# Geostatistical Modelling of an Iron Ore Deposit of Bailadila Area, Chhattisgarh, India

A thesis submitted to the University of Hyderabad
in partial fulfillment of the award of a **Ph. D degree** in
Earth and Space Sciences

by

**V. Kameshwara Rao**

**University Centre for Earth & Space Sciences**
**School of Physics**

**University of Hyderabad**
**(P.O) Central University, Gachibowli**
**Hyderabad – 500 046**
**India**

**December 2014**

# DECLARATION

I, V. Kameshwara Rao, hereby declare that this thesis entitled **"Geostatistical Modelling of an Iron ore Deposit of Bailadila Area, Chhattisgarh, India"** submitted by me under the guidance of Prof. A.C. Narayana is a bonafide research work which is also free from plagiarism. I also declare that it has not been submitted previously in part or in full to this University or any other University or Institution for the award of any degree or diploma. I hereby agree that my thesis can be deposited in Shodganga/INFLIBNET.

Date: December 30, 2014 **Name: V. Kameshwara Rao**

Signature of the student

Regd. No. 10ESPE05


# CERTIFICATE

This is to certify that the thesis entitled **"Geostatistical Modelling of an Iron ore Deposit of Bailadila Area, Chhattisgarh, India"** submitted by Mr. V. Kameshwara Rao, bearing regd. No. 10ESPE05, in partial fulfillment of the requirements for the award of **Doctor of Philosophy** in Earth & Space Sciences is a bonafide work carried out by him under my supervision and guidance which is a plagiarism free thesis.

The thesis has not been submitted previously in part or in full to this or any other university or institution for the award of any degree or diploma.

Date:

**(A.C. Narayana)**
**Research Supervisor**

**Head of the Centre**

**Dean of the school**

# ACKNOWLEDGEMENTS

I express my reverence to my research supervisor Prof. A.C. Narayana for his able supervision, guidance and support in various ways during the course of my research work. I wish to express my grateful thanks for his valuable suggestions and find words inadequate to thank him for all the discussions we have had and for his untiring efforts. I have drawn inspiration and constant encouragement from him throughout the progress of work. I am very much indebted to Prof. A.C. Narayana for his immense help and valuable guidance at every step of this research work to complete successfully.

I owe deepest gratitude to my organization and CMD, NMDC Ltd for giving permission to pursue research. I am particularly grateful to Sri N.K. Nanda, Director (Technical) for permitting me to use the data pertaining to one of the iron ore deposits of NMDC for my research purpose. I am thankful to Sri. S. Bose, former Director (Production), NMDC for the support he has extended during my work. I express my gratitude to Sri L.N. Mathur, Executive Director and Head, R.P. Dept., NMDC for his support.

I express my deep sense of appreciation and thanks to Prof. C.R. Rao, School of Computer and Information Sciences, for his valuable suggestions and critical discussion during the course of my research work as a member of Doctoral Committee. I also thank Dr. V. Chakravarthy, member of Doctoral Committee, for his help and suggestions in my research work. The support received from Dr. S. Sri Lakshmi, faculty, UCESS is acknowledged.

My sincere thanks to Head, Centre for Earth & Space Sciences, for sparing the facilities. I am extremely thankful to Prof. K.P.N. Murthy, School of Physics and Prof. Arun Agarwal, School of Computer and Information Sciences for their valuable suggestions.

I owe my sincere thanks to Sri T. Suryanarayana, formerly NMDC, for his constant encouragement, suggestions and advice. I extend my heartfelt thanks to my colleagues Sri Jayapal Reddy, Dr. P.H. Khan and Dr. Chandra Bhushan, for their support during the research work. Thanks are also due to Dr. C.h. Sravan Kumar and Dr. A. Mukherjee for the useful discussions on geological aspects.

I express my gratitude to Geovariances, France, for providing technical support as and when needed in *Isatis* software.

I acknowledge Ms. Sravanthi and Mr. Shiva Kumar and other research scholars at Centre for Earth & Space sciences for their help and support during the course. I thank all the non-teaching staff of the Centre for Earth & Space Sciences.

I express my respect and gratitude to my parents and parents-in-law whose support and blessings made this thesis possible. I am thankful to my uncle Prof. Bhanoji Rao, who has inspired and encouraged me to pursue Ph.D. and for the support in all facets of my life. I express my deepest thanks to my wife Aruna who provided continuous support by taking the entire responsibility on domestic front, during my long periods of absence from home in connection with the research work. I really feel proud of my children Archita and Ashish who have sacrificed my attention during this period.

Finally, I would like to thank everyone who helped in one way or another in making this work possible.

**V. Kameshwara Rao**

**CONTENTS**

## LIST OF TABLES

## LIST OF FIGURES

# CHAPTER 1

# INTRODUCTION

# CHAPTER 1

# Introduction

## 1.1 General introduction

The economic viability of a mineral deposit is based on the estimation of ore reserves of the deposit. Ore reserve estimates are assessments of the quantity and grade of a mineral deposit that may be profitably extracted from a mineral deposit through mining and/or mineral beneficiation. The various stages involved in reserve estimation are exploration stage and exploitation i.e., mining/production stage. In exploration stage both global (for the whole deposit) and local (block wise and bench wise) resource/reserve will be estimated using exploratory drilling data; whereas in production stage, the reserve estimation will be done using blast hole data for small portion of a particular bench. A number of disciplines such as geology, geostatistics, mining engineering, mineral process engineering, mineral economics and environmental engineering are involved in mineral exploration and ore reserve estimation (Noble, 1993).

In the exploration stage, the data from mineral deposit are sampled in a very sparse manner and thus represent only a fraction of the volume of the original sample. For mineral resource estimation, the resource modeler job is to make a very careful and sensible assessment in determining a ore body as well as the grades with the limited data available over the spatial domain as it will act as a decision for the mining company to invest huge money on a future venture (Yang, 2011). Resource estimation involves the interaction of numerous qualitative and quantitative criteria such as data quality, geological continuity and grade continuity. No prescribed criteria and rules will work for all situations or even between different ore types within the same deposit (De-vitry, 2003).

There are several interpolation methods for ore resource/reserve estimation and these methods are broadly categorized in two main categories: deterministic i.e., non-geostatistical (nearest neighborhood, triangulation, inverse distance weighting, polygonal functions (splines), linear regression and artificial neural network), and probabilistic i.e., geostatistical (ordinary

kriging, simple kriging, universal kriging, residual kriging, indicator kriging, probability kriging and disjunctive kriging) (Sluiter, 2009). The deterministic methods create a continuous surface by using only the geometric characteristics of point observations, whereas probabilistic methods are based on probabilistic theory and use the concept of randomness, spatial variability and compute the statistical significance of the predicted values. These estimation methods are used for different purposes such as global resource estimates, strategic mine planning, whole-of-life mine plans, long-term and short-term mine planning and grade control. It is important to use an unbiased estimation method which can provide a cost-effective, fit-for-purpose grade and tonnage estimate. By providing the best estimate, mining costs can be decreased by minimising the need for unplanned and unnecessary unearthing of mine area (Keogh and Moulton, 1998).

Conventional deterministic ore body modelling and resource estimation would lead to over estimation or under estimation of the grade, tonnage and other parameters related to a deposit. This will lead to improper mine planning and thus incur huge financial risk (De-vitry, 2003). On the other hand, geostatistical methods pioneered by Matheron (1963) and Krige (1951) have proved to be significant over the classical methods, and provide reliable and accurate estimates. The geostatistical method of ore reserve estimation has evolved into a theory capable of answering most of the questions raised during the development, assessment, and exploitation of a mineral deposit (Dagbert and David, 1977).

Geostatistics is a relatively new, interdisciplinary field that encompasses geology, mathematics, statistics and mining. The most common goal of geostatistics is to model the spatial data to interpolate the data at unsampled locations and provide resource estimates (Matheron, 1963). The method not only estimates the ore reserve but also gives error of estimates (Krige, 1951). There have been significant improvements in estimation techniques first with the introduction of linear methods (e.g. simple kriging or ordinary kriging) and subsequently non-linear methods (e.g. indicator kriging) and then simulation methods. These methods have proved to be significant advances over the classical methods of weighted averaging to interpolate values at some locations between known data (Khosrowshahi et al, 1998).

The ore reserve estimation is normally carried out in different stages depending upon the purpose, namely, preliminary exploration stage, project planning and development stage, or production (exploitation) stage. Depending upon the stage, the methods of estimation also vary.

Geostatistical methods are widely used at every stage. Chatterjee and Murthy (1994) discussed the details of these three stages. In the *preliminary exploration stage*, the global estimates of ore tonnage and grade of the deposit along with the optimum drilling grid at global level are determined for taking a decision whether the ore deposit is worth for further exploration and development. In the *project planning stage*, the reserves and grade estimation are to be sufficiently reliable, because any unreliable results will lead to erroneous production and economic estimates. After ensuring availability of required quantum of drilling data, subsequent action for grade and reserve estimation can be taken up. At this stage, it would be necessary to work out more detailed grade and reserve estimates like bench-wise estimates in the case of open cast mines. Kriging of the blocks of a given size, determination of the recoverable reserves, drawing a grade-tonnage curves for a given block size, and pit optimization using different method are carried out in the planning stage of the project. In *production stage*, estimating of small blocks by using production data i.e., blast-hole drilling information, and calculation of local recoverable reserves of bench is carried out. The preproduction estimates are normally carried out on large blocks. But as production proceeds, estimates of ore reserves and quality in small blocks for each bench are needed for effective planning and controlling the production. At this stage, initial estimates are compared with the production data for reconciliation and the error of estimates of grade and reserve are determined. In all these three stages, the traditional methods of computation of resource/reserves – cross-sectional methods and slice plan methods – are still largely used in India, whereas geostatistical methods are widely used elsewhere.

The quality of Fe grade plays an important role in the cost-effectiveness of an iron ore deposit. The consistent supply of quality iron ore is necessary for the steady operation of the plant and to achieve optimum plant output. It is therefore essential that all the constituents of iron ore such as Fe, silica ($SiO_2$), alumina ($Al2O_3$), supplied to the plant be within permissible limits of variation. To maintain a consistent supply of suitable Fe grades to the plant, an ore grade model is generated, based on which a grade control plan can be produced to guide the excavation of the iron ore. A good model aims to achieve reliable estimates of ore grades, representing the deposit as accurately as possible (Abdullah, 1990). The development of a good grade model is not an easy task in relation to iron ore deposits (Isaaks and Srivastava, 1989). These authors further state that the iron ore, formed under complex geological structures, typically occurs in multiple geological units. For example, in the present study there are as many as seven

lithological units and the co-existence of various geological units disrupts the spatial continuity of the deposit. In addition, the occasional presence of folds and faults further disrupts the spatial continuity of the deposit. Iron ore deposits therefore exhibit wide spatial variations (vertical and horizontal). Ideally, wide patterns of variations in grade attributes would be captured by a suitable exploratory drilling program. However, in most cases, a drilling program adequate to gather enough borehole data to produce a reliable ore grade model would be prohibitively expensive. In most cases therefore, the data available for deposit modeling is limited (Murthy and Chatterjee, 2007). Mining engineers and geologists face the challenge of delivering reliable ore grade models using limited resources and thus need to apply a variety of grade estimation techniques. Geostatistics has established itself as the most versatile of these methods for spatial input-output mapping (Chatterjee et al., 2006).

Omre (1984), in his paper 'Introduction to Geostatistical Theory and Examples of Practical Applications', states that several aspects of geostatistical analysis may be unfamiliar to statisticians. He further states that regionalized variables from the field of earth sciences tend to have skewed and heavily tailed distribution of values. Hence the well established multi-normal theory has limited applications. Omre (1984) also states that the usage of most traditional statistical methods may be prohibited as the observations are not independent but are spatially correlated.

According to Cressie (1991), in statistical methods, it is assumed that the data observations are independent, and spatial and temporal data often possess some form of correlation between observations, and to assume that each observation is taken independently is statistically incorrect. Armstrong (1998) demonstrates that two data sets having same mean and variance have a different spatial variability. This fact underlines the importance of acknowledging dependence between observations whenever such correlation exists. As stated by several authors, spatial variables are not completely random but usually exhibit an intricate relationship i.e. the nearby points usually exhibit similar or nearly equal values (Clark, 1977; David, 1988). Spatial data can often contain some form of spatial dependence or spatial correlation, and in such circumstances, it is of paramount importance that the spatial location of the data be considered. Geostatistics considers distances between sample points and target points along with their position and direction with respect to each other (Webster and Oliver, 2007).

During estimation, the variances between sample points and target points along with the variances of samples within themselves are considered (David, 1977; Davis, 1973). Geostatistics regards not only distance relation between sample points and target points but also spatial variation between them in relation with distance and direction (David, 1988). The spatial phenomenon is subjected to uncertainty which the traditional methods fail to include in their models. Traditional methods used to evaluate resources are based on sampling position and do not model the spatial continuity of the deposit. These methods are unable to provide a measure of error associated with their estimates. As they do not provide an error assessment, these methods are inappropriate to assess local or global uncertainty associated with an estimate (de Souza et al., 2004). It may lead to under-estimating or over-estimating of a reserve, which thus leads to improper mine planning and cost allocation. However, geostatistics provides a way to quantify spatial uncertainty (Chiles and Delfiner, 2009).

The resource estimation using geostatistics has made inroads into many diverse areas of the earth sciences such as mining engineering, petroleum engineering, environmental engineering and hydrology since its advent in the early 1960s. In the recent years, the mining industry has become much more conscious of the need for accurate predictions about the quantity and quality of ore reserves. This has led to surge of interest in the geostatistical methods pioneered by Krige (1951) and Matheron (1963). Application of geostatistics was carried out by several researchers in various mineral deposits such as Bauxite (Pandey and Sarkar, 2006), Copper (Emery, 2012), Coal (Armstrong, 1981; Sarkar et al., 2006; Saikia and Sarkar, 2013), diamond (Deraisme and Farrow, 2005), gold (Sarma, 2002), granite(Taboada et al., 2002), Iron ore (De-vitry, 2003; Murthy, 1989a,1989b; Sarkar et al., 2006), Limestone (Chatterjee et al., 2006), Lead and Zinc (Haldar, 1990, 2010), Nickel (Bertoli et al., 2003), Uranium (Parker et al., 1979). However, despite the increasing importance of geostatistics in mineral industry as a scientific method for resource estimation, very little work has been done on the application of geostatistics in Indian mineral industry (Sarkar, 2005a).

Many iron ore deposits have mixed distributions which are highly variable in grades and estimating the amount of ore grade material in the deposit is difficult because of its variability in grade (Isaaks and Srivastava, 1989). In such cases, the linear and non-linear geostatistical methods are advantageous when compared to the traditional methods of calculation of reserves

by cross-sections, bench plans, polygonal methods, and inverse distance square. In India, even in large mine areas, estimation of reserves and grade are assessed based on old traditional methods of cross-section and slice level plans, and the use of computerized geostatistical techniques are yet to be adapted. The geostatistical techniques can solve several problems encountered in the resource estimation.

Modeling mineral deposits to evaluate mineral resources and ore reserve is the basis for later stages of mine planning and extraction of material along the mine life. The challenge of assessment of future recoverable reserves is critical to the mining industry in that ore reserves condition both investment and profitability associated with any mining venture (Journel, 1985; Pasti et al., 2012).

In India, there is no much published work on geostatistical applications particularly in the iron ore resource estimations. Very few have applied geostatistical methods and authors restricted their work to linear methods only. It can be seen from the literature that there is no major work on the application of non-linear and simulation methods. The present study is intended to be a pilot study with the objective to investigate and evaluate the potential and applicability of various geostatistical methods, which include linear, non-linear and conditional simulation methods, in resource estimation of an iron ore deposit.

## 1.2 Iron ore

Iron, one of the most widely distributed elements in the earth's crust (ranking fourth, after oxygen, silica and aluminum), occurs as a major component of many rocks, and in small quantities in the waters of seas, lakes and rivers, in plants, etc. Iron is also the second most abundant metallic element in the Earth's crust after aluminum and accounts for 5.6% of the lithosphere. Iron, like most metals, is found in the Earth's crust only in the form of an ore, i.e., combined with other elements such as oxygen, sulfur and carbonates.

Nearly all of Earth's major iron ore deposits are in rocks that formed over 2 billions years ago. Iron ore deposits are located worldwide and the most important deposit types are: sedimentary iron deposits (iron concentration of sedimentary affiliation, banded iron formations); hematite ore from altered banded iron formations (and rarely igneous accumulations); magmatic ore deposits; hydrothermal metasomatic deposits (siderite);

hydrothermal epigenetic deposits. Earth's most important iron ore deposits are found in sedimentary rocks (Petti John, 1975).

Iron ore differs significantly in iron content. For ex, the average Fe content of Brazilian and Australian iron ore deposits is >60% Fe. Fe content in Indian iron ore is about 45-65% Fe. The average Fe content of Chinese iron ore is about 30-40% Fe. This variation affects the size of production and reserves in terms of actual iron content and also the value of the iron ore.

The iron is usually found in the form of magnetite ($Fe_3O_4$), hematite ($Fe_2O_3$), goethite (FeO(OH)), limonite ($Fe_2O_3$+H2O) or siderite ($FeCO_3$). However, two iron oxides hematite (Fe2O3) and magnetite ($Fe_3O_4$) are the primary ore minerals of iron. The maximum percent of iron that the iron ore deposits consist is 70 % Fe in hematite ($Fe_2O_3$), 72 % Fe in magnetite ($Fe_3O_4$), 50-60 % Fe in goethite (FeO(OH)), 50-66% Fe in limonite ($Fe_2O_3$+$H_2O$), and 48 % Fe in siderite ($FeCO_3$).

The iron and steel industry is the major consumer of iron ore. Iron ore is the basic raw material used in the making of pig iron, sponge iron, steel and alloy steel. Sponge iron is used as a substitute in place of scrap in electric arc furnaces and in mini-steel plants. The other important iron ore consuming industries are cement, coal washeries and ferro-alloys. As for finished products, these iron ores are used in every iron and steel object that we use today – from paper clips to automobiles. Pure iron has relatively specialized uses which include welding, enameling, manufacture of appliance parts like washing machine, electrical equipments, engineering spares etc.

### 1.2.1 World scenario

Iron ore deposits are distributed in different regions of the world under varied geological conditions and in different geological formations. The top ten countries in the world in the order of their iron resources are Russia, Australia, Canada, USA, Brazil, India, South Africa, China, Sweden and Venezuela. The world resource of iron is estimated to be 370 billion tonnes (USGS Mineral commodity summary, 2008) and the reserve is estimated to be around 160 billion tonnes.

Total production of iron ore in the world was 2.9 billion tonnes in 2013. Ranking, in descending order, of iron ore producing countries are China, Australia, Brazil, India, Russia, Ukraine, South Africa, USA, Canada, Iran, Venezuela and Sweden. India stands at fourth position with a total iron ore production of 0.15 billion tonnes in 2013 (USGS Mineral commodity summary, 2008).

World consumption of iron ore grows 10 % per annum on an average with the main consumers being China, Japan and Korea. China is currently the largest consumer of iron ore, which translates to be the World's largest steel producing country.

### 1.2.2 Indian scenario

Total resources of iron ore in India as on 1st April 2010 is about 28.5 billion tons constituting about 7.7 % of the world resources. As per UNFC system, dated 1st April 2010, the total resources of *hematit*e are estimated at 17,882 million tonnes of which 8,093 million tonnes (45%) are under 'reserves' category and the balance 9,789 million tonnes (55%) are under 'remaining resources' category. Whereas, the total resources of *magnetite* are estimated at 10,644 million tonnes of which 21.7 million tonnes are under 'reserves' category and the balance 10.622 million tonnes are under 'remaining resources' category (IBM, 2014).

Major resources of *hematite* are located in Odisha - 5,930 million tonnes (33%), Jharkhand -4,597 million tonnes (26%), Chhattisgarh - 3,292 million tonnes (18%), Karnataka - 2,159 million tonnes (12%) and Goa - 927 million tonnes (5%). The balance resources of hematite are spread in Andhra Pradesh, Assam, Bihar, Madhya Pradesh, Maharashtra, Meghalaya, Rajasthan and Uttar Pradesh. Magnetite is another principal iron ore that also occurs in the form of oxides, either in igneous or metamorphosed banded magnetite-silica formation, possibly of sedimentary origin. As per UNFC system, the total resources of *magnetite* are estimated at 10,644 million tonnes of which 'reserves' constitute a mere 22 million tonnes, while 10,622 million tonnes are placed under 'remaining resources (IBM, 2014).

India is an important producer of iron ore ranking fourth in the world in terms of quantity produced following China, Australia and Brazil. In 2009-10, world production of iron ore is 2400 MT against which Indian iron ore production was 220 MT. The world's largest producer of iron ore is the Brazilian Mining Corporation Vale, followed by Anglo-Australian companies

BHP Billiton and Rio Tinto Group. In India, Madhya Pradesh, Karnataka, Bihar, Orissa, Goa, Maharashtra, Andhra Pradesh, Kerala, Rajashthan and Tamil Nadu are the principal producers of iron ore. Among these States, Orissa recorded the highest production of 79 million tonnes i.e., about 36% of the country's production in 2009-10, followed by Karnataka 43 million tonnes (about 20%), Goa 39 million tonnes (about 18%), Chhattisgarh 26 million tonnes (about 12%) , Jharkhand 23 million tonnes (about 11%) of the total production. The remaining 3% production was reported from Andhra Pradesh, Madhya Pradesh, Maharashtra and Rajasthan (IBM, 2014)**.**

In 2009-10, Indian consumption of iron ore is 92.9 MT, whereas exports are placed at 117.38 MT (about 53.35 % of total production). China is the most important importer of Indian ores, consuming up to 93.11 % of the total iron ore exports from India (IBM, 2014).

***NMDC in iron ore exploration***

NMDC was established on 15$^{th}$ November, 1958 with the sole objective of development of mineral deposits of the nation. NMDC is a pioneer public sector organization in Iron ore exploration in India, under Ministry of Steel, Govt. of India, and has explored and developed famous iron ore deposits such as Meghahatuburu – Kiriburu Iron Ore Deposit, Bailadila Iron Ore Deposits, Malangtoli Iron Ore Deposit, Bababudan iron Ore Deposit, Kudremukh Iron Ore Deposit, Ramandurg Iron Ore Deposit, Gua Iron Ore Deposit, Donimalai and Kumarswamy Iron Ore deposit. Presently, NMDC has been exploring iron ore deposits which include Bailadila Iron Ore Deposits in Chhattisgarh, Donimalai and Kumarswamy Iron Ore deposits in Karnataka. Presently, total resources of NMDC iron ore deposits constitute more than the one third of the total Indian Iron Ore Resources. The exploration is being pursued more vividly in the brown field areas of NMDC and more than 1.5 billion tonnes have been added to the company's initial resource (1498.68 MT) base by its exploration for the last 15 years. There are many private companies in the country producing and exporting iron ore.

## 1.3 Resource estimation methods

Resource estimation methods are in complex in nature. Methods of resource estimation are generally divided into traditional (geometric or manual) methods and interpolation methods (moving average methods). An overview of the various techniques is given by Carras (1998).

### 1.3.1 Conventional methods

Conventional resource estimations are usually done manually on plan maps or cross-section maps that cut the deposit into sets of parallel slices. Data plotted on the maps include drillhole locations, assay values, and the geologic interpretation of the mineralization controls. The conventional methods, also called traditional or geometric or manual methods, are based on geometric weighting of assays and include various methods such as (i) area averaging, (ii) polygonal, (iii) nearest neighbour, (iv) cross sectional, and (v) triangular methods (David 1977).

In *area-averaging method*, the outline of the ore body for each litho type is drawn and its area is measured manually; further this area is multiplied with thickness of the ore and by the in-situ density (tones per cubic meter) of ore body to compute the tonnage of ore. Average grade is the tonnage-weighted average grade of the individual blocks (Noble, 1993).

In *Polygonal method,* the area under study is divided into a series of polygons. Tonnage is then computed using the same procedure as was used for the area-average method, except that the areas used to compute tonnage are the area of each individual polygon. Each polygon is designated a mean value equal to the value of the sample grade within its boundaries (David, 1977). *Nearest neighbor* method requires superposition of a rectangular grid of blocks over the drilled area. The grade of the nearest sample is then assigned to each block.

In *cross-sectional* approach, sectional interpretations are constructed, generally orthogonal to the strike of mineralisation. Each separate ore intersection on each drill hole is allocated its own volume of influence, which usually extends halfway to the next drill hole up and down dip, and halfway to the next section in each strike direction (Glacken and Snowden, 2001). The *triangular method* is similar to the polygonal method except that areas of triangles are estimated, and the grade of each triangle is based on the average of the grades at each of the vertices of the triangles.

Though all these traditional (geometric) methods have the advantage of simplicity and ease of implementation, some problems arise in the resource estimation employing these methods. For example, a non-uniform drill pattern will cause over estimation of grade. Sometimes it is difficult to apply geometric methods on discontinuous ore zones, especially if the ore contacts are gradational. As they provide estimate of the average grade of a deposit at a zero

cutoff grade only, it is not possible to estimate the deposit for multiple cut-off grades. The most common problem with geometric methods is that the resulting mined grades are different from the predicted distribution; some high-grade blocks usually include lower-grade material when they are mined, and low-grade blocks usually include some higher-grade material. It has been discussed by several workers that these traditional methods produce biased estimates and thus not satisfactory for estimating the reserves of mineral resources (Noble, 1993; David, 1977; Glacken and Snowden, 2001; Murthy, 2007).

There are also a number of disadvantages, including the assumption of an unrealistic model for grade variation. The major objections by users of geostatistical techniques include the issue of ignoring sample support (every sample has a different support, equivalent to the size of the polygon or the area of influence) and possible conditional bias i.e., high-grade areas are overestimated and low-grade areas are underestimated (David 1977, p309).

### 1.3.2 Interpolation methods

This estimation method, also known as the *moving average* method, uses a search area progressively moved by selected displacements across the area under evaluation. The estimated grade value of the search area is obtained by the weighted mean of all points lying within the search area. The evaluation results obtained by interpolation method are better than the traditional methods. Unlike traditional methods, which provide unsmoothed grade estimations, the interpolation methods smoothen the grade estimations. Most resource estimation techniques in common practice today, use some form of grade smoothing to interpolate values into a block based upon surrounding samples. These interpolation methods broadly divided in to *non-geostatistical interpolation* methods and *geostatistical interpolation* methods.

#### *Non-geostatistical interpolation method*

In this estimation method, also known as *weighted inverse distance method*, the weights given to observations within the search area depend on the distance of the observation from the centre location whose value is to be estimated. Weighting functions being used usually include those of 'inverse squared distance' or more generally 'inverse power distance' where the exponent is a real positive number chosen empirically. This method is simple and easy to compute, but not optimal because of its sensitivity to arbitrary weighting functions. Besides, this method does not

take in to account of spatial variability of the grade and there is no criteria to decide the optimum distance beyond which the samples are not considered for estimation.

***Geostatistical interpolation method***

All geostatistical interpolation methods, based on the theory of regionalized variables, developed by the French mathematician Matheron (1963) utilize the spatial relationship between samples, to provide weights for the estimation of the unknown block. The standard estimation method of geostatistics has many varieties, but the most commonly used is the linear kriging technique, called ordinary kriging.

The mining software packages developed in 1980s, made great advances in the visualization and modelling of complex geological domains. It was during this time that the first resource estimates were generated using kriging techniques. Subsequently, the non-linear geostatistical approaches such as indicator kriging (Journel, 1983b), disjunctive kriging (Matheron, 1975) were employed in resource estimation. A number of computationally-intensive techniques such as conditional simulation are also employed widely.

In brief, the geostatistical approaches in grade interpolation rely on variants of kriging, whereby the weights given to each sample are derived from the semi-variogram model, which defines the continuity of grades in two or three dimensions. These geostatistical methods are in turn subdivided into three categories – linear kriging, non-linear kriging, and simulation. All geostatistical methods rely to an extent on the assumption of stationarity, which is seen as the decision to pool data within a given area or domain, and not as a hypothesis which can be proven or disproven (Glacken and Snowden, 2001).

***Advantages of geostatistical methods over traditional estimation methods***

The primary purpose of any natural resource estimation is to reliably estimate the overall ore resources and recoverable tonnage and grades throughout a mineral deposit. Traditional methods may provide a global estimate of ore resource but not the error associated within such estimate. However, geostatistical modelling study provide not only global reserve estimate, but also a more reliable block-by-block mineral inventory with an indication of relative confidence i.e., error associated in the block grade estimates (Sarkar, 2014).

Classification of resources based on sectional interpretations (traditional method) is limited to the resolution of the section spacing and relies on a qualitative assessment of the continuity of the mineralization with respect to the drill hole spacing along and between section lines. A more quantitative assessment of confidence in numerical estimates can be achieved using geostatistical tools which measure spatial continuity, relative uncertainty, and absolute risk (Glacken and Snowden, 2001).

## 1.4 Objectives of the present study

There are very limited studies on the geostatistical modeling of mineral deposits particularly of iron ore deposits in the Indian context. Some of these studies are restricted to linear geostatistical methods, which are not very effective in the real mining context. Against this background, it is proposed in this study to carry out a comprehensive geostatistical modeling of an iron ore deposit employing linear, non-linear and simulation methods.

The aim of this study is to investigate and evaluate the potential and applicability of suitable linear, non-linear and conditional simulation geostatistical methods for modelling iron ore deposit. The study further focuses on evaluation of applicability and suitability of each method in resource estimation.

The study envisages the following main objectives:

- To assess grade domains of the deposit in a rapid way in 2D before the application of 3D modelling of the deposit.
- To investigate the feasibility of non-linear method indicator kriging for delineating various litho types in the iron ore deposit and to compare the grade estimation results of two different approaches.
- To correlate and validate the recoverable resource estimation results of different types of non-linear geostatistical estimation methods and evaluate the suitable methods.
- To assess the uncertainty and risk involved in the resource estimates of the deposit by employing two conditional simulation methods and compare them to find the suitable model for the deposit.

## 1.4 Literature review

A number of studies has been carried out across the world discussing the evaluation of geostatistics and application of geostatistics methods in mineral resource estimation, environmental management, geotechnical engineering etc.

***Evolution of geostatistics***

A mathematician and a mining engineer, Professor Georges Matheron, while working with the French Geological Survey in Algeria and in France during 1954-1963, discovered the pioneering work of the South African School on the gold deposits of the Witwatersrand, and formalized the major concepts of the theory that he named Geostatistics (Rivoirard, 2005). In the late 1950s and early 1960s Daniel Krige and George Matheron, both mining engineers, gave a detailed framework for the science of geostatistics. Prior to the evolution of the geostatistics, Krige (1951) presented a statistical approach to some basic mine valuation problems on the South African gold deposit of the Witwatersrand. Duval et al., (1955) presented the work of Krige (1951) in a very concise way in the French journal "Annales des Mines". The same issue of Annales des Mines published another article by Matheron (1955a) on statistical methods for evaluating the deposits. The term "geostatistics" appeared explicitly in the title of a study of a lead deposit by Matheron (1955b) in a technical report in French much before the subject 'geostatistics' was introduced.

Matheron (1962), Father of Geostatistics, introduced the first part of geostatistical theory of 'Regionalized Variables' to the evaluation of a mineral deposit, involving a study of the spatial relationships between sample values; this was followed by the second part in 1963 linking concepts of estimation variance, extension variance and kriging. Although classical linear geostatistics was essentially completed by Matheron (1963), Matheron did not introduce the concept of Random Function until he completed his thesis in 1965. The "classical" geostatistics i.e., linear geostatistics based on stationary covariance and variogram has been discussed in his thesis by Matheron (1965). The regionalized variable under study, as Matheron called it, is then modelled as a Random Function. Geostatistics has its origin as a scientific field in the work of Youden (1951), Matheron (1962) and Gandin (1963).

Even though the theory of regionalized variables and the kriging estimators were developed in the early to late 1960's, much of this work was written in French and it was not until the publications in English of Michel David's *Geostatistical Ore Reserve Estimation* and Andre Journel's and Huijbregt's *Mining Geostatistics* in the late 1970's that use of these geostatistical ideas became widespread. Armstrong and Matheron (1986a) have observed that much of earlier works on geostatistics (ex., Matheron, 1971, 1975a, b) was available in French and in the internal reports of Centre for Geostatistics (at Fontainebleau, France). Once the translation of Matheron work was available, numerous papers and books have been published on all aspects of geostatistics. Basic introduction to geostatistical theory and applications are discussed by various authors (ex., Huijbregts,1975; and Delfiner and Delhomme,1975; David,1977; Journel and Huijbregts,1978; Clark,1979a, b, c; Journel,1983a; Journel,1986; Isaaks and Srivastava, 1989; Cressie, 1993; Kitandis, 1997; Stein,1999; Sarma, 2002, 2009; Webster and Oliver, 2007; Hengh et al., 2009; Haldar, 2013; Rossi and Deutsch, 2014).

The geostatistics have been defined by various authors. Geostatistics is the application of the formalism of random functions to the reconnaissance and estimation of natural phenomena (Matheron, 1963). Geostatistics, which largely overlaps with the term '*spatio-temporal statistics*', can be defined as a branch of statistics that specializes in the analysis and interpretation of any spatially (and temporally) referenced data (Journel, 1986). Isaaks and Srivastava, 1989 state that Geostatistics offers a way of describing the spatial continuity of natural phenomena and provides adaptations of classical regression techniques to take advantage of this continuity. According to Cressie (1990), Geostatistics means "statistics applied to geology", evolved in the mining industry for a long time. Geostatistics can be regarded as a collection of numerical techniques that deal with the characterization of spatial attributes, employing primarily random models in a manner similar to the way in which time series analysis characterizes temporal data (Olea, 1999). Geostatistics is the study of phenomena that vary in space and/or time (Deutsch, 2002).

### *Application of geostatistics*

The application of geostatisitcs started with the objective to improve forecasts of ore grade and reserves in mines, but the mathematical generality of the approach led to applications of geostatistics to other problems in the earth sciences. In mineral industry, geostatistical

methods were applied by researchers for various applications such as mineral resource estimation (Glacken and Snowden, 2001; Emery and Ortiz, 2005), quantification of uncertainty in resource estimation and resource classification (Yamamoto, 1999; De-vitry, 2003), determination of optimum drilling grid (Humphreys and Shrivastava, 1997; Murthy and Chaterjee, 2007; Saikia et al., 2006; Haldar, 2013), determination of grade-tonnage relations (Mol and Gillies, 1984; Murthy, 1996; Haldar, 2004), delineation of litho types in mineral deposit (Chatterjee et al., 2006; Gossage, 1998), recoverable resource estimation (Vann and Guibal, 1998; Jones, 1998; Thwaites and Deraisme, 1998) and risk assessment of estimated grade (Jackson et al., 2003; Costa et al., 2000). Geostatistical techniques have been successfully applied also in numerous non-mining fields, ranging from soil mapping, meteorology, ecology, oceanography, geochemistry, epidemiology, human geography, and geomorphometry (Hengh al, 2009).

The various geostatistical methods employed for resource estimation are broadly categorized as '*linear methods'* (simple kriging, ordinary kriging, universal kriging), '*non-linear methods'* (indicator kriging, disjunctive kriging, uniform conditioning) and *simulation methods* (turning band, sequential Gaussian simulation, LU (Lower Upper) decomposition, simulated annealing etc). Earlier techniques, based on the works of Krige (1951) and Matheron (1963), focused on linear geostatistical methods such as ordinary kriging followed by several authors (Journel and Huijbregts, 1978; Isaaks and Srivastava, 1989; Krige, 1994a,b; Gooverts, 1997; Armstrong, 1998; Davis, 2002; Coombes, 2008).

A comparison of traditional methods and linear geostatistical methods was made by several workers with reference to mineral resource estimation. For example, Royle (1979) compared traditional methods of estimation such as polygonal method and geostatistical method such as ordinary kriging and stated that traditional methods produced biased estimates but not geostatistical method.

Geostatistical prediction of grade fluctuations of iron ore, after blasting a certain volume in El-Gedida iron ore deposit, Egypt, was carried out by Hardy et al., (1986). Authors have inferred that their study helps mining engineer to predict the grade fluctuations of different components of iron ore and to design the bench blasting dimensions accordingly.

A comparison of inverse distance, ordinary kriging and median indicator kriging estimation methods was carried out by Keogh, and Moulton (1998) in the 84 East iron ore deposit of Parabudroo mine. Authors have concluded that kriging methods gave better results as compared to inverse distance. Similarly, a computational experiment was conducted by Zimmerman et al., (1999) to compare the spatial interpolation accuracy of ordinary kriging and universal kriging and inverse distance method. In their study, they have also found that both the kriging methods consistently and substantially outperformed inverse distance method.

A comparison between ordinary kriging (OK) and inverse distance weighted (IDW) estimates was recently made by Shahbeik et al., (2013) for an iron ore deposit, and observed that the error of estimation in OK method is less than that of IDW method and that the results of OK method are more robust.

Several authors (Gouda and Moharam, 2001; De-vitry, 2003; Asghari et al., 2009) have employed OK method for estimation of grade variable Fe of iron ore deposit. All these authors have estimated only Fe variable and did not consider estimating the variables associated with Fe of iron ore deposit such as silica and alumina. Though silica and alumina are impurities in iron, it is necessary to estimate these variables from mining aspect to make sure that their contribution is minimum in the estimated blocks.

In addition to above, several researchers have employed ordinary kriging in various applications. Glacken and Snowden (2001) stated in their paper that several authors have provided an overview of the entire resource estimation and classification process. Collings et al., (1997) describe the geological modelling, resource estimation and classification aspects of a sedimentary-hosted iron ore deposit. A similar historical perspective is presented by Glacken et al. (1998) for the Kambalda nickel mines. Reeve and Glacken (1998) describe the history of resource estimation for one large Australian mining company, WMC Resources Limited. Arvidson (1998) describes the process of bringing together over 100 years of data to generate a resource estimate for the gold deposits of the Golden Mile in Kalgoorlie. Murphy et al. (1998) provide an overview of the resource estimation process at the Bronzewing and Jundee gold operations, Yandal province, WA. Lutherborrow (1999) describes the history of estimation on the broken Hill field. Moorhead et al. (1999) present the resource estimation procedures at the Cadia Hill mine in New South Wales. Pocock (1999) describes why resources at the Peak gold

deposit, Cobar, NSW, have always been underestimated. Kok and Ulker (2008) mentioned in their paper that Cochrane et al. (1998) used block modeling techniques and the application of geostatistics for resource estimation to further improve the quality of the resource model to improve the accuracy of the deposit model and the quality of the resource and reserve estimates in order to optimize capital investments and reduce the development and operating costs of underground mining projects.

Advantage of linear geostatistics is far less complex than its non-linear counterpart and its theory is also more widely accessible (Journel and Huijbregts, 1978; Wackernagel, 1995). However, a major drawback is that OK does smoothening of the grade superfluous with respect to grade cut-offs and thus provide an unrealistic estimate of tonnage and grades at these cut-offs, which means that a mining project can be exposed to undue risk (Krige, 1996). Another disadvantage of linear geostatistical method such as ordinary kriging is, it results in inaccurate recoverable resources if the data follow a skewed distribution (Isaaks and srivastava, 1989). According to Yu et al. (2004), not all the problems in the estimation of natural resources can be solved by the linear geostatistical methods. They further suggest that non-linear geostatistical methods must be used if the probability of an actual but unknown concentration at a given location exceeding a particular threshold needs to be assessed and subsequently for estimation of recoverable resources.

Non-linear geostatistical methods are based upon non-linear transformations of the sample data such as the natural logarithm, the Gaussian (normal) transform, or the indicator transform, which have gained popularity in the last ten years. A comprehensive review of most non-linear kriging methods is given by Vann and Guibal (1998). Practical implementations of non-linear kriging techniques are presented by Elliott et al. (1997), Collings et al. (1997), Matthews et al. (1999) and Glacken and Snowden (2001). Vann et al. (2000) discussed the non-linear methods commonly used in the mining industry such as disjunctive kriging (DK), indicator kriging (IK), probability kriging (PK), lognormal kriging (LK), uniform conditioning (UC), and residual indicator kriging (RIK).

These non-linear estimators can be *parametric* and *non-parametric* estimators. Non-linear Parametric estimators of recoverable reserves based on normal transforms were first introduced by Matheron (1974, 1976 a, b). Other parametric methods such as multi gaussian

method have been developed by Verly (1983, 1984), while the disjunctive kriging methods by Marechal (1976a, b), Jackson and Marechal (1979) and Young (1982). Simple lognormal kriging, which requires knowledge of the stationary mean of the grades, was introduced by Parker (1975) and Parker and Switzer (1976). Ordinary lognormal kriging, which does not require knowledge of the mean grade, was developed by Rendu (1979). Further expansion of this method was presented by Parker et al. (1979) and Journal (1980). A major drawback of the parametric method is that it is difficult to comprehend and apply because of mathematical complexity involved in this approach.

Of all the *non-linear parametric* methods, *disjunctive kriging* is widely used as it has advantage over linear kriging methods. Several authors (Matheron, 1976a, b; Marechal, 1976a, b; Kim, Myers, and Knudsen, 1977; Journel and Huijbregts, 1978; Jackson and Marechal, 1979; Rendu, 1980b) have discussed the theory and applications of disjunctive kriging.

A comparison was made between OK and DK methods by Yates et al. (1986a, b) for the electrical conductivity (EC) data which was sampled at 101 random locations in a 10 ha field. Authors have concluded that DK is better estimator than OK in the sense of average kriging variance as there was a reduction of about 6 % in kriging variance from DK as compared to OK.

An application of disjunctive kriging for earthquake ground motion estimation was presented by Carr et al. (1986). A comparison of OK and DK was carried out for peak velocity data at five locations arbitrarily selected. Estimated values of velocity yielded by OK and DK are compared to the estimated probability that these estimates exceed 6 cms/sec for an earthquake. By following the contours of high exceedance probability, likely zones of damaging earthquake ground motion are delineated. Authors have concluded that DK yielded accurate estimates reducing underestimated values to less than 10 % of the total number of estimation locations. They further stated that because of DK and OK fundamentally are different, their comparison is perhaps unfair. Each of these techniques has merit for earthquake ground motion applications.

Samui and Sitharam (2007) developed a geostatistical model based on ordinary kriging (OK) and disjunctive kriging (DK) methods to estimate spatial variability of standard penetration test (SPT) data and carried out geotechnical analysis studying several variables such as depth, density of the soil, SPT values and depth of ground water at different locations of Bangalore over

a 220 sq km area using 766 boreholes with an average depth of 30 m below the ground level. Authors have compared the results of these two methods with actual data of two boreholes and concluded that DK has shown better estimator than OK in terms of reduced kriging variance and the comparison between an estimated and actual value.

Disjunctive kriging was employed by Yang et al. (2008) for predicting the probability distribution of exceeding a Pb threshold and subsequently tracing the hotspots in sewage-irrigated land. Based on DK estimates, authors have identified the hotspots of Pb pollution which indicated higher risk in the regions of soils irrigated with sewage. Their results of DK showed that, in evaluating the land for vegetable production, if the probability that pb concentrations exceed the contamination threshold of 50 % or more, then 6.2 % of the study area (1932 $km^2$) would be classified as unsafe for this purpose.

Daya and Hassani (2010) have employed disjunctive kriging (DK) for geostatistical grade modelling and to model the uncertainty of mapping iron ore concentration in an iron ore deposit. Authors have inferred that DK is suitable for modelling iron ore deposit where data are marginally skewed. Catherine Bleinès et al. (2011a) presented a case study on application of OK, IK and DK for an iron ore deposit and inferred that ore estimates are more accurate in DK method than other methods.

Yates and Yates (1988a, b) have demonstrated how DK can be used as a management decision making tool. Moreover, they have emphasized that the conditional probability can be used as an input to a management decision-making model to provide a quantitative means for determining whether the management actions are necessary. Oliver et al. (1996) employed disjunctive kriging for environmental management and state that assessing pollution risk is a major feature of environmental analysis and this is feasible in an optimal way using disjunctive kriging. Authors concluded that disjunctive kriging is one of the techniques that provide environmental scientists with a useful decision making tool, especially where decisions could result in damage to health.

Juang and Lee (2000) investigated the feasibility of disjunctive kriging on delineation of heavy-metal contaminated soils. An application of this proposed method to a real data set of soil Cd concentrations in a contaminated site in Taiwan was used for illustration. Emery (2006b)

applied disjunctive kriging to two case studies; the first one for topsoil samples measuring the lead concentration at a smelter site in Dallas, Texas; and the second case study concerns the infestation of field crops by a caterpillar.

*Non-linear and non-parametric* methods, in contrast to parametric methods, require no assumption concerning the distribution of grades. The basis of these techniques is the indicator transform which essentially transforms the grade at each sample location into a distribution function. These transformed data are then used to estimate the local spatial distribution of grades by solving linear ordinary kriging systems to estimate mean grade within a block.

*Indicator kriging* (IK) is a non-linear non-parametric method which estimates the probabilities of exceeding pre-specified cut-offs without the smoothing effect of linear interpolation methods such as ordinary kriging. Indicator transforms were first used to estimate distributions of correlated data using statistical methods by Switzer (1977). Whereas, Journel introduced the *indicator kriging* (IK) in Geostatistics in 1982 (Journel, 1982). Further development of this estimator is presented by various authors (Journel, 1983b; Lemmer, 1984a, b; Sullivan, 1984; Glacken and Blackney,1998; Khosrowshahi et al., 1998). Median indicator kriging method, a variant of indicator kriging, was initially proposed by Journel and Huijbregts (1978), Journel (1982), and later discussed by Glacken and Blackney (1998) and Vann and Guibal (1998). Vann et al. (2000) discussed the theory behind indicator kriging in their paper. Authors stated that within the area of recoverable resource estimation IK is the most widely used method and is practical to implement. A comparison of parametric and non-parametric methods is given by Verly and Sullivan (1984).

Hill et al. (1998) compared two variants of indicator kriging - *median indicator kriging* (MIK) and *full indicator kriging* (FIK) in the analysis of a gold mineralization using exploratory drilling data of a bench. They further compared the results of MIK and FIK with the production data i.e., blast hole data by plotting grade tonnage curves and observed a little difference in the grade tonnage curves of the two indicator kriging methods which fell below that obtained from the blast hole data.

Jones (1998) applied indicator kriging method for estimating the grade in the strongly skewed gold distribution. A comparative study of two indicator kriged estimates using two

different grade thresholds - one using decile (10) thresholds (IK1 estimate) and another using 13 thresholds (IK2 estimate) was done. Author has investigated that the application of indicator kriging using grade thresholds based on the decile thresholds was shown to be a poor, but was greatly improved by modifying grade thresholds to 13. Author has concluded that the IK1 estimate resulted in only 578 kg Au reported above 50 g/t Au, approximately 1,100 kg Au less than was reported for the IK2 estimate, and IK2 estimates are much better than IK1.

A comparison of ordinary kriging (OK) and multiple indicator kriging (MIK) estimates for different cutoff grades (0.5 % and 1.0 % Ni) of nickel was done by Lipton et al. (1998) and their results have shown that these estimates are quite similar. Authors concluded that due to the strong continuity of grades in their deposit, it resulted in relatively small differences between the OK and MIK estimates. However, for deposits in which variability is greater MIK would give better results as compared to OK.

Mendes and Lorandi (2006) applied Indicator kriging to estimate the cumulative probability distribution function of three geotechnical variables – penetration resistance index, ground water table and potential collapse of the soil, in order to produce indicative maps showing the probabilistic occurrence of those variables. The indicative maps of the three variables were integrated to produce a probabilistic map for the quantitative evaluation of the more favourable sites for deep foundations. Authors have concluded that probabilistic maps from indicator kriging were used to show where the most favourable areas for constructing foundations at a specific depth and also unsuitable area for the proposed foundation which eliminated the local investigation process.

Several non-linear geostatistical techniques have been developed in the past decades not only for grade modelling but also for modelling lithological domains. Most of them are based on indicator kriging or on the conditional simulation of categorical variables. Lithological maps were generated employing indicator kriging by Chatterjee et al., (2006) for a limestone deposit in India. Further, using these litho maps, ore grade estimation of was carried out by using an artificial neural network (ANN) method and ordinary kriging (OK) method. In their study, a comparative evaluation between the NN method and the OK method demonstrated that the NN model outperformed the kriging model. The authors concluded that the NN method could be used for grade-control planning in ore deposits.

Interpolation methods such as kriging which generate smoothed representations of reality are inappropriate for modelling spatial fluctuations and related uncertainties of estimates. Also the use of the kriging variance as a measure of uncertainty is inappropriate. *Simulation* methods are more appropriate than block estimation procedures for risk assessment and uncertainty assessment of the estimates. Various authors (Journel, 1974, 1994; Luster, 1985; Isaaks, 1990) have discussed about the different methods for obtaining conditionally simulated models.

Conditional simulations were first developed for mine planning and grade homogenization (Journel, 1974; Deraisme, 1977; Marechal and Shrivastava, 1977). Subsequently simulations are employed by several authors (Nowak, et al., 1993; Dowd, 1994a, b; Sanguinetti et al., 1994; Guibal et al., 1997; Sahin and Fuseni, 1998) for risk assessment and uncertainty assessment of the estimates. Simulations are also used to estimate the global estimation variance for different drilling grids by Humphreys and Shrivastava (1997). Goria et al. (2001) state that measuring the global estimation variance as a function of the sample grid helps decision makers choose the most suitable grid.

In application fields such as mining engineering, agricultural land management, air, soil and groundwater pollution studies, the practitioner often looks for assessing the risk that a regionalized attribute (e.g. the grade of a metal of interest, a soil property or the concentration of a contaminant) exceeds a given threshold at a specific unsampled location, conditionally to a set of neighboring sampled values. The geostatistical methods currently used to address this concern are conditional simulations (Chile`s and Delfiner, 1999; Emery, 2006a). Of all the simulation methods ‘turning band simulation’ and ‘sequential Gaussian simulation’ methods are widely used and more useful in the mining industry. Several authors have applied these two methods in various applications.

Conditional simulation using sequential Gaussian simulation was employed by Costa et al. (2000) for assessing risk in coal mining. Authors have shown that conditional simulation is an appropriate framework to generate equally probable maps used for risk analysis in mine planning and the combination of multiple simulated models provided the necessary tool to asses uncertainty associated with predictions of the attributes studied i.e., coal accumulation and sulphur content.

A comparison between SGS and OK was carried out by Jang and Liu (2004) for estimating the spatial variability of hydraulic conductivity in the Choushui river alluvial fan, Taiwan. Authors have found that the OK realization smoothed out spatial variability and extreme measured values of hydraulic conductivity. The mean SGS realization yields moderate spatial variability whereas the individual SGS realization shows high spatial variability and statistically extreme variation because of the wide ranges of the mean and standard deviation. Authors have concluded that the individual SGS realization is useful in stochastically assessing the spatial uncertainty of highly heterogeneous aquifers

Emery and Gonzalez (2007) presented probabilistic modeling of lithological domains employing plurigaussian simulation model and its application to resource evaluation in a copper deposit. A comparison of grade models obtained by using a deterministic and a probabilistic modelling of the lithological domains was presented. Authors have concluded that probabilistic modelling resulted in a more homogenous distribution of copper grades for the entire deposit, closer to the assay data. This probabilistic model approach was also applied to the characterization of oil reservoirs and mineral deposits by various workers (Betzhold and Roth, 2000; Skvortsova et al., 2001; Skvortsova et al., 2002; Emery and Gonzalez, 2007).

There is no single geostatistical method or workflow that can be applied to every problem. Each study may be different from the others, in that a unique combination of methods and an individualized workflow should be selected and designed to solve each particular problem (Yunsel and Ersoy, 2011). Several geostatistical methods are available, and the choice depends on the type of the data available and the purpose of the study (Kok and Ulker, 2008). Irrespective of the methods used, it is necessary to fully test the results of the various grade estimation methods used in a study. Reconciliations must be performed between the estimated models and blast hole production data. Once the results of the estimated models are tested, then the benefits of applying a particular method can be determined examined (Keogh and Moulton, 1998). It is further suggested that the estimated models are also to be compared with the original data for reconciliation purpose.

## 1.6 Outline of the present study

The present research is focused on application of geostatistical modeling of iron ore deposit of Bailadila region. The Bailadila range in South Bastar Dantewada District, Chhattisgarh possess one of the richest concentrations of high grade iron ores in the country. There are 14 iron ore deposits distributed over two separate ridges namely eastern ridge and western ridge. The deposit under study is a green field deposit on the western ridge of Bailadila range in Dantewada District, Chhattisgarh and mining is yet to be commenced. This iron ore deposit is situated on the southern most end of the Bailadila Iron ore range and is characterized by rugged and undulating topography.

The increased demand of iron ore in the domestic market has necessitated development of a new deposit to meet the domestic and export demands for beneficiated iron ore lumps and fines by steel plants and sponge iron industries. NMDC has taken up to explore and develop this deposit to meet the national requirement. For the purpose of obtaining statutory clearances such as mining lease for this deposit, it is mandatory to estimate the resource base of the deposit and submit to Indian Bureau of Mines (IBM), and hence NMDC has carried out resource estimation but using conventional methods. As the conventional methods do not deliver the required results and are also not suitable for mine planning and production scheduling (Osterholt et al., 2009), a comprehensive geostatistical modelling of an iron ore deposit is carried employing various geostatistical methods which include linear, non-linear and simulation methods for different purposes in this study.

Ore deposit evaluation of the deposit is carried out in 2D for rapid assessment of grade domains and grade variation of Fe in the deposit employing linear geostatistical method ordinary kriging.

The traditional *geological cross-sectional* method was applied for delineating litho types and preparation of geological model of the deposit. A 3D block model is then created prior to estimation of resource and grade of the deposit. In this study, a novel method - non-linear geostatistical *indicator kriging* method is applied for categorizing the litho units in the block model and subsequently lithological maps are generated for 32 benches of the deposit.

Block model generated from geological cross section is used for estimation of volume and tonnage in different litho units. Grade estimation of Fe, $SiO_2$ and $Al_2O_3$ in two block models - traditional geological cross sectional model and novel indicator kriging model is done employing ordinary kriging, in different litho units. The estimated results obtained from both the block models are compared with the original drilling data and composited data. Subsequently, based on indicator kriged block model, Fe grade maps and error maps are generated for 32 benches of the deposit.

Resource classification is done based on error quantification method and the total estimated mineral resource is classified into 'measured', 'indicated' and 'inferred' categories in two different approaches based on *kriging standard deviation* and *kriging efficiency*.

Recoverable resources estimation is carried out for a total of eight thresholds (cut-offs) 45 %, 55 %, 60 %, 62 %, 65 %, 67 %, 68 % and 69 % Fe employing non-linear geostatistical method 'Median indicator kriging' and 'Disjunctive kriging' . For these cut-offs, grade-tonnage relationship is established in both the methods. 'Disjunctive kriging' is employed for estimation of global recoverable resources taking in to account of mineable block size 5 x 5 x 12 m (SMU size) within the block size of 25 x 25 x 12 m.

A comparison is made between the grade estimates obtained from indicator kriging, disjunctive kriging and ordinary kriging methods to find out the applicability of suitable estimation method.

Conditional simulation is carried out for 100 realizations employing turning band (TB) and sequential Gaussian simulation (SGS) methods to evaluate uncertainty of estimates. In both the methods, simulated results of 7 realizations are validated with the input data. A comparison is made between the results of total recoverable tonnage (T) and mean grade (M) obtained from turning band simulation and sequential Gaussian simulation methods for different cut-offs to find out the suitability of simulation method.

All of the statistical and geostatistical calculations and graphical output generated for this case study were made using exclusive geostatistical advanced software *Isatis* developed by Geovariances, France. Geological model and volume calculation of 3D lithological models were carried out using *Surpac* mine planning software of Dassault Systems, Australia.

# CHAPTER 2

# GEOLOGY OF THE STUDY AREA

# CHAPTER 2

# Geology of the Study Area

## 2.1 Introduction

The most important factor in resource/reserve estimation is an understanding of the geology of the deposit and the surrounding areas. Without a sound geological understanding, and a sensible application of that understanding, an estimation exercise becomes merely a mathematical treatment of results with no practical value. More seriously, any result which does not take sufficient account of geology is almost certain to give a seriously misleading impression of the value of the deposit (Stephenson, 1990). Author further states that the most important functions of the geologist are to interpret the geology of the deposit, to make a prudent assessment of the quantity and quality of the data, to identify any uncertainties in the data, and communicate to the resource/reserve estimation experts. The importance of geology in ore reserve estimation has been emphasized by several authors like Rostad (1976), King et al. (1982, 1986), and Grace (1986). In this chapter, iron ore deposits of different cratons of India, geological setting of the Bastar craton, iron ore deposits of Chhattisgarh and Bailadila range and stratigraphy of the study area are discussed.

## 2.2 Cratons of India and associated iron ore deposits

Cratons are broad central areas of continents that have remained tectonically stable for prolonged periods and are affected by younger epeirogenic movements, whereas the mobile belts are the curvilinear, high-grade, gneiss-granulite belts that surround the cratons (Ramakrishnan and Vaidyanadhan, 2010), The Indian Peninsular shield is a mosaic of such cratons and mobile belts, consisting mainly four Archean cratons (Figure 2.1): Aravalli-Bundelkhand Craton in the north, Singhbum craton in the east, Bastar craton in the center and Dharwar craton in the south (Mukhopadhyay et al., 2008). These cratons are surrounded by proterozoic mobile belts viz. Eastern Ghat Mobile Belt (EGMB), Delhi-Aravali Mobile belt, Singhbum mobile belt and Central Indian Tectonic Zone (CITZ) and Kotri-Dongargarh mobile belt (Radhakrishna, 1989). The greater part of the high grade iron ores of India are hosted by voluminous banded iron

formations of major Archean greenstone belt successions. Major iron ore deposits in different cratons of India (Figure 2.1) include (i) Noamundi-Koira Valley of the Singhbhum craton of eastern India, (ii) the Bailadila-Dalli-Rajhara deposits of the Bastar craton in Central India, (iii) the Donimalai-Hospet deposits, and (iv) the Goa deposits of the Eastern and Western Dharwar cratons, respectively in southern India. No major iron ore deposits are found in Aravalli-Bundelkhand craton and Deccan traps. Economically significant iron ore deposits in India are hosted by prominent Banded Iron Formation (BIF) successions in Archean greenstone belts with major iron ore located in States of Chhattisgarh, Jharkhand, Orissa, Goa, and Karnataka. The BIF host rock is referred to as banded hematite quartzite (BHQ), banded hematite jasper (BHJ) or banded magnetite quartzite (BMQ). The consistency of the weathered BIF ranges from friable to very hard, but it is always composed of mesobands rich in hematite alternating with quartz (chert) mesobands. Variable proportions of remnant magnetite and siderite are also present (Mukhopadhyay et al., 2008). The study area is located in Bastar craton.

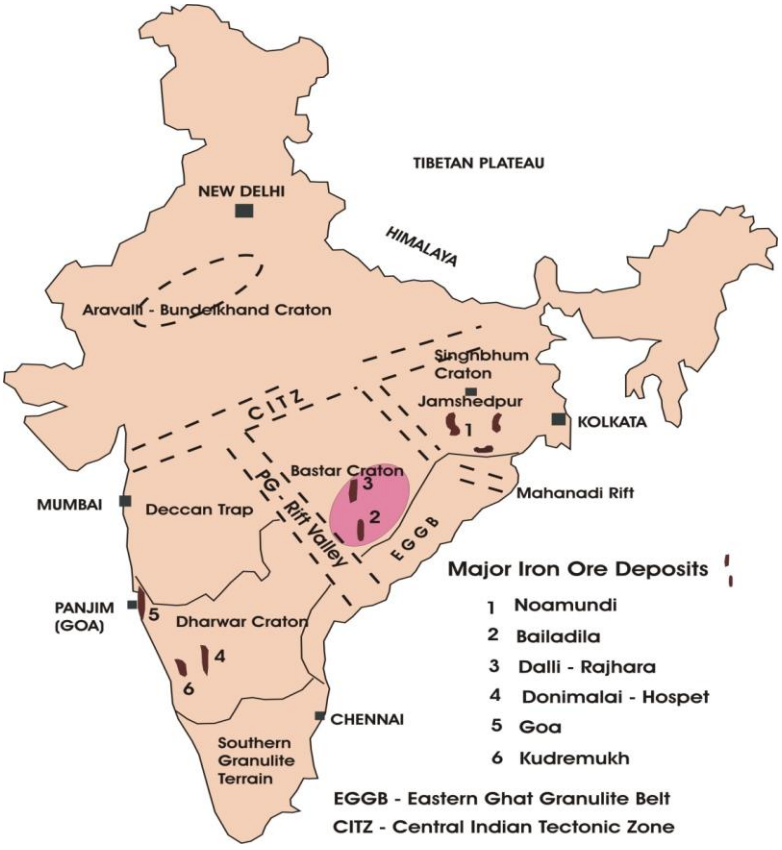


Figure 2.1 Distribution of different cratons of India that hosted iron ore deposits (Mukhopadhyay et al., 2008). The study area is located in the Bastar craton indicated as '2' in the map.

## 2.3 Geological setting of the Bastar craton

The Bastar craton in central India is bounded by the Eastern Ghats Mobile Belt in the east, the Late Mesoproterozoic Pranhita-Godavari and Mahanadi Rift Valleys in the south, the Bhopalpatnam Granulite belt in the west, and the Central Indian Tectonic Zone (CITZ) in the north (Figure 2.2). A number of Paleo-Neoarchean low-grade metamorphic greenstone or supracrustal belts, with BIF as major constituent units locally, occur in the Bastar craton (Figure 2.2) (Crookshank, 1963; Chatterjee, 1970; Mishra et al., 1988; Ramakrishna,1990; Ramachnadra et al., 2001; Roy et al., 2001; Srivastava et al., 2004). The greenstone belts are surrounded by tonnalite-trondjhemite-grandiorite complexes with enclaves of quartzite, calc silicates, cordierite-sillimanite schists, and amphibolites. Some of these complexes are paleoarchean age, making the Bastar craton one of the oldest terranes known in India. Voluminous granite intrusions are considered to reflect final consolidation of the Bastar craton (Sarkar et al., 1993). The granite-greenstone basement is uncoformably overlain by two groups of supracrustal rocks. The older group is Paleo-to Mesoproterozoic in age and comprises folded felsic volcanic and siliciclastic rocks (Figure 2.2). The younger group is late Meso-to Neoproterozoic in age and is constituted by under formed siliciclastic-carbonate successions of the Chhattisgarh Supergroup, Indravati, Albaka, and Penganga Groups (Mukhopadhyay et al., 2006). In Bastar craton, major iron ore deposits occur in Chhattisgarh and Madhya Pradesh States. The deposit under study is located in Chhattisgarh state.

## 2.4 Iron ore deposits of Chhattisgarh

Precambrian iron ore group of rocks consists of banded haematite jasper/quartzite are found in several parts of MP and Chhattisgarh State. Large deposits of excellent quality iron ore are found in Bastar, Durg, Dantewara districts and Smaller deposits occur in Raigarh, Raipur, Bilashpur, Rajnandgaon, Kanker and Jashpur districts of Chhattisgarh (formerly M. P.). Various iron ore deposits found in Chhattisgarh in different districts are shown in table 2.1.

Table 2.1 Iron ore deposits occurring in various districts of Chhattisgarh. Study area occurs in Bailadila range of Dantewara district which is highlighted in the table.

| **District** | **Iron ore Deposits** |
|---|---|
| Bastar | Rowghat area, Chhotadongar deposit |
| **Dantewara** | **Bailadila range includes fourteen deposits numbered 1 to 14** |
| Durg | Dalli-Rajhara, Kanchar, Jharandali, Kondekosa and minor occurrences near Khairagarh, Berla, Katul Kassa, Jurla Khar etc. |
| Kanker | Ari Dongri. Besides this there are smaller deposits in Dulki, Kalwar, Dongar bar, Lohattar in bordering area of Durg district. |
| Jashpur, Bilashpur, Raigarh | minor occurrences |

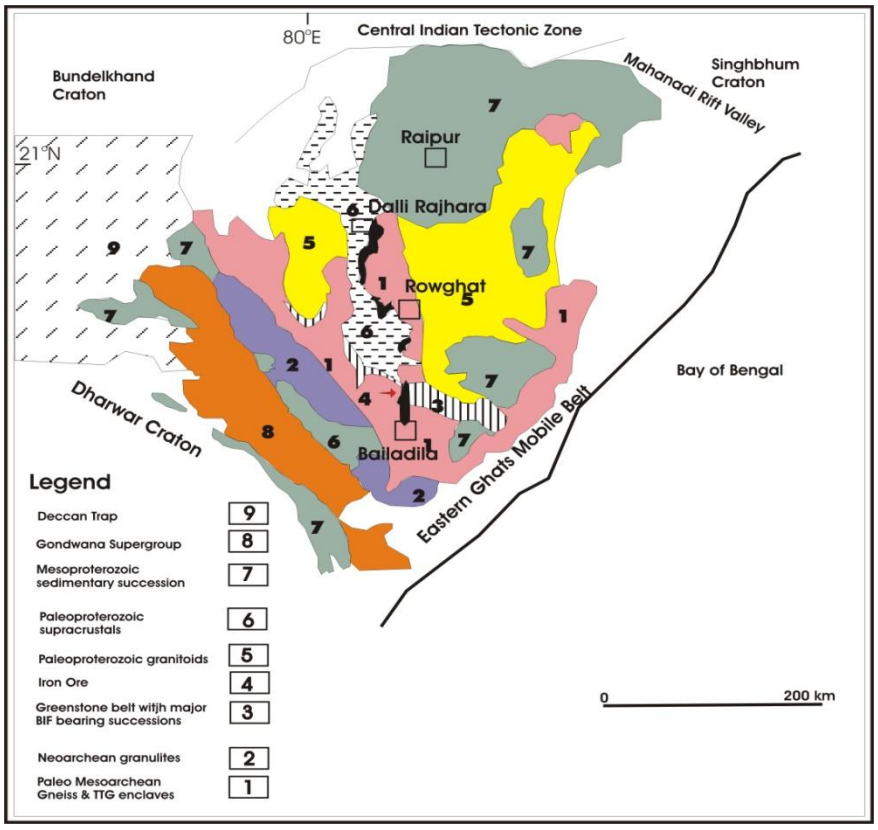


Figure 2.2 Geological map of the Bastar craton, central India, showing the distribution of BIF-bearing successions that host major iron ore deposits (Mukhopadhyay et al., 2008).

## 2.5 Iron ore Deposits of Bailadila

The largest and probably richest iron ore deposits of the Bastar craton are in the thick, BIF-bearing succession of the Bailadila Group in the Bailadila hill range. Bailadila range of deposits is perched on the southern tip of Chattisgarh in Dantewada District (Figure 2.3). The iron ore deposit is associated with the metamorphic Pre-Cambrian rocks comprising the "Bailadila Iron Ore Series", which are considered to be equivalent to the iron ore series of Jharkhand-Orissa. The ore body is developed at the junction of the banded hematite quartzite and ferruginous shale and has a general NE-SW strike, with south-easterly dips ranging between 35º and 40º.

The iron ore deposits of Bailadila range occupy a large tract of land in southern and western parts of Dantewara District in Chhattisgarh (Toposheet No. 65F/1,2,5,6) covering the area between latitude $18^0$35' - $18^0$52' N and longitude $81^0$10' - $81^o$16' E. The Bailadila range is estimated to contain over 1600 MT of resources of iron ore (Exploration Report of NMDC, 2006).

The Bailadila range, extends about 40 km long and 1 km wide range of hills that stands out as high as 1,250 m above sea level from the rolling plateau of Bastar granitoids, with a north-south-trending, tightly folded, northerly plunging synclinorium. The easterly dipping eastern limb of the synclinorium is overturned and the western limb is steeply easterly dipping to subvertical. The BIF unit is resistant to weathering and forms a range of hills that hosts 14 individual ore bodies (Figure 2.3) numbered for mining purposes, "Deposit No. 1 to Deposit No.14" (Crookshank, 1938a, b, 1963). The names of these 14 deposits are as follows: Sonadehi Dongri, Pargal hill, Khandighat Dongri, North Hahaladdi hill, South Hahaladdi hill, Tarai Kholi hill, Bajimari Dongri, Dorkenhur Dongri, Ghoradar Dongri, Pitehur Dongri, Hill west of Amapara, Hill north west of Kawachi Katel, Berahus Donger and Hakirihur Donger (GSI, 2006). In the present study, one deposit (of the 14 deposits) is evaluated for resource estimation, using linear, non-linear and conditional simulation geostatistical methods.

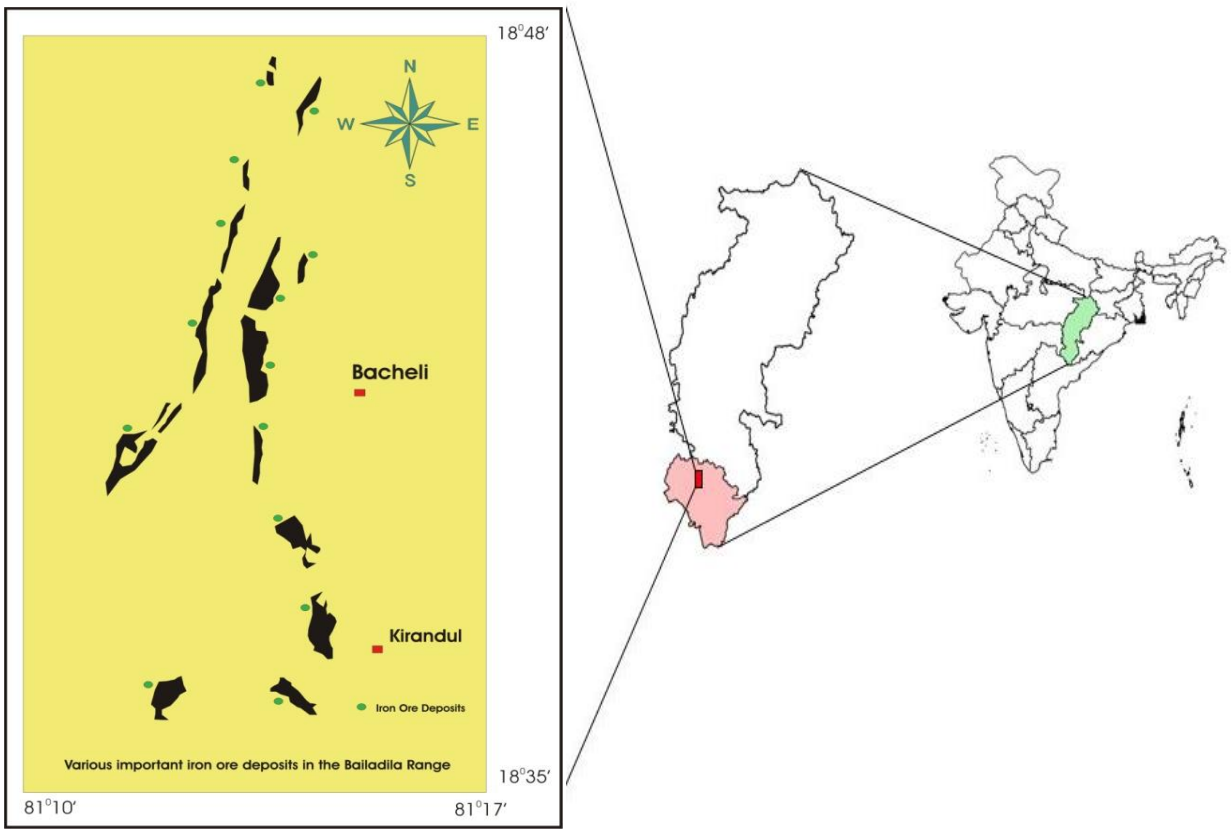


Figure 2.3 Map showing Bailadila range and its deposits in Bastar district of Chhattisgarh State in India. All the 14 deposits in Bailadila range are distributed in east and west ridges.

### 2.5.1 Geology and structure

The Bailadila hills in South Bastar, Dantewada District, Chhatisgarh contain vast deposits of high grade iron ore, ranked among the richest in the world. The iron ore deposits of range so far observed are seen to occur in the Dharwarian rocks known as Bailadila Iron Ore series. The rocks of this series have great resemblance with those of iron ore series of Singhbhum-Keonjhah-Bonai of Orissa and Jharkhand. The rocks of the "Bailadila Iron Ore Series" consist of banded haematite quartzite (BHQ), ferruginous or haematite schist, phyllites, massive quartzites, grits etc. These formations are intruded by extensive patches of granites and amphibolite. The Bailadila range is composed of slightly metamorphosed Pre-Cambrian rocks. The regional strike of the rocks is more or less persistent in N-S direction with dips ranging from 50º to 70º towards east. The series overlie the Bengpal Series consisting of meta-siliciclastic sediments and is

underlain by Pre-Cuddapah intrusives. The geological sequence in the region of Bailadila is shown in Table 2.2.

The iron ore is mostly enriched in haematite in massive and laminated forms, apart from shaly laminated, and biscuity under laminated type. Of the different types of iron ore, massive variety is of the purest quality. Laterites are normally associated with the laminated ore either as capping of varying thickness and / or along the lamina of the ore. In addition to the above types of ore, there are floats of iron ore intermixed with soil scattered all round the deposits, especially on the slopes and at the foot of the cliffs. At places, recemented ore comprising blocks of iron ore of varying sizes cemented together by a ferruginous matrix is also found (GSI, 2006).

Table 2.2 Geological sequence in the Bailadila region (Kar and Chakravarthy, 1970)

<table>
<tr><td rowspan="6">Pre-Cambrian</td><td colspan="2">Pre-Cuddapah Intrusives</td><td>Dolerites, pegmatites, charnockites, granites, greenstones, amphibolites</td></tr>
<tr><td colspan="3">Intrusive Contract</td></tr>
<tr><td colspan="2">Bailadila Iron Ore Series</td><td>Banded hematite quartzites and shale with the associated iron ore deposits.<br>Grunerite-quartzites, ferruginous phyllites etc.<br>White quartzites.</td></tr>
<tr><td colspan="3">~~~~~~~~~~~~~~~~~~~~~~~~~~~~~~Unconformity~~~~~~~~~~~~~~~~~~~~~~~</td></tr>
<tr><td>Bengal Series</td><td>Loa stage<br>Dantewada stage.</td><td>Bracciated ferruginous schists, schistose conglomerates etc.<br>Slate and shales with andalusite crystals, grunerite schists, sericite schists and quartzites.</td></tr>
<tr><td colspan="4">~~~~~~~~~~~~~~~~~~~~~~~~~~~~~~Unconformity~~~~~~~~~~~~~~~~~~~~~~~~~~~~~</td></tr>
<tr><td colspan="2">Archaean</td><td colspan="2">Granite Basement</td></tr>
</table>

The Bailadila metasedimentary sequence unconfirmably overlies the older metamorphic of Bengpal (Sukma) Group with intervening post-Bailadila Granites (Ramakrishnan, 1990). These metasediments in the Bailadila area form two approximately parallel N-S trending ridges (Figure 2.4), extending for about 30 kms from Kirandul in the South to Jhirka in the north, where they confluence and extend further northward (Crookshank, 1963). The sequence exposed on the eastern flank of east ridge forms an east dipping overturned limb of an isoclinals syncline (Figure 2.5). Primary sedimentary structures, however suggested westward younging. The Western ridge is also a synclinal ridge, with near vertical to steeply eastward dipping beds (Mukherjee et al, 2010). The phylite and conglomerate occupying the intervening valley are folded into synclines and anticlines. Thus the whole sequence in the Bailadila Group forms a northerly plunging synclinorium (Crookshank, 1963; Ramakrishna, 1990). Plunging overturned folds trending NNE in Bailadila sequence are a result of horizontal shear concomittent with flexural slip folding Chatterjee (1970).

The BHQ usually form ridges parallel to the strike direction but are at places irregular due to complicated folding. The Bailadila range comprises two NS ridges separated from each other by a narrow valley. The iron ore deposits of Bailadila range are numbered from north to south. Deposits 1 - 5 are located on the western ridge, deposits 6 - 12 on the eastern ridge, and deposits 13 & 14 on the E-W southern range. The two ridges are about 1219m in height above sea level. BHQ normally occurs along the upper portion of the eastern flank of the eastern ridge and the upper portion of the western flank of the western ridge. At places, BHQ is also seen on the top of the ridges. Structurally, the ridges have a synclinal structure and the valley between them is eroded anticlinal. It is these synclines in the ridges that the major deposits of iron ore are found.

The Bailadila group of rocks consists of meta sedimentary sequence and overlying the Bengpal group of rocks. These metasedimentary sequences are arranged in two parallel N-S trending ridges.

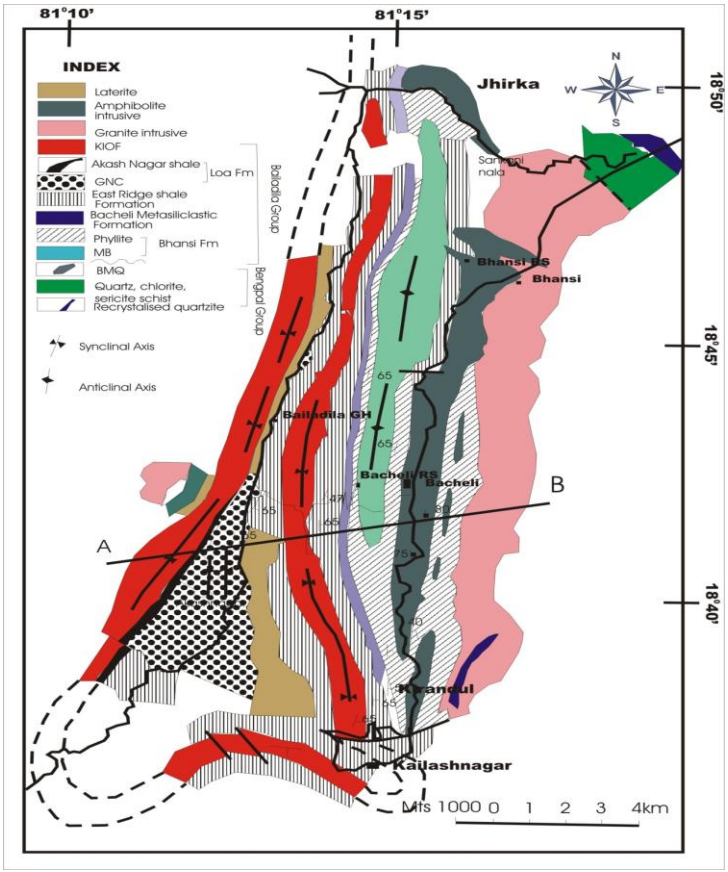


Figure 2.4 Geological map of Bailadila range (after Crookshank, 1963; Bandyopadhyay and Hishikar, 1977; Khan and Bhattacharya, 1993; and Mukherjee et al., 2010).

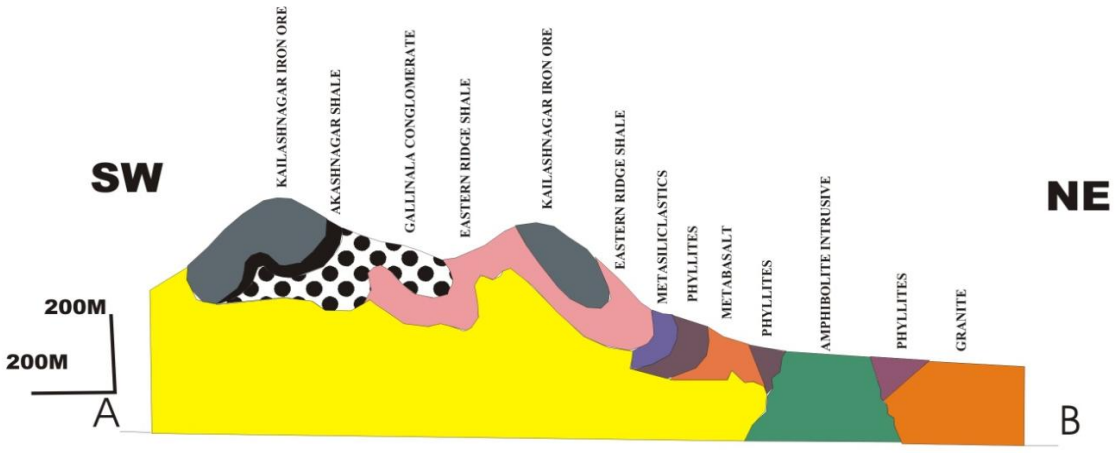


Figure 2.5 Geological cross-section (A-B) of the area given in Figure 2.4 (Bandyopadhyay and Hishikar, 1977; Khan and Bhattacharya, 1993; Mukherjee et al., 2010.

The enriched pockets of iron ore deposits associated with BIF's are mostly canoe shaped and are in linear belts of BIF which are bifurcating in nature. The enriched ore within the BIF's is concentrated in the swelled portions of the synclinal depressions of the BIF's. In general, the iron ore deposits present in the BIF's of the eastern limb are wider and shallower compared to the iron ore deposits of the western limb, where the spread is more surfacial and is reflected very clearly in the present day working mines of NMDC viz., BIOD-5 (on western limb) and BIOD-14 (on the eastern limb). This could be due to the nature of synclines, which is open in the eastern limb and tighter in the western limb (Mukherjee et al, 2010).

It is observed from the outcrop pattern and structure that the enriched ore within the BIF is concentrated in the swelled portions of the synclinal depressions of the BIF's (Figure 2.6). The southern tip of the eastern and western limbs of the BIF's is eroded because of which the older formations of the stratigraphic sequence are totally exposed. Bifurcation of the anticline and syncline is observed towards the south. A synclinal overturned folding in the south and the outcrop pattern of concavity towards south resulted in the enrichment of iron ore in Deposit-13 (Mukherjee et al, 2010).

### 2.5.2 Stratigraphy of Bailadila group

The earliest account on the geology of Bailadila Group was given by Crookshank (1963). In his three tier classication of Bastar Supracrustal rocks, the Bailadila Series (Group) is the youngest and unconfirmable overlies the Bengpals and Sukma. Subsequently, Bandyopadahyay and Hishikar (1977), based on subsurface excavations, have brought out a better picture of the stratigraphy of the Bailadila Group. Later, Mishra et al., (1988) recognized three formations in the Bailadila Group and Chatterjee (1969, 1970) who reported the amphibole series minerals, provided a short account on the metamorphism of the Bailadila Metasediments. Subsequently, Khan and Bhattacharya (1993) documented the stratigraphy of Bailadila Group in the Bhansi-Bacheli-Kirandul areas. Based on the field relations, structural disposition, conglomerate occurrence and petrographic characters, they have proposed to classify the Bailadila Group into three Subgroups, which comprises five formal stratigraphic formations (Table 2.3), namely-Bhansi metabasalt and metapelites, Bacheli metasiliciclastics, East Ridge shale/slate, Loa

conglomerates and shales and Kailash Nagar Irom Formations in the ascending order (Khan and Bhattacharya, 1994).

The Bailadila group of rocks consists of metasedimentary sequence and overlies the Bengpal Group of rocks (Ramakrishnan, 1990; Khan and Bhattacharyya, 1993). The metasedimentary sequences are arranged in two parallel N-S trending ridges (Figure 4) approximately parallel initially then confluenching near Jhirka (Crookshank, 1963; Bandyopadhyay and Hishikar, 1977). The Stratigraphic sequence of Bailadila is given in Table 2.3.

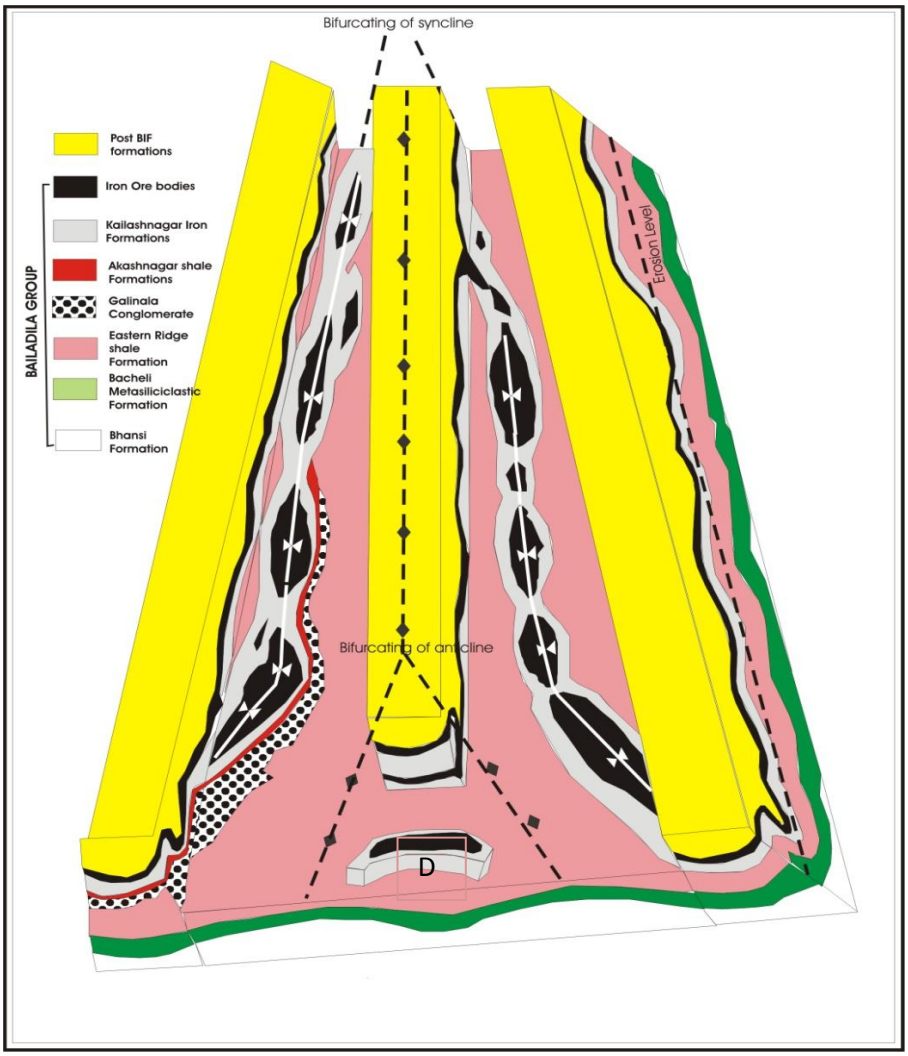


Figure 2.6 Schematic block diagram showing disposition of different litho units in Bailadila Range (Mukherjee et al., 2010). Deposit under study is shown at the bottom as D.

Table 2.3 Stratigraphic sequence of Bailadila group (after Khan and Bhattacharya, 1994)

| Subgroup | Formation | Member |
|---|---|---|
| | Kailash Nagar Iron Formation | |
| | | Akash Nagar Shale |
| Upper | Loa formation | |
| | | Galli Nala Conglomerate |
| .....Local Unconformity…… | | |
| | East Ridge Shale | |
| Middle | | |
| | Bacheli Metasiliciclastic | |
| ..... Local Unconformity ..... | | |
| Lower | Bhansi Formation | |
| ..... Angular Unconformity ..... | | |
| Quartz chlorite schists, crystalline quartzites, magnetite quartzites of Bengpal (sukma), | | |

The Bhansi Formation consists of chlorite schist, micaccous phyllite and metabasalt and forms the lower subgroup of Bailadila Group. The middle subgroup is represented by East Ridge Shale and Bacheli Metasiliciclastic Formations. The lithology of Bacheli Metasiliciclastic Formations include thin, grade, cross bedded wacke/arenites with inter bedded shaly layers becoming common upwards. Eastern Ridge Shale is reperesented by interlaminated ferrugunious shales and bedded cherts. The Upper subgroup of Bailadila Group has two formations viz., Loa Formation and Kailashnagar Iron Formation. The Loa Formation has two members namely Gallinala congomerte (Polymictic, unsorted, matrix supported conglomerates) and Akash Nagar Shale (thinly laminated, soft, ferruginous shale). The Loa formation is overlain by Kailashnagar Iron Formation and is represented by banded hematite quartzite with pockets of massive, laminated ores and blue dust (Mukherjee et al., 2010).

### 2.5.3 Previous works on Bailadila range of iron ore deposits

'Bailadila' range of hills look like '**the hump of an ox**' it is named so by the native inhabitants of this place, in the local dialect. The Bailadila iron ore range was remote, inaccessible and replete with wild life.

P.N. Bose of GSI in 1899 was the first to map geology of this region, and reported very rich and extensive iron ores with hematite quartzite in the Bailadila range. H. Crookshank and P.K. Ghose of GSI during 1934-1938 mapped and identified 14 iron ore deposits in Bailadila Range. A systematic geological mapping was done during 1932-38, through which 14 iron ore bearing hills have been demarcated from the range. In view of the urgency of assessment of the mineral potentialities of this region, a separate circle of GSI was formed in December, 1958, and in the same year Indian Bureau of Mines (IBM) was assigned the job of detailed proving of some of these deposits.

The commercial discovery of Bailadila dates back to 1955-56 when Euemura of Japanese Steel Mills Association, studying the memories of Geological Survey of India, draw the attention of the Japanese Steel Mills to the richness of the vast deposits of iron ore and its proximity to the East Coast of India. Later an agreement has been signed with the Japanese Steel Mills in 1960. During 1964-65, Chatterjee gave a detailed account of mineralogy and mode of formation of important deposits in this hill range. Subsequently, based on REE pattern and ratios of various elements in meta-pelites, Khan and Bhattacharya (1993) proposed a new stratigraphic sequence for Bailadila Iron Ore Series.

The entire area was brought to the mainstream of civilization by the spectacular effort of NMDC by opening-up of mines. Today, Bailadila is a name to reckon in the world iron ore market because of its super high grade quality. Bailadila complex possesses the world's best grade of hard lumpy ore having > 66% iron content, with negligible deleterious material and the best physical and metallurgical properties needed for steel making.

## 2.6 Study area

The Bailadila range in Dantewada District, Chhattisgarh possesses one of the richest concentrations of high-grade iron ores in the country. There are in all 14 iron ore deposits distributed over two separate ridges namely eastern ridge and western ridge. NMDC is already operating five large mechanized mines in Bailadila sector. The deposit under study is a green field deposit located a little south-eastward of the southern extension of the western ridge and mining is yet to be commenced. The highest point of the deposit is at 1218 RL and the lowest surface exposure of the ore body is seen around 930 m RL. The borehole data has indicated

average depth of the ore around 95 m. The ore body has maximum thickness of 160 m to 190 m on cross-sections S6 and N0 to N3 and gradually thins out towards the ore shale/BIF contact in the north-western and south-eastern area.

### 2.6.1 Location and geography

The deposit is located 2.5 km west of a deposit which is under operation and about 7 km southwest of Kirandul railway station (SE railway) and is connected with a fair weather road. Kirandul is well connected with Raipur (via Jagdalpur) in the north by road and Visakhapatnam in the east by both rail and road (470 km). The deposit is situated on the southern most end of the Bailadila Iron Ore Range. The deposit falls under Survey of India Toposheet No. 65F/2 confined between latitudes of 18º36′00″N - 18º37′15″N and longitudes 81°11′30″E - 81°12′30″E.

The deposit is characterised by rugged and undulatory topography rising to an altitude of 1218 m. The deposit is a crescent shaped ore body, trending roughly NE-SW and with moderate to steep dipping (38º-42º) towards south east and forms a cliff towards north. The deposit has a strike length of 1600 m and width varies from 120 to 975 m with an average of 390 m. The average depth of the deposit is around 95 m. The Malinger and Galli nalas provide the main drainage in the area. The Galli nala flows southwest of the deposit and the Malinger nala emerges from southern slopes of the deposit. These nalas are perennial in nature. NMDC has carried out detailed geological exploration work in this deposit, covering an area of 631.34 ha after obtaining prospecting licence (PL). The area falls under reserve forest.

### 2.6.2 Geology of the deposit under study

On the basis of detailed geological exploration in the deposit, the following local stratigraphic sequence (Table 2.4) has been established (Exploration report of NMDC, 2006).

Table 2.4 Stratigraphic sequence of the deposit

| | |
|---|---|
| Bailadila Iron Ore Series | Dolerites<br>Banded iron formations (BIF) with associated iron ores<br>Ferruginous shale<br>Schist |

Detailed exploration work has indicated surface exposure of ore body upto 930 reduced level (RL). Structurally, the deposit appears to be one limb of an isoclinal fold. Deposit has been traversed by number of faults and a major fault trending NE-SW, suspected to be passing along the Galli nala may have isolated the deposit from the main western ridge. One major fault east of ore body has displaced the BIF. All these faults appear to have caused change in strike of the ore body. The rock types encountered in the deposit are as follows:

***Banded Iron Formation (BIF)***

The BIF'S are distinctly banded and mainly occur in north, north-eastern and north-western flanks of the ore body. The exposures of both thickly and thinly banded BIF'S are seen in the deposit. The strike is generally NE-SW and dip angle is 60° - 70° towards SE. BIF displays alternate bands of quartz and hematite. Small quartz veins traversing across the bedding planes are sometimes seen. Well developed joints, small folds and puckers have also been observed in BIF. At depths blue dust generally grades into BIF and sometimes sharp contact between blue dust and BIF has been observed. Chemical composition of BIF exhibits Fe (51.46 %), $SiO_2$ (24.85 %), $Al_2O_3$ (0.49 %) and LOI (0.77 %).

***Ferruginous Shales***

Shale underlies the banded iron formations. Shale outcrops are mainly confined to the nala sections, low level contours and hill slopes. Shale is generally covered by surface soil and float ore. Exposures of purple and pink shale can be seen in the north-eastern and south- eastern slopes. The composition of shales indicates Fe (40.55 %), SiO2 (18.01 %), Al2O3 (12.82 %), and LOI (8.86 %).

***Dolerites and schists***

Dolerite dyke and exposures of ferruginous and micaceous schists have been traced along NNE of the deposit.

### 2.6.3 Earlier exploration works

In 1945-46, A.M. Heron examined the Deposit and estimated a reserve of 174 million tonnes of iron ore. The Geological Survey of India (GSI) carried out preliminary exploration work in north block (CS N0 to CS N5) of Deposit during 1964-1968 emphasizing on contouring

and geological mapping of deposit on 1:2500 scale with 3 m contour interval, covering contouring of 1.80 sq.km of area in north block, and geological mapping of 3.5 sq.km of area. GSI has also carried out core drilling of 15 boreholes (BH series) on 100 m grid, covering 1398.87 m, pitting 54 (deep, medium and shallow) pits totalling 412.10 m. 1023 samples were recovered and 875 samples analysed for Fe and only 41 samples for complete analyses. GSI indicated Reserves of 81.55 million tonnes of gross reserves upto 924 m. RL with Grade Fe 65.38 %, $SiO_2$ 0.45 %, $Al_2O_3$ 0.45 % and P 0.024 % .

In 1976 NMDC started initial exploration of deposit to confirm the grade that was assessed earlier by GSI. NMDC drilled 6 boreholes (NBH Series) in the northern portion of the ore body with total drilled meterage of 336.65 m. 158 samples were recovered and analysed for Fe, $SiO_2$, $Al_2O_3$ and LOI. These boreholes were drilled for quick assessment of the deposit and to confirm the grade assessed earlier by GSI. Further, NMDC took up detailed exploration in January 1993 and completed the work in November 1997. During this period, NMDC took up detailed systematic investigation of the deposit covering topographical survey, geological mapping, pitting for delineation of concealed ore body, core drilling, ore dressing tests, sampling and chemical analysis. Contouring in 1.60 sq.km area has been completed and a topographical map on 1:2000 scale with 2 m contour interval has been prepared. Borehole locations and survey stations/spot levels were fixed with the help of triangulation station network. Detailed geological mapping for an area of 1.80 sq.km in north and south blocks has been completed on 1:2000 scale. The ore body and adjoining rock types were mapped with the help of Theodolite. The variations in physical properties of various ore types were studied. Structural features of ore body like bedding planes, joints, fold axes etc. were recorded. 7,380.85 m. of core-drilling on 100 m. cross-section interval in 72 boreholes has been completed covering the entire deposit. Borehole D/18 has gone upto a depth of 169.20 m., later on it was suspended due to drilling difficulty after encountering blue dust.

A total of 9116.37 m drilling in 93 boreholes has been completed in the deposit. The cores obtained from boreholes were systematically logged. Chemical analyses of these samples were carried out by NMDC in the R & D lab of the organization. Physical and chemical variations in different ore types such as hardness, compactness, grain size, colour, laminations, friable nature, lithological and structural features were recorded. Using these core samples,

different types of samples were prepared viz., primary samples, check samples, complete analysis and pit samples. Primary samples were prepared at 2m uniform interval and the core thus obtained was split into two, one half was preserved for future reference and the other half was analysed for Fe, $SiO_2$, $Al_2O_3$ and LOI radicals. A total of 4482 assay samples were analysed for these elements and checked the accuracy of analytical results. Check sample analysis was carried out for 10 % of primary samples. A total of 415 check samples were analysed and compared with that of assay sample results. A total of 16 samples were analysed for complete analysis the elements Fe, $SiO_2$, $Al_2O_3$, LOI, P, S, MgO, CaO, MnO, $TiO_2$, $Na_2O$, to detect any possible deleterious constituents with respect to permissible tolerance limits. In order to expose and delineate the concealed portion of ore body, 5 shallow pits were excavated on south and south-western slopes of deposit. Nature and thickness of soil/overburden and ore continuity have been ascertained. 5 Pit samples were drawn by making channels in the opposite walls and were analysed for Fe and $SiO_2$. Detailed petrological studies to find out the mineral composition, structure, texture, physical properties and XRD studies were conducted on ore type and rock type samples.

Based on physical and chemical characteristics, major ore types are identified as steel grey hematite (Hard, compact and metallic with average grade 68.15 % Fe), blue grey hematite (porous, massive in appearance, dull grey in colour, less hard and compact with average grade 68.54 % Fe), laminated hematite (moderately hard compact and characterized by the presence of well developed laminations with an average grade 65.76 % Fe), lateritic/limonitic ore (Deep brown in colour characterized by intensity of weathering and lateritisation with an average grade 59.64 % Fe) and blue dust (very soft, powdery and bluish colour with an average grade 67.84 % Fe). The in-situ bulk density of different ore types was also measured. The bulk density (tonnes/$m^3$) adopted for various ore types of reserve estimation is SG (4.3 tonnes/$m^3$), BGH (4.2 tonnes/$m^3$), LH (3.4 tonnes/$m^3$), LO (3.1 tonnes/$m^3$) and BD (3.0 tonnes/$m^3$), whereas for BIF and shale, the bulk density of 2.70 and 2.5 tonnes/$m^3$ respectively have been considered.

### 2.6.4 Previous studies on resource estimation

Number of works like geological plan, contour plan, cross sections longitudinal sections and bench plans drawn on 1:2000 scale to ascertain the ore persistence. A total of 17 geological transverse sections were drawn at 100 m intervals across the strike by projecting topography, surface features, drill holes along with the intercepts of various lithological units. The chemical analysis data was used for delineating the limits of the ore body envelope and the ore types within it. Slices were extracted at 12 m vertical intervals from the geological sections and different ore types in the slices were correlated between section lines. In each slice plan, area of each ore type polygon was measured with planimeter and its grade was computed from the 12 m composite sample data by simple arithmetic average of the samples falling in the domain. Polygon area of similar ore types were summed up separately to determine the area of each ore type in each slice plan and the average grade (Fe %) is estimated by weighted average method by weighting the grade with their respective areas. Tonnages were arrived at by multiplying the areas with slice interval and the ore type-wise insitu bulk density. On the basis of exploration work in the deposit, NMDC indicated Mineral Resources of 354.18 MT with an average grade of 67.14 % Fe with a cut-off of 55 % Fe.

# CHAPTER 3

# DATA AND STATISTICAL ANALYSIS

# CHAPTER 3

# Data and Statistical Analysis

## 3.1 Introduction

Data, either primary or secondary, are important to arrive at conclusions. The data treatment, processing and geostatistical computations are important to make significant and valid applications. In earth sciences, data is represented either in discrete or continuous values depending upon the type of variable. Discrete data, such as lithologies, are represented by integer values, where as continuous data, such as grades and drillhole intervals, are represented by continuous values. Further, the spatial data of any earth science involves geographical coordinates, which are very important for geostatistical /geo spatial analysis.

A fundamental step in any scientific investigation is the quantitative-description stage. This is particularly true today in the geological sciences, which in the past had depended largely on qualitative description. Until the facts are gathered and described quantitatively, analysis of their causes is premature. Statistics deals with quantities of data, and so requires those data in manageable form. Organized data are the clearest data. Thus, much of statistical analysis deals with the organization, presentation, and summary of information. In this study, exploratory drilling data is organized in several categories such as exploratory raw data, domain data and regularized data.

Computation of basic statistics and evaluation of grade distributions are basic tools for geostatistical analysis and resource modelling (Davis, 1986). Statistical analysis of the data provide information on high or/and low grade outlier values, evaluation of favourability of different lithologies, data subsets within each domain, grade distributions, correlations and choice of thresholds for non-linear methods such as indicator kriging and disjunctive kriging.

Spatial aspects of the data, such as the degree of continuity or heterogeneity and directionality are important in developing a resource model of the deposit. However, a study of descriptive statistics and inferential statistics is prerequisite to understanding geostatistical

concepts (Krige, 1951; Isaaks and Srivastava 1989). In this study, descriptive statistical measures (e.g., Number of samples, minimum, maximum, mean, standard deviation, variance and coefficient of variation), and inferential statistical measures i.e. graphical data representation (e.g., histograms and scatter plots) are used to understand the nature of data sets.

## 3.2 Exploratory raw data

The main data used in this study are the drillhole data consisting of collar, survey, assays and geological logging to create the geological model, block model and for grade estimation. The other set of data available are the data collected while exploring the deposit specially pitting, trenching, check samples and bulk samples.

The Geological Survey of India was the first organisation to carry out preliminary exploration work in north block of the deposit, during 1964-1968. 15 boreholes (BH Series) (Figure 3.1) were drilled on 100 m grid scale covering total meterage of 1398.87 m. A total of 1023 samples were recovered of which 875 samples were analysed for Fe. NMDC has drilled 6 boreholes (NBH Series) in 1976 in the northern portion of the ore body, which covered a total meterage of 336.65 m, for quick assessment of the deposit and to confirm the grade earlier assessed by GSI. A total of 158 core samples were recovered and analysed for Fe, $SiO_2$, $Al_2O_3$ and loss on ignition (LOI). NMDC has completed 7380.85 m of drilling on 100 m grid interval in 72 boreholes (D Series) covering the entire deposit during 1991-93. In total, the available data comprise of 4537 samples recovered from 93 vertical boreholes (Figure 3.1) with a total meterage of 9116.37 m for the present study. The boreholes were spaced in a more or less grid pattern with a spacing of 60-120 m (average 100 m) between each borehole. The depth of boreholes varies from 13.75 to 169.25 m and with an average depth of 97.5 m. The histogram showing depth variation in 93 boreholes is given in Figure 3.2

The data available are categorized into collar data (Borehole Id, Easting, Northing, RL and Depth), and assay data (Sample Number, from, to, Z, Fe, SiO2, Al2O3, LOI, P and Lithology). All the data are obtained from NMDC.

Prior to geostatistical modelling, both basic (quantitative) and graphical representation of the exploratory data are carried out. The extent of the deposit in x, y and z direction and

range (minimum and maximum) of the data are analysed from collar data and represented in Table 3.1. Chemical analyses of Fe, $SiO_2$, $Al_2O_3$ and LOI for 4482 samples with the information on the lithology were obtained. Descriptive statistics of these chemical variables of assay data is given in Table 3.2 and the grade distributions of Fe, $SiO_2$, and $Al_2O_3$ are given in Figure 3.3.

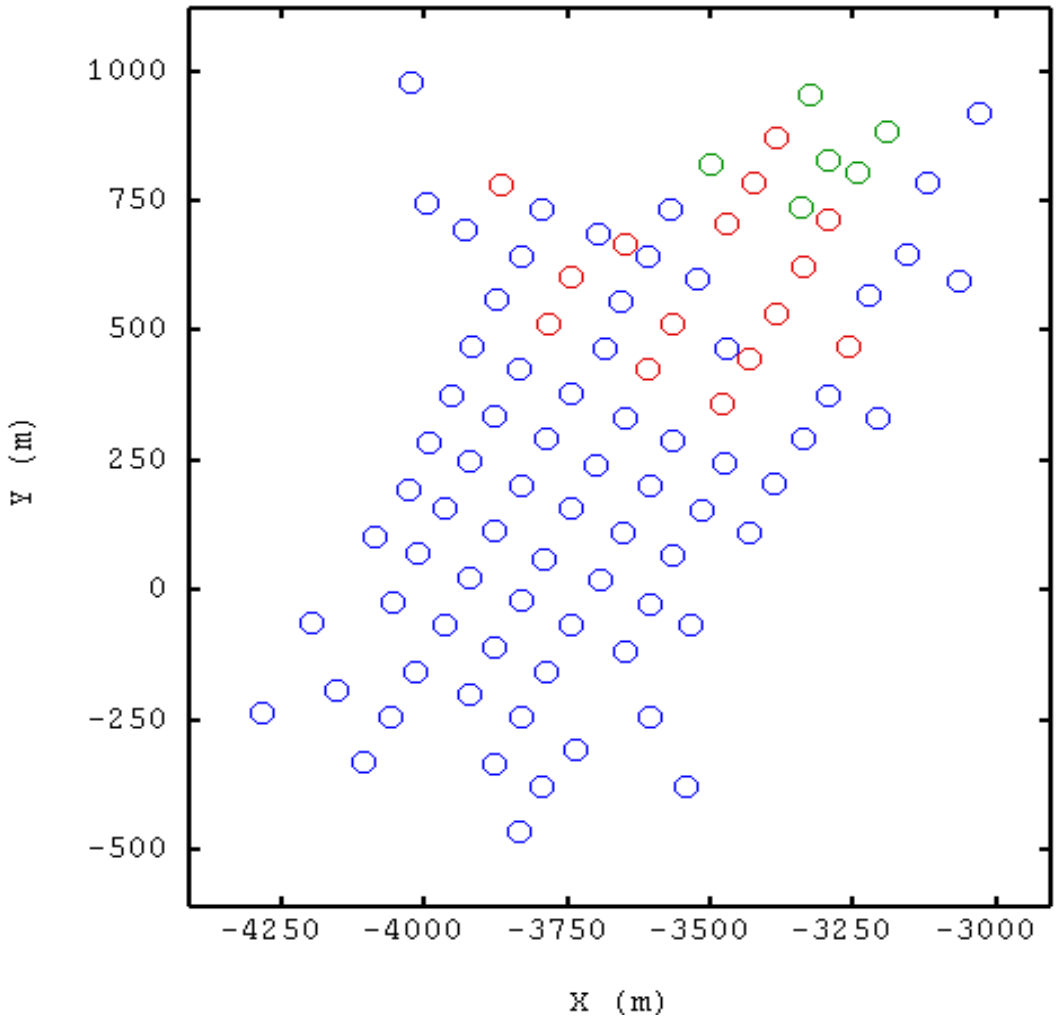


Figure3.1 Spatial distribution of 93 boreholes (red: 15 boreholes drilled by GSI during 1964-68, green: 6 old boreholes drilled by NMDC in 1976, blue: 72 new boreholes drilled by NMDC during 1991-93).

In the present study, although the data on Fe, $Sio_2$, $Al_2O_3$ and LOI variables are available, Fe, $Sio_2$ and $Al_2O_3$ are chosen for grade estimation in different litho units using linear estimation method; on the other hand, the primary variable Fe is chosen for global estimation using linear and for recoverable resource estimation using non-linear methods.

In this study, the iron ore is associated with eight different lithologies such as steel grey hematite (SGH), blue grey hematite (BGH), laminated hematite (LH), lateritic/limonitic ore (LO), blue dust (BD), banded hematite quartzite (BHQ), shale (Sh) and transition zone (TZ). The statistical parameters of Fe, $Sio_2$, and $Al_2O_3$ in different litho units are given in Table 3.3 and histograms showing grade distributions of these three variables are presented in Figures 3.4 to 3.6.

## 3.3 Domaining

One of the most important aspects of geostatistics is to ensure that any data set is correctly classified into a set of homogenous "domains". The key to the validity of any resource model is appropriate definition of domains (Glacken and Snowden, 2001; Bertoli et al., 2003; Sarkar, 2005). The variables estimated within these domains display a level of statistical homogeneity compatible with an assumption of stationarity (Journel and Huijbregts, 1978; Rossi and Deutsch, 2014). A domain is either a 2D (area) or 3D (volume) region within which all data is related. In other words, within a domain, the characteristics of the mineralization are more similar than outside the domain. Mixing data from more than one domain or not classifying data into correct domains can often be the source of estimation errors (Bristol, 2009). It is important to recognize separate "regions" or "domains" within a deposit. It is also important to group sampled data from each domain into distinct subsets (For ex., litho types).

The geological data will have a number of domains, and in many cases, the geological units are the same as the mineralogical domains, such as in iron ore deposits. Further, the grade modeling is constrained entirely by the geological modeling, and the resource grade model will be true reflection of the geology (Glacken and Snowden, 2001). The domain boundaries are defined by either geology or a grade boundary, which involves the cut-off grade. Domains may be defined by a combination of statistical and geostatistical means, in addition to a cut-off grade. When grade alone is used to define the domain boundaries, it would be risky to use a cut-off grade too close to the overall economic cut-off of the deposit. In such a case, the result is often the overestimation of grades within the domain, and the underestimation of grades outside the domain. Some deposits show a rapid change from ore to non-ore, so selecting a natural cut-off is relatively safe. These boundaries may be termed hard, and greatly facilitate resource estimation.

The other extreme is the gradual or soft boundary, requiring much more careful treatment when estimating resources (Glacken and Snowden, 2001).

Deposits which are structurally complex display a combination of hard and soft boundaries. Soft domain boundaries allow grades from either side of the boundary to be used in estimating both domains, to varying degrees. Hard domain boundaries do not permit interpolation of grades across domains. Soft domains are often used in estimation, data within a high-grade domain is not used to estimate within an adjacent low-grade domain, but estimation of the high-grade domain will use data from within low-grade domain (Glacken and Snowden, 2001). Stegman (1999) discusses the effects of domaining on resource estimation in the Cobar region of New South Wales.

In this study, the iron ore is associated with eight different lithologies such as steel grey hematite (SGH), blue grey hematite (BGH), laminated hematite (LH), lateritic/limonitic ore (LO), blue dust (BD), banded hematite quartzite (BHQ), shale (Sh) and transition zone (TZ). The ore body is made of several types of *ore* and *waste* minerals. Separating the ore from the waste is a prerequisite for geostatistical modelling of the deposit. Based on geology, litho types, and chemical analysis of samples, the data are divided into two domains - *ore* and *waste*. The domain of *ore* consists of borehole data pertaining to litho units - SGH, BGH, LH, LO, BD and TZ; where as the domain *waste* contains data pertaining to litho units - BHQ and Sh. The statistical parameters of assay data in different domains are presented in Table 3.4 and 3.5, and Figures 3.7 and 3.8.

## 3.4 Regularization

In geostatistics, regularization is a process of compositing assay data, which is an essential step in 3D data. The geostatistical estimations which involve linear combinations of data will be biased unless all samples have the same length. Usually in drilling data, samples have different lengths, and thus the grades along boreholes are regularized in order to work with composite samples on a regular support (Deraisme, 1996). This support is usually a multiple of the size of the smallest sample, and is related to the height of the benches (Catherine Bleines, 2011). In general, various methods of compositing are used such as *bench compositing*, *constant length compositing*, and ore zone compositing i.e. *compositing by domain*.

In the present study, the *bench compositing* and *compositing by domain* are employed. Since the exploratory data are classified into two domains 'ore' and 'waste', regularization was done using *compositing by domain* method for each domain separately for estimation of grade by linear geostatistical method. As global estimates using linear methods and recoverable resources using non-linear geostatistical methods are applied for the whole data set, regularization is also done using *bench compositing*.

In *bench compositing*, composite intervals are chosen at the crest and toe of the mining benches. Several authors (David, 1977; Clark, 1983b; Isaaks and Srivastava, 1989; Catherine Bleines, 2011b) have emphasized that the composited length must be equal to the bench height. In bench compositing, the input data is fully diluted to the bench height, which is taken as basis for mining, it provides constant elevation data that are simple to plot and interpret on plan maps.

When the deposit has 2 or more domains, sometimes the use of bench compositing may distort the grade distributions by adding low grade to the ore population and high grade to the waste population, results in underestimation of ore grade or overestimation of waste grades. In our study, the deposit has two domains, and therefore *compositing by domain* gives better results in resource estimation. In the present study, a composite length of 12 mts is considered. The *compositing by domain* gives composited data in each domain.

In both the methods, assay data are combined by computing a weighted average over longer intervals to provide a smaller number of data with greater length, while compositing the data. Mathematically, compositing is usually a length-weighted average, computed using the equation (Asghari et al., 2009):

$$G_c = \frac{\sum L_p G_p}{\sum L_p} \quad Where \ \sum L_p = \text{Composite length} \qquad 3.1$$

where $G_c$ is an equivalent grade obtained from making composites; $L_p$ is the analyzed core length of primary sample and $G_p$ is the grade of primary sample.

In the deposit under study, 4537 samples extracted from 93 vertical boreholes are not of equal length (Figure 3.9), thus it was required to make equal composites for the variables Fe, $SiO_2$ and $Al_2O_3$ using equation 3.1. The results on *compositing by domain* are presented in Tables

3.6and 3.7 and in Figures 3.10 and 3.11, whereas the results on *bench compositing* are presented in Table 3.8 and Figure 3.12.

## 3.5 Data Analysis in 2D

Before a detailed geostatistical analysis, the deposit is modelled in 2D for assessing grade domains in a rapid way. All 4537 samples recovered from 93 boreholes are converted to 2-D for analysing the variation of Fe within the boreholes. For each borehole, the weighted mean of Fe grade 'wFe' and its coefficient of variation (CV) are calculated. Basic statistics of these two variables are presented in Table 3.9.

***Scatter Diagrams***

Scatter diagrams are useful to understand the relationship between two grade variables. In spatial variables, there is every possibility of having a good correlation between two variables and the study of this correlation is very essential prior to modelling a deposit. In this study, scatter diagrams are generated between (i) Fe and $SiO_2$, (ii) Fe and $Al_2O_3$, and (iii) $SiO_2$ and $Al_2O_3$ for raw data and bench composited data. The results are presented in Figures 3.14 (raw data) and 3.15 (composited data).

## 3.6 Results and Discussion

The results of basic statistics and inferential statistics of three data sets - exploratory data, domaining data and regularized data are presented in this section:

### 3.6.1 Basic Statistics

It is inferred from Table 3.1 that the 93 bore holes are spread in about 1250 mts in 'x' direction, 1450 mts in 'y' direction and 265 m in 'z' direction. The depths of boreholes vary from 13.75 m to 169.25 m, with an average depth is 97.52 m.

Table 3.1 Range of collar data (n=93 boreholes)

| Variable | Minimum | Maximum |
|---|---|---|
| Easting | -4287.33 | -3030.19 |
| Northing | -465.84 | 975.10 |
| RL | 946.78 | 1212.38 |
| Depth | 13.75 | 169.25 |

The basic statistics of exploratory borehole data (Table 3.2) reveal that the overall Fe content is very high in the iron ore deposit with an average grade of 64.62 %. It is also observed from Table 3.2 that the grade attributes are highly contrasting between a very low minimum and high maximum, especially for the variables Fe, $SiO_2$ and $Al_2O_3$. Therefore, basic statistics of the assay data are studied for each lithological type as suggested by Chatterjee et al., (2006) and Noble (2011).

Table 3.2 Basic Statistics of Assay Data (n=4537 samples)

| Variable | Samples | Min. % | Max. % | Mean % | Std.Dev | CV % |
|---|---|---|---|---|---|---|
| Fe | 4482 | 2.00 | 70.30 | 64.62 | 7.66 | 11.85 |
| SiO2 | 4480 | 0.02 | 65.50 | 3.12 | 7.39 | 236.85 |
| $Al_2O_3$ | 4478 | 0.01 | 41.53 | 1.77 | 3.31 | 187.00 |
| LOI | 4475 | 0.01 | 22.01 | 2.35 | 2.80 | 119.15 |
| P | 421 | 0.001 | 0.72 | 0.04 | 0.06 | 150.00 |

It is observed from table 3.3 that Fe grade variability is very high in the litho types BHQ and Shale as compared to other litho types viz., SGH, BGH, LH, LO and BD. This is because the litho units BHQ and Shale exhibit low Fe values due to presence of high impurities like silica and alumina, whereas other litho types consist of moderate to high Fe (45 to 70 %) values and low silica and alumina values. Keogh and Moulton (1998) have also reported similar observations in the Hamersley Iron ore deposits of the Pilbara region in Western Australia.

Based on geology, grade and litho types, the data is divided into two domains - *ore* and *waste*. The domain of *ore* consists of borehole data pertaining to litho units - SGH, BGH, LH, LO, BD and TZ; where as the domain *waste* contains data pertaining to litho units - BHQ and Sh. The basic statistics of exploratory data in the domains i.e., ore and waste (Table 3.4 and 3.5) indicate that majority (91 %) of the samples in the iron ore deposit represents the domain *ore* and

has Fe grade > 45 % with an average of 66.55 %, whereas only 9 % of the samples represents the domain *waste*. Surprisingly the average Fe in domain waste is 46.12 %, which indicates that there are some samples in the litho units BHQ and Shale that possess high Fe % though these are considered as waste. In case of Fe variable, coefficient of variation (CV %) has come down to 4.85 % in the domain *ore* and increased to 25.9 % in the domain *waste* as compared to 11.85 % in total raw data. This indicates that the separation of *ore* and *waste* in the raw data is necessary before modelling the deposit.

Table3.3. Litho - wise basic statistics of exploration data (n=4482 samples)

| Litho type | Samples | Variable | Minimum | Maximum | Mean | Std. Dev |
|---|---|---|---|---|---|---|
| SGH | 585 | Fe | 62.10 | 70.00 | 68.19 | 1.49 |
| | | $SiO_2$ | 0.04 | 7.4 | 0.45 | 0.60 |
| | | $Al_2O_3$ | 0.01 | 5.4 | 0.57 | 0.66 |
| BGH | 1158 | Fe | 59.70 | 70.30 | 68.20 | 1.28 |
| | | $SiO_2$ | 0.03 | 9.02 | 0.57 | 0.80 |
| | | $Al_2O_3$ | 0.01 | 5.57 | 0.65 | 0.65 |
| LH | 1077 | Fe | 59.00 | 69.60 | 65.84 | 2.03 |
| | | $SiO_2$ | 0.04 | 8.90 | 1.15 | 1.27 |
| | | $Al_2O_3$ | 0.01 | 6.63 | 1.55 | 1.20 |
| LO | 334 | Fe | 45.18 | 67.80 | 58.55 | 2.80 |
| | | SiO2 | 0.04 | 12.62 | 2.74 | 2.58 |
| | | $Al_2O_3$ | 0.24 | 17.08 | 5.67 | 2.42 |
| BD | 833 | Fe | 56.20 | 70.00 | 67.69 | 1.61 |
| | | $SiO_2$ | 0.02 | 7.00 | 1.31 | 1.47 |
| | | $Al_2O_3$ | 0.01 | 7.26 | 0.55 | 0.65 |
| BHQ | 215 | Fe | 23.00 | 61.00 | 51.40 | 8.27 |
| | | SiO2 | 10.92 | 65.50 | 24.93 | 11.71 |
| | | $Al_2O_3$ | 0.01 | 3.25 | 0.50 | 0.49 |
| Shale | 209 | Fe | 2.00 | 57.30 | 40.69 | 12.71 |
| | | $SiO_2$ | 0.42 | 55.32 | 17.91 | 13.57 |
| | | $Al_2O_3$ | 0.15 | 41.53 | 12.76 | 6.86 |
| TZ | 71 | Fe | 55.40 | 64.40 | 61.27 | 1.90 |
| | | $SiO_2$ | 7.06 | 15.26 | 9.85 | 1.99 |
| | | $Al_2O_3$ | 0.01 | 7.43 | 1.02 | 1.62 |

(SGH: steel grey hematite; BGH: blue grey hematite; LH: laminated hematite;
LO: lateritic/limonitic ore; BD: blue dust; BHQ: banded hematite quartzite; TZ: transition zone).

Table 3.4 Basic Statistics of domain *ore* of assay data (n=4059 samples)

| Variable | Samples | Min. % | Max. % | Mean % | Std.Dev | CV % |
|---|---|---|---|---|---|---|
| Fe | 4058 | 45.18 | 70.30 | 66.55 | 3.23 | 4.85 |
| $SiO_2$ | 4056 | 0.02 | 15.26 | 1.20 | 1.85 | 154.17 |
| $Al_2O_3$ | 4054 | 0.00 | 17.08 | 1.28 | 1.75 | 136.72 |

Table 3.5 Basic statistics of domain *waste* of assay data (n=475 samples)

| Variable | Samples | Min. % | Max. % | Mean % | Std. Dev | CV % |
|---|---|---|---|---|---|---|
| Fe | 424 | 2.00 | 61.00 | 46.12 | 11.96 | 25.93 |
| $SiO_2$ | 424 | 0.42 | 65.50 | 21.47 | 13.14 | 61.20 |
| $Al_2O_3$ | 424 | 0.01 | 41.53 | 6.54 | 7.80 | 119.27 |

Both these data sets (*ore* and *waste* domains) are regularised separately using '*compositing by domain'* method. After regularization of each domain, it is observed from basic statistics of composited data of domain *ore* (Table 3.6), that the minimum value of Fe in domain *ore* increased from 45.18 % to 55.14 % and not much change in mean Fe % (66.55 % to 66.61 %) whereas in domain *waste* (Table 3.7) mean Fe % slightly decreased from 46.12 % to 44.48 %. This is due to dilution effect in regularization of data to 12 mts. No major change is observed in $SiO_2$ and $Al_2O_3$ average grades after compositing in both the domains. It is also observed that after compositing by domain, CV values of composited data in both the domains (Tables 3.6 and 3.7) are in accordance with CV values of raw data (Tables 3.4 and 3.5).

Table 3.6 Basic statistics of regularized data in domain *ore* (n=715)

| Variable | Samples | Min. % | Max. % | Mean % | Std. Dev | CV % |
|---|---|---|---|---|---|---|
| Fe | 715 | 55.14 | 70.00 | 66.61 | 2.70 | 4.05 |
| $SiO_2$ | 715 | 0.070 | 12.99 | 1.35 | 1.92 | 142.22 |
| $Al_2O_3$ | 715 | 0.001 | 8.39 | 1.21 | 1.39 | 114.87 |

Table 3.7 Basic statistics of regularized data in domain *waste* (n=124)

| Variable | Samples | Min. % | Max. % | Mean % | Std. Dev | CV % |
|---|---|---|---|---|---|---|
| Fe | 124 | 10.85 | 60.80 | 44.88 | 11.69 | 26.04 |
| $SiO_2$ | 124 | 0.98 | 62.70 | 22.52 | 12.34 | 54.79 |
| $Al_2O_3$ | 124 | 0.02 | 32.69 | 6.86 | 7.26 | 105.83 |

For the purpose of global estimation using linear method and for recoverable resource estimation using non-linear methods, total raw data is composited by 'bench compositing' method. After compositing the total data using 12 mts bench height, it is observed that the average Fe grade is 64.84 % (Table 3.8) which is in line with original raw data having a mean Fe of 64.62 % (Table 3.2). It is also observed that there is no much variation in both $SiO_2$ and $Al_2O_3$ after regularization. In Fe, CV is decreased from 11.85 % to 10.11 after compositing.

Table 3.8 Basic statistics of bench composited data (n=725)

| Variable | Samples | Min. % | Max. % | Mean % | Std.Dev | CV % |
|---|---|---|---|---|---|---|
| Fe | 725 | 11.04 | 70.00 | 64.84 | 6.56 | 10.11 |
| SiO2 | 725 | 0.08 | 46.42 | 3.13 | 6.43 | 205.43 |
| $Al_2O_3$ | 725 | 0.001 | 33.16 | 1.67 | 2.81 | 168.26 |

After converting 3D data to 2D data, it is observed from the basic statistics (Table 3.9) that the overall Fe content is very high in the deposit which ranges from a minimum of 40.78 % to a maximum of 69.66 %, and with an average of 63.71 % Fe.

Table 3.9 Basic statistics of Fe and its CV of the Borehole data in 2D

| Variable | Samples | Minimum | Maximum | Mean | CV |
|---|---|---|---|---|---|
| wFe | 93 | 40.78 | 69.66 | 63.71 | 9.2 |
| CV | 93 | 0.22 | 45.70 | 9.92 | 89.3 |

### 3.6.2 Inferential Statistics

Inferential statistics is an approach for data analysis that employs a variety of graphical techniques to maximize insight into a data set, detect outliers to understand distribution pattern of data and to find correlation between two variables. The graphical techniques employed are plotting the raw data such as base map, histograms and scatter diagrams (correlations). The histogram of depth variation in 93 boreholes (Figure 3.2) shows that the depth variation in boreholes is not consistent varying from 13.75 m to 169.25 m and with an average depth of 97.5 m. It also exhibits that about 45 % of boreholes have depth < 100 mts, 50 % have depth 100 – 150 mts and 5 % have depth > 150 mts.

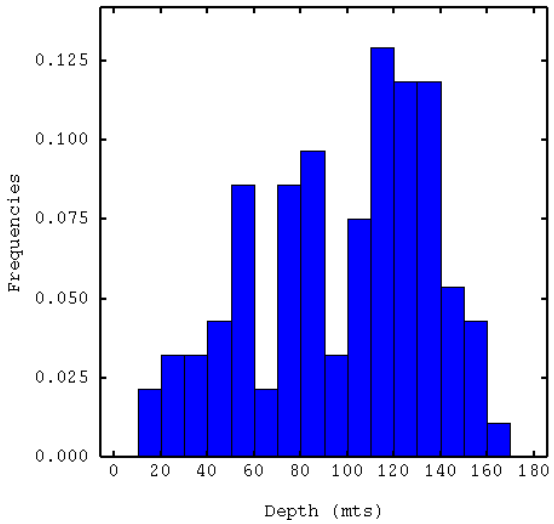


Figure 3.2 Histogram showing the depth variation in 93 boreholes.

Grade distributions of Fe, $SiO_2$ and $Al_2O_3$ in the raw data are studied using histograms. This study enables to understand the skewness and presence of outliers in the original data. Histogram of Fe (Figure 3.3 A) shows that the distribution is asymmetric and skewed to the left. It is observed that nearly 86 % of the samples have Fe ranging between 60 and 70 %. Only 5 % samples of the total assay data, whose Fe < 40 % are considered as outliers. It is observed from the histograms of $SiO_2$ (Figure 3.3 B) and $Al_2O_3$ (Figure 3.3 C) that these distributions are also asymmetric but skewed to the right. Nearly 92 % of the samples show $SiO_2$ values ranging from 0 and 10 % and 97 % of the samples show $Al_2O_3$ ranging from 0 and 10 %.

The grade distributions are further analysed in each lithological type, and histograms are plotted for Fe, $SiO_2$ and $Al_2O_3$ in different lithological units (Figures 3.4 to 3.6). Figure 3.5 suggest that the litho units - steel grey hematite, blue grey hematite, laminated hematite, lateritic/limonitic ore and blue dust - posses very high grade Fe, varying between 55-70 %, whereas the litho units - banded hematite quartzite and shale - exhibit low grade Fe values and very few high grade Fe values.

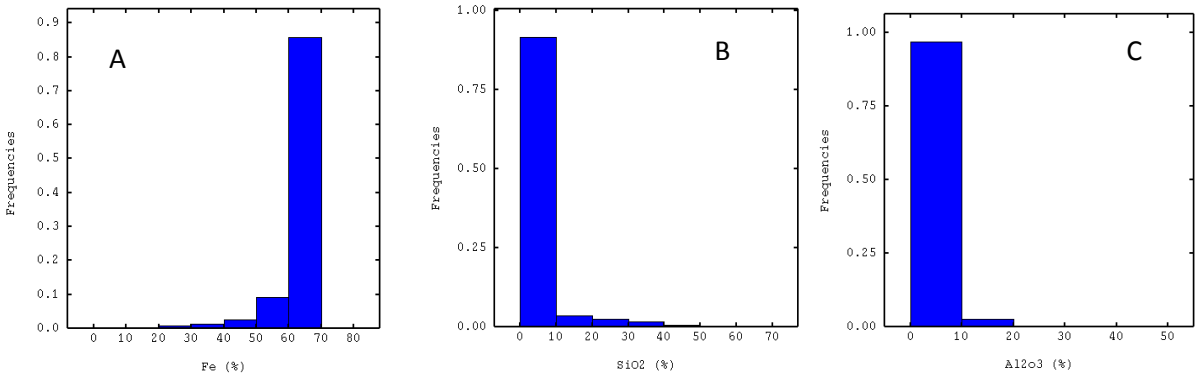


Figure 3.3 Grade distributions of (A) Fe, (B) $SiO_2$ and (C) $Al_2O_3$ in raw data. The uni-modal asymmetric distribution is observed in all the three. Histogram of Fe is skewed to left, whereas histograms of $SiO_2$ and $Al_2O_3$ are skewed to right.

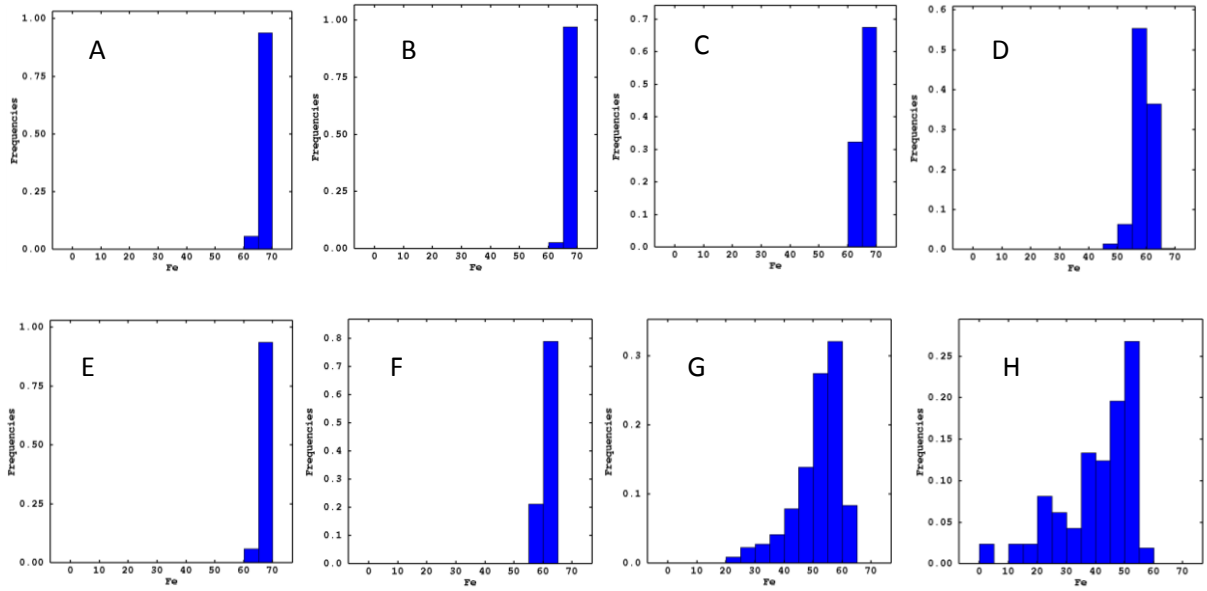


Figure 3.4 Histograms showing grade distribution of Fe % in the borehole samples of different litho units. (A) SGH, (B) BGH, (C) LH, (D) LO, (E) BD, (F) TZ, (G) BHQ and (H) Shale. Fe grade variability is very high in the litho types BHQ and Shale as compared to other litho types viz., SGH, BGH, LH, LO and BD. This is because the litho units BHQ and Shale exhibit low Fe values due to presence of high impurities like silica and alumina.

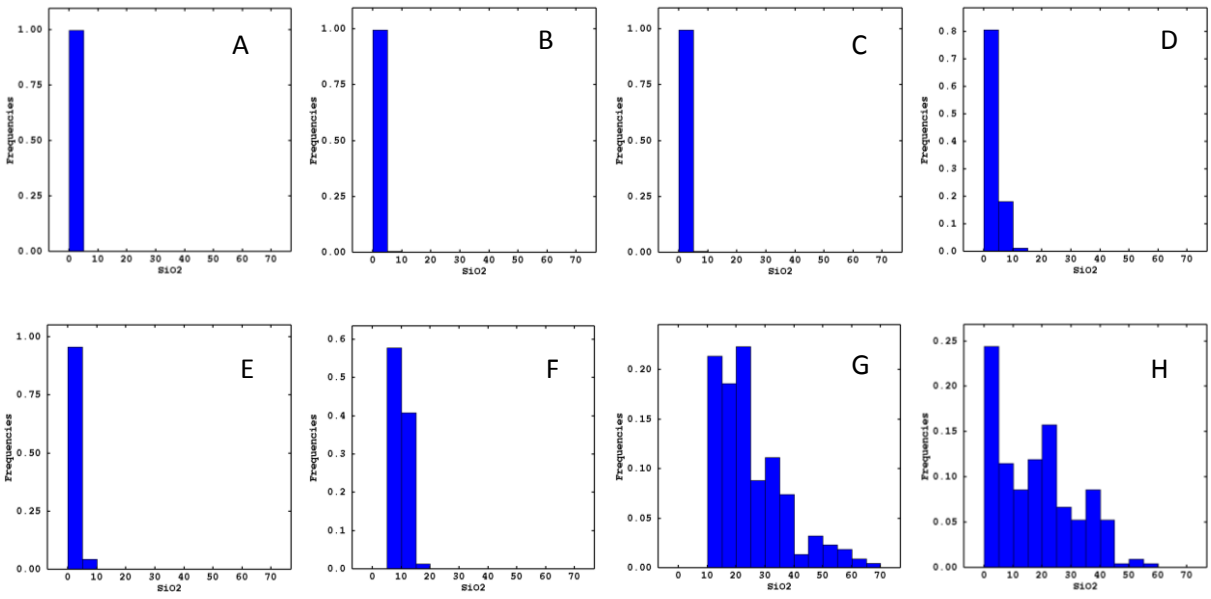


Figure 3.5 Histograms showing grade distribution of $SiO_2$ % in the borehole samples of different litho units. (A) SGH, (B) BGH, (C) LH, (D) LO, (E) BD, (F) TZ, (G) BHQ and (H) Shale.

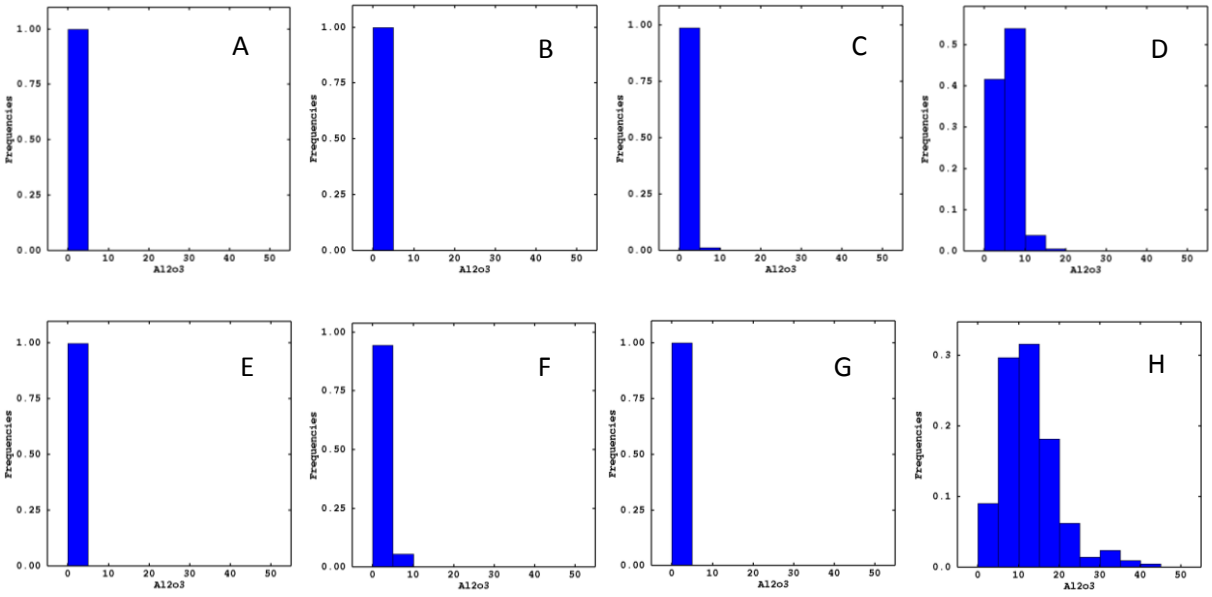


Figure 3.6 Histograms showing grade distribution of $Al_2O_3$ % in the borehole samples of different litho units. (A) SGH, (B) BGH, (C) LH, (D) LO, (E) BD, (F) TZ, (G) BHQ and (H) Shale.

In the domain *ore*, histogram of Fe (Figure 3.7 A) exhibit that majority (78 %) of samples posses grade > 65 %, 16 % posses grade between 60-65% and 6% of samples posses < 60 % and average grade is 66.55 %. Histograms of both $SiO_2$ and $Al_2O_3$ (Figures 3.7 B and C) exhibit that about 95 % of samples posses grade < 5 % and both have an average grade of about 1.2 %.

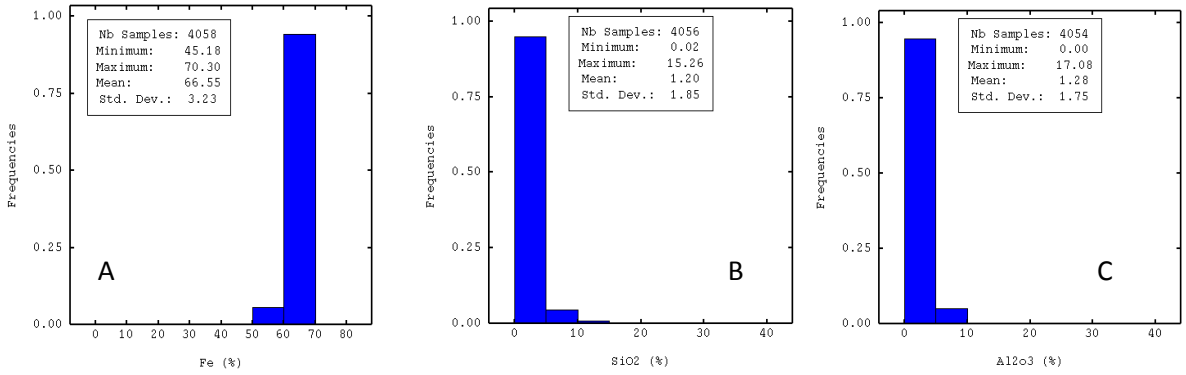


Figure 3.7 Histograms of the raw data in the domain ore (A) Fe, (B) $SiO_2$ and (C) $Al_2O_3$. High Fe, and low $SiO_2$ and $Al_2O_3$ values are recorded in the domain ore.

In the domain waste, histogram of Fe exhibit (Figure 3.8 A) that about 35 % of samples posses grade < 45 % , about 44 % of samples posses grade between 45 -55 % and surprisingly 21% of samples posses > 55 % and average grade is 46.12 %. Histogram of $SiO_2$ (Figure 3.8 B) exhibit 12 % of samples posses grade < 5 % with an average grade of 21.47 % and histogram of $Al_2O_3$ (Figure 3.8 C) exhibit that about 55 % of samples posses grade < 5 % with an average grade of 6.54 %. Low grade Fe values and high grade $SiO_2$ and $Al_2O_3$ are noted in the domain waste due to presence of high impurities such as silica and alumina.

The variation in length of samples extracted from 93 boreholes is computed using assay data of boreholes. Histogram of sample length (Figure 3.9) shows that the samples extracted from boreholes are not of equal length varying from 0.03 m to 57.34 m and with an average of 2 m. 30.35 % samples exhibit 0-2 mts sample length, and 66.92 % of samples exhibit highest abundance of 2-4 mts length.

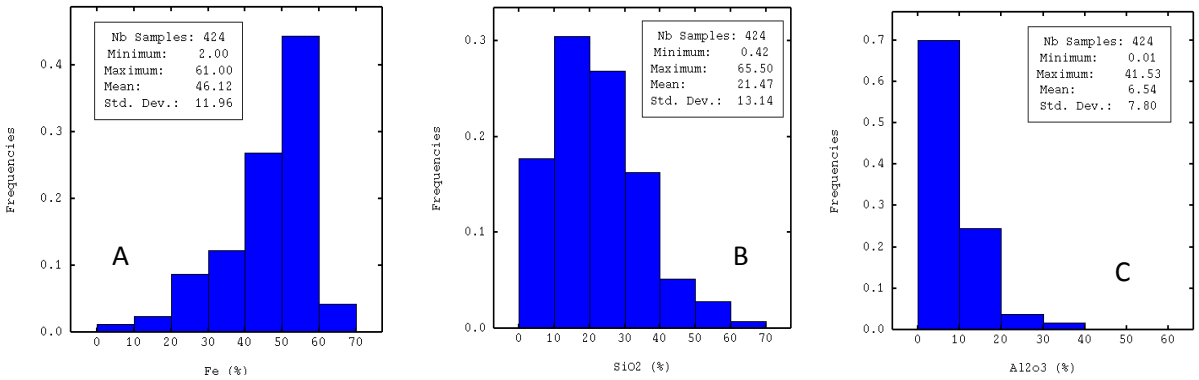


Figure 3.8 Histograms of the raw data in the domain waste (A) Fe, (B) $SiO_2$ and (C) $Al_2O_3$. Low grade Fe values and high grade $SiO_2$ and $Al_2O_3$ are noted in the domain waste due to presence of high impurities such as silica and alumina.

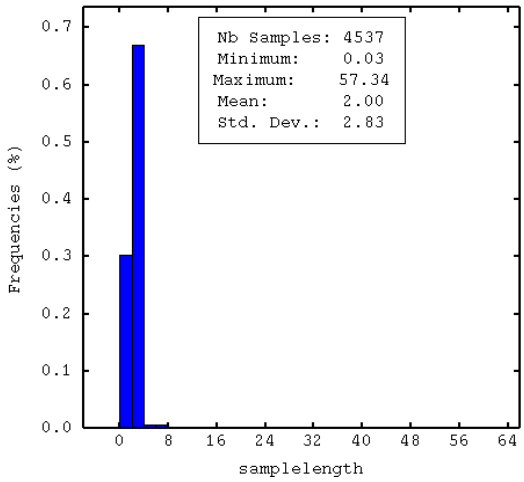


Figure 3.9 Histogram showing the sample length variation in boreholes. 30.35 % samples exhibit 0-2 mts sample length, and 66.92 % of samples exhibit highest abundance of 2-4 mts length.

Histograms of the composited data in both the domains - *ore* and *waste* (Figures 3.10 and 3.11) show that the grade distributions of Fe, $SiO_2$ and $Al_2O_3$ are similar to the grade distributions of Fe, $SiO_2$ and $Al_2O_3$ of raw data (Figures 3.7 and 3.8) in the respective domains. This indicates that the composited data is in accordance with raw data in both the domains.

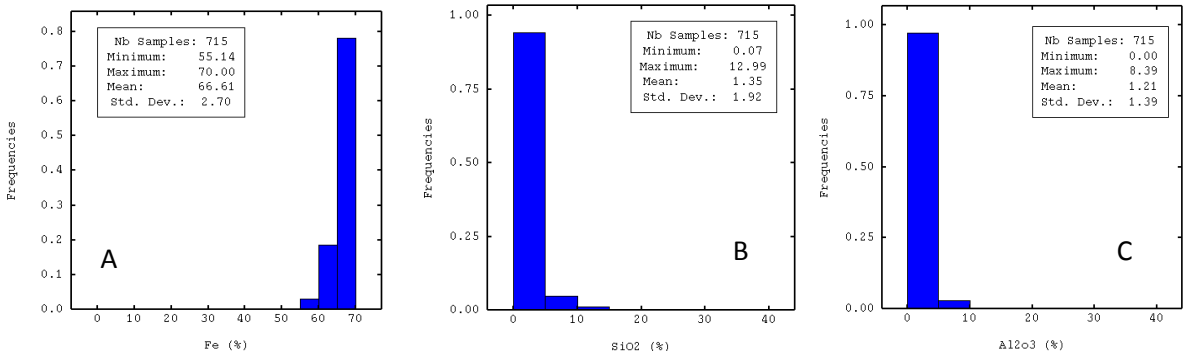


Figure 3.10 Grade distributions of the composited data in the domain ore (A) Fe, (B) $SiO_2$ and (C) $Al_2O_3$.

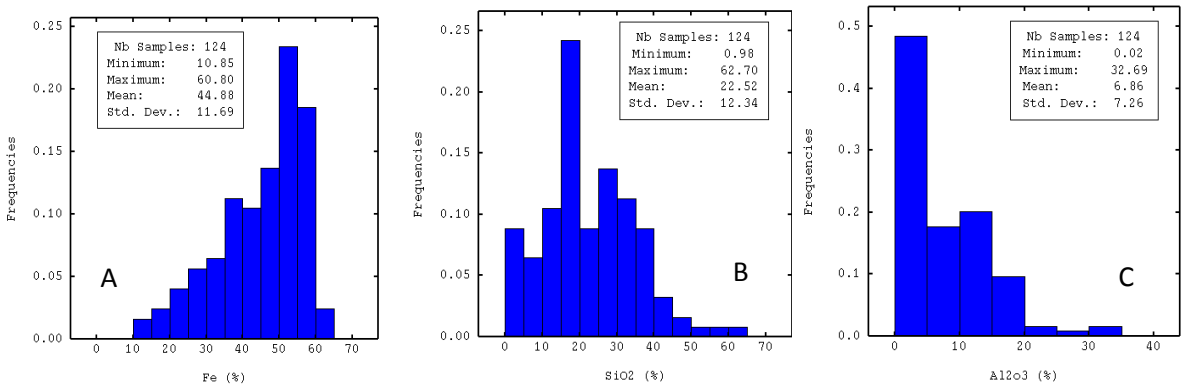


Figure 3.11 Histograms of the composited data in the domain waste (A) Fe, (B) $SiO_2$ and (C) $Al_2O_3$.

Grade distributions of bench composited data (Figure 3.12) shows that nearly 86 % of the samples have Fe ranging between 60 and 70 % (which is also same in raw data), 11 % of samples have Fe ranging between 45 and 60 % and only 3 % of samples have Fe < 45 %. The average grade is 64.84 % which is in line with original raw data having a mean of 64.62 %. It is also observed that there is no significant variation in both $SiO_2$ and $Al_2O_3$ distributions after regularization.

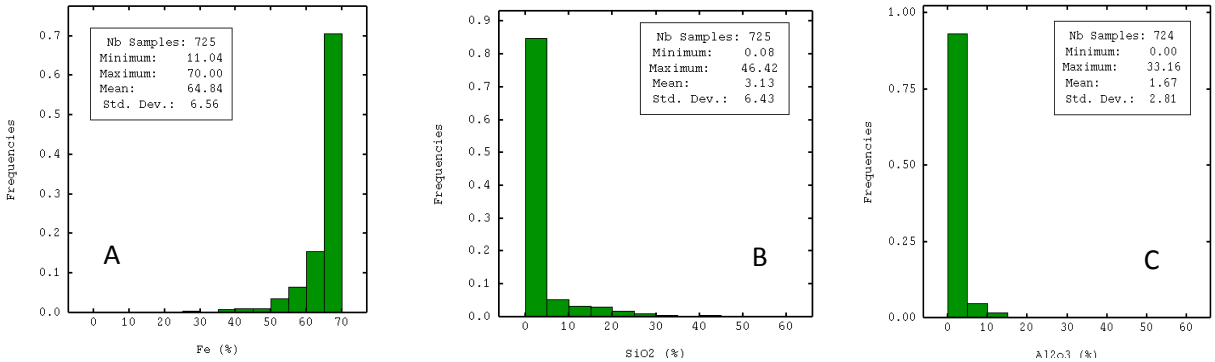


Figure 3.12 Histogram showing grade distributions of bench composited data (A) Fe, (B) $SiO_2$ and (C) $Al_2O_3$. These histograms show that in the overall deposit, composites of Fe are high with low silica and alumina.

The histogram of 2D data for the weighted mean of Fe grade (Figure 3.13) shows that majority (85 %) of the boreholes have Fe grade >60 % and very few boreholes (4 %) have Fe grade <50 %

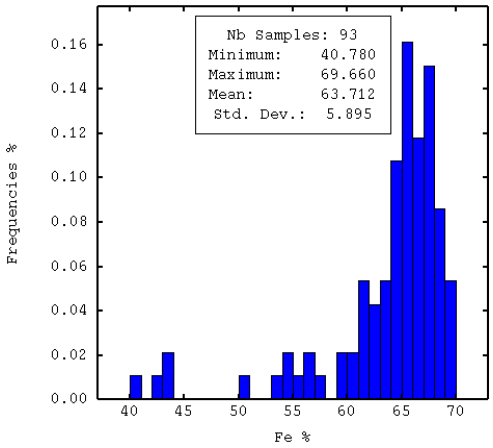


Figure 3.13 Histogram showing grade distribution of Fe % in the borehole samples of 2D data. It is observed that majority (85 %) of the boreholes exhibit Fe grade >60 %; 10% of boreholes exhibit 50 - 60 %, and the remaining boreholes exhibit <50 % Fe grade.

### *Scatter Diagrams*

Scatter diagrams are generated between Fe and $SiO_2$, Fe and $Al_2O_3$ and $SiO_2$ and $Al_2O_3$ for raw data (Figure 3.14) and bench composited data (Figure 3.15) to understand the relationship between two grade variables. The scatter diagrams for both the data sets (Figure 3.14 A and 3.15 A) show a very good negative correlation (-0.8) between Fe and $SiO_2$ and a good negative correlation (-0.7) between Fe and $Al_2O_3$. However the scatter plots between $SiO_2$ and $Al_2O_3$ (Figure 3.14 C and 3.15 C) show that there is no significant correlation between these two variables in both raw data and composited data.

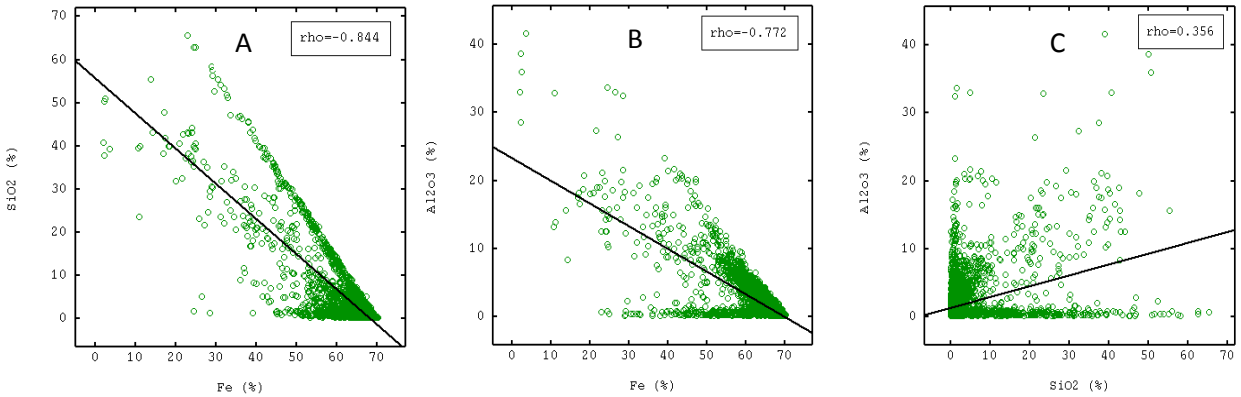


Figure 3.14 Scatter diagrams plotted for different variables of raw data. (A) Fe vs $SiO_2$, (B) Fe vs $Al_2O_3$ and (C) $SiO_2$ vs $Al_2O_3$. Fe has good correlation with both the variables $SiO_2$ and $Al_2O_3$. But there is no correlation between $SiO_2$ and$Al_2O_3$

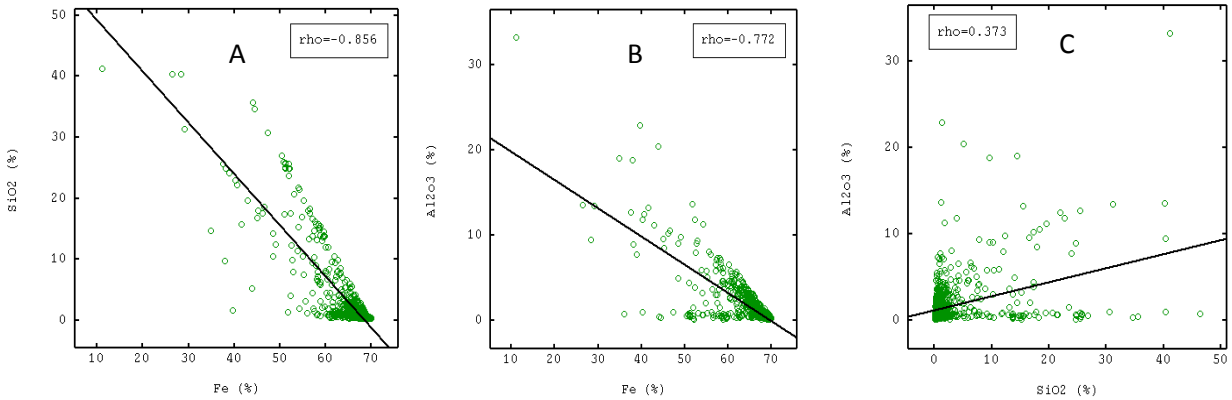


Figure 3.15 Scatter diagrams plotted for different variables of bench composited data. A) Fe vs $SiO_2$, B) Fe vs $Al_2O_3$ and C) $SiO_2$ vs $Al_2O_3$. After compositing the correlation coefficients between Fe, $SiO_2$ and $Al_2O_3$ remained almost same as of raw data.

## 3.7 Summary

In the present study, the exploratory data used for geostatistical modelling comprise of 4537 samples recovered from 93 vertical boreholes are subjected to statistical analysis. The boreholes are spaced in a more or less grid pattern with an average spacing of 100 m between each borehole and have an average depth of 97.5 m. From the extents of the boreholes, it is inferred that the 93 bore holes spread about 1250 mts in x direction, 1450 mts in y direction and 265 m in z direction. Chemical analyses of Fe, $SiO_2$, $Al_2O_3$ and LOI for 4482 samples with the information on the lithology are obtained. The iron ore is associated with eight different lithologies such as steel grey hematite (SGH), blue grey hematite (BGH), laminated hematite (LH), lateritic/limonitic ore (LO), blue dust (BD), banded hematite quartzite (BHQ), shale (Sh) and transition zone (TZ). The data are divided into two domains - *ore* and *waste* - based on geology, litho types and chemical analysis. The domain *ore* consists of 4058 samples pertaining to litho units - SGH, BGH, LH, LO, BD and TZ; whereas the domain *waste* contains 424 samples pertaining to litho units - BHQ and Sh. In the deposit, as the samples extracted from 93 boreholes are not of equal length, thus regularization is done using two different methods *compositing by domain* and *bench compositing*. *Compositing by domain* is done in each domain separately for estimation of Fe, $SiO_2$, and $Al_2O_3$ grades by linear geostatistical method and bench compositing is done for estimation of Fe grade by non-linear geostatistical methods.

The basic statistics of exploratory borehole data reveal that the overall Fe content is very high in the iron ore deposit with an average grade of 64.62 %. The basic statistics of exploratory data in both the domains ore and waste indicate that majority (91 %) of the data in the iron ore deposit has Fe grade > 45 % represents the domain ore with an average Fe 66.55 % and only 9 % of the data represents the domain waste. After regularization of each domain, it is observed that the minimum value of Fe in domain ore increased from 45.18 % to 55.14 % and not much change in mean Fe % (66.55 % to 66.61 %) whereas in domain waste mean Fe % is decreased from 46.12 % to 44.48 %. This may be due to dilution effect in regularization of data to 12 mts bench height. No significant variations are observed in $SiO_2$ and $Al_2O_3$ average grades after compositing the data in both the domains. After compositing the total data using bench compositing, it is observed that the average Fe grade is 64.84 % which is in line with original raw data, which has a mean Fe

64.62 %. It is also observed that there is no much change in $SiO_2$ and $Al_2O_3$ values after regularization.

Scatter diagrams are generated between Fe vs $SiO_2$, Fe vs $Al_2O_3$ and $SiO_2$ vs $Al_2O_3$, for raw data and bench composited data for understanding the relationships between two grade variables. In both the data sets, correlation results showed that Fe has good negative correlation with both the variables $SiO_2$ (-0.85) and $Al_2O_3$ (-0.77) and there is no significant correlation (0.3) between $SiO_2$ and$Al_2O_3$.

# CHAPTER 4

# GEOSTATISTICAL ANALYSIS

# CHAPTER 4

# Geostatistical Analysis

## 4.1 Introduction

Geostatistics is an important subject for modelling the spatial variability of any spatial data. The basis of geostatistics is the study of the spatial correlation of data measured at various points in three-dimensional space. Examples of spatial data include particularly in mineral exploration such as ore grade, thickness, lithology. The geostatistical evaluation of ore deposit avoids economic failures (Matheron, 1963). Matheron, formalized the geostatistical theory in the early 1960s. His primary aim was to understand and solve problems of the mining industry. Matheron (1965) states that the geostatistical theory is based on concept of the theory of regionalized variables. Since then, basic introductions to geostatistical theory and applications were discussed by many researchers (Ex., Huijbregts, 1975; David, 1977; Journel and Huijbregts, 1978; Clark, 1979a, 1979b and 1979c; Kitandis, 1997; Delfiner, 1979; Rendu, 1980a; Journel, 1983a and 1989; Isaaks and Srivastava, 1989; Wacknernagel, 1995; Armstrong, 1998; Sarma, 2002 and 2009; Haldar, 2013; Rossi and Deutsch, 2014).

In this study, geostatistical analysis has been carried out in three stages - modelling, estimation and simulation. The spatial modelling is essential for estimation and simulation. The different methods of geostatistical estimation (linear and non-linear) and simulations used in this study are presented in chapters 5, 6 and 7. In this chapter, the prerequisites such as variogram modelling, cross-validation of model, neighborhood analysis and block modelling required for geostatistical estimation are discussed.

Of all the geostatistical tools, the semi-variogram is an essential tool, which measures spatial the distribution of a regionalized variable in the form of a geo-mathematical function representing degree of continuity of mineralization (Matheron, 1963; Clark, 1976a). Semi-variogram helps in estimation or simulation of the deposit with probable grade concentrations. Various researchers have applied this tool and successfully modelled the spatial variability of the grade of elements associated with mineral deposits viz., gold (Guibal, 1987; Schofield, 1989a),

copper (Emery, 2005a, b), limestone (Chatterjee et al., 2006), iron ore (Clark, 1983a, Sarkar and Roy, 2005; Marzeihe et al., 2013) etc.

The conventional way of assessing the suitability of a particular ore grade modeling technique is to collect ground-truth data from various locations to be mined. The estimated grade of a model is then compared with the true grade. However, it is rare to have anything other than exploratory borehole data at the initial stage of mine planning. If no grade-related information about mined material was made available to test the model performance, in such cases, geostatistics provide a unique tool of 'cross-validation' to measure model performance (David, 1977). Several authors (Clark, 1986; Isaaks and Srivastava, 1989; Goovaerts, 1997; Deutsch & Journel, 1998) have appreciated this unique tool in geostatistics and emphasized the importance of this method.

The neighbourhood chosen in the estimation of ore grade has a significant impact on the outcome of the kriging estimate and kriging, 'minimum variance estimator', is true only when the neighbourhood is adequately chosen (De-vitry, 2003). The choice of neighborhood parameters was extensively discussed by various researchers (Rivoirard, 1987; Murthy, 1989a; Vann et al., 2003; Marzeihe et al., 2013).

The block model is created into a three-dimensional representation of the volume of the deposit to be estimated and also to delineate the different lithological units in the block model. The Block model consists of interpolated values rather than true measurements and it provides a method of estimating volume, tonnage, and average grade of a 3-D body from a sparse drill hole data. The advantages of a block modelling is that it provides the framework for a good local estimation, lends itself readily to reserve estimation, and allows the modelling of mining selectivity (Murthy,1989a).

In the mineral resource estimation, it is important to classify the mineral deposit into different lithological units. Inaccurate categorization of litho types in a block model will have negative impact on resources estimation as bulk density of various lithological units varies. However, the classification cannot be properly done on a point-by-point or block-by-block basis as it ignores the geological continuity (Henstridge, 1998). Thus, the modelling of lithological domains is a critical step in mineral reserve evaluation (Emery and Gonzalez, 2007). In any

deposit, the lithological information was available only at the exploratory borehole locations and using this information; spatial interpolation of lithological units can be done to get information on litho types of each block. It is necessary to assign a litho type for each block before grade estimation.

In general, a conventional classification method was used to delineate different lithological units using geological cross sections derived from borehole logs. In this study, a novel approach based on geostatistical non-linear indicator kriging is employed to delineate different lithological units of an iron ore deposit. The geological cross-sectional method mostly rely on interpretation of the available drill hole data and do not account for the uncertainty in the spatial extent of the lithological units (Emery and Gonzalez, 2007). An alternative model to the geological cross sectional model approach has been suggested by Chatterjee et al. (2006) in which lithological type is assigned to blocks using a non-linear geostatistical indicator kriging method. In this approach, a probabilistic model based on indicator kriging is used to map the probabilities of occurrences of the litho units within the deposit, which reflects the spatial extent of the lithological units at unsampled locations. Application of indicator kriging (IK) in the modelling of geological data which includes lithology and geochemical drilling data for a gold deposit was discussed by Gossage (1998). Author has compared IK results with original geological model and discussed the relative merits of IK model.

This concept of probabilistic modelling of lithological domains and its application to resource evaluation of copper deposit using conditional simulation was discussed by Emery and Gonzalez (2007). Geostatistical modelling of rock type domains with spatially varying proportions employing plurigaussian simulation and its application to a porphyry copper deposit was discussed by Emery et al., (2008). Pasti et al. (2012) have used multi point geostatistics approach using simulation for modelling lithological domains for an iron ore deposit. Authors state that the delineation of litho units is conventionally based on vertical and horizontal sections interpreted by a mine geologist, and in more advanced cases, geostatistical methods such as indicator kriging and/or simulations are used which allow to automate the modelling process. These methods are probabilistic and employ variogram models to represent the geological continuity of each litho unit.

In the present study, for the purpose of categorizing litho units in the block model, two approaches - *geological cross sectional* method and a novel approach non-linear geostatistical *indicator kriging* method - are adopted. This chapter presents the methodology and results on variogram modelling, cross validation and block modelling.

## 4.2 Semi-variogram analysis

In nature, the grade of a particular sample in three dimensional space is expected to be affected by its position and its relationship with its neighbours, i.e., mineralization is not totally random. Semi-variogram is an essential tool and fundamental tool in geostatistical analysis that takes spatial dependency into account to measure spatial continuity (or correlation) of grade data (Matheron, 1963, Gholamnejad et al., 2010).

As a precursor to either kriging and/or conditional simulation methods, spatial analysis of the domained data i.e., the calculation of experimental semi-variogram and its modelling is a necessary step (Clark, 1979a; Glacken and Snowden, 2001), as it defines the 'range of influence' of the data in terms of the direction and magnitude of ranges. Geostatistical techniques for spatial analysis are discussed by Vann and Sans (1995), Coombes (1997), and Longley-Sinitsyna and Snowden (1997).

### 4.2.1 Experimental semi-variograms

The first step in geostatistical estimation is the construction of an experimental semi-variogram, which is calculated from a sample set (Matheron, 1963; Singh, 1982; Mendis and Lorandi, 2006). The semi-variogram is a graph (Figure 4.1) of the average variability between samples $\gamma(h)$ vs the distance between samples h, which is computed by averaging the squared differences of grades between pairs of samples that are a given distance apart (Matheron, 1963), which can be expressed as:

$$\gamma(h) = \frac{1}{2N(\mathrm{h})} \sum_{i=1}^{N(h)} \left[ Z(x_i) - Z(x_i + h) \right]^2 \qquad (4.1)$$

where N(h) is the number of pairs at distance h, and h is the distance between two samples; $Z(x_i)$ is the value of regionalized variable at location $x_i$ and $Z(x_i + h)$ is the value of the regionalized variable at 'h' distance away from $x_i$. Experimental semi-variograms reflect the continuity – or

lack of continuity – of mineral values within the deposit or the area under study (Clark, 1983b). It is expected that the samples geographically close to each other are more alike to each other than those at greater distances (Huijbregts 1975). Thus, it is expected that semi-variogram represented by $\gamma(h)$, a function of increment h, increases with distance h.

According to Bachmaier and Backes (2011), there is a confusing situation in geostatistical literature: Some authors (Wackernagel, 2003; Worboys, 1995; Gneiting et al., 2001) write varigoram, and some authors (Matheron, 1963; Journel and Huijbregts, 1978; Cressie, 1991) write semi-variogram and some others use the terms variogram and semi-variogram synonymously (Isaaks and Srivastava, 1989; Webster and Oliver, 2007). In the present study, the term semi-variogram is used as most of the researchers use this term.

While constructing variograms, it is important to consider that, samples must belong to one domain (or zone) in order to represent the spatial variability of the data. These domains can be defined by studying the geology of the ore body, including its structural, mineralogical, and chemical properties (Gouda and Moharam, 2001). A database is created for a specific domain which has the same geological features and similar assay values. Checking and detecting anisotropy is another important process as it has larger or shorter spatial correlation (range) in some directions, and can be useful in selecting neighboring data to improve the performance of kriged estimates. However, as no significant anisotropy was found in the deposit in XY direction, omnidirectional experimental semi-variograms are computed in XY direction with anisotropy modelled in the Z-direction (vertical direction). Thus horizontal and vertical semi-variograms are constructed for each domain separately in this study as suggested by Gouda et al. (1995).

### 4.2.2 Semi-variogram modelling

The experimental semi-variogram calculated using equation (4.1) gives spatial variability of grade for discrete distances. It requires to be modelled to measure the variability of the grade for continuous distances. Thus, after calculation of the experimental semi-variogram, it is necessary to fit a mathematical model to represent the variability as realistically as possible. The modelling procedure is iterative and the choice of suitable model is very important. A fit of the

theoretical semi-variogram to the experimental semi-variogram with features close to the ideal one is shown in Figure 4.1.

*Range* (a) indicates the distance between locations beyond which observations appear independent, i.e. variance no longer increases. This distance is called 'Range of influence'. The grades of samples separated by distances greater than the range of influence are uncorrelated.

*Sill* ($C+C_0$) is the value on ordinate where variogram stabilizes which corresponds to range.

*Nugget* ($C_0$) describes the vertical jump from the value of zero at the origin to the variogram value at extremely small distances due to short scale variability.

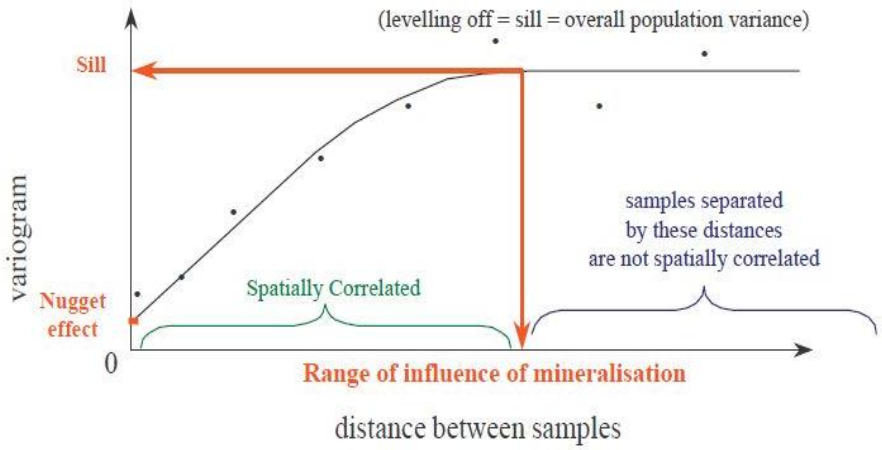


Figure 4.1 Theoretical semi-variogram fitted to an experimental semi-variogram (Snowden, 2001). Dotted points representing experimental semi-variogram and thick line showing fitted semi-variogram model.

In order to ensure that the variance of any linear combination of a stationary regionalized variable is always non-negative, only certain functions can be used as variogram models and these must be positive definite functions (Cressie and Hawkins, 1980; Armstrong and Jabin, 1981; Armstrong, 1984 and 1998). Some of the standard theoretical models are exponential, spherical and Gaussian models as shown in Figure 4.2.

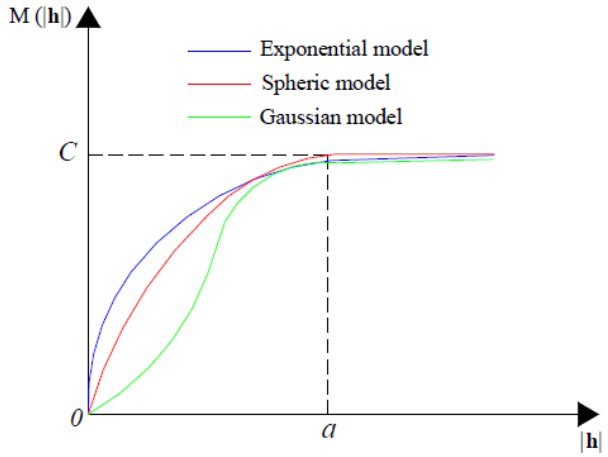


Figure 4.2 Theoretical semi-variogram models (Mendis and Lorandi, 2006). Both exponential and spherical models are linear near origin whereas Gaussian model is parabolic.

The mathematical expressions of these models are:

*Exponential Model* is expressed as

$$\gamma(h) = C_0 + C_1\left[1 - e^{(-\frac{h}{a})}\right] \quad for\, h \neq 0 \tag{4.2}$$

*Spherical Model* is expressed as

$$\gamma(h) = C\left[\frac{3}{2}.\frac{|h|}{a} - \frac{1}{2}.\frac{|h|^3}{a^3}\right] + C_0 \quad if \quad h < a$$
$$= C + C_0 \qquad\qquad if \quad h \geq a \tag{4.3}$$

*Gaussian Model* is expressed as

$$\gamma(h) = C_0 + C\left[1 - e^{(-\frac{h^2}{a^2})}\right] \quad for\, h \neq 0 \tag{4.4}$$

In some situations, the experimental semi-variogram does not seem to follow any of the standard structures. It is possible to combine structures to obtain a variogram with the characteristics of more than one of the standard structures. A linear combination of valid variogram structures is also a valid variogram model and is called a 'nested variogram structure' (Gholamnejad et al., 2010). In this study, experimental semi-variograms of variables viz., wFe and CV of 2D data and of variables Fe, $SiO_2$, and $Al_2O_3$ of 3D data for different domains in horizontal and vertical directions are modelled using a combination of 2 structures and a nugget effect.

***2-D Modelling***

Before a detailed geostatistical analysis, the 3-D data is converted to 2-D for assessing grade domains in a rapid way. Due to importance of iron, geostatistical modelling was carried out for Fe variable. Thus, sampled data recovered from 93 boreholes were converted to 2-D for analysing the variation of Fe within the boreholes. For each borehole, the weighted mean of Fe grade 'wFe'and its coefficient of variation 'CV' within the borehole are calculated. Spatial modelling has been done for both 'wFe' and 'CV' using 2 - nested structures of spherical model. The modelling parameters are presented in Table 4.1 and fitted model is shown in Figure 4.3.

Table 4.1 Semi-variogram modelling parameters of wFe and CV for 2D data

| | wFe | | CV | |
|---|---|---|---|---|
| Structure | Range (m) | Sill $(\%)^2$ | Range (m) | Sill $(\%)^2$ |
| 1 | 450 | 10 | 400 | 19 |
| 2 | 700 | 24 | 700 | 58 |

It is observed from Figure 4.3 that the semi-variograms steadily increase in terms of the variability and get stabilized at 700 m (the range of influence), and beyond 700 m distance the semi-variogram models get tend flat which suggests that no sample-to-sample correlation exists beyond 700 m distance in the deposit (Table 4.1 & Figure 4.3).

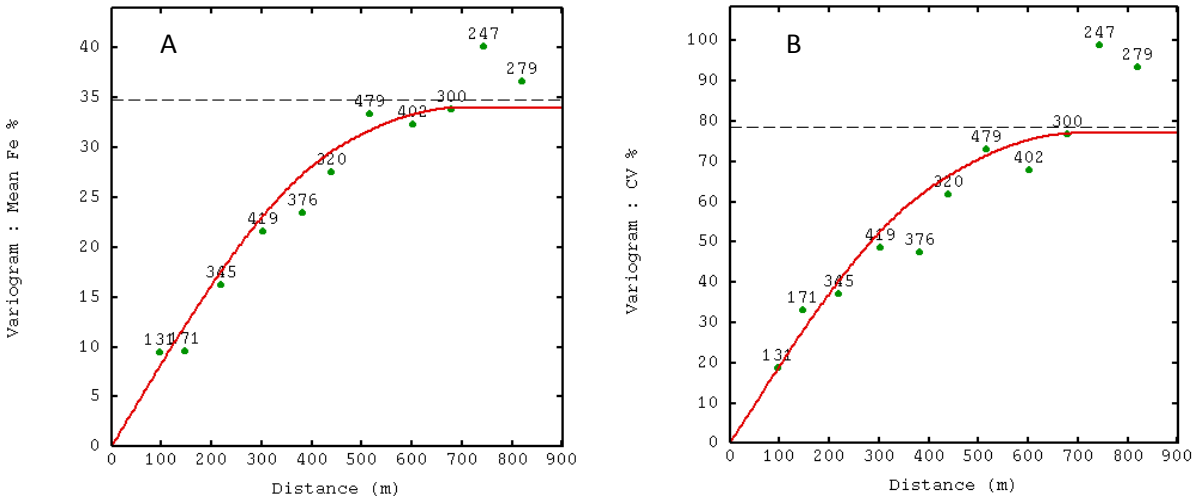


Figure 4.3 Semi-variogram models of (A) Fe % and, (B) Coefficient of Variation (CV). Both the variograms show a very good spatial structure with nested models. No nugget effect is observed in both the models (Kameshwara Rao et al., 2014)

The fitted spherical functions, derived from equation 4.3, are presented below:

$$\text{For Fe: } \gamma(h) = 10\left(1.5\frac{h}{450} - 0.5\frac{h3}{4503}\right) + 24\left(1.5\frac{h}{700} - 0.5\frac{h3}{7003}\right) \text{ if } h < 450 \text{ m} \qquad (4.5)$$

$$\gamma(h) = 10 + 24\left(1.5\frac{h}{700} - 0.5\frac{h3}{7003}\right) \text{ if } 450 < h < 700$$

$$\gamma(h) = 10 + 24 \text{ if } h \geq 750 \text{ m}$$

$$\text{For CV: } \gamma(h) = 19\left(1.5\frac{h}{400} - 0.5\frac{h3}{4003}\right) + 58\left(1.5\frac{h}{700} - 0.5\frac{h3}{7003}\right) \text{ if } h < 400 \text{ m} \qquad (4.6)$$

$$\gamma(h) = 19 + 58\left(1.5\frac{h}{700} - 0.5\frac{h3}{7003}\right) \text{ if } 400 < h < 700$$

$$\gamma(h) = 19 + 58 \text{ if } h \geq 700 \text{ m}$$

### *3-D Modelling*

Spatial analysis was performed on 3D data set for the variables Fe, $SiO_2$ and $Al_2O_3$ variables in both the domains - *ore* and *waste*. In order to examine the composites for any anisotropy and directions of continuity, semi-variogram map was generated for principle variable Fe. The semi-variogram maps for both these domains show no anisotropy in the XY plane of Fe and no direction of maximum continuity, whereas in vertical direction the variability is different from XY. On this basis, omni directional experimental semi-variograms for both the domains were calculated in the XY plane (horizontal direction) with anisotropy modelled in the Z direction (vertical direction). According to Clark (1976b), most mineral deposits particularly those of low concentration minerals such as nickel, copper, uranium, etc., follow the spherical model. However, in this study, in addition to the nugget effect, the semi-variograms of Fe, $SiO_2$ and $Al_2O_3$ are modelled using one exponential and one spherical model. The modelling parameters of these three variables for both the domains are represented in Table 4.2 to 4.4. The fitted variogram models are shown in Figures 4.4 - 4.9.

It is observed from the semi-variogram models of Fe (Figure 4.4) in domain *ore* that both the horizontal and vertical directions show a very good spatial structure with a small nugget effect. Anisotropy is observed in both the directions with ranges 400 m and 90 m respectively (Table 4.2). On the other hand, the horizontal and vertical semi-variograms of domain *waste* are less structured (Figure 4.5), which may be due to low grade Fe values and presence of impurities like silica and alumina.

Table 4.2 Domain-wise semi-variogram modelling parameters of Fe % in horizontal and vertical directions.

| Domain | Direction | Model-1 | Model-2 | Range-1 | Range-2 | Sill-1 | Sill-2 | NE |
|---|---|---|---|---|---|---|---|---|
| ore | Horizontal | Exponential | Spherical | 90 | 400 | 5.4 | 2.3 | 0.5 |
| | Vertical | Spherical | Spherical | 50 | 90 | 2.1 | 3.6 | 1.5 |
| waste | Horizontal | Exponential | Spherical | 100 | 325 | 40 | 36 | 9 |
| | Vertical | Spherical | Spherical | 35 | 60 | 24 | 46 | 9 |

(Domain **‘**ore’**:** SGH, BGH, LH, LO and BD; Domain ‘waste’: BHQ and Shale)

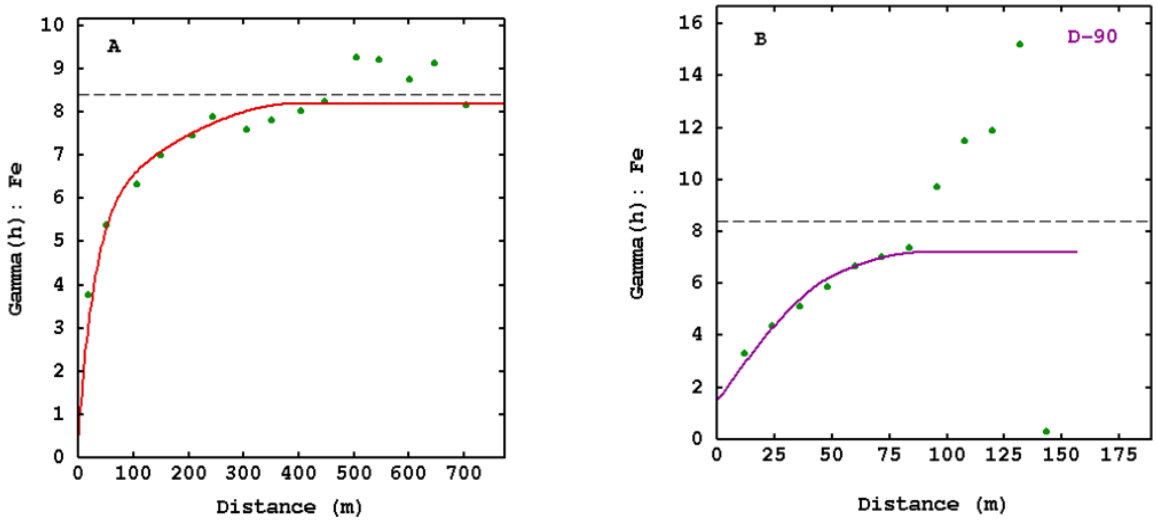


Figure 4.4 Omni-directional semi-variogram models of Fe % for domain 'ore' in horizontal direction (A), and in vertical direction (B). Both the semi-variograms show a very good spatial structure with nested models. Small nugget effect is observed in both the models.

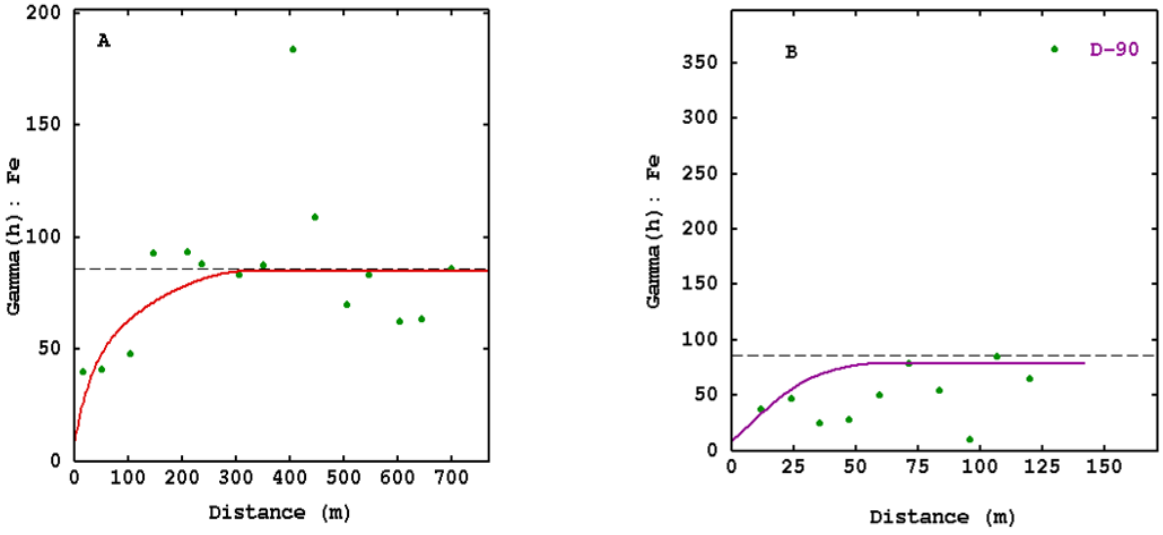


Figure 4.5 Omni-directional semi-variogram models of Fe % for domain 'waste' in horizontal direction (A), and in vertical direction (B). Both the semi-variograms show a reasonably good spatial structure with nested models.

It is observed from the semi-variogram models of $SiO_2$ (Figure 4.6) in domain *ore* that both the horizontal and vertical directions show a very good spatial structure with a small nugget effect. Anisotropy is observed in both the directions having ranges 375 m and 90 m respectively (Table 4.3). It is also observed that range is same in the vertical direction in both Fe and $SiO_2$ and not much change in the horizontal direction, which may be due to a very good correlation between these two variables. The horizontal and vertical semi-variogram models of $SiO_2$ in domain *waste* are less structured (Figure 4.7) as observed in Fe.

Table 4.3 Domain-wise semi-variogram modelling parameters of $SiO_2$ % in horizontal and vertical directions

| Domain | Direction | Model-1 | Model-2 | Range-1 | Range-2 | Sill-1 | Sill-2 | NE |
|---|---|---|---|---|---|---|---|---|
| ore | Horizontal | Exponential | Spherical | 100 | 375 | 1.5 | 1.6 | 0.8 |
| | Vertical | Spherical | Spherical | 30 | 90 | 0.8 | 1.5 | 0.6 |
| waste | Horizontal | Exponential | Spherical | 40 | 350 | 9 | 33 | 9 |
| | Vertical | Spherical | Spherical | 30 | 70 | 55 | 35 | 0.5 |

(Domain **'**ore'**:** SGH, BGH, LH, LO and BD; Domain 'waste': BHQ and Shale)

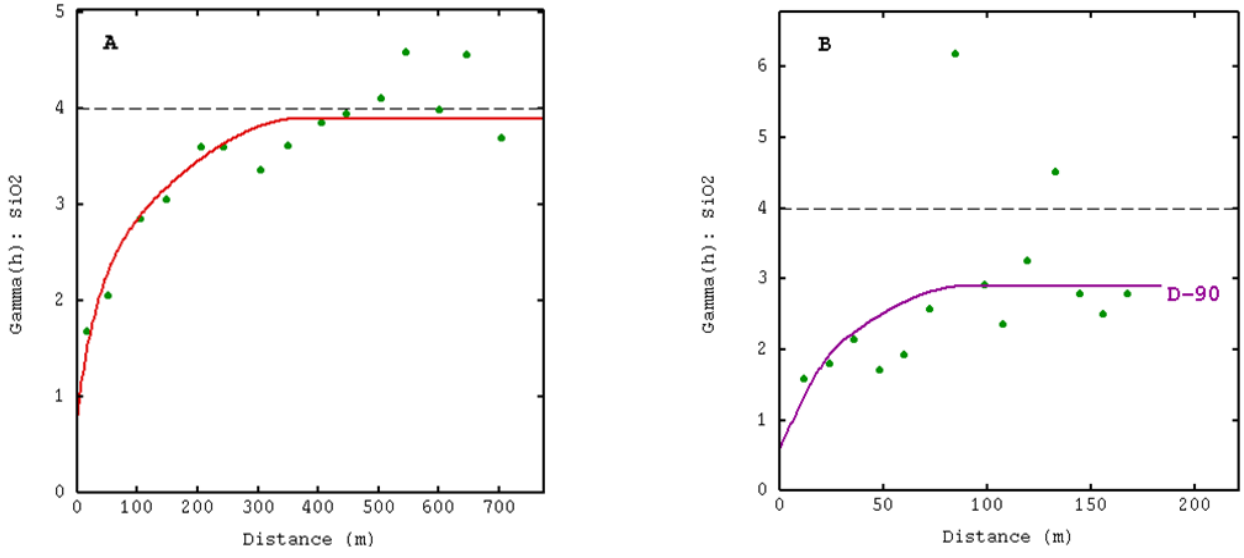


Figure 4.6 Omni-directional semi-variogram models of $SiO_2$ % for domain 'ore' in horizontal direction (A), and in vertical direction (B).

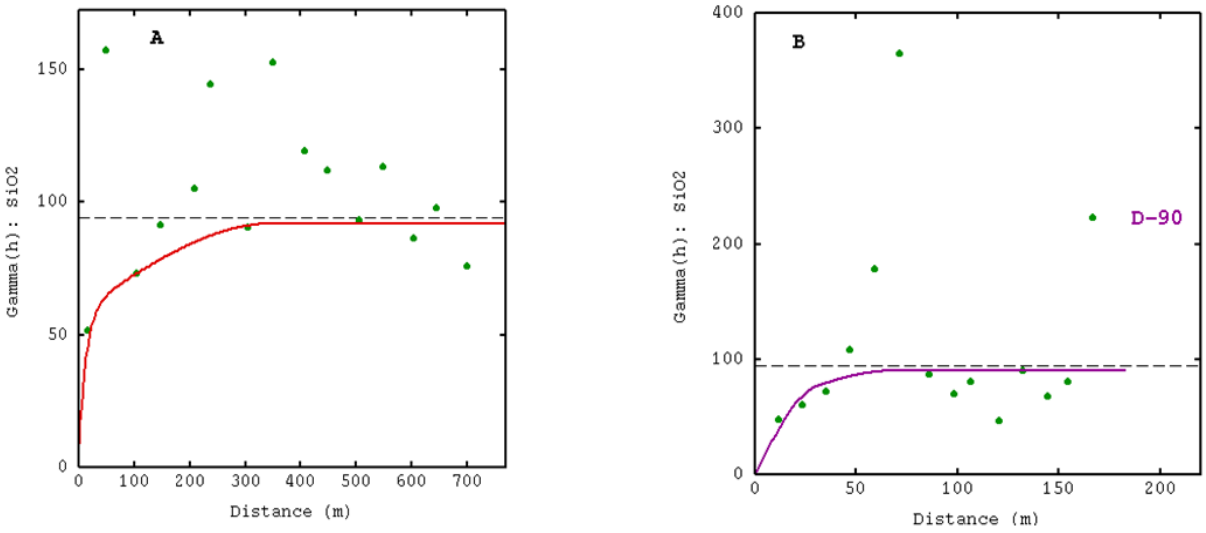


Figure 4.7 Omni-directional semi-variogram models of $SiO_2$ % for domain 'waste' in horizontal direction (A), and in vertical direction (B).

It is observed from the semi-variogram models of $Al_2O_3$ (Figure 4.8) that both the horizontal and vertical directions exhibit good spatial structure with a small nugget effect in domain *ore*. Anisotropy is observed in both the directions having ranges 400 m and 70 m respectively (Table 4.4). It is also observed that range is less in the vertical direction for $Al_2O_3$, and not much change in the horizontal direction, when compared to Fe and $SiO_2$ variables. The horizontal and vertical semi-variograms of domain 'waste' are less structured (Figure 4.9) as in the case of Fe and $SiO_2$.

Table 4.4 Domain-wise semi-variogram modelling parameters of $Al_2O_3$ % in horizontal and vertical directions

| Domain | Direction | Model-1 | Model-2 | Range-1 | Range-2 | Sill-1 | Sill-2 | NE |
|---|---|---|---|---|---|---|---|---|
| ore | Horizontal | Exponential | Spherical | 100 | 400 | 1.1 | 0.53 | 0.2 |
| | Vertical | Spherical | Spherical | 50 | 70 | 0.7 | 0.75 | 0.2 |
| waste | Horizontal | Exponential | Spherical | 130 | 425 | 14 | 28 | 1 |
| | Vertical | Spherical | Spherical | 40 | 90 | 10 | 16 | 1 |

(Domain 'ore': SGH, BGH, LH, LO and BD; Domain 'waste': BHQ and Shale)

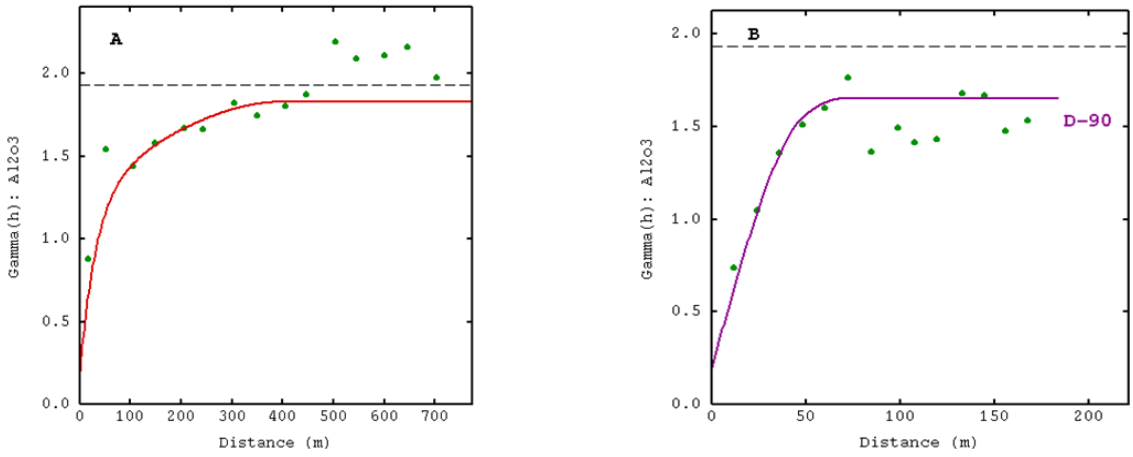


Figure 4.8 Omni-directional semi-variogram models of $Al_2O_3$ % for domain 'ore' in horizontal direction (A), and in vertical direction (B).

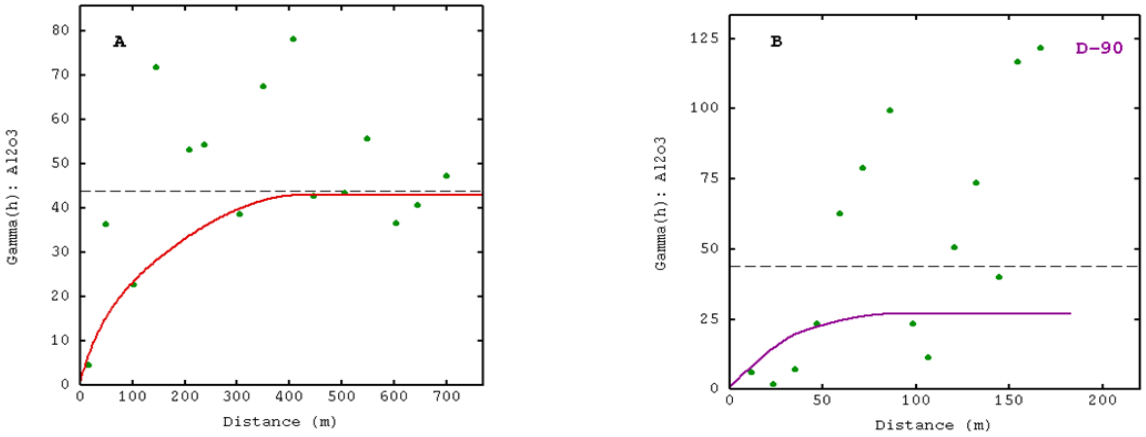


Figure 4.9 Omni-directional semi-variogram models of $Al_2O_3$ % for domain 'waste' in horizontal direction (A), and in vertical direction (B).

## 4.3 Cross validation of semi-variogram models

Fitted variogram models are validated using cross validation, a unique tool in geostatistics. In cross validation, using the fitted variogram model, one of the data $Z_i$ will be eliminated in every step and its value is estimated (a kriged grade $Z_i^*$) based on the data existing in the neighborhood search and then this estimated grade is compared with the known grade. This process is repeated for all the data points available. Then, the difference between the estimated and known values ($Z_i$ - $Z_i^*$) is observed, leading to a correlation coefficient between

the estimated and known points. The variogram model is a good model and is appropriate for the data set used if the following criteria are satisfied (Clark, 1986; David, 1988; Armstrong, 1998):

A. The mean of the actual kriging errors E ($Z_i$ - $Z_i^*$) should be very close to zero and the variance of standard error should be close to 1.
B. The percentage of the kriging errors within two standard deviations of the mean should be about 95%.
C. The histograms of kriging errors ($Z_i$ - $Z_i^*$), and standardized kriging errors ($Z_i$ - $Z_i^*$) /s* should both show a normal distribution, with a mean around zero.
D. The scatter plot of the standardized kriging errors ($Z_i$ - $Z_i^*$) /s* versus the estimated grade z* should show a cloud of points around the zero line running across from the vertical axis.

In the present study, cross validation of semi-variogram models were carried out for the variables - Fe, $SiO_2$ and $Al_2O_3$ in the *ore* domain, as variogram models in the domain *waste* are less structured and not of much importance in mining. The above four conditions are checked and the results of cross validation are presented in Table 4.5 and Figure 4.10 - 4.12. It is observed from the Table 4.5 that the mean of the actual kriging errors E ($Z_i$ - $Z_i^*$) is very close to zero (0.09, -0.04 and -0.05 for Fe, SiO2 and $Al_2O_3$ respectively) and the variance of standard error is close to 1 (1.003 and 0.95 for Fe and SiO2 respectively) and slightly high (1.31) in case of $Al_2O_3$.

Table 4.5 Cross validation results of Fe, $SiO_2$ and $Al_2O_3$ estimates (n=715 samples)

| Variable | Mean of kriging error | Variance of standard error | Robust data* |
|---|---|---|---|
| Fe | 0.09 | 1.003 | 687 |
| SiO2 | -0.04 | 0.95 | 686 |
| Al2O3 | -0.05 | 1.31 | 675 |

**A data is robust when its standardized error lies between -2.5 and 2.5.*

It is observed from Figures 4.10 (A), 4.11 (A) and 4.12 (A) that the scatter diagrams show a good correlation between estimated values and true values. It is further observed from Figures 4.10 (B), 4.11 (B) and 4.12 (B) that the histograms of standardized kriging errors

($Z_i$ - $Z_i^*$) /s* show a normal distribution, with a mean around zero (0.03, -0.02 and -0.03 for Fe, SiO2 and $Al_2O_3$ respectively) for all the three variables. Figures 4.10 (C), 4.11 (C) and 4.12 (C) show that the scatter plot of the standardized kriging errors ($Z_i$ - $Z_i^*$) /s* versus the estimated grade z* exhibit a cloud of points around the zero line running across from the vertical axis. It also shows the robust data i.e., standardized error lies between -2.5 and 2.5 as 687, 686 and 675 (out of 715 samples) for Fe, SiO2 and $Al_2O_3$ respectively. These results suggest that as nearly 96 % of total samples are estimated correctly for Fe, SiO2 and $Al_2O_3$ grades using corresponding semi-variogram model, these models can be used for further estimation purpose.

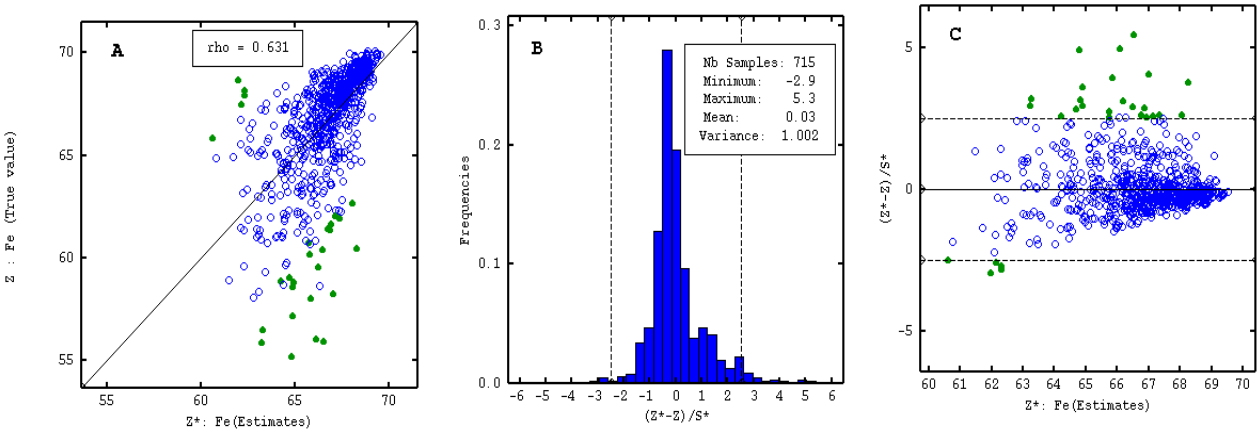


Figure 4.10 Cross validation results of Fe. (A) scatter plot between estimates and true values, (B) histogram of standard errors, and (C) scatter between estimates and standard errors.

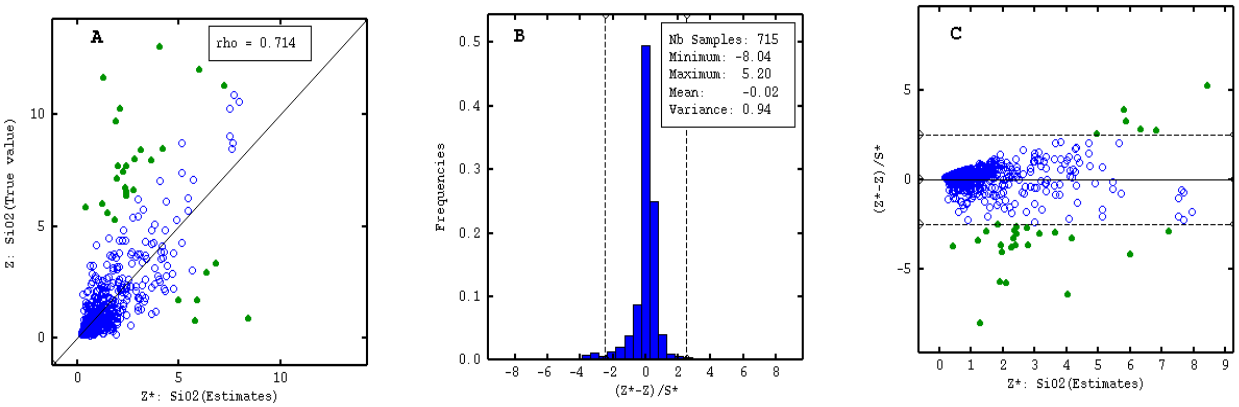


Figure 4.11 Cross validation results of $SiO_2$. (A) scatter plot between estimates and true values, (B) histogram of standard errors, and (C) scatter between estimates and standard errors.

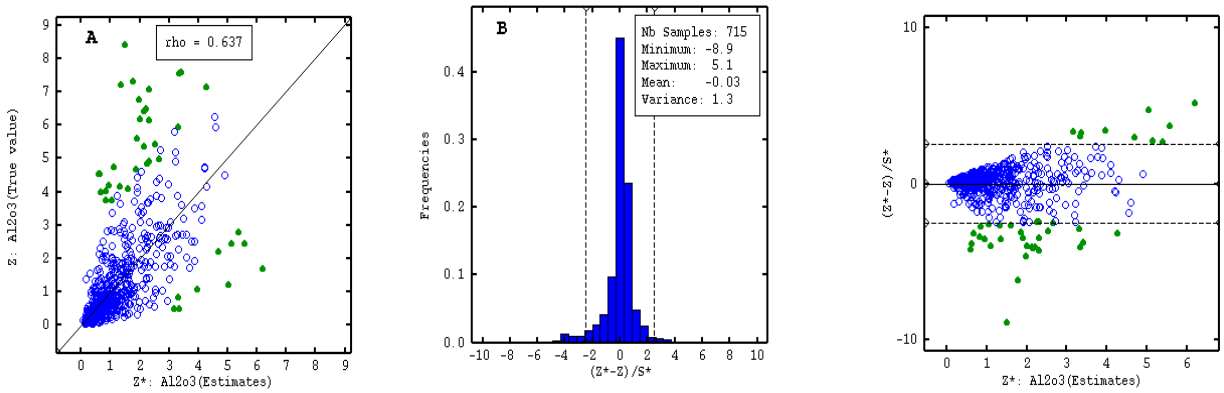


Figure 4.12 Cross validation results of $Al_2O_3$. (A) scatter plot between estimates and true values, (B) histogram of standard errors, and (C) scatter between estimates and standard errors.

## 4.4 Neighbourhood analysis

The neighbourhood chosen in the estimation of ore grade has a significant impact on the outcome of the kriging estimate. Kriging, 'minimum variance estimator', is true only when the neighbourhood is adequately chosen (De-vitry, 2003; Marzeihe et al., 2013). The two key parameters for choosing the kriging neighbourhood are '*search radius'* and *'sample selection'*.

### *Search radius*

In the neighbourhood analysis, search radius, the maximum distance of a sample that contributes in the estimation of an unknown point, is an important parameter in estimation of grade. An inappropriate search radius reduces the accuracy of estimates. For example, long search radius considers the points which have no spatial correlation whereas short search radius reduces the number of data points. According to Rivoirard (1987), the larger the neighbourhood the more precise are the estimates. A neighbourhood that is too restrictive will result in serious conditional biases (Krige, 1996).

Generally, the semi-variogram range is used as a criterion for determining the search radius of neighbourhood, which can be equal to or less than the semi-variogram range (Hassani Pak, 2005; Marzeihe et al., 2013). Vann et al. (2003) suggest that the choice of neighbourhood may be influenced more by the slope of the semi-variogram model at short lags and the relative

nugget effect (i.e., the ratio of the nugget variance to the total variance, expressed in percentage) than by the ranges. It was suggested by various researchers that the optimized radius can be 2/3 of the variogram range (Annels, 1996; Hassani Pak, 1998; Marzeihe et al., 2013). Asghari et al. (2009) also suggest that search radius is usually 2/3 of the range of the semi-variogram or can be less in some cases where sampling is done in a very fine grid to avoid more number of data within the domain of the search radius.

Against this background, the search radius was chosen as rounded to two-third of range of the semi-variogram in this study. Thus, 2/3 * 700 m (range being 700 m) =467 m. Taking this into account and deposit is isotropic, equal search radius of 450 m was taken for estimation of mean Fe grade and CV in 2D analysis. Subsequently, in 3D analysis of linear (ordinary kriging) and non-linear (Indicator kriging and Disjunctive kriging) estimation methods, equal search radius of 300 m was taken in horizontal direction and 36 m in vertical direction for comparison purpose.

***Sample selection***

Another important parameter to be considered in the neighbourhood analysis is the sample selection which involves number of sectors made in the circle of defined search radius and the number of samples used in the estimation. The samples may be considered from several directions either as quadrant or octant search methods, to avoid biasness, as suggested by Murthy (1989a) and Vann (2003). In this study, octant search method is used i.e., the circle with defined radius is divided into eight parts equally and samples are considered for estimation from each sector.

The minimum and maximum number of samples used for the estimation depends upon the distribution of samples in the deposit (Asghari et al., 2009). As there are no fixed criteria to fix minimum and maximum number of samples, applying trial and error method, as suggested by Murthy (1989a), 2 and 16 were found to be optimal values as the minimum and maximum number of points, respectively. If the number of samples within the search radius is less than 2, then the block will not be estimated. If the number of samples exceeds 16 within the search radius, then the 16 nearest samples to the block are considered for estimation and other samples

are ignored. For example, neighborhood analysis carried out for a block of 25 x 25 x 12 mts is shown in Figure 4.13.

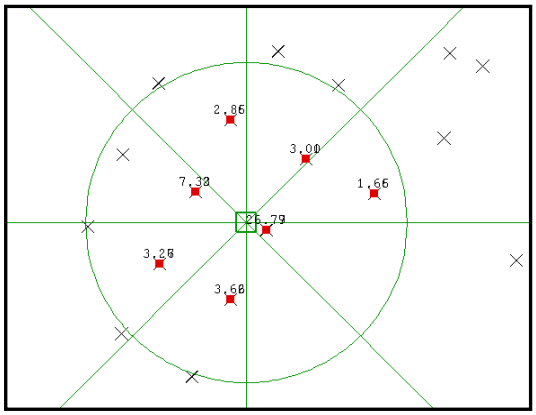


Figure 4.13 Neighborhood analyses for a block with an index 32, 32 and 15 along x, y and z directions respectively in the block model. A circle is drawn with the centre of block as centre and given search radius. Block shown in green colour is estimated using samples shown in red within 8 sectors and samples shown in black are ignored to estimate this block.

## 4.5 Block modelling and categorization of litho units

A 3D block model has been created covering the total deposit, taking into account of minimum and maximum of northing (Y), easting (X) and elevation (Z) of the samples in the drill holes, topography and geological model of the deposit before estimating grade and resources of the deposit. The centroid of each block defines its geometric dimensions in each axis, i.e., its coordinates, X, Y, and Z. Each block contains attributes with numeric (such as grades) and categorical values (such as lithological units).

In any deposit, the lithological information was available only at the exploratory borehole locations, hence spatial interpolation of lithological units was done and the information on litho types in each block was obtained. It is necessary to assign a litho type in each block for grade estimation. Two approaches - *geological cross sectional* method and a non-linear geostatistical *indicator kriging* method, - are adopted for categorizing litho units.

### 4.5.1 Geological cross sectional method

Cross-sections generated from exploratory boreholes enable to understand the structure of the mineralization and delineation of the orebody. In the conventional method, the lithological type will be assigned in blocks using a geological cross sectional model approach. In this approach, sectional interpretations are constructed, generally orthogonal to the strike of mineralization. Each litho intersection in each drill hole is allocated its own volume of influence, which usually extends halfway to the next drill hole up and down dip, and halfway to the next-section in each strike direction (Glacken and Snowden, 2001). According to Pasti et al., (2012), these sections provide information about the contacts between lithologies.

A detailed statistical analysis by zones, combined with the geological interpretation given on maps and cross-sections is necessary to identify the statistically homogenous populations (Fouquet, 1996). Based on contour data, digital terrain model (DTM) was generated for the deposit (Figure 4.14) and subsequently profile lines are generated for each cross section.

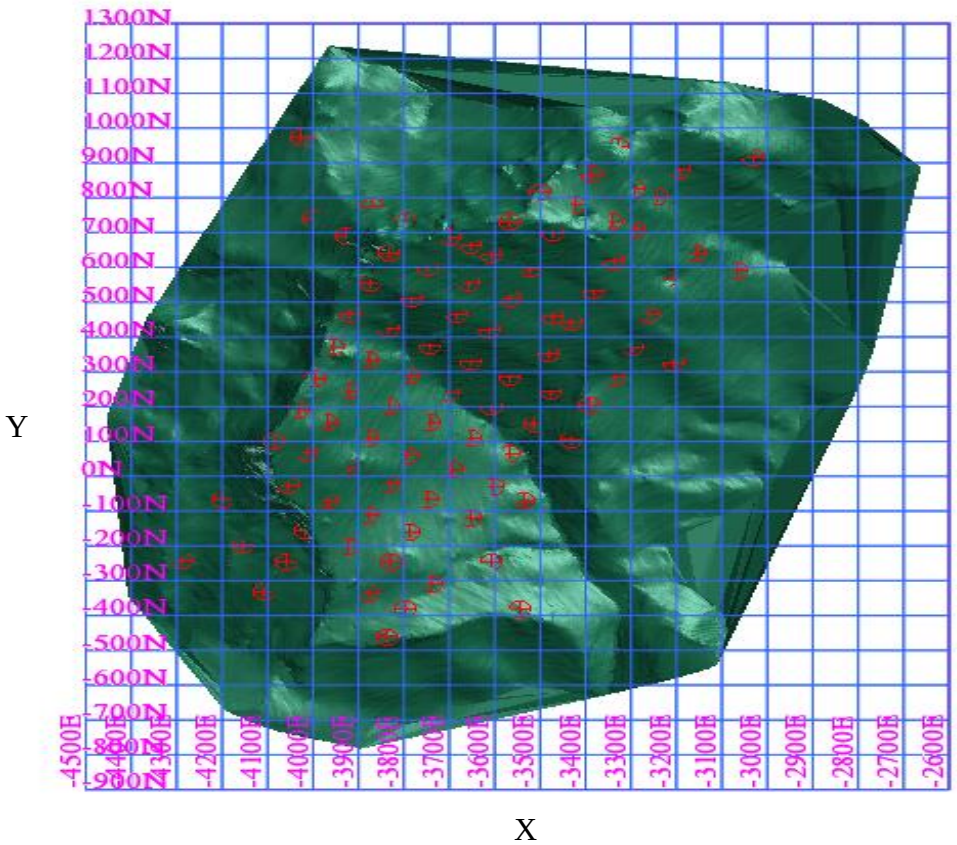


Figure 4.14 Showing digital terrain model (DTM) of the deposit in XY plane with boreholes.

Considering the profile line and lithological log of boreholes, litho boundaries were digitized taking into account their lateral influence based on the overall dip of the ore body. A total of 17 cross sections were prepared covering all the boreholes with a distance 100 mts between cross sections and a tolerance distance of 50 mts. Details of boreholes available on each section line are given in Table 4.6 and Figure 4.15. Figure 4.16 shows a typical geological cross section, interpreted and built in the traditional way.

Table 4.6 Details of boreholes available on each section line. Bore holes drilled by GSI and NMDC are included.

| **Section No.** | **Section ID** | **Number of Boreholes** | **Borehole ID's** |
|---|---|---|---|
| 1 | N7 | 1 | D69 |
| 2 | N6 | 2 | NBH-1, NBH-3A |
| 3 | N5 | 4 | BH-12, NBH-3, NBH-2, D59 |
| 4 | N4 | 6 | NBH-6, BH-1, NBH-5, BH-5, D58, D65 |
| 5 | N3 | 5 | D71, D18, BH-6, BH-13, D60 |
| 6 | N2 | 8 | BH-14, D55, D10, BH-2, D41, D1, BH-7, BH-10 |
| 7 | N1 | 10 | D68, D52, D32, BH-4, D2, BH-15, D47, BH-8, |
| 8 | N0 | 6 | D29, BH-3, D34, BH-11, BH-9, D44 |
| 9 | S1 | 7 | D26, D9, D21, D3, D37, D35, D70 |
| 10 | S2 | 7 | D43, D4, D6, D22, D28, D51, D40 |
| 11 | S3 | 6 | D46, D3, D25, D11, D30, D36 |
| 12 | S4 | 7 | D31, D5, D7, D17, D24, D48, D42 |
| 13 | S5 | 6 | D39, D4, D20, D12, D23, D27 |
| 14 | S6 | 5 | D15, D8, D16, D19, D33 |
| 15 | S7 | 6 | D66, D63, D45, D49, D38, D72 |
| 16 | S8 | 4 | D62, D61, D54, D53 |
| 17 | S9 | 3 | D67, D64 D56 |

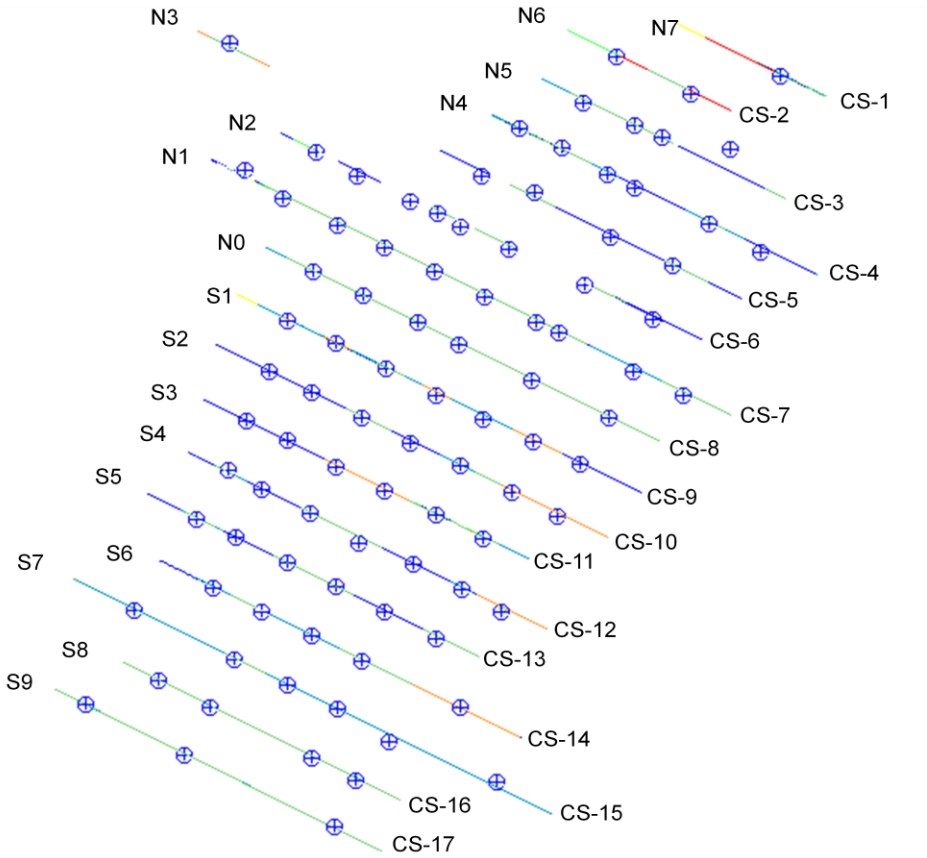


Figure 4.15 Representation of boreholes available on each section line in XY plane.

From 17 cross sections, litho wise digitized boundaries are extracted and solids were generated for each litho type. Solids generated for each litho unit are shown in Figure 4.16. Finally, a solid model ie geological model was obtained by combining all the litho type solids.

Further, block model is created by considering the extents of geological model and topography of the deposit for geostatistical grade estimation by kriging. After creating block model (parent or mother block), constrained block models are generated for each litho type, using corresponding geological ore body represented in Figure 4.16 and are shown in Figure 4.17.

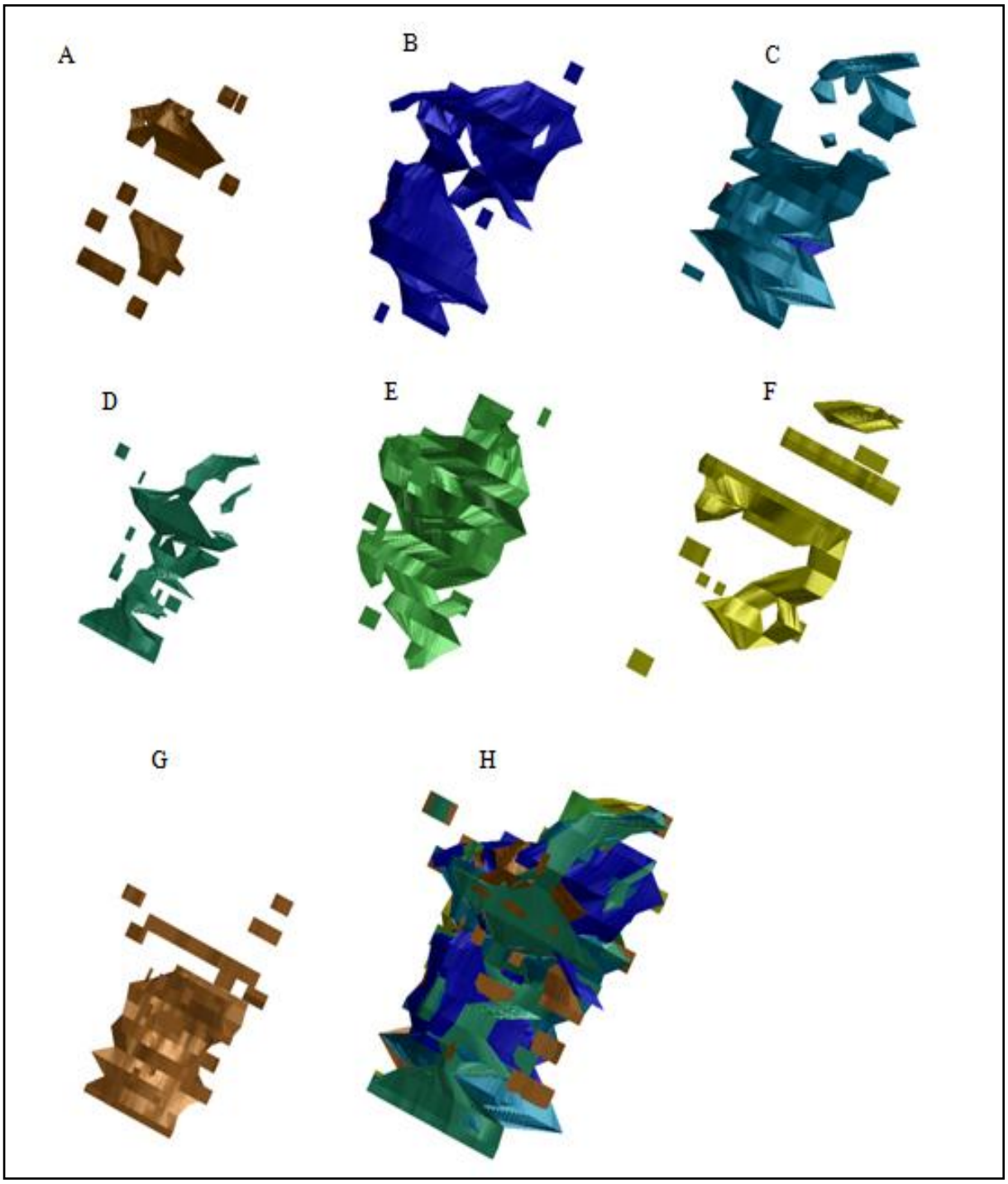


Figure 4.16 Geological model generated for each litho unit. (A) SGH, (B) BGH, (C) LH, (D) LO, (E) BD, (F) BHQ, (G) Shale, and (H) All litho types together.

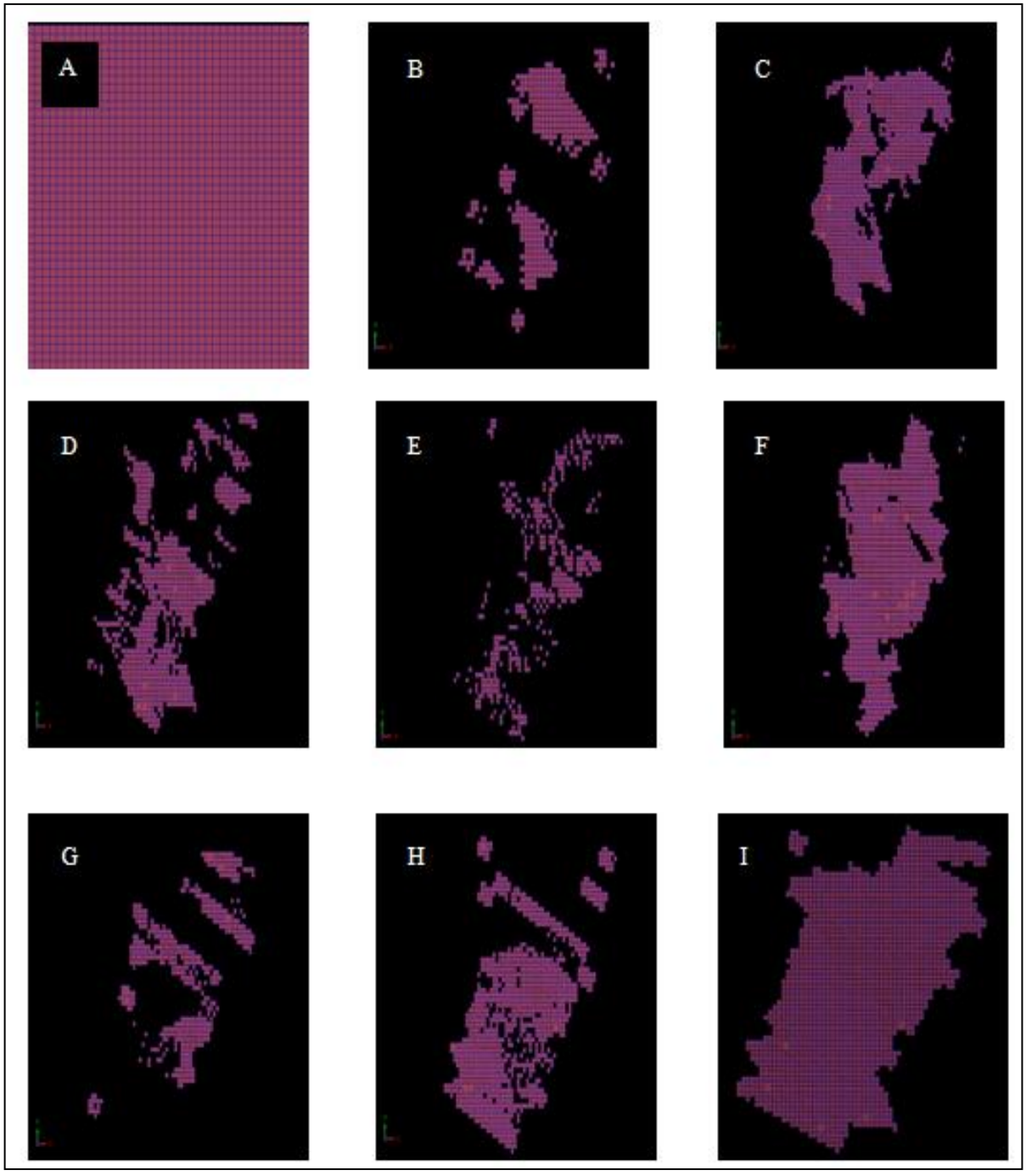


Figure 4.17 Block model (parent) and constrained block models of different lithological units. (A) Parent Block, (B) SGH, (C) BGH, (D) LH, (E) LO, (F) BD, (G) BHQ, (H) Shale, and (I) All litho units.

### 4.5.2 Indicator Kriging method

In indicator kriging, original random variable needs to be transformed into indicator data instead of using the variable itself. The concept of indicator coding of data has been proposed by Journel (1983b) for estimation of spatial distributions. Indicator transformation is an estimator applied on a set of variables whose values are modified according to a non-linear transform, and it transforms each value of the set of variables into indicator values i.e., 0s and 1s (Deutsch and Journel, 1998). The main advantage of the indicator transformation is that it is non-parametric and it need not follow any distribution pattern. In this study, Indicator transformation was done on categorical variables i.e., lithological units for delineating litho units of the deposit. While using an indicator kriging for categorical data such as lithological type, a series of indicator values corresponding to each lithological type are chosen. These indicator values are used to numerically build up the probability of occurrence for different lithologies at each estimation point or block. Indicator kriging is carried out in 3 steps: (i) Indicator transformation, (ii) Indicator semi-variogram modelling and (iii) Indicator kriging.

***(i) Indicator transformation***

An indicator transform is necessary for the estimation of categorical data, which are not continuous but which have discrete values. Composited data in each of the available sample location are transformed into 0s and 1s. It is '1' if the data belong to the particular litho type, and '0' if the data do not belong to that particular litho type. A categorical indicator transformation is carried out for each of the seven lithological units of the deposit. At a sample location 'x' in the deposit, for a particular lithological unit $L_i$, an indicator transformation is expressed as:

$$I_i(x) = 1 \text{ if } x \varepsilon L_i, \qquad (3.2)$$

$$= 0 \text{ otherwise}$$

where 'i' varies from 1 to 7 lithological units. After transformation, a different set of indicator data were generated for each lithological unit. The transformed data are further used in semi-variogram modelling and in indicator kriging.

### *(ii) Indicator semi-variogram modelling*

Iron ore has been broadly grouped into eight litho units based on physical and chemical characteristics of the drill hole samples. Soares (1992) suggests single average semi-variogram model in determining lithofacies in a petroleum reservoir as this approach saves the time. A single average semi-variogram model was constructed for all the lithological units in a limestone deposit, assuming the same spatial continuity for all lithological units by Chatterjee et al (2006). As this approach has limitations in terms of spatial continuity, a separate indicator semi-variogram model for each lithological unit for obtaining a better spatial variability has been constructed. The typical indicator semi-variogram was calculated using the following formulae (Chatterjee et al., 2006):

$$\gamma(h) = \frac{1}{2MN} \sum_{n=1}^{N} \sum_{m=1}^{M} \left[ i_n(x_m) - i_n(x_m + h) \right]^2 \qquad (3.3)$$

where M is the number of pairs for lag h and N is the number of lithological units.

These semi-variograms are modelled with a small nugget effect and using two variogram models – exponential and spherical. The parameters used for modelling of indicator semi-variograms are presented in Table 4.7, and the omni-directional indicator semi-variogram models of each lithological unit are shown in Figure 4.18. The indicator semi-variogram models of different lithological unit (Figure 4.18) show a good spatial structure with an average range of around 290 m.

Table 4.7 The parameters of indicator semi-variograms used for modelling in different lithological units.

| Litho type | Nugget Effect | Structure 1 | | | Structure 2 | | |
|---|---|---|---|---|---|---|---|
| | | Model | Sill | Range (m) | Model2 | Sill | Range (m) |
| SGH | 0.008 | Exponential | 0.060 | 75 | Spherical | 0.020 | 275 |
| BGH | 0.050 | Exponential | 0.150 | 125 | Spherical | 0.015 | 300 |
| LH | 0.030 | Exponential | 0.099 | 50 | Spherical | 0.037 | 300 |
| LO | 0.005 | Exponential | 0.039 | 75 | Spherical | 0.001 | 275 |
| BD | 0.040 | Exponential | 0.100 | 50 | Spherical | 0.036 | 200 |
| BHQ | 0.015 | Exponential | 0.008 | 100 | Spherical | 0.026 | 325 |
| Shale | 0.020 | Exponential | 0.001 | 100 | Spherical | 0.020 | 350 |

### *(iii) Indicator kriging (IK)*

Geostatistical non-linear indicator kriging is employed to delineate different lithological units of iron ore deposit, i.e., indicator categorical variables. Before applying indicator kriging for delineation of litho units in the deposit, a block model for the deposit is created by dividing the total area into smaller blocks, as block size plays an important role. For example, if large size blocks are selected for kriging, the estimation variance will be less, and hence, such estimates will not serve any purpose for practical mining purposes (Guibal, 1987; Murthy, 1989a). If very small blocks are considered, the estimation variance will be high and erroneous (Jackson and Marechal, 1979). David (1977, p. 283) gives a practical rule that one should not consider the blocks of the size less than ¼ $^{th}$ of the spacing of the boreholes. Based on these considerations, the block dimensions are assigned as 25 m x 25 m in XY direction, while in Z direction the block size considered is 12 m i.e., bench height.

#### *Preparation of lithological maps*

Based on IK estimates, the lithological maps are prepared. A single litho type was assigned to each block, based on the maximum probability of occurrence of kriged estimates of seven litho types in that block. For example, in a block, the probability of occurrence of the lithological units - SGH, BGH, LH, LO, BD, BHQ and shale are 0.06, 0.57, 0.05, 0.06, 0.16, 0.01, 0.04 and 0.56 respectively. As BGH shows maximum probability of 0.57, the lithological unit assigned to that block is BGH. This methodology was employed by Chatterjee et al., (2006) in lime stone deposit. The lithological maps for all the 32 benches in the deposit are constructed. For example, the lithological maps of 4 benches at reduced levels (RL) of 1152 m, 1068 m, 996 m and 912 m are shown in Figure 4.19. It is observed from the lithological maps of all the 32 benches that the low grade Fe content bearing litho units - BHQ and shale - occur mostly in the peripheral blocks, whereas high grade Fe bearing litho units occur in the middle portion of the deposit.

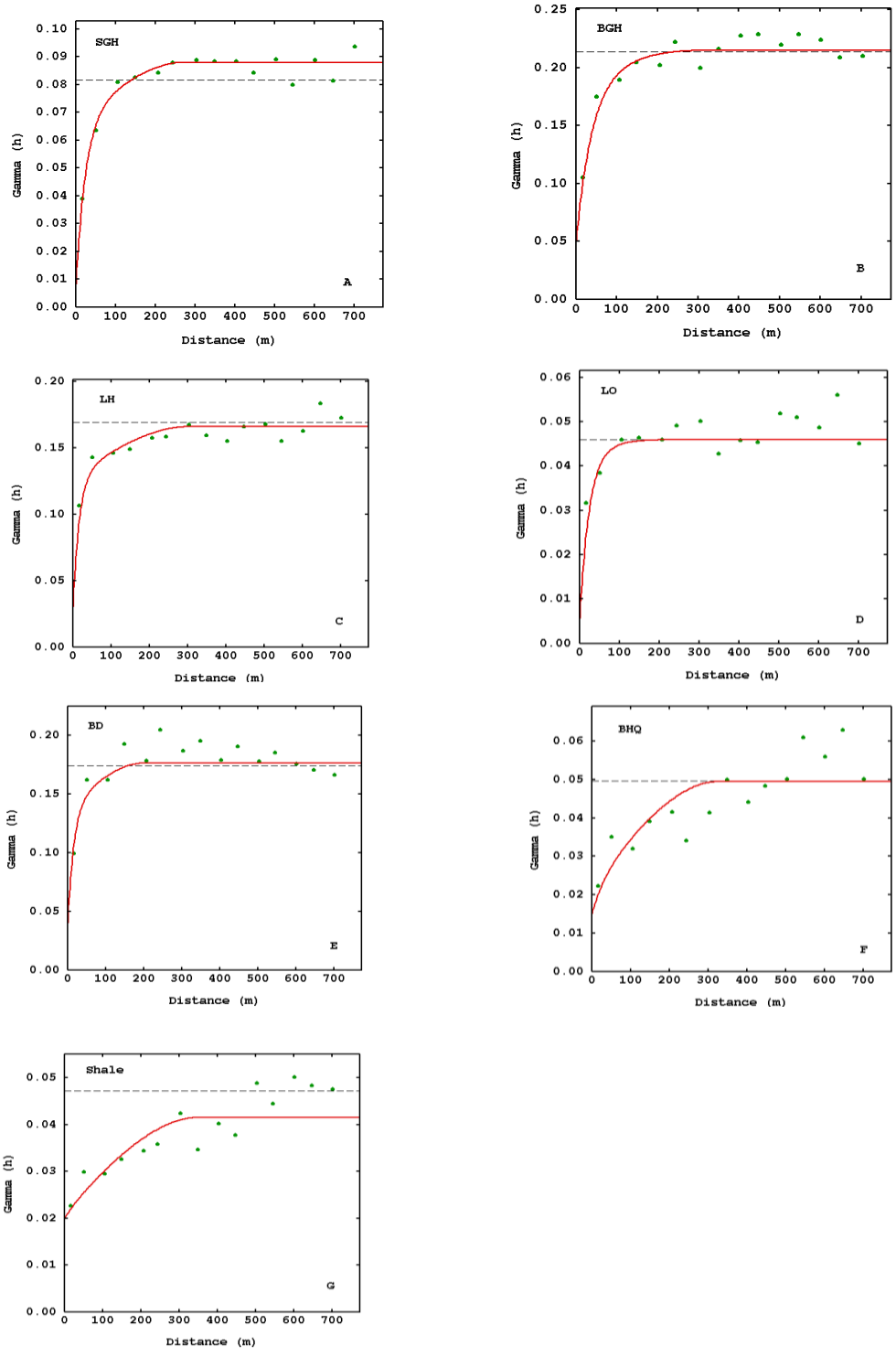


Figure 4.18 The omni-directional indicator semi-variogram models of different lithological units. Semi-variogram models of all seven litho units show a good spatial structure with low nugget values.

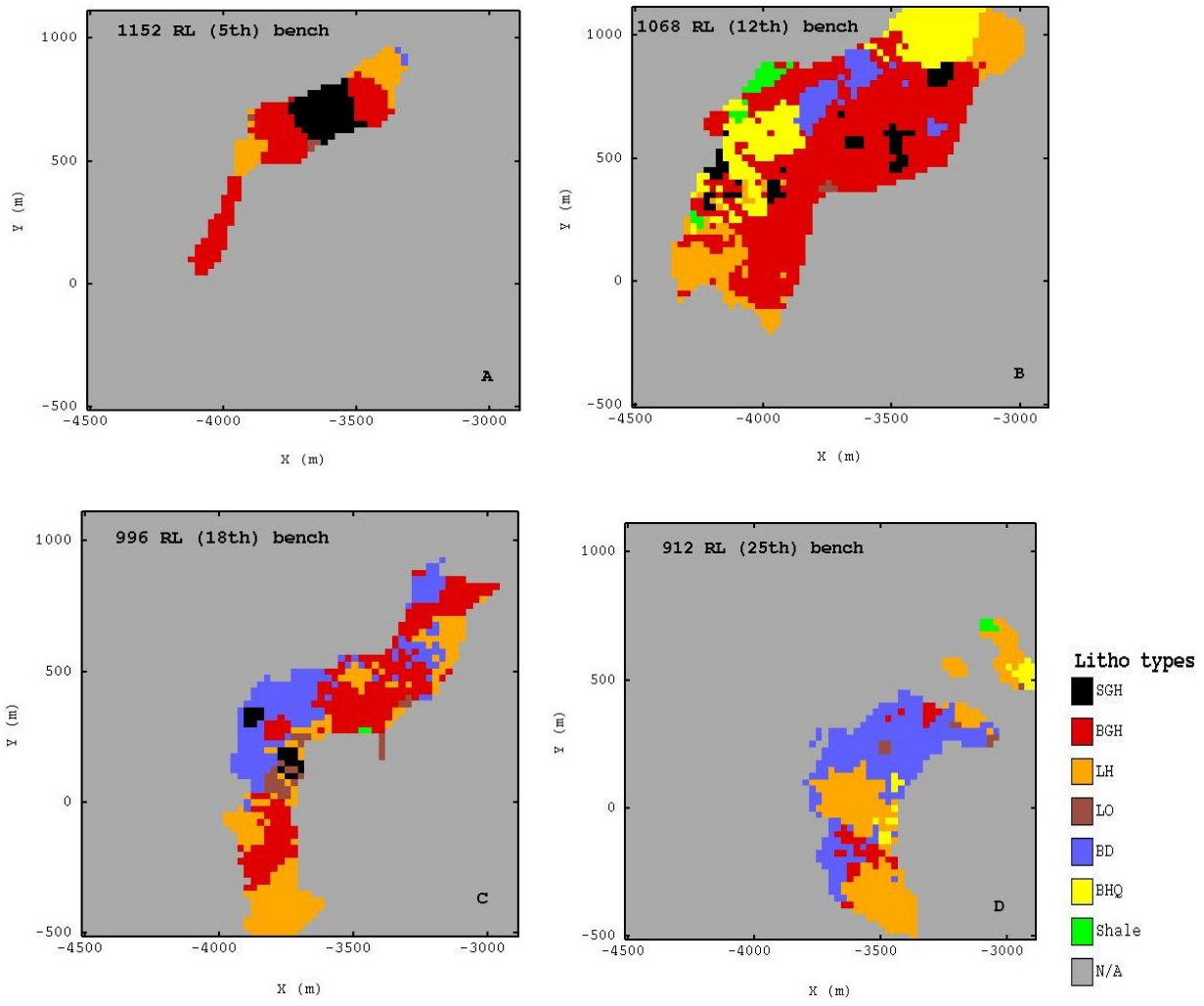


Figure 4.19 Showing lithological maps of four mining benches located at 1152 m, 1068 m, 996 m and 912 m. Majority of the blocks in each bench are categorized into high grade Fe litho units. Litho units – BHQ & Shale containing low Fe grade are observed in peripheral areas.

## 4.6 Summary

In this chapter, the prerequisites for geostatistical estimation such as variogram modeling, cross-validation of model, neighborhood analysis and block modelling are discussed. Detailed spatial analysis was performed on 3D composited data for the variables Fe, $SiO_2$ and $Al_2O_3$ in both the domains *ore* and *waste*. In order to examine the composites for any anisotropy and

directions of continuity, semi-variogram map was generated for principle variable Fe. The semi-variogram maps for both these domains do not show anisotropy in the XY plane. On this basis, omni directional experimental semi-variograms for both the domains were calculated in the XY plane (horizontal direction) with anisotropy modelled in the Z direction (vertical direction). The semi-variograms of Fe, $SiO_2$ and $Al_2O_3$ were modelled using two structures and with a nugget effect in both the domains.

It is observed from the semi-variogram models of Fe that both the horizontal and vertical directions show a very good spatial structure with a small nugget effect in domain 'ore'. Anisotropy is observed in both the directions having ranges 400 m and 90 m respectively (Table 4.2; Figure 4.4). On the other hand, the horizontal and vertical semi-variograms of domain 'waste' are less structured (Figure 4.5), which may be due to low grade Fe values and presence of impurities like silica and alumina. It is observed from the semi-variogram models of $SiO_2$ that both the horizontal and vertical directions show a very good spatial structure with a small nugget effect in domain 'ore'. Anisotropy is observed in both the directions having ranges 375 m and 90 m respectively (Table 4.3; Figure 4.6). It is also observed that range is same in the vertical direction in both Fe and $SiO_2$ and not much change in the horizontal direction, which may be due to a very good correlation between these two variables. The horizontal and vertical semi-variograms of domain 'waste' are less structured (Figure 4.7) as observed in Fe. It is observed from the semi-variogram models of $Al_2O_3$ that both the horizontal and vertical directions show a very good spatial structure with a small nugget effect in domain 'ore'. Anisotropy is observed in both the directions having ranges 400 m and 70 m respectively (Table 4.4; Figure 4.8). It is also observed that $Al_2O_3$ range is less in the vertical direction and very little change in the horizontal direction when compared to both Fe and $SiO_2$. The horizontal and vertical semi-variograms of domain 'waste' are also less structured in $Al_2O_3$ (Figure 4.9) as observed in Fe and $SiO_2$.

Cross validation of semi-variogram models are carried out for the variables Fe, SiO2 and Al2O3 in the *ore* domain, as it has bearing for mining of the deposit. All the results of cross validation indicate that the models are satisfactory and can be further used in estimation.

A 3D block model is created taking into account the extent of samples in the drill holes, topography and geological model of the deposit prior to grade estimation and resources of the

deposit. *Geological cross sectional method* and a non-linear geostatistical *indicator kriging method* are employed in categorizing the litho units in the block model.

The indicator semi-variogram models for each lithological unit show a good spatial structure with an average range of ~350 m. It is observed from the lithological maps of 32 benches that the low grade Fe content bearing litho units - BHQ and shale - occur mostly in the peripheral blocks, whereas high grade Fe bearing litho units occur in the middle portion of the deposit.

# CHAPTER 5

# RESOURCE ESTIMATION BY ORDINARY KRIGNG

# CHAPTER 5

# Resource Estimation by Ordinary Kriging

## 5.1 Introduction

Resource estimation i.e., the assessment of the quantity (tonnage) and grade of a mineral deposit, is an important aspect of mining and mining economics. There are, in general, two approaches of resource estimation - (i) non-geostatistical methods i.e., traditional methods that are done manually on plans or sections using weighted average or inverse-distance technique, and (ii) geostatistical methods such as kriging that require the use of a computer. In the computer aided interpolation methods, most resource estimation techniques, use some form of grade smoothing to interpolate values into a block based upon surrounding samples (Glacken and Snowden, 2001).

Manual resource estimations are usually done on plan maps or cross-section maps that cut the deposit into sets of parallel slices. Data plotted on the maps include drillhole locations, assay values, and the geologic interpretation of the mineralization controls. The manual estimations such as area averaging, polygonal, cross sectional, and triangular are based on geometric weighting of assays (Noble, 1993). The most common problem with these manual methods is that they may imply more selective mining. It results in high-grade blocks usually include lower-grade material when they are mined, and low-grade blocks usually include some higher-grade material. The resulting mined grades are usually different from the predicted distribution; In these methods, it is also not clear up to what distance samples must be considered, and number of samples to be used during estimation. There is a limitation with these methods as they do not take spatial variability of a variable in to account (Matheron, 1971).

The geostatistical approaches to grade interpolation all rely on some form of kriging, whereby the weights given to each sample are derived from the semi-variogram model, which defines the continuity and spatial variability of grades. The geostatistical methods are categorized into three types – linear, non-linear, and simulation (Glacken and Snowden, 2001).

In linear geostatistics, the fundamental estimation technique is called ordinary kriging, in recognition of the work carried out by Dr. Krige on gold deposits in South Africa. Ordinary kriging not only estimates the data at unsampled locations but also assess error of estimates in the form of kriging variance (David, 1977).

Ordinary kriging and its applications were discussed by various researchers (Matheron, 1965; Journel and Huijbregts, 1978; Clark, 1979b; David, 1988; Isaaks and Srivastava, 1989; Armstrong, 1998; Wacknernagel, 1995; Sharma, 2002; Sarkar, 2014). In mining industry, ordinary kriging was extensively applied for grade estimation of a tin deposit (Clarke, 1979), coal deposit (Clark, 1989), iron ore deposit (Mol and Gillies, 1984; Murthy, 1989b, 1996; Gouda and Moharam, 2001; De-vitry, 2003; Fitzgerald et al., 2009; Asghari et al., 2009; Osterholt et al., 2009) copper deposit (Deraisme, 1998; Emery and Ortiz, 2005), nickel deposit (Glacken et al., 1998; Bertoli et al., 2003), zinc deposit (Clark, 1999), gold deposit (Champigny and Armstrong, 1993) Sarma, 2002; Jackson et al., 2003), and bauxite deposit (Samanta et al., 2005). Interestingly ordinary kriging was also applied in non-mining industry such as in archaeology (Lloyd and Atkinson, 2004), ecology modelling (Monestiez et al., 2006), forestry (Berterretche et al., 2005), geotechnical engineering (Hammah and Curran, 2006), rainfall (Kamel et al., 2010), environment (Zirschky, 1985), ground water (Yang et al., 2008), and hydrology (Virdee and Kottegoda, 1984).

In this chapter, prior to initiating detailed ore reserve estimation of the deposit, the preliminary ore deposit evaluation was carried out in a rapid way in 2D, to assess grade domains and grade variation of the deposit employing ordinary kriging. Further, volume and tonnage estimation are carried out in 3D by considering block model categorization using geological cross section method. Ordinary kriging is employed also for grade estimation for the attributes Fe, $SiO_2$ and $Al_2O_3$, in different litho units separately, in both the block models - block model categorized using *geological cross section* approach and block model categorized using *indicator kriging* approach. As suggested by Keogh and Moulton (1998), both the resulting estimated model grade distributions are compared with input composited grade distributions and raw data. Ordinary kriging is employed also for grade estimation of Fe variable using the complete bench composited data for the purpose of global estimation of resources and for comparing with non-

linear methods (Chapter 6 and 7). Based on kriged results of global estimates, Fe grade maps and Fe kriged standard deviation maps (error maps) are generated for the 32 benches in the deposit.

In addition to the resource estimation, the quantification of uncertainty in mineral resources estimation is essential for the economic planning in any mineral deposit as the resource/reserve evaluation is the base on which economic feasibility studies are established. Activities such as mine planning, production scheduling, mining orientation, projection of cash flows and the operation of processing plants require the correct classification of these resources, besides the estimate of the available resources (de Souza et al, 2004). Thus, error associated with an estimate is of paramount importance in classifying resources/ reserves. Authors further state that the estimate and the subsequent classification of resources into different classes or categories, according to the possible variations of these resources must provide a model that quantifies the risk on each category.

As traditional methods unable to provide a measure of error associated with their estimates, these methods are inappropriate to assess local or global uncertainty associated with an estimate. However, geostatistics provides the technical criteria required for uncertainty assessment and, consequently, the identification of resources/reserves categories (Sabourin, 1983; Mwasinga, 2001). Several geostatistical methods can be used to assess uncertainty.

In this study, error quantification is done based on 'kriging standard deviation' and 'kriging efficiency' and subsequently the total estimated mineral resource is classified into *measured, indicated and inferred* categories based on these two error quantification methods.

## 5.2 Ordinary Kriging

Kriging is a linear geostatistical optimal spatial interpolation and estimation method that gives the best linear unbiased estimates of point values or of block averages of regionalised variable. Kriging is referred to as 'Best Linear Unbiased Estimator' (BLUE) because it provides best estimates (with minimum estimation variance) and it is unbiased (error of estimates is zero) (David, 1977). Kriging estimates are weighted moving averages of the original data values; thus they have less spatial variability than the original data.

Semi-variogram model is a prerequisite for ordinary kriging. Using the semi-variogram model, the block grades together with their associated variances are estimated adopting ordinary kriging (Krige, 1962; Matheron, 1971; Sarkar, 2014). Kriging calculates an estimated value $Z_v^*$ of a real value *z* in a block by using a linear combination of weights, $\lambda_i$ of the selected surrounding values such that:

$$Z_v^* = \sum_{i=1}^{N} \lambda_i Z(x_i) \tag{5.1}$$

where *N* is the number of scatter points in the set, $z(x_i)$ are the values of the scatter points, $\lambda_i$ are weights assigned to each scatter point and * denotes the estimated value as opposed to original value. This equation (Journel and Huijbregts, 1978) is essentially the same as the equation used for inverse distance weighted interpolation except that rather than using weights based on an arbitrary function of distance, the weights used in kriging are based on the model variogram.

Kriging calculates the weighting factors $\lambda_i$ in equation (5.1) in the best way, choosing the weights so that the estimator is (i) unbiased, expressed as $E [ Z^*_v - Z_v] = 0$ and (ii) minimum variance, expressed as $Var [Z^*_v - Z_v]$ is a minimum (Matheron, 1963; David, 1977).

If Z(x) is stationary with mean m, then $E [Z (x_i)] = m$ and so $E [Z_V] = m$, then

$$E [ Z^*_v - Z_v] = E [ \sum \lambda_i Z(x_i) - Z_V] = \sum \lambda_i m - m \tag{5.2}$$

$$= m [\sum \lambda_i - 1] = 0$$

Consequently, for the estimator to be unbiased the weights add up to 1. ie $\sum \lambda_i = 1$. (5.3)

The variance of error $[Z^*_v - Z_v]$ is called the kriging variance and can be expressed in terms of the variogram as

$$\sigma^2_k = 2\sum_{i=1}^{N} \lambda_i \gamma(x_i, v) - \sum_{i=1}^{N}\sum_{j=1}^{N} \lambda_i \lambda_j \gamma(x_i, x_j) - \gamma(v, v) \tag{5.4}$$

where $\gamma (x_i, V)$ is the average of the variogram between $x_i$ and the volume V and $\gamma (V, V)$ is the average of the variogram in the volume V.

In order to minimize the estimation variance under the constraint that the sum of the weights must be equal to 1 (from equation 5.2), kriging introduces a Lagrange multiplier μ.

$$\phi = \mathrm{Var}\,(Z^{*}_{V} - Z_{V}) - 2\mu\,[\sum\lambda_i - 1] \qquad (5.5)$$

Since the sum of the weights must be 1.0, adding the term in μ does not change the value of the expression. The partial derivatives of the quantity are then set to zero. This leads to a set of N + 1 linear equations called the Kriging System. Mathematically it is expressed as:

$$\sum_{j=1}^{N} \lambda_j\, \gamma(x_i, x_j) + \mu = \gamma(x_i, V) \qquad i=1, 2. ..N \qquad (5.6)$$

$$\text{Where} \sum_{i}^{N} \lambda_i = 1$$

(N+1) equations in equation (5.6) are solved to get kriging weights of equation (5.1). The minimum variance is called the kriging variance and is expressed as

$$\sigma^2_k = \sum\lambda_i\gamma(x_i, V) - \gamma(V, V) + \mu \qquad (5.7)$$

## 5.3 Assessing grade domains of the deposit in 2D

Ordinary kriging provides estimates of ore deposit with minimum variance at unsampled locations. Prior to detailed ore reserve estimation of the deposit in 3D, the preliminary ore deposit evaluation was carried out in a rapid way in 2D, to assess grade domains and grade variation of the deposit (Kameshwara Rao et al., 2014). This two-dimensional (2D) geostatistical estimation approach for a 3D nickel deposit with narrow vein- or layer – like geometry was discussed by Bertoli et al., (2003).

In this study, the 3-D data was converted to 2-D for analysing the variation of Fe within the boreholes. For each borehole, weighted mean of Fe grade 'wFe' and its coefficient of variation (CV) are calculated and further statistical analysis, variogram analysis and ordinary kriging are carried out for these two variables. wFe and CV were estimated by using block kriging method, which provides an estimate of the grade of the *in situ* resources from which low

and high grade areas of the deposit can be identified. Block dimensions have been assigned as 25 m x 25 m in 2D modelling. A total number of 3863 blocks were recorded in the study area. wFe grade and CV are estimated in each block by ordinary kriging using corresponding semi-variogram models (Figure 4.3) and neighbourhood search parameters defined in section 4.4. The kriged results of wFe and CV are presented in Table 5.3 and domain maps of wFe and CV based on kriged estimates are presented in Figure 5.2. The scatter plot between these two estimates is shown in Figure 5.3.

## 5.4 Resource estimation of the deposit in 3D

The whole ore body of the deposit is divided in to blocks, with each block of size as 25 x 25 x 12 m for estimation of reserve and grade. The geological reserves in different lithological units of the deposit are computed using the block model which was categorized using geological cross sections (Figure 4.18). Tonnage of each block is obtained by multiplying the volume of each block with tonnage factor i.e., in situ density of litho type to which block belongs. Tonnage of each litho type is obtained by taking sum of tonnages of all those litho blocks. The volume and estimated tonnage in different litho types are shown in Table 5.4.

Grade estimation was carried out for Fe, $SiO_2$ and $Al_2O_3$ using both the block models i.e., block model categorized using geological cross section approach (Figure 4.18) and block model categorized using indicator kriging approach (Figure 4.20). In both the approaches, grades are estimated for each block employing ordinary kriging. As the original data of main variable Fe % are strongly skewed, composited data is categorized into two domains to avoid mixing of populations and for computation of semi-variograms, as suggested by Glacken and Snowden (2001). Domain *ore* - consisting of samples from lithological units SGH, BGH, LH, LO and BD, and Domain *waste* - consisting of samples from lithological units BHQ and Shale. Subsequently, semi-variograms for both the domains are calculated in the horizontal and vertical directions. Grade estimation is carried out for each block using the composites of domain type of that particular block and the semi-variogram model of the corresponding domain. It means the grade of all blocks of litho units SGH, BGH, LH, LO and BD are estimated using composites and semi-variogram model of domain *ore*, whereas grade estimation of all blocks of litho units BHQ and Sh are estimated using composites and semi-variogram model of domain *waste*.

Basic statistics of kriged estimates i.e., kriged grades and kriged standard deviations of Fe, $SiO_2$ and $Al_2O_3$ for different litho units in both the approaches – *geological cross section* and *indicator kriging* are presented in Tables 5.5 and 5.6 respectively. A comparison is made between the results of the estimated grades obtained from these two approaches in order to test and validate the estimated Fe grades for each litho type in novel approach as compared to traditional method. Keogh and Moulton (1998) suggest that, the kriged estimates are to be validated with original data with respect to basic statistics. Thus, the resulting estimated model grade distributions are also compared with input composited grade distributions and raw data i.e., borehole data to test whether estimated results are in line with original data (Table 5.7; Figure 5.4).

For the purpose of global estimation and for comparison with non-linear methods (Chapter 6 and 7) ordinary kriging is employed for Fe variable using total bench composited data and the corresponding semi-variogram model. The basic statistics of the global estimates of Fe are given in Table 5.8. Based on kriged results of global estimates, Fe grade maps and Fe kriged standard deviation maps (error maps) are generated for the 32 benches in the deposit. The toe of top bench is 1200 m and bottom bench is 828 m above mean sea level with a bench height of 12 mts. Grade maps and kriged standard deviation maps of twelve benches (1200 m, 1164 m, 1116 m, 1068 m, 1020 m, 972 m, 924 m, 876 m, 864 m, 852 m, 840 m and 828 m) are shown in Figures 5.5 and 5.6. The scatter plot between kriged grades and kriged standard deviation of Fe is shown in Figure 5.7.

## 5.5 Resource classification

'Mineral Resources' confidence classification takes into account practical considerations such as drilling, sampling, and assay integrity, drill hole spacing, geological control and continuity, grade continuity, estimation method and block size, potential mining method and reporting period. Based on these factors, three categories of mineral resources, namely *Measured*, *Indicated* or *Inferred* resources, reflecting decreasing levels of geological confidence are defined (Snowden, 2001). On the other hand, 'Ore Reserves' confidence classification takes into account the confidence classification of the mineral resources and does not include *Inferred* resources. Cut-off grades, economic, mining and metallurgical factors or assumptions, cost and

revenue factors, market assessment, legal, and other risk factors such as environmental, social or governmental are considered in terms of their impact on confidence in the Ore Reserve estimate (AusIMM, 1996; Snowden, 2001). A widely accepted model (Figure 5.1) for estimating reserves from resources was presented by Yamamoto (1999).

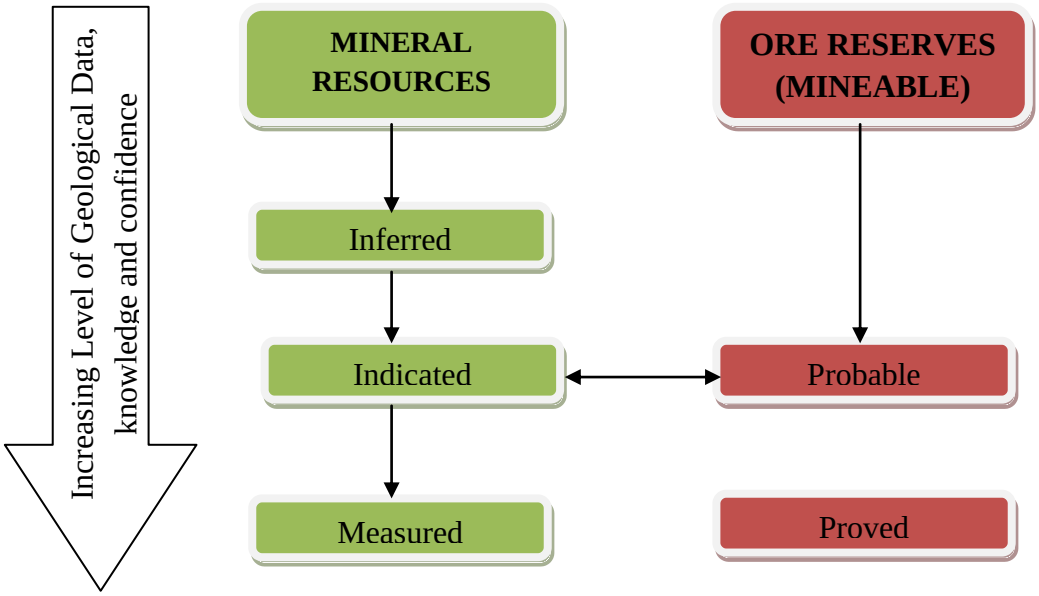


Figure 5. 1. Model for estimating reserves from resources (after AusIMM, 1996; Yamamoto, 1999)

According to this model, identified mineral resources are classified in increasing degree of assurance from inferred, indicated to measured. Actually geologist gives a figure of available resources, based on exploration data. If some technical, economical, and mining constraints are imposed, mineable reserves are recalculated within new boundary conditions. The degree of assurance is based on geological data, knowledge, and confidence (Table 5.1)

***Measures of relative Uncertainty***

Authors have used various methods to compute the estimated error and then classified estimated resource in to various classes based on this estimated error. Several authors, such as Froidevaux (1982), Isaaks and Srivastava (1989), Vallee and Cote (1992), and Wober and Morgan (1993), have proposed to compute the confidence interval using the normal theory.

Other authors (Diehl and David, 1982; Wellmer, 1983) have used the Central Limit theorem to compute the error around an estimate, because it provides a good approximation to a normal distribution. Confidence intervals based on normal distributions are computed when the number of samples is large enough (> 40) to justify its use, otherwise the *t* distribution is considered Yamamoto (1999). Author further stated that if the number of samples is less than 40, which is the general situation in ore-reserve estimation, *t* distribution must be used to compute the confidence interval using equation (5.8):

$$Error = \frac{\sigma_{ok}.t}{Z^*(x_o).\sqrt{nV}} * 100 \qquad (5.8)$$

Where $\sigma_{ok}$ is the ordinary kriging standard deviation, t is the table value of t-distribution used to compute the error around the estimate and nV is the number of discretized points in the block used to estimate $Z^*(X_0)$.

Using percentage error computed within a confidence level of 90 %, and expression (5.8), for an evaluation block, a resource classification scheme (Table 5.2) was proposed by Wellmer (1983), which is suitable for geological data as recommended by Koch and Link (1971). According to Yamamoto (1999), the above expression (5.8) is adequate for ore-reserve classification as shown in Table 5.2. Author applied this approach for resource classification in a copper deposit.

Table 5.1 Mineral Resources classes in relation to level of geological data, knowledge, and confidence (after AusIMM, 1996; Yamamoto, 1999).

| **Class** | **Level of geological data, knowledge, and confidence** |
|---|---|
| Inferred | Continuity cannot be predicted with confidence and geo-scientific data may not be known with a reasonable level of reliability |
| Indicated | Geological data gives a reasonable indication of continuity and a reasonable level of reliability |
| Measured | Reliably known; geological data confirms continuity, which allows a clear determination of shapes, sizes, densities, and grades. |

Table 5.2 Ore resource classification based on error quantification using kriging standard deviation

| | **Measured** | | | |
|---|---|---|---|---|
| | **Proved** | **Probable** | **Indicated** | **Inferred** |
| Error | ± 10 % | ± 20 % | ± 30 % | ± 40 % |
| Confidence Level | 90 % | 90 % | 90 % | 90 % |

***Kriging Efficiency***

Another resource classification method based on 'kriging efficiency' was proposed by Krige (1996). Kriging efficiency, directly linked to the kriging variance, is a number between 0 and 1 with 1 representing a perfect estimate. It is computed using expression (5.9) as

$$KE = (BV-KV)/BV \tag{5.9}$$

Where BV=theoretical variance of blocks within the domain and KV = kriging variance.

According to Krige (1996), a block kriging efficiency less than 0·3 is inferred, 0·3–0·5 is indicated and above 0·5 is measured.

## 5.6 Results and Discussion

The success of a mining operation depends on the accuracy of the tonnage evaluation and the distribution of ore grade. Choosing the proper method for estimation of reserves with a minimum error is very important in mining engineering (Shahbeik et al., 2013). Linear geostatistical estimation method such as ordinary kriging is widely used for ore grade estimation to get reliable estimates with minimum estimation variance (Tahmesebi and Hezarkhani, 2010).

A comparison of traditional methods and linear geostatistical methods was made by several workers with reference to mineral resource estimation. For example, Royle (1979) compared traditional methods of estimation such as polygonal method and geostatistical method such as ordinary kriging and stated that traditional methods produced biased estimates but not geostatistical method.

A geostatistical reserve estimation of the Itakpe iron ore deposit was undertaken by Emmanuel et al., (1993) employing conventional estimation methods viz., triangular, rectangular and cross-sectional methods. Authors have composited mineral content in each borehole to obtain the average grade for the particular borehole. The Pearson correlation coefficient was calculated for each borehole in order to establish the relationship between the grade and length of ore. As correlation exists for only five boreholes out of 29, authors have estimated the grade of each borehole by taking simple average of grades of Fe in the borehole. Though the title of their paper reflects 'geostatistical reserve estimation', neither grade nor tonnage was estimated employing geostatistical estimation method such as ordinary kriging. Though authors have computed variogram modelling, its use in grade or reserve estimation is questionable. Atleast weighted mean would have been better than simple mean while computing borehole grades. Authors have concluded that rectangular method was considered the most appropriate and accurate method in estimating the reserves of the deposit.

Geostatistical prediction of grade fluctuations of iron ore, after blasting a certain volume in El-Gedida iron ore deposit, Egypt, was carried out by Hardy et al., (1986). Authors have inferred that their study helps mining engineer to predict the grade fluctuations of different components of iron ore and to design the bench blasting dimensions accordingly.

A comparison of inverse distance, ordinary kriging and median indicator kriging estimation methods was carried out by Keogh, and Moulton (1998) in the 84 East iron ore deposit of Parabudroo mine. Authors have concluded that kriging methods gave better results as compared to inverse distance. Similarly, a computational experiment was conducted by Zimmerman et al., (1999) to compare the spatial interpolation accuracy of ordinary kriging and universal kriging and inverse distance method. In their study, they have also found that both the kriging methods consistently and substantially outperformed inverse distance method.

In general, iron ore occurs in different litho units and thus delineation of litho units in the block model is essential prior to estimation of grade. The research work on delineation of litho units of an iron ore deposit using a block model is scanty. Indicator kriging approach was employed by Chatterjee et al., (2006) for a limestone deposit for delineation of litho units. They compared OK estimates with neural networking model estimates and concluded that neural networking model outperformed OK. In this study, two approaches – geological cross sectional

model (GCM) and indicator kriging model (IK) are employed for delineation of litho units of iron ore deposit in the block model. As IK model estimates gave satisfactory results as compared to GCM, further grades maps are prepared using IK model.

Although authors (Catherine Bleines et al., 2011a; Noble, 1993; Glacken and Snowden, 2011), have expressed that the domaining of the assay data is essential for geostatistical modelling of the deposit, several authors (For ex., Rocha and Yamamoto, 2000; Asghari et al., 2009) have not considered the domaining aspect in geostatistical modeling. Catherine Bleines et al., (2011a) provided a case study of iron ore deposit in which domaining of the deposit was done based on litho units and the same method was employed in this study. The effect of domaining in kriged results of this study and in case study provided by Catherine Bleines et al., (2011a) is similar. For ex., variographic analysis showed that the semi-variogram model of domain 'ore' has a better structure than semi-variogram model of domain 'waste' and subsequently kriged estimates of Fe indicate that average grade of Fe is high in domain 'ore' than in domain 'waste'.

A comparison between ordinary kriging (OK) and non-geostatistical inverse distance weighted (IDW) estimates was recently made by Shahbeik et al., (2013) for an iron ore deposit, and observed that the error of estimation in OK method is less than that of IDW method and that the results of OK method are more robust. However, IDW estimation method was not employed in this study, but OK estimates are compared with non-linear methods.

In this section, results of ordinary kriging which include (i) the kriged estimates of the variables wFe and CV to assess the grade domains in 2D, (ii) estimated tonnage in different litho units of block model categorized using geological cross section approach, and (iii) kriged estimates of the variables Fe, SiO2 and Al2O3 for different litho units in block models categorized using *geological cross section* approach and *indicator kriging* approach, (iv) kriged results of global estimates and (v) resource classification based on global estimates are presented.

### 5.6.1 Kriged estimates in 2D

Bertoli et al., (2013) employed 2D geostatistical estimation of a 3D nickel deposit and estimated the variables such as nickel, thickness and accumulation using ordinary kriging for blocks of 10 x 10 m size with grid spacing of 20 x 20 m. They have inferred that 2-D estimates

of the deposit are very useful for mine planning purposes. In the present study, for assessing grade domains of the 3D deposit in 2D, in addition to the primary variable Fe, its coefficient of variation (CV) is also estimated using ordinary kriging (OK). Estimation of CV gives a value addition for the estimates in the form of variation in Fe, which was not considered by Bertoli et al., (2013) in their study.

It can be observed from the comparison of kriged grade (Table 5.3) with basic statistics of borehole data (Table 3.9 of Chapter 3) that, the minimum and maximum values are almost the same whereas the mean of wFe has come down from 63.71 % to 59.7 %). This may be due to estimation carried out for smaller blocks of 25 m x 25 m size using samples with average drill hole spacing of 100 m and because of conversion of 3D data to 2D data. It is interesting to note that CV of wFe has come down from 9.2 to 6.97 suggesting lesser variation of kriged estimates of Fe than that of raw data.

Table 5.3 Kriged estimates of wFe and co-efficient of variation (CV) (n=3863 blocks).

| Variable | Minimum (%) | | Maximum (%) | | Mean (%) | | CV | |
|---|---|---|---|---|---|---|---|---|
| | wFe | CV | wFe | CV | wFe | CV | wFe | CV |
| Kriged Grade | 40.53 | 0.48 | 69.63 | 45.46 | 59.7 | 15.91 | 6.97 | 10.75 |
| Kriged Std. Dev % | 0.48 | 0.72 | 7.46 | 11.16 | 3.57 | 5.40 | 1.60 | 2.40 |

It is observed from domain maps (Figure 5.2) that the deposit is broadly distributed in three zones based on the estimated Fe grade and CV. It is also inferred that the central part of the ore body has very high grade (60-70%) of Fe with a less coefficient of variation (0 – 20%). The medium grade (50-60 %) Fe is scattered in pockets and low grade (40-50%) Fe occurs only in two locations i.e., in N-W and S-W corners.

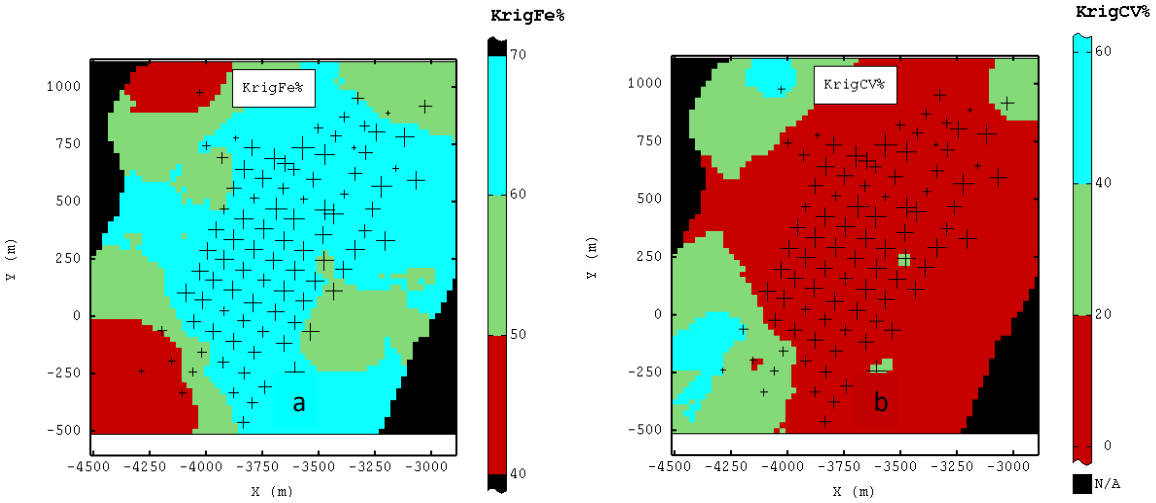


Figure 5.2 Represents grade map for kriged estimates of (a) Fe, and (b) Coefficient of Variation (CV). Broadly, 3 grade domains are observed. NE-SW trend of ore body can be clearly seen from the figures.

A correlation plot (Figure 5.3) between kriged estimates of Fe and CV shows very strong negative correlation (-0.93) between these two variables. It is observed that there is a thick cloud for the data with a cutoff grade of Fe 55 % and above, and it is scattered in other regions where Fe grade is <55 %. In totality, it can be inferred that the estimated grades in the potential zones are highly correlated with estimates of CV, which is a good indication for mining operation.

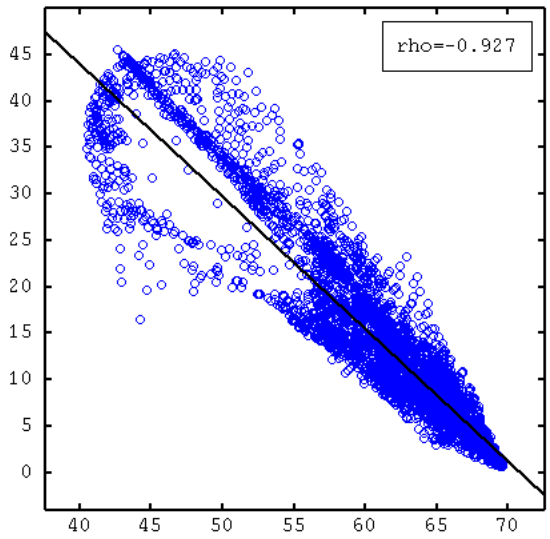


Figure 5.3 Correlation between kriged estimates of Fe and CV. The overall estimated grade of Fe has a good negative correlation with estimated CV.

### 5.6.2 Resource estimation in 3D

The results of resource estimation in 3D which includes estimated tonnage in different litho types, total tonnage of the deposit and estimated kriged grades in Fe, $SiO_2$ and $Al_2O_3$ are presented.

**(i) Estimation of tonnage**

It is observed from estimated volume and tonnage in different litho units of block model, categorized using geological cross section approach (Table 5.4) that of the total resource, the domain *ore* is ~ 362 MT and the domain *waste* is ~ 46 MT. It is also observed that the litho units BGH (36 %) and LH (32 %) are predominant litho types whereas LO with only about 2 % is scanty in the ore body of the total deposit. It is further observed that, in the total deposit the ore : waste is in the ratio of 1:0.13 which indicates that the quantum of waste is very less as compared to ore and hence very profitable for mining.

Table 5.4 The estimated volume and tonnage for different litho types

| **Litho Type** | **Volume** | **Tonnage (MT)** |
|---|---|---|
| Steel Grey Hematite (SGH) | 6,761,250 | 32,183,550 |
| Blue Grey Hematite (BGH) | 27,806,250 | 129,577,125 |
| Lateritic Hematite (LH) | 26,483,438 | 117,586,462 |
| Laminated Ore (LO) | 2,079,375 | 7,797,656 |
| Blue Dust (BD) | 24,955,313 | 74,865,938 |
| **Total (Domain *ore*)** | | **362,010,731** |
| Banded Hematite Quartzite (BHQ) | 10,470,938 | 10,470,938 |
| Shale | 35,738,438 | 35,738,438 |
| **Total (Domain *waste*)** | | **46,209,376** |

**(ii) Estimation of grades**

Several authors (Gouda and Moharam, 2001; De-vitry, 2003; Asghari et al., 2009) have employed OK method for estimation of grade variable Fe of iron ore deposit. All these authors have estimated only Fe variable and did not consider estimating the variables associated with Fe of iron ore deposit such as silica and alumina. Though silica and alumina are impurities in iron, it is necessary to estimate these variables from mining aspect to make sure that their contribution is minimum in the estimated blocks. Hence, all the variables Fe, SiO2 and Al2O3 are estimated using OK.

It is observed that in both geological cross-section and indicator kriging approaches, the kriged grade of Fe in the litho units SGH, BGH, LH and BD in Domain 'ore' are almost similar and exhibit Fe grade > 65 % (Table 5.5 and 5.6), whereas LO is different in these two approaches, exhibiting Fe grade > 65 % in geological cross section approach (Table 5.5) and 60.4 % in indicator kriging approach (Table 5.6). In case of $SiO_2$, it is observed that the kriged estimates in different litho units varying between 0.83-1.72 % in geological cross section approach (Table 5.5) and between 0.57 and 2.17 % in indicator kriging approach (Table 5.6). It is further observed that the kriged results of the litho units SGH, BGH, LH and BD in Domain 'ore' are almost similar in both the approaches and exhibit $Al_2O_3$ grade < 2 %, whereas litho unit 'LO' exhibits $Al_2O_3$ grade as > 2 %. The variations observed in domain 'waste' are not considered as this domain does not carry any significance.

Table 5.5 Kriged grades and kriged standard deviation of Fe, $SiO_2$ and $Al_2O_3$ for different litho units in the block model categorized using '*geological cross section*' approach.

| **Domain** | **Litho Type** | **Krig Fe** | **Krig StdFe** | **Krig $Sio_2$** | **Krig $StdSio_2$** | **Krig $Al_2O_3$** | **Krig $StdAl_2O_3$** |
|---|---|---|---|---|---|---|---|
| Ore | SGH | 67.11 | 1.96 | 0.83 | 0.97 | 1.02 | 0.72 |
| | BGH | 67.34 | 2.13 | 0.91 | 1.06 | 1.03 | 0.75 |
| | LH | 65.95 | 2.35 | 1.72 | 1.18 | 1.54 | 0.80 |
| | LO | 65.10 | 2.07 | 1.27 | 1.02 | 2.13 | 0.73 |
| | BD | 67.01 | 2.08 | 1.61 | 1.10 | 0.88 | 0.77 |
| Waste | BHQ | 43.45 | 7.19 | 27.45 | 8.72 | 5.35 | 4.54 |
| | Shale | 36.24 | 8.02 | 26.84 | 8.12 | 10.48 | 5.18 |

Table 5.6 Kriged grades and kriged standard deviation of Fe, $SiO_2$ and $Al_2O_3$ for different litho units in the block model categorized using '*indicator kriging*' approach.

| **Domain** | **Litho Type** | **Krig Fe** | **Krig StdFe** | **Krig $Sio_2$** | **Krig $StdSio_2$** | **Krig $Al_2O_3$** | **Krig $StdAl_2O_3$** |
|---|---|---|---|---|---|---|---|
| Ore | SGH | 67.55 | 2.03 | 0.57 | 1.91 | 1.05 | 1.35 |
| | BGH | 68.04 | 2.08 | 0.71 | 1.89 | 0.90 | 1.34 |
| | LH | 65.18 | 2.25 | 2.17 | 2.00 | 1.79 | 1.42 |
| | LO | 60.40 | 2.00 | 1.54 | 1.95 | 4.44 | 1.37 |
| | BD | 66.98 | 2.12 | 2.17 | 1.95 | 0.99 | 1.38 |
| Waste | BHQ | 52.19 | 8.02 | 21.71 | 10.62 | 0.53 | 6.10 |
| | Shale | 46.86 | 7.07 | 16.09 | 10.36 | 9.79 | 5.82 |

***Comparison of estimated grades in different methods***

The comparative results of IK model and geological cross sectional model (Table 5.7; Figure 5.4) indicate that the estimated mean grades of litho units SGH, BGH, LH and BD are almost same, whereas estimated mean grade of litho unit LO is higher by 4.6 % in case of geological model. The difference observed in estimated grades in the litho units BHQ and shale is not much significant; however these litho units are not considered as 'ore' in this deposit.

The results of kriged estimates are compared with original data by Keogh and Moulton (1998) in their study of an Australian iron ore deposit and they have found that the results of kriged estimates are in line with original data. It is observed in this study that the results of kriged estimates of litho units SGH, BGH, LH and BD are same in all the four data sets i.e. kriged estimates of geological cross section model, kriged estimates of indicator kriging model, composited data and raw data. However, estimated mean grade of litho unit LO by indicator kriging approach is matching with composited data as compared to geological cross section approach.

Table 5.7 Comparison of kriged estimates and exploratory data of Fe of in different lithological units.

| Litho type | Estimated Grades | | Exploratory Data | |
|---|---|---|---|---|
| | Geological cross-section | Indicator kriged | Composited data | Assay data |
| SGH | 67.11 | 67.55 | 67.58 | 68.19 |
| BGH | 67.34 | 68.04 | 68.05 | 68.20 |
| LH | 65.95 | 65.18 | 65.25 | 65.84 |
| LO | 65.10 | 60.40 | 60.38 | 58.55 |
| BD | 67.01 | 66.98 | 66.95 | 67.69 |
| BHQ | 43.45 | 52.19 | 53.89 | 51.40 |
| Shale | 36.24 | 46.86 | 45.09 | 40.69 |

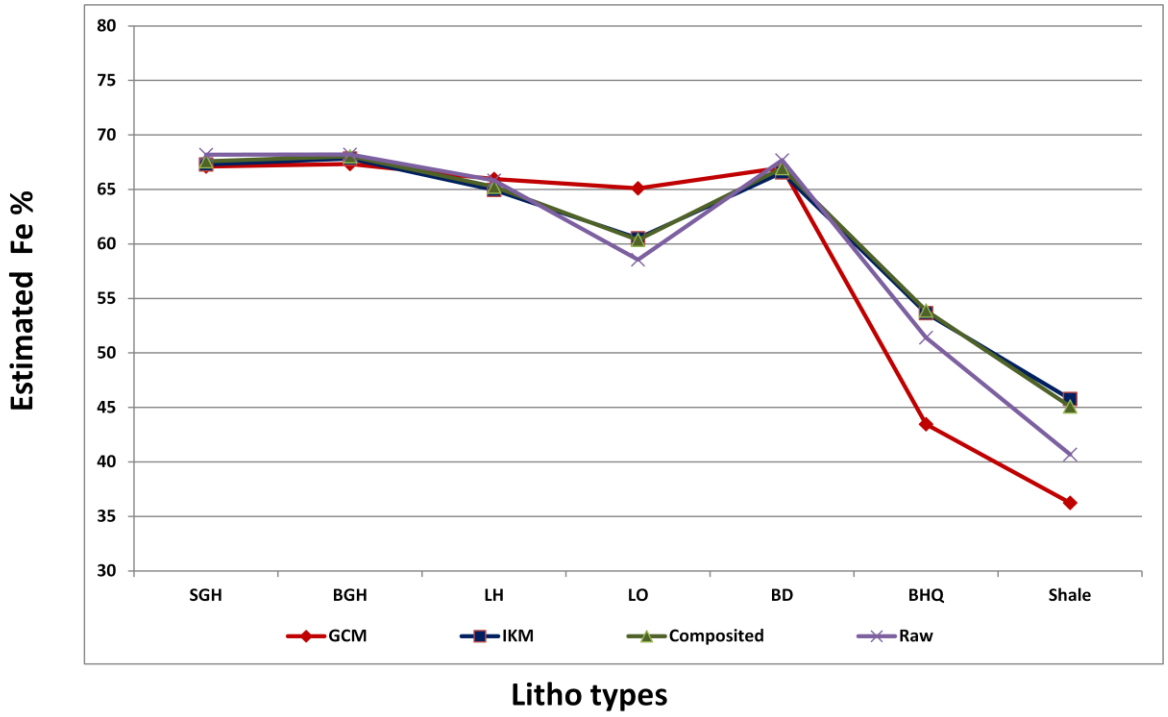


Figure 5.4 Comparative Results of Fe kriged grade in both the methods viz., GCM and IKM show that the estimated grades are matching well in all the litho units in the ore category namely, SGH, BGH, LH and BD except in case of litho unit LO where conventional estimation model differs from the remaining methods.

It is observed from the global estimates of Fe (Table 5.8) that the kriged grade of Fe ranges from 33.83 % to 69.72 % with a mean of 64.73 % and standard deviation of 3.77 %. It is further observed that the error of estimation i.e., kriged standard deviation ranges from 3.58 to 7.96 with a mean of 5.32 and standard deviation of 0.54.

Table 5.8 Basic statistics of global estimates of Fe (n=17057)

| Varible | Minimum | Maximum | Mean | Std. Dev | Variance |
|---|---|---|---|---|---|
| Kriged Grade % | 33.83 | 69.72 | 64.73 | 3.77 | 14.21 |
| Kriged Std. Dev | 3.58 | 7.96 | 5.32 | 0.54 | 0.29 |

Grade maps generated using global estimates of Fe (Figure 5.5) show that the Fe grade is distributed mostly between 65 -70 % and partly between 60-65 % in the entire deposit. The medium grade (50-60 %) Fe is scattered in pockets and low grade (40-50%) Fe occurs only in peripheral areas of the deposit and mostly in lower benches. Also to determine the error of estimates of Fe grade, the kriged standard deviation maps are generated for these twelve benches (Figure 5.6). It is inferred from figure 5.6, that the central part of the ore body has a very less kriged standard deviation as compared to peripheral areas. Majority of the blocks in each bench have estimated Fe above 55 % and very few peripheral blocks have estimated grade below 55 % in the lower benches.

The correlation coefficient between kriged grades and kriged standard deviation of Fe are plotted to find the overall correlation between kriged estimates and the error of estimates of the deposit (Figure 5.7). The kriged grades of Fe and kriged standard deviation show very strong negative correlation (-0.85). It indicates that most of the estimated grades of Fe have less error of estimate. Further, this suggests that overall, global estimates of ordinary kriging model are satisfactory.

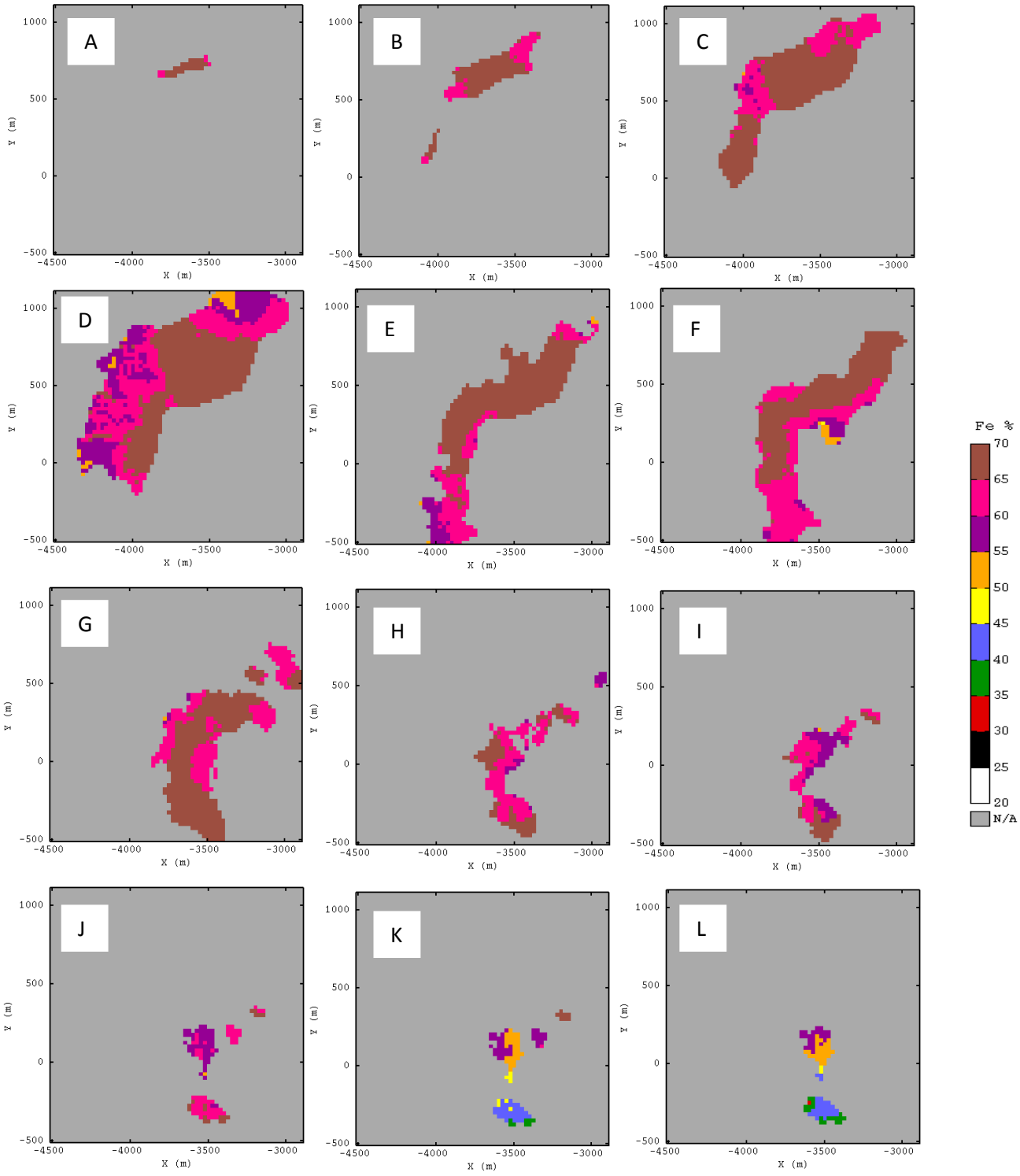


Figure 5.5 Grade maps of 12 benches of reduced levels (A)1200, (B)1164, (C)1116, (D)1068, (E)1020, (F)972, (G)924, (H)876, (I)864, (J)852, (K)840, and (L)828.

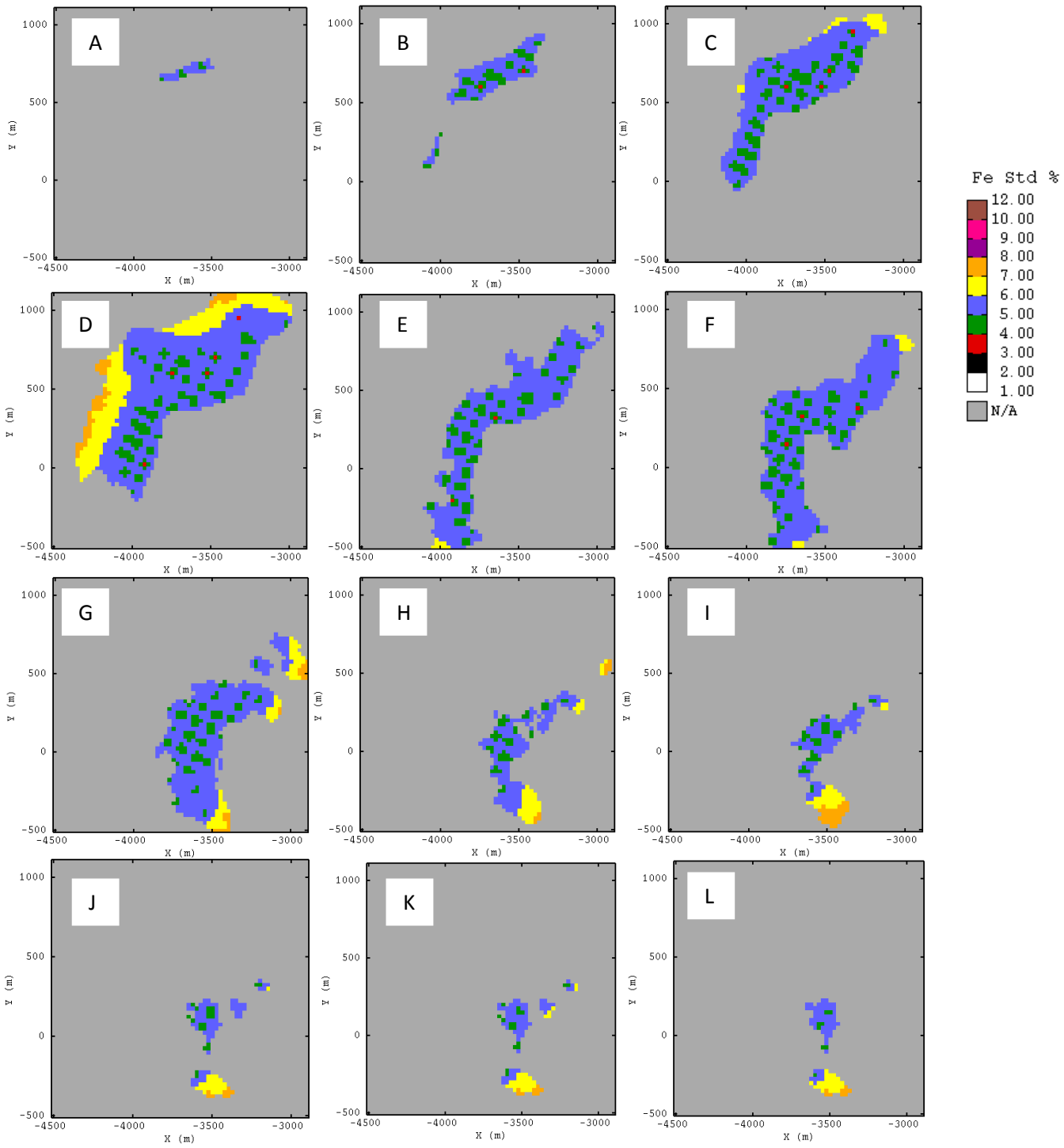


Figure 5.6 Kriged standard deviation maps of 12 benches of reduced levels (A)1200, (B)1164, (C)1116, (D)1068, (E)1020, (F)972, (G)924, (H)876, (I)864, (J)852, (K)840, and (L)828. It can be observed that only peripheral blocks have high estimation error as compared to central blocks.

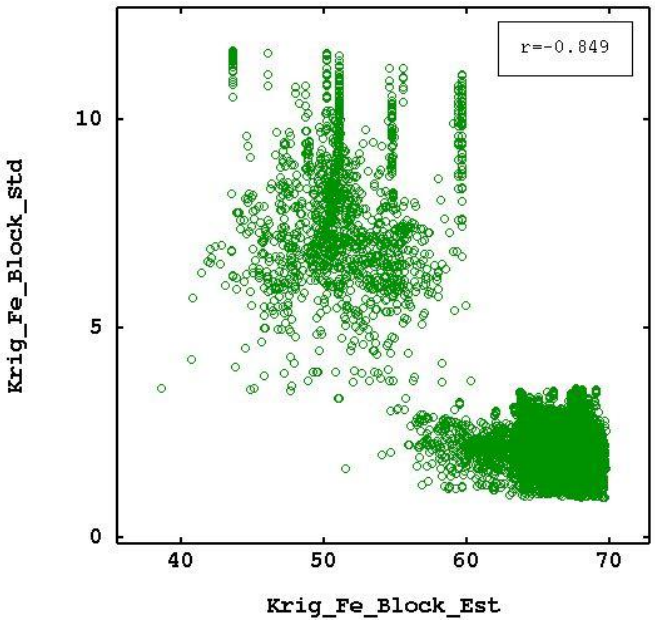


Figure 5.7 Correlation diagram between kriged grades and kriged standard deviation of Fe.

### 5.6.4 Categorization of Resources

Shahabeik et al., (2013) classified reserves in an iron ore deposit based on calculation of estimation errors employing ordinary kriging and inverse distance methods. Authors computed the estimation error proposed by Noppe (1994) using the following expression:

$$\% \text{ Error} = (1.64\sigma \times 100) / Z^* \times \sqrt{N} \qquad (5.10)$$

Where 1.64 is the value for the confidence level of 90 %, σ is the standard deviation of the estimate, Z* is the estimated grade and N is the number of samples that participated in the grade estimation. Authors have found that most estimated values by OK method have low values of errors, which are lower than 20 % as compared to ID method. Most parts of the estimated block model derived via OK method (higher than 99 %) is classified in *Measured* category. Very few blocks (0.12 %) are classified in *Indicated* category with 20 - 40 % error and (0.1 %) blocks are classified in *Inferred* category with 40 - 60 % error.

It can be observed from the basic statistics and histogram of error of kriged estimates (Figure 5.8) that the error of estimates in this study ranges from 2.27 % to 45.23 % with a mean error of 7.35 % and standard deviation of 6.39. It can be further observed from Figure 5.8 that the mineral resource classification carried out as per table 5.2, indicate that most parts (92.16 %) of the estimated block model is classified in *Measured* category with 0-20 % error. Very few blocks (5.41 %) are classified in *Indicated* category with 30-40 % error and remaining (2.39 %) blocks are classified in *Inferred* category with 40-50% error.

On the other hand, mineral resource classification carried out using kriging efficiency (Equation 5.9) of Fe show that 87.8 % of the estimated block model is classified in *Measured*, 3.11 % blocks are classified in *Indicated* category and remaining 9.08 % blocks are classified in *Inferred*' category. It is concluded from both the methods that majority of the blocks are classified as *Measured* category whose confidence of estimates is very high. Similar conclusion was also made by Shahabeik et al., (2013) in their classification of resources where 99 % are *Measured* category.

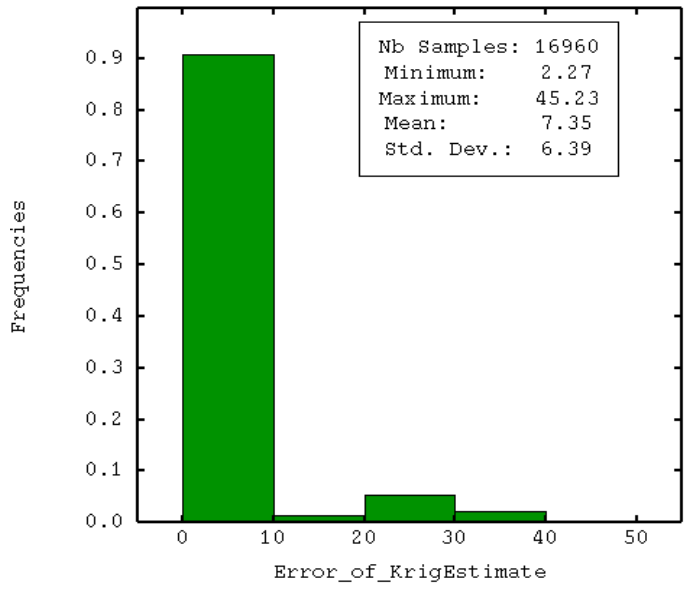


Figure 5.8 Histogram showing error of estimates computed using equation (5.8).

## 5.6 Summary

Prior to a detailed ore reserve estimation for the deposit in 3D, ore deposit evaluation of the deposit is carried out in 2D model for rapid assessment of grade domains and grade variation of the deposit. The comparison of kriged results with descriptive statistics of Fe of borehole data suggest that minimum and maximum values are almost the same whereas the mean value changed from 63.71 % to 59.7 % and CV has come down from 9.2 to 6.97 indicating lesser variation of kriged estimates of Fe than that of raw data. Domain maps (Figure 5.1) show that the deposit broadly can be distributed in to three zones depending on the estimated Fe grade and CV. It is also inferred that the central part of the ore body has very high grade (60-70%) of Fe with a very less variation (0 – 20%) (Figure 5.1). The medium grade (50-60 %) Fe is scattered in pockets and low grade (40-50%) Fe occurs only in two locations. The scatter plot between kriged estimates of Fe and CV shows very strong negative correlation (-0.93) between these two estimates (Figure 5.2). It is observed that there is a thick cloud for the data with a cutoff grade of Fe 55 % and above, and it is scattered in other regions where Fe grade is <55 %. In totality, it can be inferred that the estimated grades in the potential zones are highly correlated with estimates of CV, which is a good indication for mining operation.

For the purpose of volume and tonnage estimation in different litho units, block model that was categorized using geological cross section approach was taken in to account. It is observed that the total reserves of the domain 'ore' is ~ 362 MT and of the domain 'waste' is ~ 46 MT. It is further observed that, in the total deposit, the ratio of ore to waste is 1:0.13, which indicates that the quantum of waste is very less suggesting high profitable of mining.

Grade estimation was carried out for the attributes Fe, $SiO_2$ and $Al_2O_3$ using ordinary kriging, in both the block models i.e., block model categorized using geological cross section approach and block model categorized using indicator kriging approach. It is observed that in both these approaches, kriged grades of the litho units SGH, BGH, LH and BD in domain 'ore' are almost similar and exhibit Fe grade > 65 %, whereas LO is different exhibiting Fe grade > 65 % in geological cross section approach (Table 5.3) and 60.5 % in indicator kriging approach (Table 5.4). In case of $SiO_2$, it is observed that the kriged estimates in different litho units vary between 0.83-1.72 % in geological cross section approach (Table 5.3) and between 0.57 and 2.17 % in indicator kriging approach (Table 5.4). It is further observed in both the approaches that, the

kriged results of the litho units SGH, BGH, LH and BD in domain 'ore' are almost similar and exhibit $Al_2O_3$ grade < 2 %, whereas LO is exhibiting $Al_2O_3$ grade > 2 %. The resulting estimated model grade distributions are compared with input composited grade distributions and raw data. The comparative results of IK model and geological cross sectional model (Table 5.5; Figure 5.3) indicate that the estimated mean grades of litho units SGH, BGH, LH and BD are almost same, whereas estimated mean grade of litho unit LO is slightly higher (4.6 %) in case of geological model. The results obtained from IK modelling reflect the original drilling data and composited data as compared to the results of geological model. It is suggested that the indicator kriging approach is more suitable to assign the litho types in block model, and can be used as an alternative method to the traditionally used geological cross sectional model approach.

Based on kriged results of global estimates, Fe grade maps and Fe kriged standard deviation maps (error maps) are generated for the 32 benches in the deposit. Grade maps (Figure 5.4) show that the Fe grade is distributed mostly between 65 -70 % and partly between 60-65 % in the entire deposit. The medium grade (50-60 %) Fe is scattered in pockets and low grade (40-50%) Fe occurs only in peripheral areas of the deposit. It is also inferred from error map (figure 5.5), that the central part of the ore body has a very low kriged standard deviation as compared to peripheral areas.

The correlations between kriged grades and kriged standard deviation of Fe are plotted and observed that the kriged grades of Fe and kriged standard deviation show very strong negative correlation (-0.85), which indicates that most of the estimated grades of Fe show less error of estimate.

Mineral resource classification carried out using kriging standard deviation of Fe show that most parts (92.16 %) of the estimated block model is classified in 'Measured' category with 0-20 % error. Very few blocks (5.41 %) are classified in 'Indicated' category with 30-40 % error and remaining (2.39 %) blocks are classified in 'Inferred' category with 40-50% error. On the other hand, mineral resource classification carried out using kriging efficiency of Fe show that 87.8 % of the estimated block model is classified in 'Measured', 3.11 % blocks are classified in 'Indicated' category and remaining 9.08 % blocks are classified in 'Inferred' category.

# CHAPTER 6

# RECOVERABLE RESOURCES ESTIMATION BY INDICATOR KRIGING

# CHAPTER 6

# Recoverable Resources Estimation by Indicator Kriging

## 6.1 Introduction

Recoverable resources are the portion of in-situ resources that are recovered during mining. Estimation of recoverable resources is one of the most critical aspects of modern mining geology. The accurate assessment of the tonnage and grade of run of mine ore, may be the difference between a healthy profitable operation and an expensive early mine closure (Lipton et al., 1998).

The concept of recoverable resources involves both technical considerations, such as cut-off grade, SMU definition, machinery selection etc., and also economic/financial considerations such as site operating costs, commodity prices outlook, etc (Vann and Guibal, 1998; Vann et al., 2000). In this study, only technical factor cut-off grade is considered. Recoverable resources can be categorised as either global or local recoverable resources. According to Vann and Guibal, global recoverable resources are estimated for the whole field of interest; e.g., estimation of recoverable resources for the entire orebody (or a large well-defined subset of the orebody like an entire bench), whereas the local recoverable resources are estimated for a local subset of the orebody; e.g., estimation of recoverable resources for a block. In this study, global recoverable resources are estimated for the whole deposit and local recoverable resources for a block of 25m x 25m x 12m.

In the context of recoverable resources estimation, the requirement is not to estimate the grade of each block, but to estimate the proportion of in-situ resources exceeding some threshold or cut-off of grade, that are recovered during mining (Journel, 1985). For this, it is required to estimate the probability distribution of grade rather than simply an average grade value for each block. This cannot be accomplished by applying linear estimator like Ordinary kriging (OK). Further, ordinary kriging is not a suitable option for highly skewed data such as Fe (Badel et al., 2011). When the grade distributions show near normal shape, a linear estimator is ideal. However, when the grade distribution is highly skewed or contains a mixture of populations, the

underlying assumption of linear estimation methods such as ordinary kriging can be invalidated. In such cases, non-linear estimation methods can deal appropriately with these more complex distributions (Isaaks and Srivastava, 1989). The specific problem of dealing with skewed distributions and estimating recoverable resources was the origin of non-linear geostatistical estimation (Matheron, 1976b; Journel 1982; Vann and Guibal, 1998).

In geostatistical applications, non-linear estimation is to estimate the conditional expectation, and further the conditional distribution of grade at a location, as opposed to simply predicting the grade itself. In this case, we estimate the mean grade (expectation) at some location under the condition that we know certain nearby sample values (conditional expectation). In non-linear geostatistical estimators, non-linear functions of the data to obtain the conditional expectation through the probability distribution are employed.

$$P[\ Z(X_v) \mid Z(X_i)]$$

i.e., the probability of the grade at location (block) $X_V$ given the known sampling information at locations $Z(x_i)$ (i.e. $Z(x_1)$, $Z(x_2)$ ….$Z(x_N)$. This is the conditional distribution of grade at that particular location. Once the probability distribution is known, grade tonnage relationships (eg. "how much of this block is above a cut-off $Z_C$ ?) can be estimated.

In geostatistics, there are different non-linear methods such as disjunctive kriging (DK) (Matheron, 1976; Armstrong and Matheron, 1986a, 1986b); indicator kriging (IK) (Journel and Huijbregts, 1978; Journel, 1982, 1988), and variants of indicator kriging (multiple indicator kriging; median indicator kriging, etc.); probability kriging (PK) (Verly and Sullivan, 1985); lognormal kriging (LK) (Dowd, 1982); multigaussian kriging (MK) (Verly and Sullivan, 1985, Schofield, 1989a, 1989b); uniform conditioning (UC) (Rivoirard, 1994; Humphreys, 1998); and residual indicator kriging (RIK) (Rivoirard, 1989). In particular, non-linear methods such as indicator kriging (IK), disjunctive Kriging (DK), uniform conditioning (UC), service variables (SV) and conditional simulation are more useful for estimation of recoverable resources (Didier, 2010; Catherine Bleines et al., 2011a; Rambert, 2014). Non-linear methods employed in this study are (i) indicator kriging, (ii) disjunctive kriging and (iii) conditional simulations. In this chapter, estimation of recoverable resources using indicator kriging is discussed.

Based on the work of Switzer (1977), Journel and Huijbregts (1978) have introduced indicator kriging (IK) method to estimate recoverable resources. IK method has been widely in non-linear grade resource estimation, despite the complexity of application. Many researchers (Clark, 1993; Hill et al., 1998; Marinoni, 2003; Mendes and Lorandi, 2006; Tavares et al., 2008; Gholamnejad et al., 2010; Badel et al., 2011) have applied the IK method in various mineral deposits.

The IK method is non-parametric and does not rely upon the assumption of a particular distribution model. It is one of the few techniques that address mixed data populations (Jones, 1998). Indicator kriging was introduced to infer a model for the conditional cumulative density function (cdf), e.g., the recovered tonnage and quantity of metal above the cut-off (Perez, 1988). Indicator kriging is used to estimate the proportion of the ore body above a certain cut-off grade by considering weighting factors for the data above the cut-off grade. In general, Indicator kriging can be applied in two ways - (i) multiple indicator kriging (MIK) which performs the kriging of the indicator variables with their own variograms, independently for the different cut-offs, and (ii) median indicator kriging (median IK) based on assumption that all the indicator variables have the same variogram i.e., the variogram of the indicator based on the median value of the grade. Multiple indicator kriging is very time consuming as it requires a separate variographic analysis for each cut-off, and also requires considerable amount of data for each cut-off during modelling. Therefore, median indicator kriging has been proposed as an alternative approach (Hill et al., 1998).

Various researchers have applied the median indicator kriging (Journel and Huijbregts, 1978; Journel, 1982; Glacken and Blackney, 1998; Vann and Guibal, 1998; Gouda and Moharam, 2001). According to Glacken and Blackney (1998), median IK might be considered in early stage of resource estimation, where sample data is sparse and is difficult to define the grade continuity for a full range of indicators. Four steps are involved in the application of median indicator kriging: (i) Indicator transformation of raw data, (ii) calculation of median indicator semi-variogram, (iii) median indicator kriging, and (iv) indicator post-processing.

As the Bailadila iron ore deposit shows mixed distribution, applying a linear estimator (such as an ordinary kriging) may give inaccurate local estimates. Thus, IK was initially selected

as the preferred non-linear method of recoverable reserves estimation and subsequently disjunctive kriging and conditional simulation are applied.

In general, for economic evaluation of the deposit, all the variables of iron ore deposit viz., Fe, $SiO_2$ and $Al_2O_3$ at a given cut-off grade are evaluated. In linear estimation methods that produce whole block estimates, this is possible and ideal but for non-linear methods such as MIK some difficulties arise (Lipton et al., 1998). According to Lipton et al., (1998), MIK is a probabilistic method that defines the distribution of grades of samples within each search window, providing a discrete approximation to the Conditional Cumulative Distribution Function (CCDF) for each block. Authors further state that the spatial relationships between the variables must be retained in the representations of the individual CCDFs whenever multiple variables are considered. That is, the model should provide estimates of each variable for the same portion of the CCDF, which is not possible. Thus, in MIK interpolation, the local CCDFs are usually based on one variable, for which multiple indicator parameters are modelled. Thus, in the present study, due to importance of iron content, Fe variable is considered for MIK analysis.

## 6.2 Indicator transformation

The grade estimation by non-linear geostatistical methods such as indicator kriging requires indicator transformation, whereas disjunctive kriging and simulation methods require Gaussian transformation. Further, modelling, estimation and simulations are carried out on the transformed data instead of original raw data.

The concept of indicator transformation has been proposed by Journel (1983b) in estimation of spatial distribution. Indicator transformation is a transformation applied on a set of variables whose values are modified according to a non-linear transform, and it transforms each value of the set of variables into indicator values i.e. 0s and 1s (Deutsch and Journel, 1998). The main advantage of the indicator transformation is that it is non-parametric and does not follow any distribution pattern. In this study, indicator transformation is applied to both - categorical variables i.e., lithological units for delineating litho units in the deposit (see chapter 4), and to grade variable ‘Fe’ for estimation of recoverable reserves with different cut-offs.

The indicator transformation is the binomial coding of Fe data into either 1 or 0 depending upon its relationship to a given cut-off value *Zc*. For a given Fe value *Z(x)* at location 'x' is expressed as (Dimitrakopoulos, 1997); which is a non-linear transformation

$$I_k(x) = 1 \quad \text{if } Z(x) \geq Z_c \tag{6.1}$$

Otherwise it is 0 (zero), if $Z(x) < Z_c$

values which are much greater than a given cut-off $Z_c$, will receive the same indicator value as those values which are only slightly greater than that cut-off. Thus, indicator transformation of data is an effective way of limiting the effect of very high values and by definition does not contain extreme values (Vann and Guibal, 1998). Indicator transformation allows common coding of diverse data types and their integration into the single process. Since all data is transformed to 0→1 space (Glacken and Blackney, 1998). The transformed data thus form a binomial distribution, having mean m=p and variance $\sigma^2$= p(1-p), where p is the proportion of 1's as defined in equation 6.1 (for example, if the cut-off, $Z_c$ is equal to the median of the grade distribution, *p* takes a value of 0.5, and the maximum variance is defined as 0.25).

***Choice of cut-off's / thresholds***

Indicator transformation is applied on the whole bench composited data, and the 'k' number of thresholds '$I_n$' for different cut-off values $Z_c$, where n=1, 2, …, k are defined according to the number of samples and based on the distribution of assay data (Mendis and Lorandi, 2006). While applying indicator kriging to resource estimation, a finite number of thresholds that adequately represent the input data distribution are chosen (Glacken and Blackney, 1998). Isaaks and Srivastava (1989) and Jones (1998) suggest that the thresholds are chosen from the histogram such as deciles, i.e, the indicators $I_1$, $I_2$, $I_3$….. $I_9$ have thresholds of the 10th, 20th, 30th … 90th percentiles. An alternative method for choosing the thresholds was also suggested by Isaaks and Srivastava (1989), where the choice of thresholds depends on the distribution of data and more number of thresholds can be included at the location where data is dense.

In this study, the detailed grade distribution of Fe for the bench composited data is computed using histogram (Figure 6.1) of class interval '1' for the purpose of choosing cut-off values.

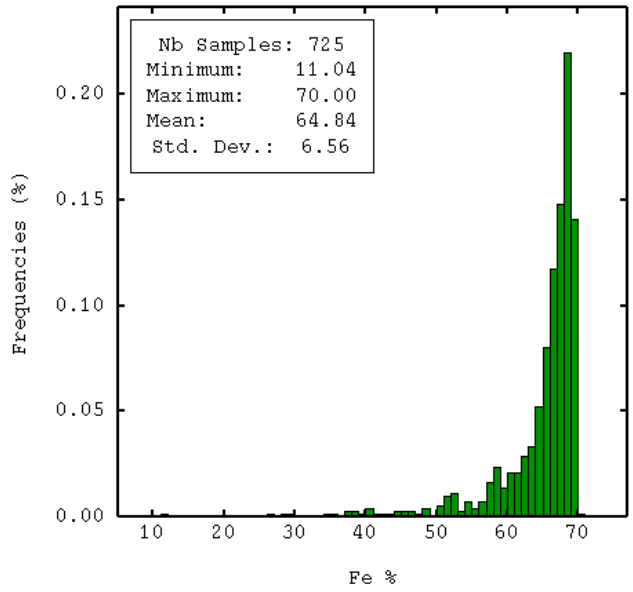


Figure 6. 1 Grade distribution of Fe composited data with class interval of 1.

It is observed from the histogram that about 50 % of composited data has greater than 67 % Fe (~ median value). It is further observed that only 2 % of samples are present below the $40^{th}$ percentile of Fe grade. Thus, there is a disadvantage in choosing deciles based thresholds because first four thresholds are of no use and it is not possible to define the continuity of grades for thresholds set below the $40^{th}$ percentile of Fe grade as only ~ 2% of samples are present.

Based on this observation, instead of decile choice of cut-offs, a total number of eight thresholds (one threshold at median value of Fe, five thresholds below median value of Fe, and two thresholds above median value of Fe) are taken in the present study. The details of these eight cut-offs are - first cut-off $I_1$ is taken as 45 % because it is the cut-off grade in this deposit to distinguish between *ore* and *waste*. The cut-off grade below 45 % is not considered as only about 8 % of data is below Fe 45 %. Four cut-offs $I_2$ , $I_3$, $I_4$ and $I_5$ below the median grade of Fe (67.2 %) are selected which constitute 55 %, 60%, 62% and 65 % Fe. Close to median grade of Fe, a cut-off $I_6$=67 % Fe is taken. Lastly, two cut-offs $I_7$ and $I_8$ are taken above the median grade of Fe which are 68 % and 69 % Fe respectively.

In total eight cut-offs viz., 45 %, 55 %, 60 %, 62 %, 65%, 67 % , 68 % and 69 % Fe in the indicator kriging study of this deposit are chosen. Indicator transformation has been done for Fe bench composited data using equation (6.1) for all these eight thresholds and data is

transformed into 0s and 1s. These transformed data have been used in variography and estimation of resources by IK and are presented in sections 6.3 and 6.4.

## 6.3 Indicator semi-variogram

The indicator semi-variogram for a specified cut-off grade $Z_c$ represents the spatial variability of samples with grades exceeding $Z_c$. The indicator semi-variogram can be defined (Journel, 1982; Lemmer, 1984a; Gouda and Moharam, 2001) as

$$\gamma\,(h) = 0.5\ E\ [(I(x+h,\ Z_c) - I(x\ ,\ z_c))^2] \qquad (6.2)$$

Indicator semi-variograms computed using equation 6.2 are more structured than normal variograms because they are computed on the transformed data i.e., 0s and 1s.

The practice of IK involves calculating and modelling of indicator semi-variograms for each cutoff or threshold considered during indicator transformation to cover the range of the input data (Gholamnejad et al., 2010). This approach is termed 'multiple indicator kriging' (MIK). However, this method is time consuming. So the best variation computing is obtained for a cut-off value equal to (or close to) the median computed from the sample set as suggested by Isaaks & Srivastava (1989). One approximation is to simply infer the indicator semi-variogram for the median of the input data and to use this indicator semi-variogram for all cut-offs during estimation. Since the variogram used in this approximation to indicator kriging is based on the median indicator, it is referred to as 'median indicator kriging'. Median indicator semi-variogram is considered to be 'representative' of the indicator semi-variograms at other cut-offs. In this study, median indicator semi-variogram is considered and subsequently median indicator kriging is employed for estimation of recoverable reserves.

### *Median indicator semi-variogram*

In the present study, median indicator semi-variogram is calculated for indicator transformed data of Fe with a cut-off 67 % (which is close to median value 67.2 %) using equation 6.2 . The experimental indicator semi-variogram is calculated in horizontal direction with 12 lags of 50 m and in vertical direction with 15 lags of 12 m respectively. The indicator semi-variograms in both the directions are modelled using a small nugget effect and two nested

structures. It is observed that the median indicator semi-variogram models of Fe in both the horizontal and vertical directions (Figure 6.2) show a very good structure with a small nugget effect. Anisotropy is observed in both the directions with ranges 320 m and 60 m respectively (Table 6.1). This median indicator semi-variogram model is further used in median indicator kriging.

Table 6.1 Median indicator semi-variogram modelling parameters in horizontal and vertical directions.

| Direction | Model-1 | Model-2 | Range-1 | Range-2 | Sill-1 | Sill-2 | NE |
|---|---|---|---|---|---|---|---|
| Horizontal | Spherical | Spherical | 40 | 320 | 0.1 | 0.09 | 0.06 |
| Vertical | Spherical | Spherical | 35 | 60 | 0.11 | 0.02 | 0.06 |

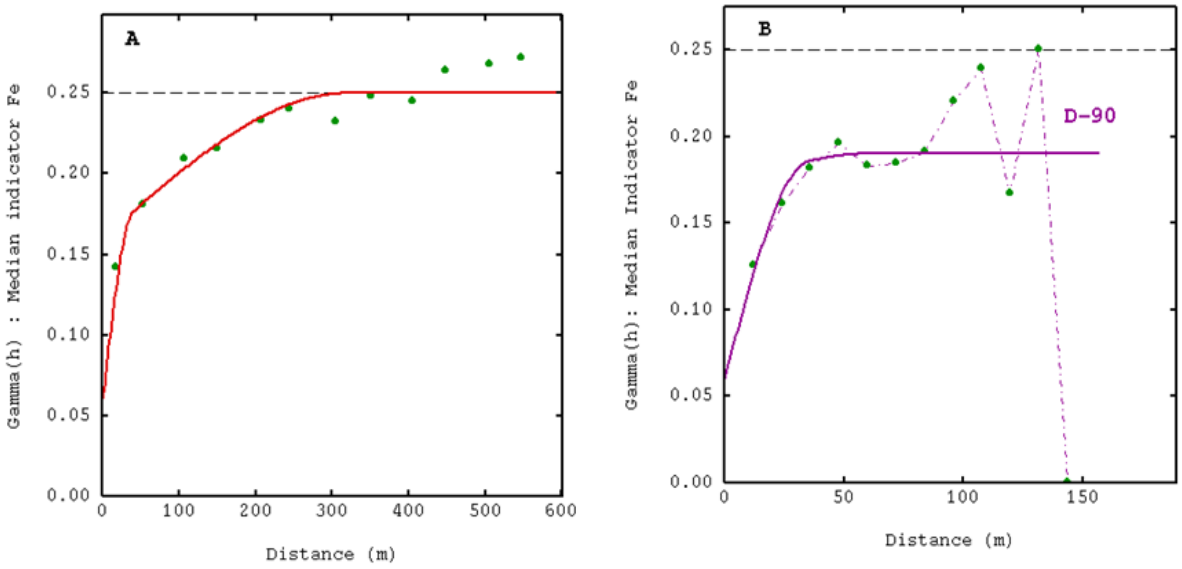


Figure 6.2 Showing median indicator semi-variogram models in horizontal (A) and vertical direction (B).

## 6.4 Estimation of recoverable resources using median indicator kriging

Median Indicator kriging is a process of kriging (estimating) each block using indicator transformed values and the median indicator semi-variogram. In general the kriging employed in median indicator kriging is ordinary kriging (OK). Ordinary kriging of a set of indicator-

transformed values provides an estimated value between 0 and 1 for each block estimate, which can be interpreted either as (Isaaks and Srivastava, 1989) - probabilities (the probability that the grade is above the specified indicator) or as proportions (the proportion of the block above the specified cut-off).

In this way, median indicator kriging is not creating a single value for the entire block, but rather describing the amount of material in the block above a given cut-off. The outcome of median IK is a conditional cumulative distribution function (ccdf) of estimates. Several cut-off s are selected and the cut-off classes vary from block to block to reflect the local variability of the samples within the search volume (Lipton et al., 1998). After the CCDFs are estimated at each block centroid, the model is further processed to provide probabilities and grades within blocks, for a range of given cut-offs that cover the range of potential mining cut-off grades.

In this study, as mentioned in section 6.2, eight cut-offs for Fe grade viz., 45 %, 55 %, 60 %, 62%, 65%, 67 %, 68 % and 69 % are chosen. Block model and neighbourhood parameters considered in this analysis are the same that are used in linear geostatistical analysis. The median indicator kriging technique gives the cumulative tonnage of the whole area above each of these eight cut-offs. Indicator kriged statistics of Fe for different cut-offs are calculated. Probability maps were produced in each level for the whole deposit for different cut-offs of Fe. Further, recoverable resources estimates are obtained using grade-tonnage curves generated from the probabilistic distribution model of indicator kriging and performing indicator post-processing.

## 6.5 Indicator post-processing

After indicator kriging, the indicator post-processing for estimation of recoverable reserves based on the IK estimate is carried out. IK generates conditional probabilities for a restricted set of specified cut-offs. In indicator post-processing, starting from these probabilities, the cumulative density function (cdf) of tonnage for each block is rebuilt, in order to derive the tonnage and grade for a new set of cutoffs. This enabled to calculate the probability for the variable to exceed any cut-off or to calculate the average value of the variable above or below this cutoff (Deutsch and Journel, 1992). For this purpose, two important parameters 'histogram interpolation' and 'Volume Correction' are defined.

### 6.5.1 Histogram Interpolation

Cumulative density functions are always available at a discrete number of cutoff values. Assumptions must be made for extrapolation beyond the smallest cut-off value (lower tail), the largest cut-off value (upper tail), and for interpolation between two consecutive cut-offs data.

An indicator kriging provides an estimate of the proportion (or probability) of a block above each of the indicator grades or thresholds assessed. Thus, kriging the indicators for a given location produces a result between 0 and 1 which cannot be transformed back to a sample grade (Khosrowshahi et al., 1998). To reduce this data into an estimate of grade above a cut-off or mean block grade (E-type estimate), it is a requirement that each indicator class interval be assigned a grade. A number of sensitivities must be considered when undertaking the task of class interval grade assignment (Gholamnejad et al., 2010).

If indicator cut-off grades have been carefully selected with adequate regard to the input grade distribution, then the distribution of grades within many classes will be nearly linear. The average grade of the input data or of the bounding indicator grades will normally suffice for the assignment of grade in these classes (Glacken and Blackney, 1998). However, the distribution of sample grades in the uppermost (above the highest grade threshold of the indicators) and lowermost (below the lowest threshold of the indicators) grade classes of the distribution will not normally be linear and therefore require special treatment. In the case of a negatively-skewed grade distribution, such as Fe, the greatest estimation sensitivities relate to the grade assigned to the lower most class. Skewed distribution and grade outliers both influence the grade distribution in this class, which requires a more sophisticated method of mean grade selection to avoid over-estimation or under-estimation of grade. Deutsch and Journel (1992) propose a modelling method based upon a hyperbolic distribution for representing the grade distribution above the uppermost indicator grade. The class mean grade calculated by this method is dependent upon the rate of decay of the hyperbolic function and the upper grade limit applied to the grade distribution. Authors further proposed a power model for the estimation of lower class. The power model was used for the lowest class estimate because, even though the class is the lowest class, the grades are still of economic interest (Jones, 1998).

In this study, the upper class was estimated using a linear model and lower class was estimated using power model with a 'p' value of 3.5. An attempt was made to estimate upper class using hyperbolic model but the estimates were erroneous and abnormal. Several attempts were also made to estimate lower class using different values of 'p' and finally a pvalue of 3.5 provided a relatively good fit to the data and found to be suitable. As suggested by Glacken and Blackney (1998) distribution of grades within the classes are estimated using linear model.

### 6.5.2 Correction for the volume-variance relationship

While estimating recoverable resources, the variance of grades based on selecting mining unit (SMU) support, as opposed to sample support, is important. The SMU block size represents the smallest practically mineable volume that can be extracted, at the grade control stage. The variance of the SMU grades will be smaller than the variance of the samples. In order to convert the prior CCDFs based on sample support to posterior CCDFs reflecting SMU support, a 'volume or variance correction' is required. However, Khosrowshahi et al. (1998) state that there is no theoretical evidence that the change of support correction has correctly modelled the impact of effective SMU size in IK approach. Authors have strongly recommended for using conditional simulation for the effective results while dealing with SMU sized blocks. Against this background, SMU size blocks are not considered in this study and hence no change of support is required. However, SMU size blocks are considered during conditional simulation.

### 6.5.3 Grade -tonnage curves

The IK method allows resource estimates to be reported mainly in two ways – (i) grade-tonnage curves for QTM (Metal quantity, Tonnage, Mean grade) variables and (ii) E-Type estimates ('E' stands for expectation i.e., mean) for the whole deposit (Lipton et al., 1998). For given cut-offs, indicator kriging method provides the estimates of the recoverable resources, in the form of the total or recovered tonnage T, the metal quantity Q, and the mean or recovered grade M (Geovariances 2013a, 2013b).

***Total or Recovered tonnage (T):***

The total tonnage is expressed as the percentage or the proportion of blocks that have a grade above the given cut-off. Mathematically, $1z_i \geq z_c$ is the recovered proportion of tonnage for a single block (it is 1 if $Z_i \geq z_c$ and 0 otherwise). The average proportion of all the blocks is

the total or recovered tonnage of 'ore' expressed as a proportion which is given by the following equation (Rivoirard, 1994):

$$T(z_c) = E[1z_i \geq z_c] = 1/N \sum 1z_i \geq z_c \quad (6.3)$$

Similarly, the tonnage of 'waste' is obtained using other indicator: $1z_i < z_c$.

As $1z_i \geq z_c + 1z_i < z_c = 1$, we have the following decomposition :

$$1/N \sum 1z_i \geq z_c \text{ (ore)} + 1/N \sum 1z_i < z_c \text{ (waste)} = 1$$

***Metal quantity (Q):***

The metal quantity (also referred sometimes as the 'metal tonnage') is the quantity of metal relative to the tonnage proportion T for a given cut-off grade. The recovered quantity of metal for a single block labeled i is proportional to $Z_i$ if the block is selected that is the indicator is equal to one: $1z_i \geq z_c = 1$ and is zero otherwise. So quantity of metal is the product $Z_i \,.\, 1z_i \geq z_c$ . It is expressed for the total deposit as (Rivoirard, 1994)

$$Q(z_c) = E[Z_i \,.\, 1z_i \geq z_c] = 1/N \sum Z_i \,.\, 1z_i \geq z_c \quad (6.4)$$

***Mean or Recovered grade (M):***

The mean or recovered grade (M) in the total deposit is the average grade of all the blocks whose mean grade is above the given cut-off. As a function of the cut-off $Z_c$ , the recovered grade is given by the following equation (Rivoirard, 1994):

$$M(z_c) = E[Z_i \mid Z \geq z_c] = Q(z_c) / T(z_c) \quad (6.5)$$

All the three variables are related by the equation Q = T x M. (6.6)

Although all the three variables Q, T, and M are computed, only the results on total tonnage (T) and mean grade (M) are presented, and metal quantity (Q) is not considered as there is no significance of this parameter in the iron ore deposit. The basic statistics of indicator kriged results for total tonnage and mean grade for different cut-offs are presented in tables 6.2 and 6.3 respectively.

Basic statistics shown in Table 6.2 and 6.3 provide the recovered tonnages and mean grade for a fixed number of cut-offs i.e 45, 55, 60, 62, 65, 67, 68 and 69 % Fe. Keeping in view

of the market dynamics, it is required to know the recovered tonnages for any cut-off, i.e., a continuous model is needed. For this, non-linear geostatistical methods such as indicator kriging and disjunctive kriging provide a tool called 'grade tonnage curves'. Based on indicator kriged estimates, the grade tonnage curves (i) cut-off grade vs total tonnage, and (ii) cut-off grade vs mean grade are calculated and presented in Figure 6.3 and 6.4 respectively.

### 6.5.4 E-type estimates

E-type estimate is the mean value of the conditional cumulative density function (ccdf), and the standard deviation of the variable the input indicators are derived from. Estimates are calculated on the cumulative density function interpolated for each block from the indicators and without applying any cutoff (Lipton et al., 1998; Catherine Bleines, 2011a, b). In other words, The E-type estimate is simply the average grade of the block determined by weighting the grade in each cut-off class using the probability for that class. While assessing the resource in terms of E-type estimates, it is assumed that the entire block has a single grade and that selective mining is not possible. Once a cut-off grade is applied, the E-type estimate incorporates high dilution and high ore loss (Lipton et al., 1998). Statistical parameters of E-type estimates of IK are provided in Table 6.4. Based on E-type estimates, grade maps and standard deviation maps are generated for the 32 benches of the deposit and results are presented for typical 12 benches in Figure 6.6 and 6.7 respectively.

## 6.6 Results and Discussion

For recoverable resource estimation, unlike ordinary kriging, inverse distance and other linear estimation methods, one cannot average sample data linearly, and thus cannot obtain a block distribution by averaging a series of point distributions. The ordinary kriging outcome is to discretise a block by a series of points, estimate the grade at each point (or sub-block), and carry out the arithmetic mean to derive the block grade. Whereas, in IK approach, block is subdivided in to sub-blocks (actually points), estimated the cdf by MIK at each point based on a cut-off grade, and then the distribution results are averaged based on the cut-off, to derive the tonnage and mean grade of each block (Glacken and Blackney, 1998). Thus IK approach is more accurate than OK for recoverable resource estimation.

Median Indicator Kriging method was used by Keogh and Moulton (1998) for grade estimation of an iron ore deposit, which was originally estimated by non-geostatistical inverse distance technique. Authors have applied median indicator kriging using two medians to represent the ore and banded iron formation (BIF) populations, to try to improve the estimates of Fe and $SiO_2$ in the geological model. A comparison was made between the results of inverse distance, ordinary kriging and median indicator kriged estimates. They have also compared these estimates with original data distribution (Drill hole composites). Authors have concluded that each method has a different effect on geological block model grade distributions and local grade estimates. In total there was an improvement from ID to the kriged models.

A comparison between cumulative ore reserves resulting from the indicator kriged model and ordinary kriged model was performed by Gouda and Moharam (2001) in an iron ore deposit. Authors have concluded that the average iron content of the recoverable tonnage at each cut-off was higher with indicator kriging than with ordinary kriging and low iron content values have only a small effect on the recoverable ore estimate. However, authors have neither attempted to validate the results with any other non-linear method nor compared with original data. No proper conclusion about the superiority of IK results as compared to OK were given in the paper.

To determine ore/waste boundary in an iron ore mine, Gholamnejad et al., (2010) used indicator kriging method. Authors have assumed the cut-off grade of 20 % for iron and generated probability maps using IK method. Comparison of resultant probability maps with the real ore/waste boundaries on the extracted levels showed that block with the probability of more than 0.85 lay within the ore body and remaining blocks can be considered as waste. This approach was applied to the rest of levels and estimated that the total amount of remaining iron ore.

The application of median indicator kriging and neural network in modelling mixed population in an iron ore deposit was carried out by Badel et al., (2011). To compare the results, authors have plotted scatter diagrams between the data (x-axis) and the respective MIK and ANN estimates (y-axis). They have concluded that the MIK estimates have a better local precision than the ANN estimates as quantified by a higher regression slope and R value associated with MIK scatter plot. And by comparison of both ANN and MIK results around the drill holes, it has been recognized that the MIK estimates are more similar to the raw data in drillholes and thus MIK procedure has been more affected by variability of the grades rather than the ANN estimates.

The results of indicator kriged estimates such as statistical parameters of recovered tonnage and mean grade for different cut-offs, grade-tonnage curves, statistical parameters of E-type estimates, grade maps and standard deviation maps based on the E-type estimates are presented in this chapter. However, a comparison of grade tonnage curves obtained from various methods viz., ordinary kriging, indicator kriging and disjunctive kriging are presented in Chapter 7.

### 6.6.1 Basic statistics of indicator kriged estimates

The cut-off grade considered in iron ore deposit to classify the mineral as 'ore' is 45 % Fe as per (Indian Bureau of Mines) IBM guidelines. In this study, it is observed from Table 6.2 that the total recovered tonnage is 97 % with a cut-off of 45 % Fe. Thus only 3 % of tonnage is estimated as 'waste' whose Fe is < 45 % in the deposit. It can be further observed from Table 6.3 that for a cut-off of 45 %, Fe content ranges from 45.50 % to 69.5 % with a mean of 65.19 %. The grade between 45 % and 55 % Fe is considered as 'sub-grade' in iron ore deposit (IBM, 2012) which is about 6 % in this case. In the existing working mines of NMDC of the Bailadila region, the high grade material is beneficial in two ways – blending with low grade material i.e. Fe grade < 45 % or selling directly with out blending with low grade which results in getting incentive in price, which is decided between NMDC and buyers. It is observed that about 50 % of the blocks have greater than 67 % Fe, with a mean grade of 68.4 % and about 15 % of blocks have greater than 69 % Fe with a mean grade of 69.50 % (Table 6.2 and 6.3). These blocks will fetch additional revenue to NMDC in the form of incentive as practiced in the existing working mines nearby to this deposit.

IK generates a cumulative distribution function (cdf) for each block with a non-decreasing value between zero and one. These requirements are sometimes not met, (for example, because of negative weights) leading to so-called '*order relations*' problems (Glacken and Blackney, 1998). Hence, the results need to be corrected. Various researchers have proposed different methods to solve the order relations issue – the most commonly-used involves direct correction of the indicator values (eg. Deutsch and Journel, 1998, p.82). It consists of the average of an upward and a downward correction of the cdf. It can be observed from Table 6.2 that the minimum and maximum values of tonnages are 0 and 1 respectively for all the cut-offs. This indicates that, in this study, no '*order relation*' problems were observed.

Table 6.2 Basic statistics of indicator kriged estimates for different cut-offs for recovered tonnage T (n=17057)

| Cut-off % Fe | Minimum | Maximum | Mean | Std. Dev | Variance |
|---|---|---|---|---|---|
| 45 | 0.00 | 1.00 | 0.975 | 0.064 | 0.004 |
| 55 | 0.00 | 1.00 | 0.915 | 0.141 | 0.020 |
| 60 | 0.00 | 1.00 | 0.854 | 0.185 | 0.034 |
| 62 | 0.00 | 1.00 | 0.807 | 0.202 | 0.041 |
| 65 | 0.00 | 1.00 | 0.693 | 0.245 | 0.060 |
| 67 | 0.00 | 1.00 | 0.505 | 0.287 | 0.082 |
| 68 | 0.00 | 1.00 | 0.358 | 0.279 | 0.078 |
| 69 | 0.00 | 1.00 | 0.149 | 0.199 | 0.040 |

Table 6.3 Basic statistics of indicator kriged estimates for different cut-offs for mean grade M (n=17057)

| Cut-off | Minimum | Maximum | Mean | Std.Dev | Variance |
|---|---|---|---|---|---|
| 45 | 45.50 | 69.50 | 65.19 | 2.89 | 8.37 |
| 55 | 55.43 | 69.50 | 66.16 | 1.96 | 3.85 |
| 60 | 60.99 | 69.50 | 66.79 | 1.40 | 1.97 |
| 62 | 63.47 | 69.50 | 67.11 | 1.19 | 1.42 |
| 65 | 65.93 | 69.54 | 67.69 | 0.84 | 0.71 |
| 67 | 67.44 | 69.54 | 68.40 | 0.50 | 0.25 |
| 68 | 68.37 | 69.57 | 68.83 | 0.32 | 0.10 |
| 69 | 69.34 | 69.66 | 69.50 | 0.02 | 0.0002 |

### 6.6.2 Grade - tonnage curves

It is observed from grade-tonnage curve plotted between *cut-off grade vs total tonnage* (Figure 6.3) that there is no significant change in the total tonnage up to a cutoff of 45 % Fe. It is further observed that the total recovered tonnage is 95 % with a cut-off of 45 % Fe, and total tonnage is gradually decreasing with increasing in cut-off up to 69 % Fe. It can be further observed from the grade-tonnage curve (Figure 6.4) *cut-off grade vs mean grade* that that there is no much difference in the average grade estimated with a cut-off of zero (i.e no cut-off) and 45

% Fe and the linear trend is observed up to 45 % Fe (Figure 6.4). Beyond this threshold the curve is steadily increasing which depicts the gain in the mean grade.

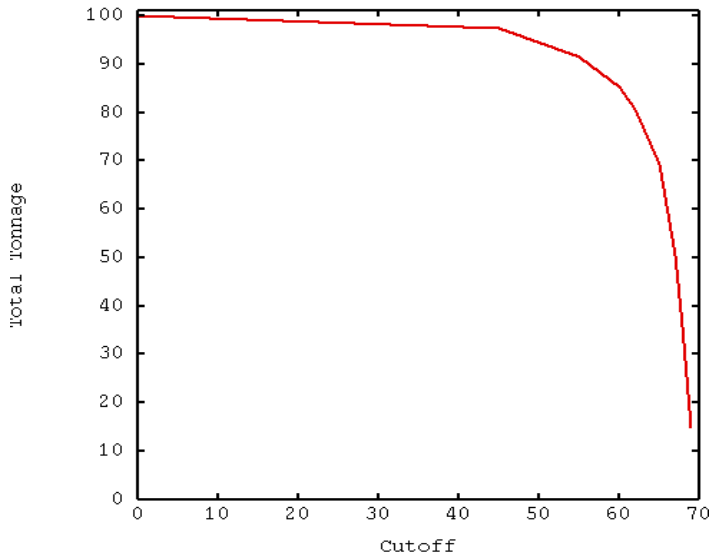


Figure 6.3 Grade tonnage curve plotted between cut-off grade and total tonnage. X axis shows cut-off grade of Fe and Y axis shows the total tonnage recovered.

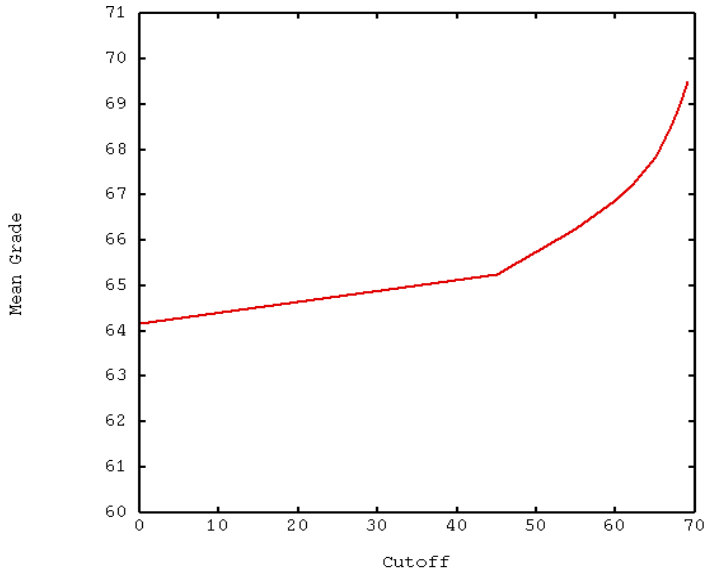


Figure 6.4 Grade tonnage curve plotted between cut-off grade and mean grade. X axis shows cut-off grade of Fe and Y axis shows the mean grade of the recovered tonnage.

### 6.6.3 E-type estimates

It can be observed from E-type estimates (Table 6.4) that indicator kriged estimates of Fe for the whole deposit i.e., without applying any cutoff ranges from 35.44 to 69.50 with a mean of 64.18. Comparing with mean grade of 65.19 for a cut-off of 45 % Fe (Table 6.3), mean of E-type estimates is slightly low which is due to mixing of all 'ore' and 'waste' blocks. It can also be observed from Table 6.4 that the indicator kriged standard deviation i.e., error of estimates ranges from 0.29 to 24.04 with average kriged standard deviation of 5.65. CV of standard deviation (~ 87 %) indicates that the variation in the error of estimation is very high. To get further insight, histogram (Figure 6.5) is computed to study the distribution of variation in the estimated blocks. It is observed from the histogram (Figure 6.5) that about 68 % of the estimated blocks are having standard deviation below 6 and about 18 % of the blocks are having standard deviation above 10. This may be due to intermixing of high grade and low grade blocks in some areas which mostly happen in BHQ dominated areas. To identify these areas, grade maps and standard deviation maps based on E-type estimates are plotted for 32 benches of the deposit.

Table 6.4 Basic statistics of E-type estimates of Fe % (n=17057 blocks)

| Variable | Minimum | Maximum | Mean | Std. Dev | CV |
|---|---|---|---|---|---|
| Indicator kriged Estimates | 35.44 | 69.50 | 64.18 | 4.31 | 6.71 |
| Indicator kriged Std. Dev | 0.29 | 24.04 | 5.65 | 4.92 | 87.08 |

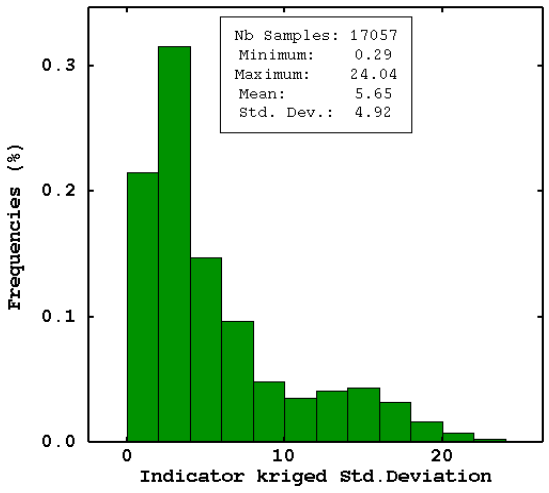


Figure 6.5 Histogram showing the distribution of indicator kriged standard deviation of E - type estimates of Fe.

Grade maps generated using indicator kriged e-type estimates show that most of the blocks are having Fe grade between 65 % and 70 %. It can be observed from the typical 12 out of 32 benches (Figure 6.6) that majority of the blocks are having Fe grade +55%. It is further observed that in the three benches (1068 RL, 1020 RL and 972 RL) very few peripheral blocks are having Fe grade between 45 % and 55%, and blocks with Fe < 45 % can be seen in the last two benches, i.e., 840 RL and 828 RL. This indicates that iron ore deposit encountered shale i.e., waste rock below 828 RL and therefore the occurrence of orebody below this level is questionable. It is also very interesting to observe that, the distribution of grades in ordinary kriging (Figure 5.5) and in median indicator kriging (Figure 6.6) are almost similar for all the benches, except the last three benches, where OK slightly overestimated.

It is observed from standard deviation maps generated using indicator kriged e-type standard deviation of 12benches (Figure 6.7) that the top benches i.e 1200 RL, 1164 RL, and 1116RL are showing less variation (< 5 %) in the estimates. It is further observed that the middle benches i.e 1068 RL, 1020 RL and 972 RL have blocks showing both high (> 10 %) and low variation (< 5 %), where as the bottom benches all are showing high variation. This is quite obvious as much drilling data is not available in that portion.

Both the figures (6.6 and 6.7) are very useful during excavation of the material. These bench plans provide estimated grades and variation in the grade in different locations of the bench and enable for the mines manager to take the decision for selective mining based on the requirement and the targets during short term scheduling. Accordingly, the mining activity can take place.

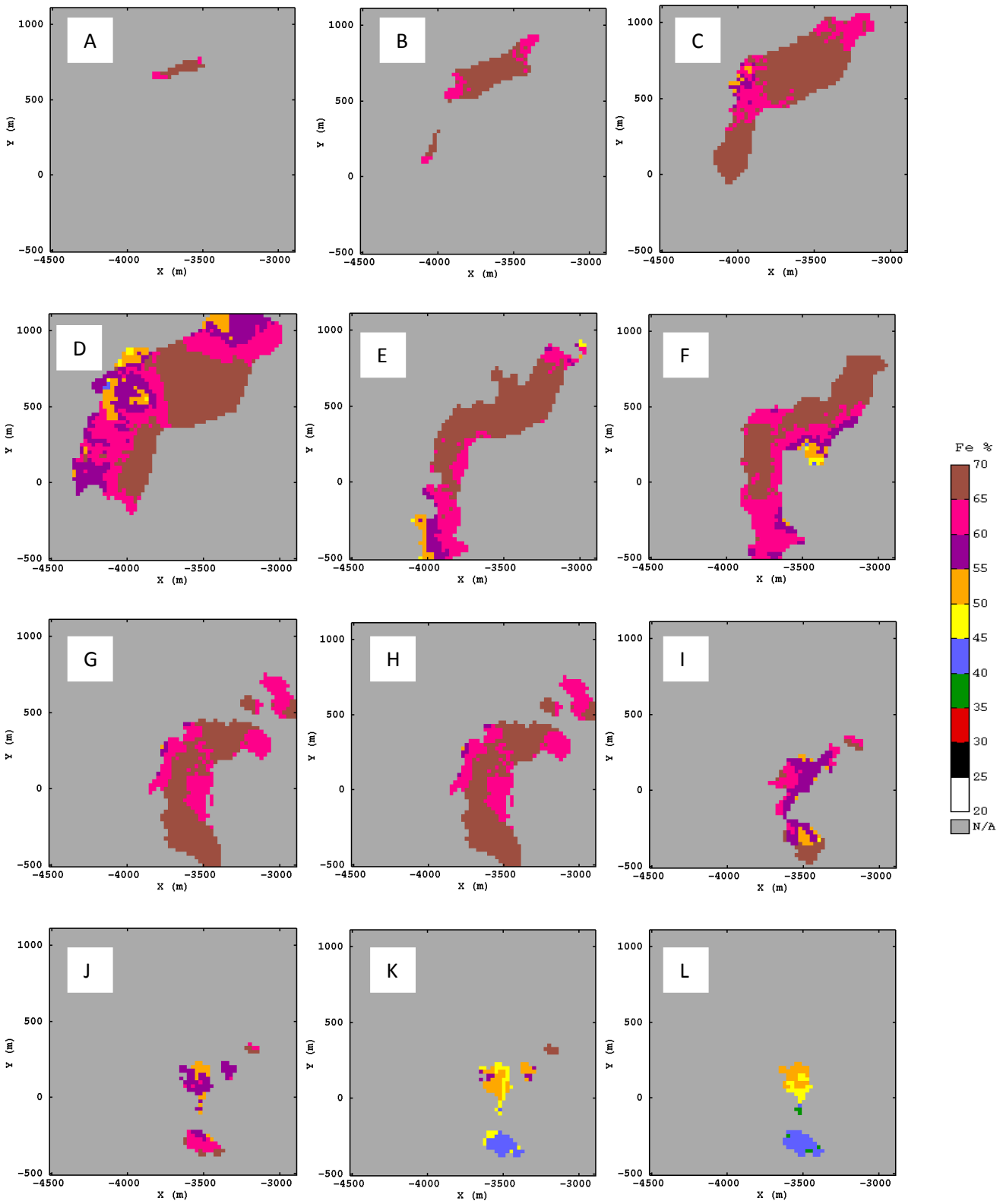


Figure 6.6 Grade maps generated using indicator kriged e-type estimates of 12benches of reduced levels (A)1200, (B)1164, (C)1116, (D)1068, (E)1020, (F)972, (G)924, (H)876, (I)864, (J)852, (K)840, and (L)828

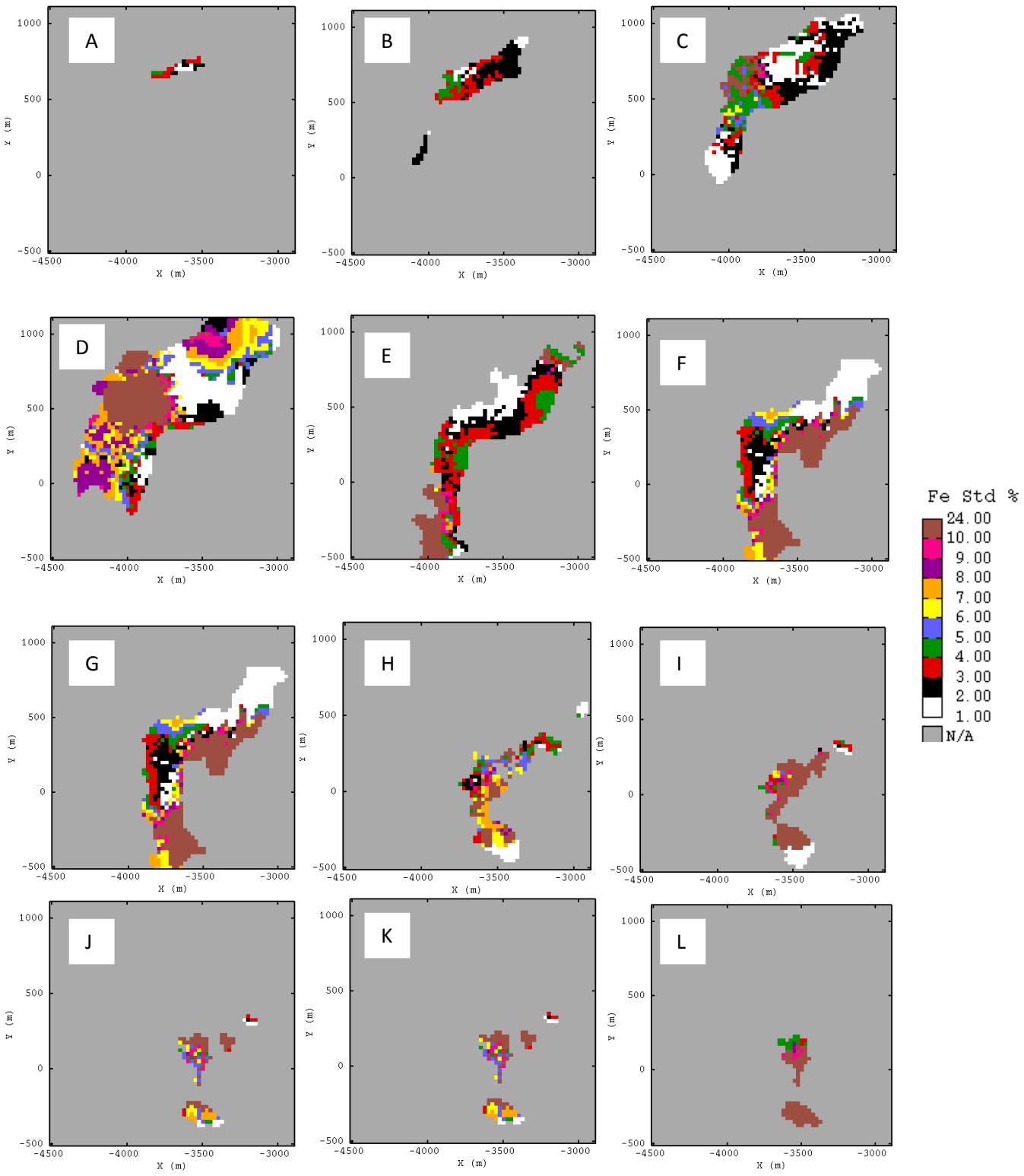


Figure 6.7 Standard deviation maps generated using indicator kriged e-type standard deviation of 12benches of reduced levels (A)1200, (B)1164, (C)1116, (D)1068, (E)1020, (F)972, (G)924, (H)876, (I)864, (J)852, (K)840, and (L)828

## 6.7 Summary

Recoverable resources are estimated using non-linear geostatistical estimation method 'Median indicator kriging' (a variant of indicator kriging). For the purpose of recoverable resources, a total of eight thresholds (or cut-offs) values are chosen i.e, 45 %, 55 %, 60 %, 62 %, 65 %, 67 %, 68 % and 69 % Fe. Bench composited data have been transformed to indicator data based on each cut-off.

Indicator semi-variograms are modelled in both horizontal and vertical directions for the indicator transformed data of 67 % Fe cut-off, which is the median value of Fe composited data. It is observed from the median indicator semi-variogram models of Fe that both the horizontal and vertical directions show a very good structure with a small nugget effect. Anisotropy is observed in both the directions with ranges 320 and 60 respectively.

The median indicator kriging is applied to calculate the total tonnage and mean grade of Fe of the whole area above each of the eight cut-offs. Indicator kriged statistics of Fe for different cut-offs are calculated. Further, recoverable resources estimates are computed using grade-tonnage curves generated from the probabilistic distribution model of indicator kriging and performing indicator post-processing.

It is observed from indicator kriged estimates of total tonnage for different cut-offs and grade tonnage curve that the total recovered tonnage is 97 % with a cut-off of 45 % Fe. In the existing working mines of NMDC of the Bailadila region, the high grade material is beneficial in two ways – blending with low grade material i.e. Fe grade < 45 % or selling directly with out blending with low grade which results in getting incentive in price, which is decided between NMDC and buyers. It is observed that about 50 % of the blocks have greater than 67 % Fe, with a mean grade of 68.4 % and about 15 % of blocks have greater than 69 % Fe with a mean grade of 69.50 % . These blocks will fetch additional revenue to NMDC in the form of incentive as practiced in the existing working mines nearby to this deposit.

The basic statistics of E-type estimates indicate that indicator kriged estimates of Fe for the whole deposit ranges from 35.44 to 69.50 with a mean of 64.18 and average kriged standard deviation of 4.31. Fe grade maps and Fe kriged standard deviation maps (error maps) are generated for the 32 benches in the deposit using global estimates. Grade maps (Figure 6.6) show

that the Fe grade is distributed mostly between 65 -70 % and partly between 60-65 % in the entire deposit. The medium grade (50-60 %) Fe is scattered in pockets and low grade (40-50%) Fe occurs only in peripheral areas of the deposit. It is also inferred from error map (Figure 6.7), that the central part of the ore body has a very low kriged standard deviation as compared to peripheral areas. The comparison of indicator kriging results with those of other methods is presented in Chapter 7.

# CHAPTER 7

# RECOVERABLE RESOURCES ESTIMATION BY DISJUNCTIVE KRIGING

# CHAPTER 7

# Recoverable Resources Estimation by Disjunctive Kriging

## 7.1 Introduction

The aim of drill hole sampling and mapping is to predict grades of ore deposit at locations that have not been sampled. A linear geostatistical estimation method such as ordinary kriging provides estimates of grades at unsampled locations. However, even the best linear estimator such as ordinary kriging may not provide satisfactory results in recoverable resource estimation and also in short term mine planning, and has a few problems in its applications. One such problem is to estimate the probability distribution of block grades as a function of different cut-off grades (Knudsen and Kim, 1978). It is required for the miners to decide for each block based on its sampling estimate, whether to extract it for processing (if its concentration exceeds the economic threshold) or segregate it as a waste. Therefore, the probability of the true value that exceeds the threshold is needed rather than a single estimate for the entire block which ordinary kriging generally provides. Matheron (l973) developed the method known as 'disjunctive kriging' to solve this problem. The main advantage of disjunctive kriging over ordinary kriging that it provides probabilities, which enable a miner to assess the risks associated with imprecise estimates. Using this probability distribution, a grade - tonnage relationship can be estimated, and the tonnage and grade of ore in each block are determined. The procedure of disjunctive kriging (DK) is aimed at solving 'tonnage' problems in recoverable resource estimation.

Some of the geostatistical methods used to calculate the probability that the true value exceeds the threshold are - multi-gaussian kriging (Verly, 1983; Schofield, 1989b; Emery, 2005a), non-parametric estimators such as indicator kriging and its variants (Deutsch and Journel, 1998), disjunctive kriging (Rendu, 1980b; Yates et al., 1986a, 1986b; Yates and Yates, 1988; Webster and Oliver, 1989, 2001; Wood et al., 1990; Oliver et al., 1996; Chica-Olmo and Luque-Espinar, 2002) and conditional simulation (Chile's and Delfiner, 1999).

Although, indicator kriging is useful to estimate the recoverable resources for different cutoffs but it ignores the relationship existing between different cut-offs. An indicator co-kriging is required to be performed instead of an univariate kriging to achieve the relation between different cut-offs. According to Vann and Guibal (1998), in general, any practical function of the data $f(Z)$ can be expressed as a linear combination of indicators: $f(Z) = \sum f_{n.} I(Z, Z_n)$ . Thus, estimating f ($Z$) amounts to estimating the various indicators. The best linear estimate of these indicators is their full co-kriging, which takes into account the existing correlations between indicators at various cut-offs. Full indicator co-kriging theoretically ensures consistency of the estimates reducing 'order relationships' to a minimum or eliminating them altogether. However, if $n$ indicators are used, $n^2$ variograms and cross-variograms need to be modelled, but this is impracticable once $n$ is > 5 or 6, even if we use modern automatic variogram modelling software (Vann and Guibal, 1998).

Rivoirard (1994), suggest various non-linear estimation methods, for simplifying the full indicator co-kriging, such as (i) multiple indicator kriging (ignores the correlations between indicators), (ii) median IK (assumes that there is intrinsic correlation, i.e all the variograms and cross-variograms are multiples of one unique variogram. In this case, cokriging is strictly equivalent to kriging), and (iii) residual indicator kriging (the indicators are expressed as linear combinations of uncorrelated orthogonal functions, which can be calculated from the data, co-kriging of the indicators which is equivalent to separate kriging of the orthogonal functions, which is decomposition of the indicators, a basis of residual indicator kriging (RIK) and of disjunctive kriging).The mathematics of DK is complex and the numerical integration process. Rivoirard (1994, p.90) yet describes it as a mathematically consistent model. Deutsch and Journel (1992, p.83) note that the DK method is a generalisation of the bivariate Gaussian model.

In practice, it is difficult to establish a model of corregionalization acceptable for a large number of cut-offs. Disjunctive kriging solves this problem by transforming the cokriging problem into N krigings performed independently. One model offering this possibility is the Gaussian anamorphosis model using Hermite polynomials where the change of support is explained by a coefficient (Catherine Bleines et al., 2011b). Further, while estimating large size blocks by kriging, kriging error, in general, is less when compared to the kriging error of small size blocks. But such estimation is more toward global estimation and not of much use mining

(Guibal, 1987, p.158). On the other hand, if small blocks are kriged by linear kriging methods when the borehole grid is large, confidence limits on the estimates would be so large as to render the values as useless (Jackson and Marechal, 1979, p. 249; Armstrong and Champigny, 1989).

Disjunctive kriging (DK) helps in estimating the percentage of small blocks in a big block, which can be considered as ore at a given cut-off $z_c$. Principles of disjunctive kriging and its application for estimating recoverable resources were given in detail by earlier works (Matheron, 1973, 1976, 1978; Marechal, 1976a, 1984; Journel and Huijbregts, 1978; Jackson and Marechal, 1979; Marechal and Touffait, 1980; Marechal, 1981; Guibal and Remacre, 1984; Armstrong and Matheron, 1986a, 1986b; Rivoirard, 1994; Chiles and Delfiner, 1999; Emery, 2006b). Disjunctive kriging is extensively applied by various researchers in several applications such as coal deposit (Armstrong, 1981), Iron ore deposit (Murthy, 1989b; Daya and Hassani, 2010, 2014), Copper deposit (Deraisme, 1998), cadmium (Juang and Lee, 2000), Tin and Zinc (Yu et al., 2004). Disjunctive kriging is also applied in non-mining applications such as earth quake ground motion estimation (Carr et al., 1986), to model areas of high fish density in acoustic fisheries surveys (Petitgas, 1993), geotechnical engineering (Samui and Sitharam, 2007), and pollution (Yang et al., 2008)

Broadly, four steps are involved in the application of disjunctive kriging: (i) Gaussian transformation (Gaussian anamorphosis modelling on point support), (ii) Support correction (Gaussian anamorphosis modelling on block support, (iii) Block Gaussian semi-variogram, and (iv) Estimation using disjunctive kriging. The process flow involved in disjunctive kriging is shown in Figure 7.1

In this chapter, the recoverable resource estimates at different cut-off grades from the distribution of sample values employing disjunctive kriging method is discussed. The Fe grade is estimated using disjunctive kriging for each 25 m x 25 m x 12 m block. A comparison is also made between the resource estimates inferred from ordinary kriging, indicator kriging and disjunctive kriging.

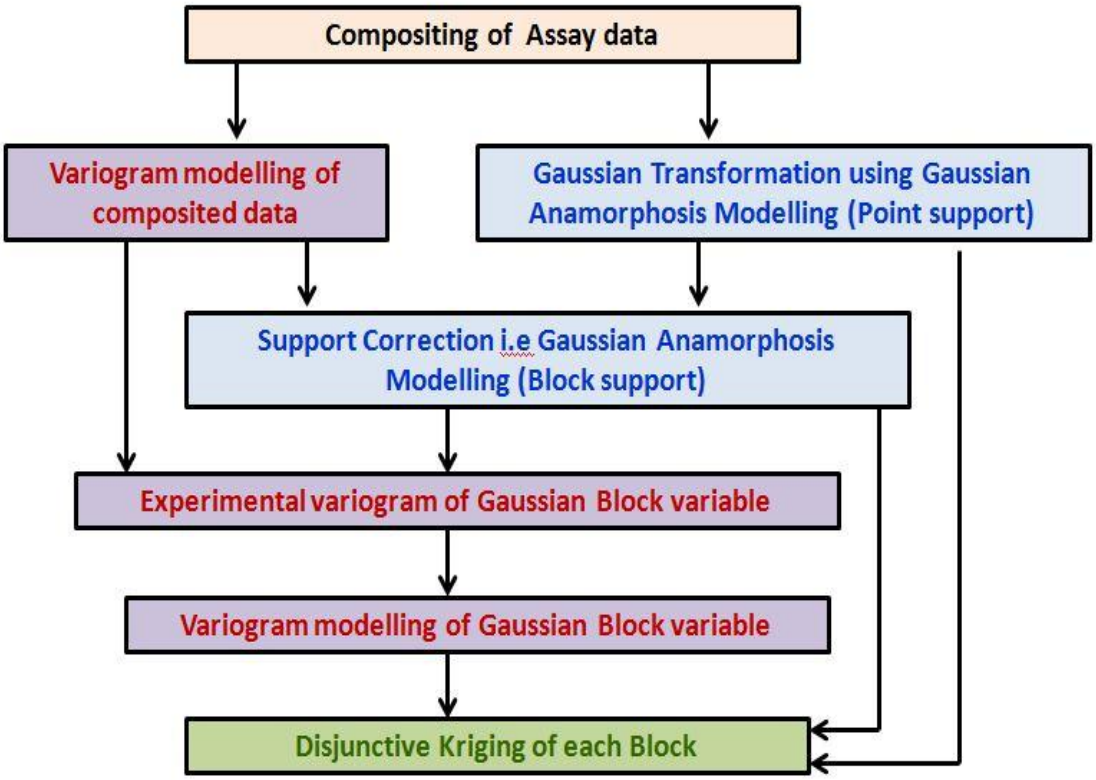


Figure 7.1 Flow chart showing steps involved in disjunctive kriging

## 7.2 Gaussian transformation (Gaussian anamorphosis on point support)

Disjunctive kriging requires the raw data to be transformed into Gaussian transformation prior to the grade estimation. In Gaussian transformation, the composited raw data of Fe is transformed into a normal distribution using Gaussian anamorphosis modelling (Rivoirard, 1994). Gaussian anamorphosis modelling, also called 'punctual histogram modelling', is a mathematical technique which allows modelling the anamorphosis function φ linking the raw data (Y) and their associated gaussian values (Z) as shown in equation 7.1

$$Z = \varphi(Y) \qquad (7.1)$$

The anamorphosis function φ in the equation 7.1 is modelled by using Hermite Polynomials and it is decomposed into Hermite polynomials up to degree 'N'. Mathematically this function is expressed (Murthy, 1989b) as

$$\phi(Y) = \sum_{i=1}^{N} \Psi_i H_i(Y) \tag{7.2}$$

where $H_1(Y)$, $H_2(Y)$, $H_3(Y)$…….. $H_N(Y)$ are Hermite Polynomials.

In practice, the number of Hermite polynomials is fixed by trail and error method till the fit between raw data and transformed data is precise. In this study, a precise fit is obtained using 30 number of Hermite polynomials. Using these 30 polynomials, the $\psi_i$ coefficients of the expansion (7.2) and subsequently the gaussian transformation was carried out using 'frequency inversion' method.

***Frequency inversion method***

In the frequency inversion method, the raw data is sorted first and a cumulative frequency (CF) is calculated for each sample $FC_i$ from the smallest value adding the frequency of each sample using the equation (Catherine Bleinès et al., 2011b)

$$FC_i = FC_{i-1} + W_i \tag{7.3}$$

The frequency $W_i$ is given as $W_i = 1/N$. Finally, the gaussian value is calculated using

$$Y_i = \left(G^{-1}(FC_i) + G^{-1}(FC_{i-1})\right)^{\frac{1}{2}} \tag{7.4}$$

the resulting Gaussian variable and the gaussian anamorphosis function are used further in block anamorphosis i.e., support correction, gaussian block variogram modelling and disjunctive kriging.

The statistical parameters of raw data and gaussian transformed data are given in Table 7.1 and the histograms of the raw data and transformed data are shown in Figure 7.2. The Figure 7.3 shows the Gaussian anamorphosis model with raw data on Y-axis and Gaussian data on X-axis.

Table 7.1 Statistical parameters of raw data and gaussian transformed data of Fe % (n= 725 samples)

| Nature of Data | Minimum | Maximum | Mean | Variance |
|---|---|---|---|---|
| Raw (Composited) | 11.04 | 70.00 | 64.84 | 42.97 |
| Gaussian (Transformed) | -3.06 | 3.06 | 0.00 | 0.99 |

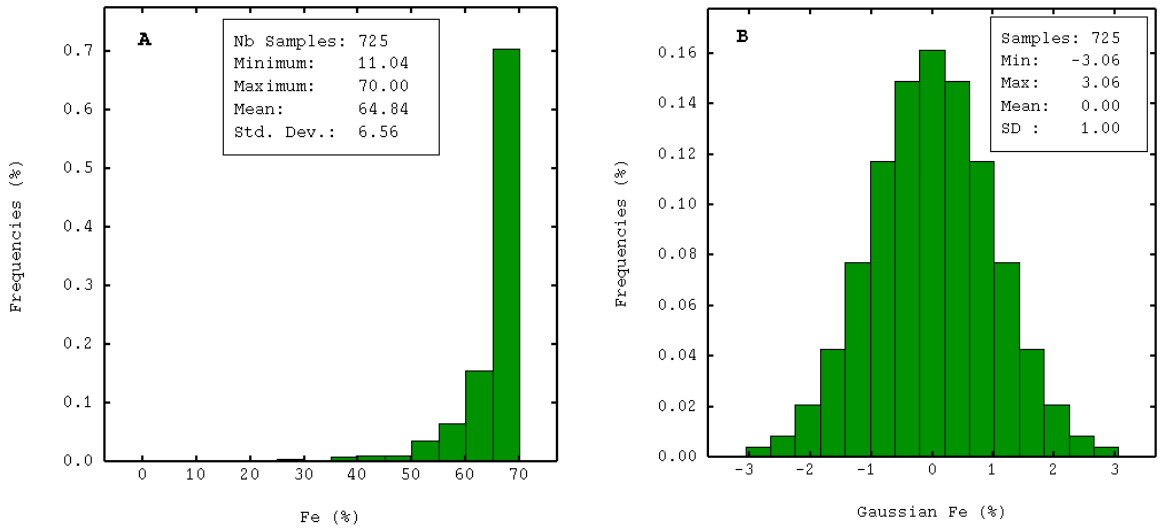


Figure 7.2 Histograms of the raw data (A) and Gaussian transformed data (B). Original data (A) which is asymmetric is successfully transformed to symmetric data (B).

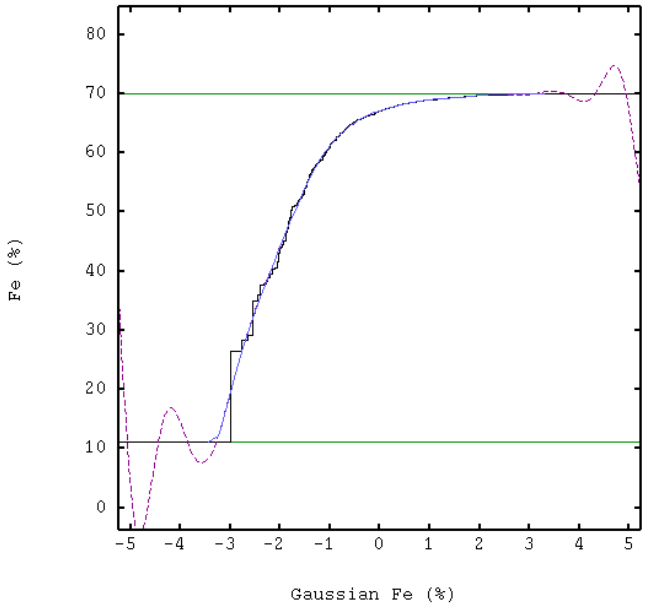


Figure 7.3 Showing the Gaussian anamorphosis model of Fe with raw data on Y-axis and Gaussian transformed data on X-axis. Raw data is in black and the anamorphosis is in blue. The two horizontal lines are the lower and upper bounds of raw Fe data.

## 7.3 Support correction (Gaussian anamorphosis on block support)

In estimation of recoverable resources, *support correction* is an important parameter to be considered. During exploration stage it is assumed that the sampled data is representative of the deposit and a histogram is modelled using the composited data. But in practice, the cut-off will be applied on blocks instead of on composited data, for the purpose of recoverable resource estimation. Therefore, a 'support correction' or 'change of support' to the composite histogram model is required to estimate a histogram model on the block support (De-vitry et al., 2007). The 'support' is the geometrical volume i.e., a block, on which the grade is defined.

Support correction computes the histogram of blocks using point anamorphosis i.e Gaussian anamorphosis modelling discussed in section 7.2 and a variogram model of the raw composited data (Geovariances, 2013b). Before performing the support correction, variogram model of the raw composited data for Fe is computed. The semi-variogram of Fe is modelled in both horizontal and vertical directions, using exponential and spherical models with a nugget effect. The modelling parameters are given in Table 7.2 and fitted models of Fe in horizontal and vertical directions are shown in Figure 7.4.

Table 7.2 Semi-variogram modelling parameters of raw Fe in horizontal and vertical directions.

| Direction | Model-1 | Model-2 | Range-1 | Range-2 | Sill-1 | Sill-2 | NE |
|---|---|---|---|---|---|---|---|
| Horizontal | Exponential | Spherical | 65 | 400 | 14 | 16 | 7 |
| Vertical | Exponential | Spherical | 30 | 90 | 16 | 6 | 4 |

It is observed that the semi-variogram models of Fe in horizontal and vertical directions (Figure 7.4) show a very good structure with a small nugget effect. Anisotropy is observed in both the directions with ranges of 400 and 90 respectively (Table 7.2). It indicates that no correlation is recorded beyond 400 m in horizontal direction, and 90 m in vertical direction.

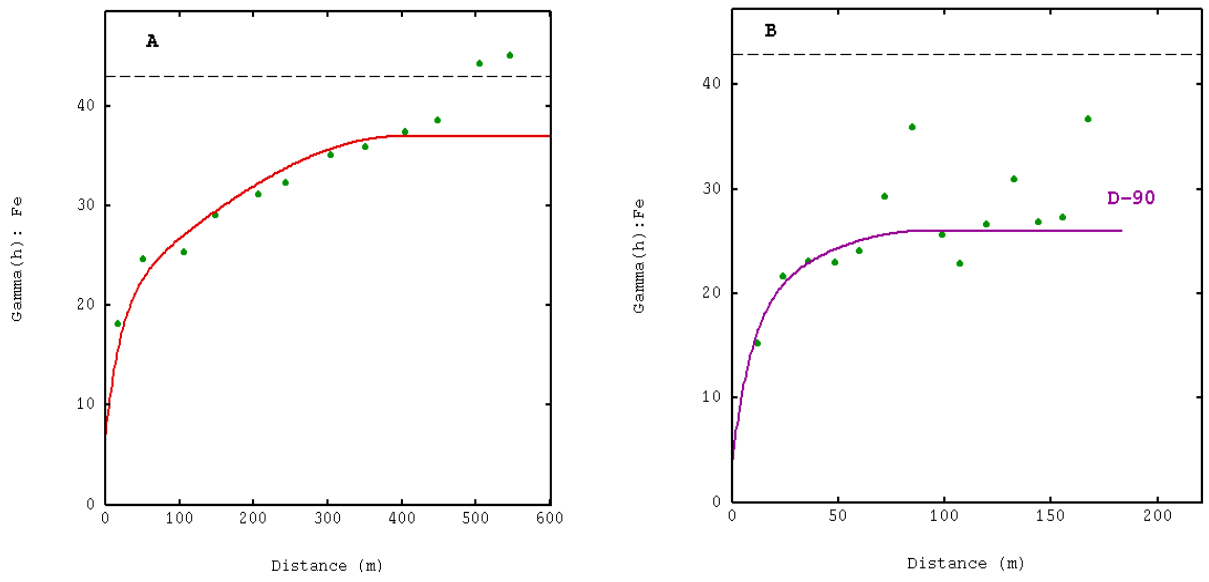


Figure 7.4 Semi-variogram models of raw composited Fe in horizontal (A) and vertical direction (B).

In support correction, the Hermite Polynomial Expansion of the punctual histogram modelling i.e., equation 7.2 provides a correction of the $\psi_i$ coefficients to get an anamorphosis on a block support. The block support anamorphosis is expressed (Catherine Bleinès et al., 2011b) as

$$Z_v = \phi_r(Y_v) = \sum_{i=1}^{\infty} \psi_i r^i H_i(Y_v) \tag{7.5}$$

where 'r' is the block support correction coefficient, determined from the variance of the blocks using the expression,

$$Var\, Z_v = \sum_{i=1}^{\infty} \Psi_i^2 . r^{2i} \tag{7.6}$$

Finally, the value of 'r' is obtained using anamorphosis model $\psi_i$ and a variogram model of composited Fe data. Block variance is calculated using the expression,

$$\text{Var } Z_v = \text{Var } Z - \gamma\,(v,v) \tag{7.7}$$

$$where \;\; Var\, Z_v = \sum_{i=1}^{\infty} \Psi_i^2 \tag{7.8}$$

This support correction coefficient ‘r’ is used to get the anamorphosis model of the histogram of the blocks.

In this study, the size of the support considered is the Selective Mining Unit (SMU) size which is fixed as 5 x 5 x 12 m along X, Y and Z directions. Thus, the support correction is calculated for a block support of 5 x 5 x 12 m. The same block model which was used in ordinary kriging and median indicator kriging is used in disjunctive kriging. Each block of 25 x 25 x 12 m is discretized by 5 x 5 x 1m for the calculation of the average variogram value in the block. No discretization is taken in the vertical direction as the composites are regularized to the bench height (12 m). Using all these parameters, the block variogram value ‘Gamma (V,V)’ is calculated and is the base for calculating the real block variance and the real block support correction coefficient ‘r’. The results of the block support correction indicate that the block grades ranges from 11.04 to 70 % Fe, with block variance 10.07 and block support correction 0.91. Comparisons of block values and the punctual values in anamorphosis models and the histograms are presented in Figure 7.5.

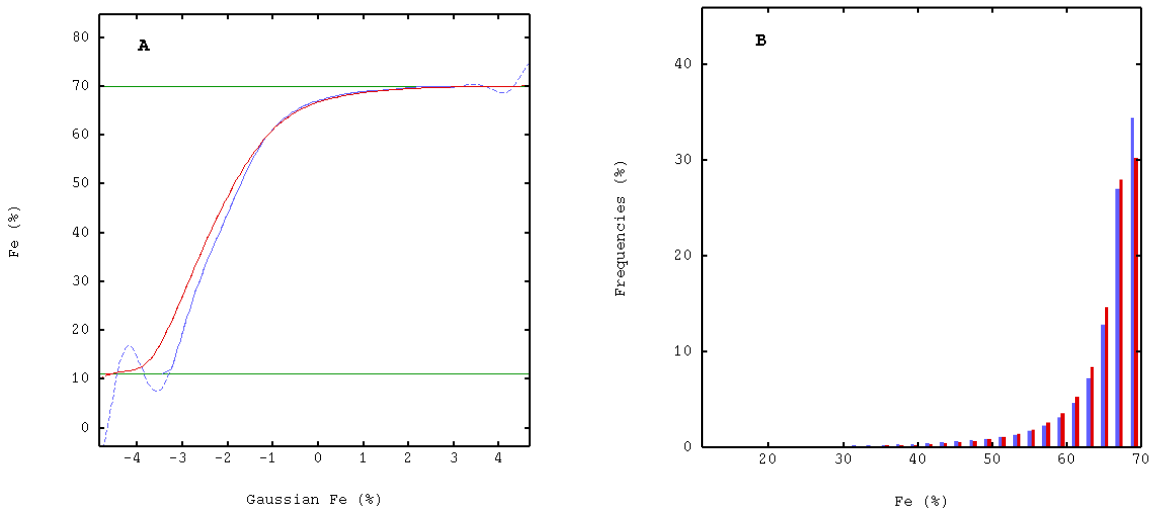


Figure 7.5 Showing comparison of block values and the punctual values in anamorphosis models (A), and histograms after support effect correction (B). The punctual values are in blue and block values are in red. After the support effect correction, the histogram of blocks is smoother and has smaller variance than the punctual histogram model.

## 7.4 Block Gaussian semi-variogram

A semi-variogram model computed on a gaussian block variable is the prerequisite for the disjunctive kriging. For this, an experimental semi-variogram for gaussian block variable is calculated using the semi-variogram model of raw data (composited data) and the block anamorphosis. A relationship between the covariance of raw variable and covariance of the gaussian transformed variable for 'point support' is calculated in terms of Hermite polynomials coefficients obtained from the equation (7.2), using the following equation as suggested by Catherine Bleinès et al., (2011b)

$$C(h) = \sum_{i=1}^{n} \Psi_i^2 . \rho^i (\mathrm{h}) \tag{7.9}$$

where ρ(h) is the covariance of the gaussian variable, and C(h) is covariance of the raw variable.

Further, the relationship between the covariance of raw variable and covariance of the gaussian transformed variable for 'block support' i.e., after change of support is expressed as

$$C_v(h) = \sum_{i=1}^{\infty} \Psi_i^2 . r^{2i} . \rho_v^{\ i} (\mathrm{h}) \tag{7.10}$$

where 'r' is the change of support coefficient in the block anamorphosis.

Using the relationship on $C_v$ (h) i.e., the gaussian covariance for the block support v obtained using equation (7.10), the relationship on variograms is derived. Finally, the gaussian experimental semi-variogram is obtained from the raw semi-variogram by inverting the relationship in each lag of variogram. Subsequently, this experimental semi-variogram is fitted and block gaussian semi-variogram model is obtained which is further used in resource estimation.

The modelling parameters of block gaussian semi-variograms in horizontal and vertical directions are given in Table 7.3. The fitted models of block gaussian semi-variograms in horizontal and vertical directions are presented in Figure 7.6.

Table 7.3 Modelling parameters of block Gaussian semi-variograms in horizontal and vertical directions.

| Direction | Model-1 | Model-2 | Range-1 | Range-2 | Sill-1 | Sill-2 | NE |
|---|---|---|---|---|---|---|---|
| Horizontal | Spherical | Spherical | 130 | 400 | 0.24 | 0.64 | 0.12 |
| Vertical | Spherical | Spherical | 35 | 90 | 0.4 | 0.45 | 0.15 |

Anisotropy is observed in both horizontal and vertical directions with ranges 400 and 90 respectively (Table 7.3). It is observed from the block Gaussian semi-variogram models of Fe (Figure 7.6) that both the horizontal and vertical directions show a very good structure with a small nugget effect. It is interesting to note that the ranges of semi-variogram models in horizontal and vertical directions are same for punctual Fe data and block Gaussian Fe data (Tables 7.2 and 7.3). This indicates that Gaussian block anamorphosis modelling using 30 Hermite polynomials and semi-variogram modelling are very accurate. It is also observed that semi-variogram models in both horizontal and vertical directions are showing similar spatial variability of semi-variograms in Murthy (1989b). This may be due to the fact that both the deposits are from the same region.

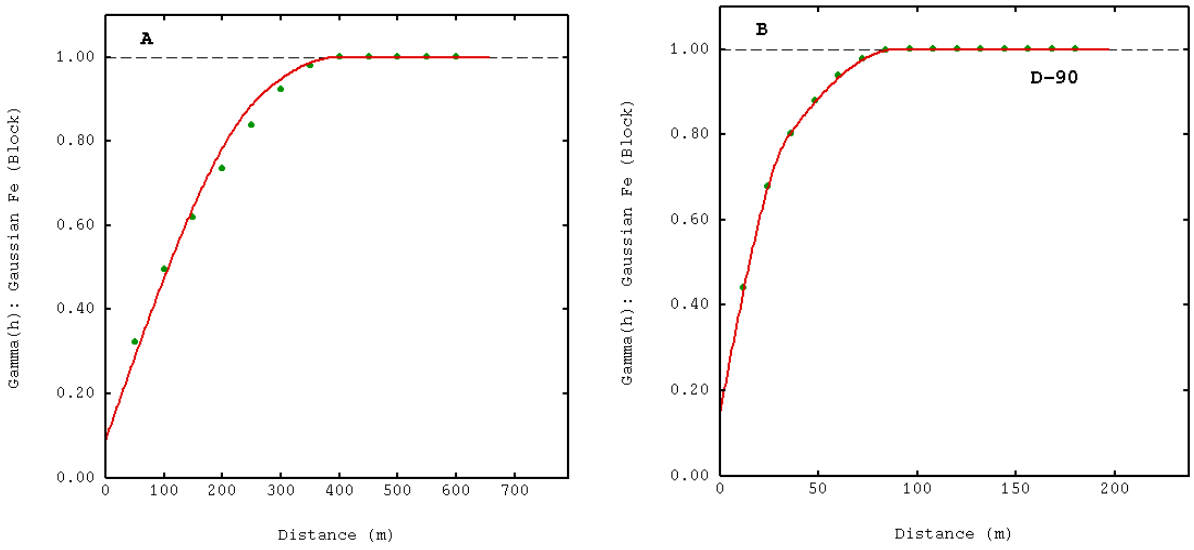


Figure 7.6 Semi-variogram models of block Gaussian Fe after support correction in horizontal (A), and vertical direction (B).

## 7.5 Estimation of recoverable resources using disjunctive kriging

Disjunctive kriging is employed to estimate recoverable resources of the deposit which include tonnage and grade for different cut-offs using gaussian transformed data, block anamorphosis model and the block gaussian semi-variogram model. In disjunctive kriging, each factor in Hermite polynomials is kriged separately using the variogram of the Gaussian transformed values on the SMU support and then the estimates of all factors are combined to form the DK estimate of that block. Thus, the DK estimation $Z_v$ of an unknown block expanded in hermitian polynomials (which provide a sequence of uncorrelated components) consists of the sum of the kriging estimators H* of each polynomial term (Murthy 1989b; Daya and Hassani, 2010).

Disjunctive kriging provides an estimated value between 0 and 1 for each block estimate, which can be interpreted either as probabilities (the probability that the grade is above the specified indicator) or as proportions (the proportion of the block above the specified cut-off on data support) (Isaaks and Srivastava, (1989). While doing so, disjunctive kriging does not give a single value for the entire block, but gives the probability of the block content above a given cut-off. The outcome of DK is a conditional cumulative distribution function (CCDF) of estimates for different cut-offs. The CCDFs are estimated at each block centroid, and the model is further processed to get the probabilities and grades in each block, for a range of given cut-offs.

In this study, nine cut-offs were chosen for Fe grade viz., 0%, 45 %, 55 %, 60 %, 62%, 65%, 67 % , 68 % and 69 % as in the case of indicator kriging. Fe grade has been estimated for each block of dimensions 25 m × 25 m × 12 m. The same block and neighbourhood parameters considered in ordinary kriging and median indicator kriging are considered in disjunctive kriging for the purpose of comparison. The disjunctive kriging technique gives the probabilistic distribution model of Fe for the whole area for different cut-offs. Further, recoverable resources estimates are obtained using grade-tonnage curves generated from the probabilistic distribution model of disjunctive kriging.

In this study, though all the three variables Q, T, and M are computed, only total tonnage (T) and mean grade (M) are discussed as the metal quantity (Q) is of no significance in case of iron ore. The basic statistics of disjunctive kriged results for total tonnage and mean grade for

different cut-offs are presented in tables 7.4 and 7.5 respectively. Based on disjunctive kriged estimates, the grade tonnage curves - cut-off grade vs total tonnage, and cut-off grade vs mean grade - are calculated and presented in Figure 7.7. Probability maps and mean grade maps were produced for 32 benches of the deposit for different cut-offs of Fe. For a typical four benches of different reduced levels, probability maps of Fe 65 % cut-off and mean grade maps of Fe 45 % cut-off are presented in Figure 7.8 and 7.9 respectively.

***Comparison of estimated recoverable resources of different methods (OK, IK and DK)***

A comparison is made between the results of the estimated recoverable resources obtained from non-linear methods such as indicator kriging (IK) and disjunctive kriging (DK) with a linear estimation method ordinary kriging (OK) and the results are presented in Table 7.6 and Figure 7.10.

## 7.6 Results and Discussion

In the context of recoverable resources, the grade and tonnage above a cutoff, estimated based on the distribution of sample grades, would result in bias and underestimation because the borehole grid is much larger than the mineable block (Knudsen and Kim, 1978). Authors further state that attempting to estimate the grade of each mineable block i.e., selective mining unit (SMU) by ordinary kriging is inappropriate because the estimation variance would be very large. If the recoverable grade and tonnage is made on these large blocks, a bias is again made due to the variance of the estimated block grades being less than the true block grades. Williamson and Mueller (1976) discussed this problem at the Cyprus Pima Mine. Authors found that overestimation of ore tonnage by 14% occurred when cutoff criteria were applied to block grades estimated using ordinary kriging. When it was planned in the mine for 30,000 tons to be mined, it was found that only 25,000 tons of it was above cutoff, when the block was actually mined.

To overcome this problem, Matheron (1976) has developed an estimation method called disjunctive kriging which solves the problem of vanishing tonnage and gives more information than regular ordinary kriging. Disjunctive kriging is useful to assess the local probabilities that the actual concentrations exceed a threshold value and to divide the ore into economic and uneconomic parts (Daya and Hassani, 2010).

Comparison of ordinary and disjunctive kriging in an iron ore deposit of Bailadila Range was employed by Murthy (1989b) in which author has estimated variable Fe for blocks of size 100 x 100 x 12 m for a grid spacing of 100 x 100 m using ordinary kriging. In disjunctive kriging the panel size considered was 100 x 100 x 12 m and the blocks within the panel are of size 25 x 25 x 12 mts. It is felt that the panel dimensions should be 25 x 25 x 12 mts and block size within the panel is 5 x 5 x 12 considering the SMU size. The main objective of DK is to consider the mining aspects i.e. SMU size while estimating recoverable resources. Thus, in this study, taking into account of SMU size, panel dimensions of 25 x 25 x 12 mts and block size within the panel is 5 x 5 x 12 are considered. It is observed that author has not provided any information related to the thresholds considered in the study and also not presented any grade-tonnage curves in the results which is very important in the context of DK. However, the bench wise reserves estimated by DK were provided at 55 % cut-off grade Fe. Author has inferred that good agreement exists between OK and DK estimates and future blast holes samples from mine going to contribute more information on quality of both the estimates.

Daya and Hassani (2010) have employed disjunctive kriging for geostatistical grade modelling of an iron ore deposit. Prior to employing DK, authors have computed variography in different azimuths and different dips and inferred that there was no anisotropy detected. All the directions they have considered were only along XY and the direction Z was not considered in their study. In Iron ore deposit, the variability in the vertical direction always differs from horizontal direction and thus it results anisotropy in the vertical direction which was not considered in their paper. Whereas, Murthy (1989b) considered vertical direction and found anisotropy. Similar observation was also made in this study. Daya and Hassani (2010) have taken threshold of 20 % Fe in their study to estimate block averages of iron by DK and subsequently generated grade and error variance maps based on DK estimates for 20 % cut-off. In their paper, it is observed that basic statistics of raw data, block dimensions considered during estimation, block gaussian variogram models and the most important statistics of estimates are all missing. There is neither validation of DK results nor comparison of DK method with any other method in the paper. Authors have inferred that DK can be used to model the uncertainty of mapping iron ore concentration in an iron ore deposit and if data are relatively marginally skewed and the goal is to predict non linear function, then DK would be suitable.

Catherine Bleinès et al., (2011a) presented a case study on application of OK, IK and DK for an iron ore deposit. Authors have compared the Fe estimates of these three methods and found that DK estimates are more accurate relatively. The results of recoverable resources estimates and grade tonnage curves estimated by disjunctive kriging in this study are presented and discussed. A comparison of grade tonnage curves obtained by different methods viz., ordinary kriging, indicator kriging and Disjunctive kriging is also presented.

In this study, it is observed from disjunctive kriged estimates of recovered tonnage (Table 7.4) and the grade tonnage curve *cut-off grade vs total tonnage* (Figure 7.7A) that the total recovered tonnage is about 98 % with a cut-off of 45 % Fe. It can be further observed from disjunctive kriged estimates of mean grade (Table 7.5) and the grade tonnage curve *cut-off grade vs mean grade* (Figure 7.7B) that for a cut-off of 45 %, Fe content ranges from 45.35 % to 69.5 % with a mean of 65.44 %. The grade between 45 % and 55% Fe is considered as *sub-grade* in iron ore deposit, which is estimated about 4 % of the total tonnage. It is also observed that about 48 % of blocks have greater than 67 % Fe, with a mean grade of 68.16 % and about 12 % of blocks have greater than 69 % Fe with a mean grade of 69.42 % (Table 7.4 and 7.5). As discussed in Chapter 6, these high grade blocks can be used for selling directly which results in getting incentive price or by blending with low grade i.e < 55 % Fe to meet the customer requirement of 62 % Fe.

Table 7.4 Basic statistics of disjunctive kriged estimates of recovered tonnage T for different cut-offs (n=17057 blocks)

| Cut-off % Fe | Minimum | Maximum | Mean | Std.De | Variance |
|---|---|---|---|---|---|
| 0 | 1.00 | 1.00 | 1.00 | 0.00 | 0.0000 |
| 45 | 0.55 | 1.00 | 0.984 | 0.02 | 0.0007 |
| 55 | 0.27 | 1.00 | 0.940 | 0.08 | 0.0061 |
| 60 | 0.05 | 1.00 | 0.874 | 0.13 | 0.0175 |
| 62 | 0.00 | 1.00 | 0.823 | 0.16 | 0.0270 |
| 65 | 0.00 | 1.00 | 0.682 | 0.23 | 0.0517 |
| 67 | 0.00 | 1.00 | 0.485 | 0.26 | 0.0705 |
| 68 | 0.00 | 1.00 | 0.322 | 0.25 | 0.0642 |
| 69 | 0.00 | 1.00 | 0.118 | 0.15 | 0.0239 |

Table 7.5 Basic statistics of disjunctive kriged estimates of mean grade M for different cut-offs (n=17057 blocks)

| Cut-off | Minimum | Maximum | Mean | Std. Dev | Variance |
|---|---|---|---|---|---|
| 45 | 45.35 | 69.50 | 65.44 | 2.49 | 6.19 |
| 55 | 54.63 | 69.50 | 66.03 | 1.89 | 3.59 |
| 60 | 60.29 | 69.50 | 66.59 | 1.45 | 2.12 |
| 62 | 62.67 | 69.40 | 66.90 | 1.34 | 1.79 |
| 65 | 65.45 | 69.45 | 67.50 | 1.61 | 2.58 |
| 67 | 67.24 | 69.45 | 68.16 | 0.98 | 0.97 |
| 68 | 68.70 | 69.67 | 68.48 | 1.88 | 3.54 |
| 69 | 69.43 | 69.76 | 69.42 | 1.65 | 2.72 |

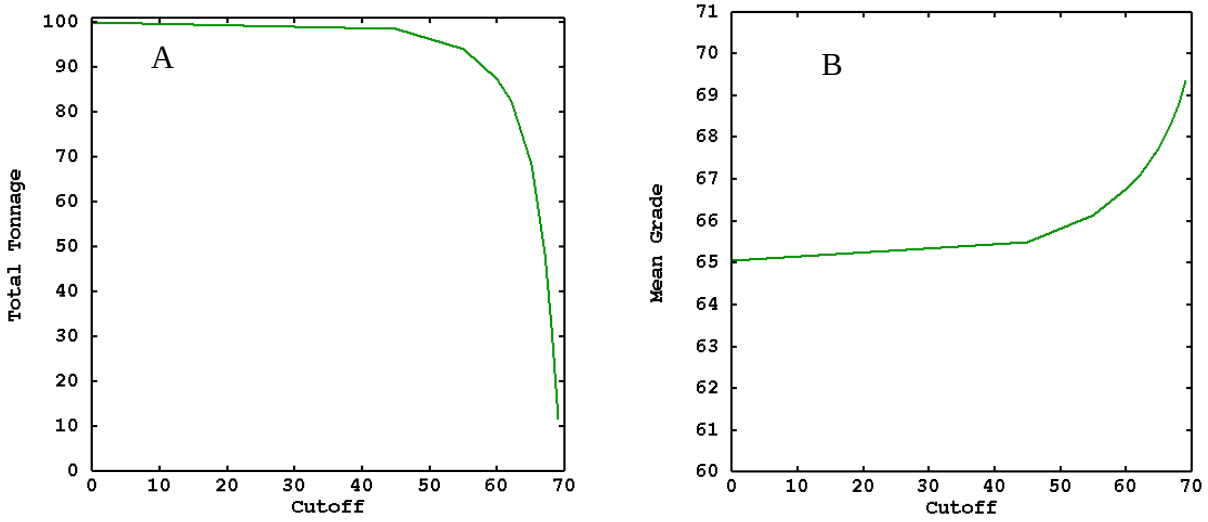


Figure 7.7 Grade tonnage curves estimated using disjunctive kriging (A) cut-off grade vs total tonnage (B) cut-off grade vs mean grade.

Probability map (Figure 7.8) generated using disjunctive kriging estimates show the probabilities that the Fe concentration exceeds the threshold value 65 %. It can be observed from the typical 4 benches that majority of the blocks are having 80-90 % probability that Fe value exceeds 65 % and very few blocks with low probability 30-60% occur in peripheral blocks.

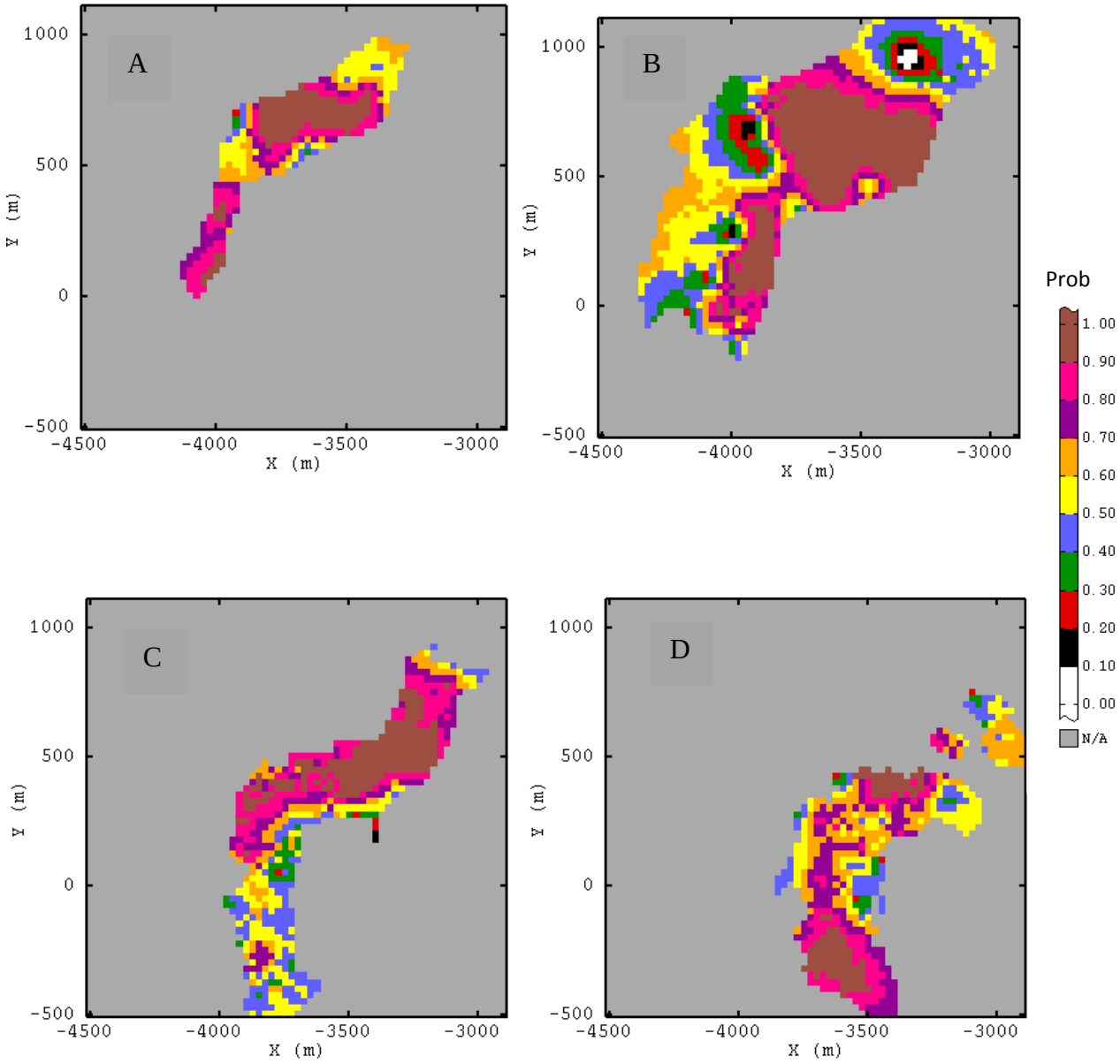


Figure 7.8 Showing probabilities that the Fe concentration exceeds the threshold value 65% in 4 typical benches of reduced levels (A) 1140, (B) 1068, (C) 996, and (D) 924

Grade maps generated using disjunctive kriging estimates with a cut-off of 45 % Fe indicate that most of the blocks are having Fe grade between 65 % and 70 %. It can be observed from the typical 4 benches (Figure 7.9) that majority of the blocks are having Fe grade + 60 %. It is further observed that very blocks are occurring in peripherals (Figure 7.9B) having Fe between 57-60 %. In the total deposit, very few blocks in the bottom benches have Fe grade between 45-55%.

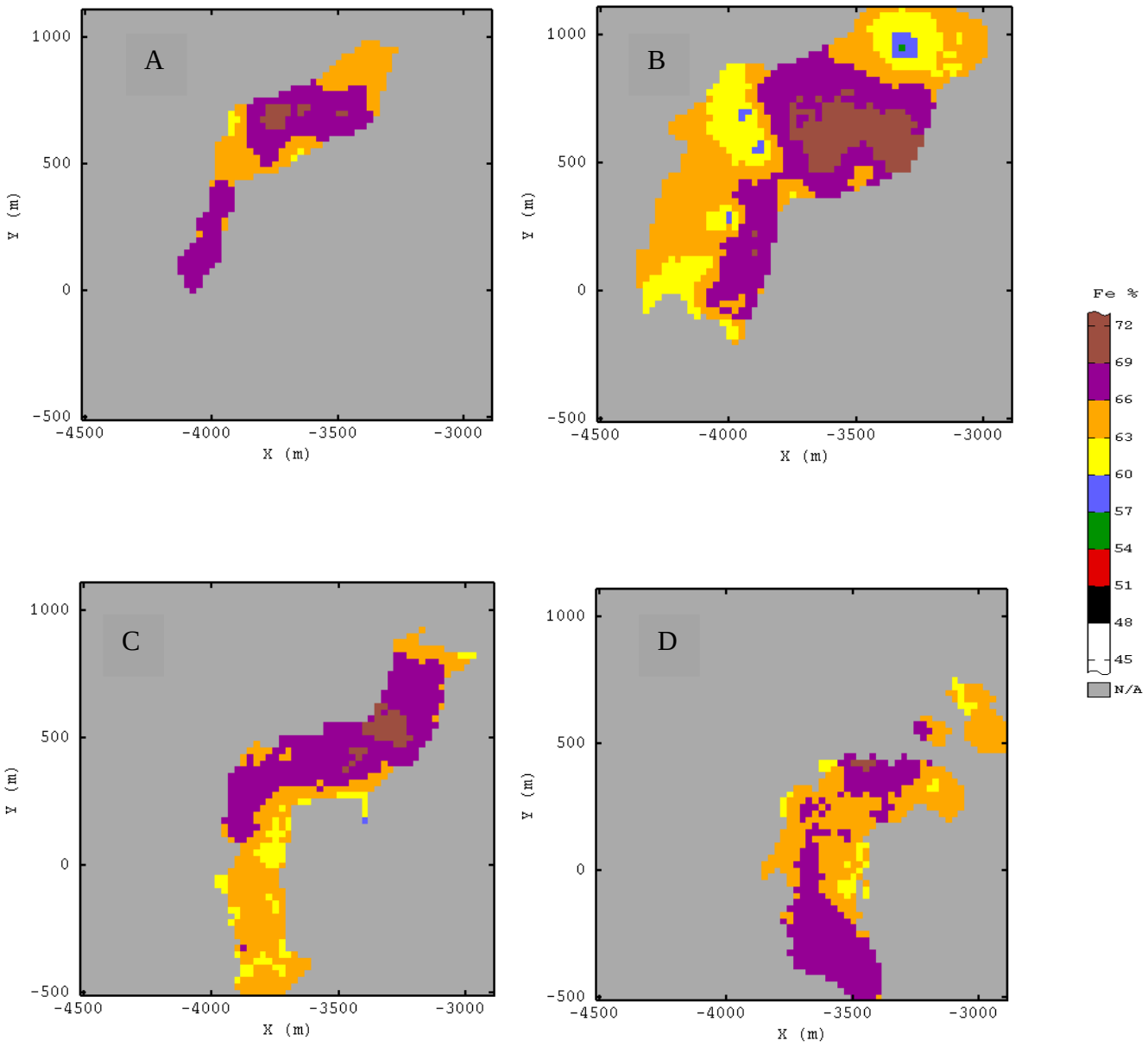


Figure 7.9 Estimates of Fe concentration by disjunctive kriging with 45 % Fe cut-off in 4 typical benches of reduced levels (A) 1140, (B) 1068, (C) 996, and (D) 924

## 7.7 Comparison of estimated recoverable resources (OK, IK and DK)

A comparison is made between the results of the estimated recoverable resources obtained from non-linear methods such as indicator kriging (IK) and disjunctive kriging (DK) with a linear estimation method ordinary kriging (OK) based on basic statistics of estimates and grade-tonnage curves. It can be observed from Table 7.6 and Figure 7.10(A) that the total tonnages estimated by IK is less than DK and OK for the cut-offs 45, 55 , 60 and 62 % Fe, whereas OK over estimated the total tonnage as compared to DK and OK at these cut-offs. It can be further observed that for the cut-offs 67 and 68 % Fe, the total tonnage estimated by DK and IK are almost same, but OK underestimated. For the cut-off 69 % Fe, OK estimates are underestimated as compared to DK and OK showing only 1.4 % of the total tonnage when both OK and DK showing more than 10 % of the total tonnage. In totality, it can be observed that DK estimates are globally consistent.

It can also be observed from Table 7.6 and Figure 7.10(B) that the mean grade estimated by DK is slightly higher than IK and OK for the cut-offs 45 % Fe. It is very interesting observation that from the cut-off 55 % Fe onwards for all the remaining cut-offs, DK and IK estimated grades are almost same. On the other hand, OK estimated grades are less for cut-offs 55, 60 and 62 % Fe as compared to IK and DK. It can be further observed that the mean grade estimated by OK, IK and DK are almost same for the cut-offs 67, 68 and 69 % Fe. In totality, it can be observed from Figure 7.10(B) that IK estimated mean is less than OK estimated mean up to a cutoff of 30 % Fe and IK estimates are more than OK above 30 %Fe, whereas DK estimates are globally consistent. This indicates that DK estimates are comparatively better and accurate for resource estimation of the deposit.

Table 7.6 Basic statistics of estimated total tonnage and mean grade in OK, IK and DK for different cut-offs

| Cut-off | Total Tonnage | | | Mean Grade | | |
|---|---|---|---|---|---|---|
| | OK | IK | DK | OK | IK | DK |
| 0 | 100.00 | 100.00 | 100.00 | 64.73 | 64.18 | 65.07 |
| 45 | 98.44 | 97.49 | 98.45 | 64.87 | 65.19 | 65.44 |
| 55 | 96.18 | 91.49 | 94.00 | 65.02 | 66.16 | 66.03 |
| 60 | 89.98 | 85.36 | 87.38 | 65.64 | 66.79 | 66.59 |
| 62 | 81.88 | 80.69 | 82.34 | 66.09 | 67.11 | 66.90 |
| 65 | 57.79 | 69.31 | 68.22 | 67.09 | 67.69 | 67.50 |
| 67 | 30.68 | 50.50 | 48.49 | 67.99 | 68.40 | 68.16 |
| 68 | 14.79 | 35.79 | 32.29 | 68.52 | 68.83 | 68.48 |
| 69 | 1.40 | 14.99 | 11.76 | 69.18 | 69.50 | 69.42 |

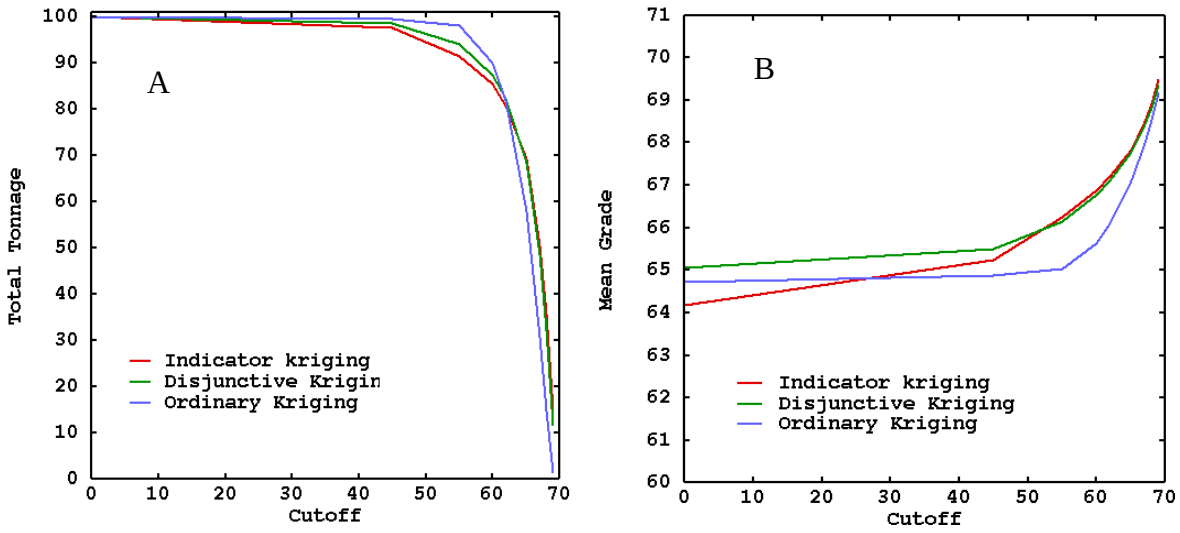


Figure 7.10 Comparison of grade-tonnage curves estimated using OK, IK and DK (A) cut-off grade vs total tonnage (B) cut-off grade vs mean grade.

## 7.8 Summary

In this chapter, bench composited data is transformed to Gaussian data using Gaussian anamorphosis modelling for different cut-offs. Semi-variograms are modelled in both horizontal and vertical directions for the raw Fe data which is required for support correction and for Gaussian variogram. It is observed from the semi-variogram models of Fe that both the horizontal and vertical directions show a very good structure with a small nugget effect. Anisotropy is observed in both the directions with ranges 400 and 90 respectively.

An experimental semi-variogram for gaussian block variable is calculated using the semi-variogram model of raw data (composited data) and the block anamorphosis. It is observed from the block Gaussian semi-variogram models of Fe (Figure 7.6) that both the horizontal and vertical directions show a very good structure with a small nugget effect. It is interesting to observe that the ranges of semi-variogram models in horizontal and vertical directions are same for punctual Fe data and block Gaussian Fe data (Tables 7.2 and 7.3). This indicates that gaussian block anamorphosis modelling using 30 Hermite polynomials and semi-variogram modelling are very accurate.

For the purpose of recoverable resources estimation by disjunctive kriging, a total nine number of thresholds (or cut-offs) are chosen i.e, 0 %, 45 %, 55 %, 60 %, 62%, 65%, 67 %, 68 % and 69 % Fe. The disjunctive kriging is applied to calculate the total tonnage and mean grade of Fe of the whole deposit above each of these nine cut-offs. It is observed from disjunctive kriged estimates of recovered tonnage (Table 7.4) and the grade tonnage curve *cut-off grade vs total tonnage* (Figure 7.7A) that the total recovered tonnage is about 98 % with a cut-off of 45 % Fe. It can be further observed from disjunctive kriged estimates of mean grade (Table 7.5) and the grade tonnage curve *cut-off grade vs mean grade* (Figure 7.7B) that for a cut-off of 45 %, Fe content ranges from 45.35 % to 69.5 % with a mean of 65.44 %. It is also observed that about 48 % of blocks have greater than 67 % Fe, with a mean grade of 68.16 % and about 12 % of blocks have greater than 69 % Fe with a mean grade of 69.42 % (Table 7.4 and 7.5). These high grade blocks can be used for selling directly which results in getting incentive price or by blending with low grade i.e < 55 % Fe to meet the customer requirement of 62 % Fe.

It is observed from probability maps of typical 4 benches (Figure 7.8) generated using disjunctive kriging estimates that majority of the blocks are having 80-90 % probability that Fe value exceeds 65 % and very few blocks with low probability 30-60% occur in peripheral blocks. Grade maps of the typical 4 benches (Figure 7.9) generated using disjunctive kriging estimates indicate that majority of the blocks are having Fe grade + 60 %. It is further observed that very blocks are occurring in peripherals (Figure 7.9B) having Fe between 57-60 %. In the total deposit, very few blocks in the bottom benches have Fe grade between 45-55%.

A comparison is made between the results of the estimated recoverable resources obtained from non-linear methods such as indicator kriging (IK) and disjunctive kriging (DK) with a linear estimation method ordinary kriging (OK). It can be observed from Table 7.6 and Figure 7.10(A) that the total tonnages estimated by IK is less than DK and OK for the cut-offs 45, 55 , 60 and 62 % Fe, whereas OK over estimated the total tonnage as compared to DK and OK at these cut-offs. It can be further observed that for the cut-offs 67 and 68 % Fe, the total tonnage estimated by DK and IK are almost same, but OK underestimated. For the cut-off 69 % Fe, OK estimates are underestimated as compared to DK and OK showing only 1.4 % of the total tonnage when both OK and DK showing more than 10 % of the total tonnage. In totality, it can be observed that DK estimates are globally consistent.

It can also be observed from Table 7.6 and Figure 7.10(B) that the mean grade estimated by DK is slightly higher than IK and OK for the cut-offs 45 % Fe. It is very interesting observation that from the cut-off 55 % Fe onwards for all the remaining cut-offs, DK and IK estimated grades are almost same. On the other hand, OK estimated grades are less for cut-offs 55, 60 and 62 % Fe as compared to IK and DK. It can be further observed that the mean grade estimated by OK, IK and DK are almost same for the cut-offs 67, 68 and 69 % Fe. In totality, it can be observed from Figure 7.10(B) that IK estimated mean is less than OK estimated mean up to a cutoff of 30 % Fe and IK estimates are more than OK above 30 %Fe, whereas DK estimates are globally consistent. This indicates that DK estimates are comparatively better and accurate for resource estimation of the deposit.

# CHAPTER 8

# RECOVERABLE RESOURCES ESTIMATION BY CONDITIONAL SIMULATION

# CHAPTER 8

# Recoverable Resources Estimation by Conditional Simulation

## 8.1 Introduction

In a field investigation, only a small fraction of *in-situ* data can be analysed, owing to time and cost constraints and the sparse measured data contain a considerable degree of uncertainty (Jang and Liu, 2004). Grades at unsampled locations are mostly determined by the minimum error variance interpolation algorithms such as kriging (Goovaerts, 1999). However, the kriging variances do not adequately reflect the uncertainty of estimates because the estimation variances are independent of the value being estimated and are related only to the spatial arrangement of the sample data and to the model variogram (Baskan et al; 2010). As kriging variances are observed to be proportional to the magnitude of the values, their use in constructing confidence intervals is suspected (Isaaks and Srivastava, 1989). It is also known that kriging may cause smoothing effects when variation is especially excessive among measured properties. This is a significant shortcoming as it gives overestimated values or of underestimated ones (Baskan et al., 2010). They further state that the conditional variances generated by simulation models depend not only on data configuration but also on data values, and theoretically provide a more realistic assessment of the uncertainty across space than the error variances obtained with simple kriging estimations.

Simulation, in general, is the process of designing a model of a real system and conducting experiments with this model for understanding the behavior of a system or of evaluating various strategies for the operation of the system (Shannon, 1975; Ingalls, 2001). Geostatistical simulation is a generalization of the concepts of Monte Carlo simulation to include three-dimensional spatial correlation (Dowd, 1992; Journel and Alabert, 1989, 1990; Journel and Huijbregts, 1978; Journel and Isaaks, 1984; Jackson et al., 2003). Geostatistical simulation which typically uses a kriging technique produces multiple sets of possible values (models) distributed in space; one set of possible outcomes is referred to as a ‘realization’ (Leuangthong et al., 2004). The major difference between the traditional estimation and geostatistical simulation is that the

simulation produces, a number of equally-likely images i.e., realizations of the grade estimation, which shows a range of possible events, as opposed to estimation methods, which output a unique result as shown in Figure 8.1 (Godoy et al., 2001). Each of the realizations honours the distribution reproducing the data histogram and also honours the spatial variability of data, characterised by a variogram model (Mata Lima, 2005). If the simulations also honour the data values themselves, they are called 'conditional simulations' (Jang and Liu, 2004).

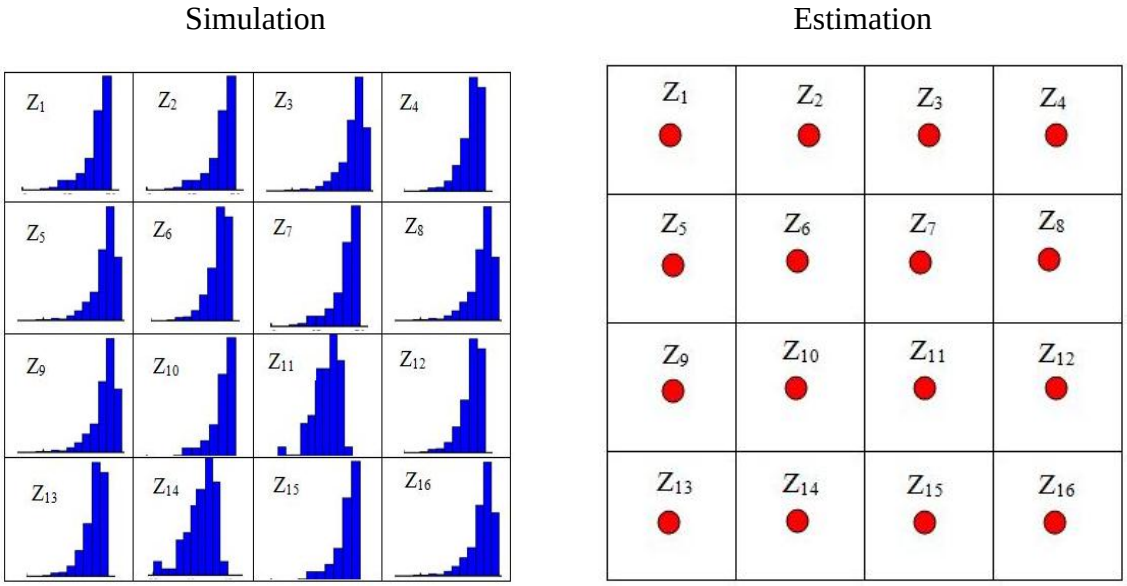


Figure 8.1 Range of possible values from simulation (left) and single estimated values (right) (Godoy et al., 2001)

A simulated map, which is some realization of the adopted random function model, looks more ''realistic'' than the kriged map from the statistically ''best'' estimates because it reproduces the spatial variability modeled from the sample information (Baskan et al., 2010). Condition simulation is thus increasingly preferred to kriging for application where the spatial variation of the measured field must be preserved (Srivastava 1996). Many geostatisticians (For ex., Goovaerts 2000; Pebesma et al. 2000; Hengl and Toomanian 2006) recommend that only simulations should be used to visualize maps because they offer the true representation of the stochastic component i.e., short-range variation. Furthermore, these techniques were developed largely in direct response to the inadequate measures of spatial uncertainty associated with the classical methods and are explicitly linked to the assessment of uncertainty. Geostatistical simulation is an approach to modeling the spatial data that attempts to reproduce the range of

values present in the data, as well as the spatial variability described by the variograms (Chiles and Delfiner 1999).

Conditional simulation of stationary variable was introduced in geostatistics by Journel (1974). Subsequently, geostatistical simulations and its applications were discussed by various researchers (Luster, 1985; Christakos, 1987; Michael Davis, 1987; Mantoglou, 1987; Chiles, 1977; Delfiner and Delhomme, 1973; Delfiner and Chiles, 1977; Dimitrakopoulos, 1988, 1990, 1994; Armstrong and Dowd, 1994; Goovaerts, 1997; Chiles and Delfiner, 1999; Lantuejoul, 2002; Vann et al., 2002; Mata lima, 2005; Phillipe Renard, 2011; Emery, 2012). An overview of conditional simulation for resource estimation is given by Khosrowshahi and Shaw (1997) and practical aspects are presented by Rossi and Alvarado (1998), Dowd (1996), and Glacken (1996).

The simulation approach has received considerable attention in various applications such as visualization of fluctuations in major geologic patterns, simulation of mining processes, evaluation of recoverable resources, optimization of exploitation parameters, modeling subsurface flow, and weather forecasting (Christakos, 1987)). Besides, simulations provide a path to evaluation and analysis of drill spacing, selectivity, blending and sensitivity to different mine scheduling approaches (Humphreys and Shrivastava, 1997; Jackson et al., 2003; Sanguinetti et al., 1994). Geostatistical simulation applications also include remediation of soil deficiencies, clean-up of polluted soils and aquifers, fluid flow and oil recovery evaluation in reservoirs, mine planning and grade control in mineral deposits (Xavier Emery, 2007). Geostatistical simulation is widely used and accepted as a method of generating stochastic models of mineral deposits, hydrocarbon reservoirs and geological structures (David et al., 1974; Dowd, 1994; Dowd and David, 1976) and also for design, analysis and risk assessment (Dowd, 1997). A series of conditionally simulated models allows the assessment of the uncertainty about the actual distribution of grades (Dimitrakopoulos, 1998). A growing area of application for geostatistical conditional simulation is as a tool for risk assessment and uncertainty modeling in environmental engineering, soil science, hydrology, reservoir characterization, and ore reserve evaluation (Lantue´joul 1994, 2002; Chile`s and Delfiner 1999; Jackson et al., 2003). In these applications, accurate field measurement of a variable at a specific location is difficult and measurement of variables at all locations is impossible. Conditional simulation provides a means of generating stochastic realizations of spatial variables at unsampled locations, using

constraints, eg statistical moments imposed by the data, thereby quantifying the uncertainty associated with limited sampling and providing stochastic models for applications such as risk assessment (Dowd and Pardo-Iguâ Zquiza, 2002; Dowd 1994a, 1997). Thus, in simulation, requirements of stationarity are stricter than for kriging (Vann et al., 2002; Jackson et al., 2003).

Non-linear estimation and conditional simulation have been rarely used in iron-ore deposits, though these techniques have wide application in other mineral deposits such as gold and base metals (De-vitry et al., 2007). Recently, conditional simulation is extensively applied for grade estimation of copper deposit (Emery and Silva, 2009; Emery 2012), iron ore deposit (Guibal et al., 1997; De-vitry, 2003; Asghari et al., 2009), uranium and arsenic deposit (Journel and Isaaks, 1984), gold deposit (Jackson et al., 2003), for optimization of drilling grid in zinc and lead deposit (Miller, 1991), and for determining an optimal sampling configuration in kimberlite ore bodies (Deraisme and Farrow, 2005). Interestingly, conditional simulation was also applied in non-mining industry such as in prediction of earth quake (Torcal et al., 1999), ice penetration in Arctic (Christakos, 1987) pollution (Fabbri and Trevisani, 2005; Wang and Zhang, 1999), forestry (Xavier Emery 2005b) and hydrogeology (Philippe Renard et al., 2011).

There are several mathematical algorithms for geostatistical simulation viz., Turning Bands, Sequential Gaussian, LU (lower upper) Decomposition, Sequential Indicator, Truncated Gaussian, Plurigaussian, Direct Sequential and Annealing simulation. A brief description of these methods is given in David Grimes and Pardo Iguzquiza (2010). In this study, the two methods of conditional simulation, more useful in the mining industry, are used for extracting multiple realizations of Fe grade distribution and for estimation of recoverable resources with different cut-offs. These two methods are - '*Turning bands'* (TB), which was the first large-scale 3D Gaussian simulation algorithm (Journel, 1974) and '*Sequential Gaussian simulation'* (SGS), which is efficient and widely used (Lantuejoul, 2002).

Both TB and SGS methods rely on the data having Gaussian distributions. In practice, drilling data never meets this criterion, thus the original drilling data of Fe are first transformed into a Gaussian variable and variogram modelling is carried out for this Gaussian Fe. A search neighbourhood is defined because conditional simulation by both methods (SGS and TB) involves kriging step. Subsequently, conditional simulation is employed on a grid with a node spacing of 25 x 25 x 12 m. In each method a total number of 100 realizations are generated for

Fe variable. After simulation of Gaussian values, the simulated data are back-transformed into a raw data distribution (De-Vitry et al., 2007; Pardo_Iguzquiza, 2010). Comparisons between the results of turning band method and the sequential Gaussian method are made and the results are discussed.

## 8.2 Gaussian transformation and Gaussian semi-variogram

Both *turning band* and *sequential Gaussian simulation* methods require the data in Gaussian space. Thus, prior to simulation, the original drilling data of Fe are transformed into a Gaussian variable (Figure 8.2) and semi-variogram modelling is carried out for Gaussian Fe (Figure 8.3). It can be observed from Figure 8.2A that the raw data is successfully transformed to Gaussian (normal) distribution (Figure 8.2 B) showing mean 0 and variance 1.

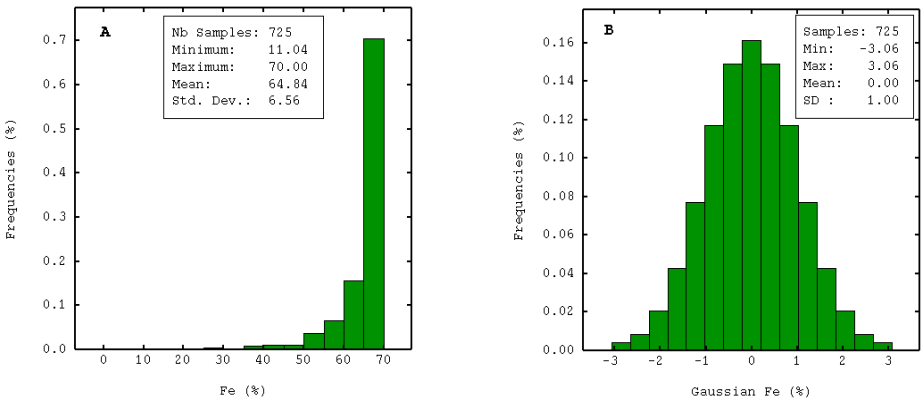


Figure 8.2 Histograms of Fe data. (A) raw data and (B) Gaussian transformed data. Raw data is transformed successfully to normal distribution by Gaussian anamorphosis modelling resulting mean 0 and variance 1.

Semi-variogram model of Gaussian Fe data (Figure 8.3) reveals a good structure with a small nugget effect of 0.15 and consists of 2 nested structures of spherical models having a short range of 80 m and long range of 425 m in the horizontal direction (Figure 8.3 A) and a range of 90 mts in the vertical direction (Figure 8.3 B). It implies that there is no correlation in Gaussian transformed data beyond 425 m distance in samples in XY plane and 90 mts in Z direction.

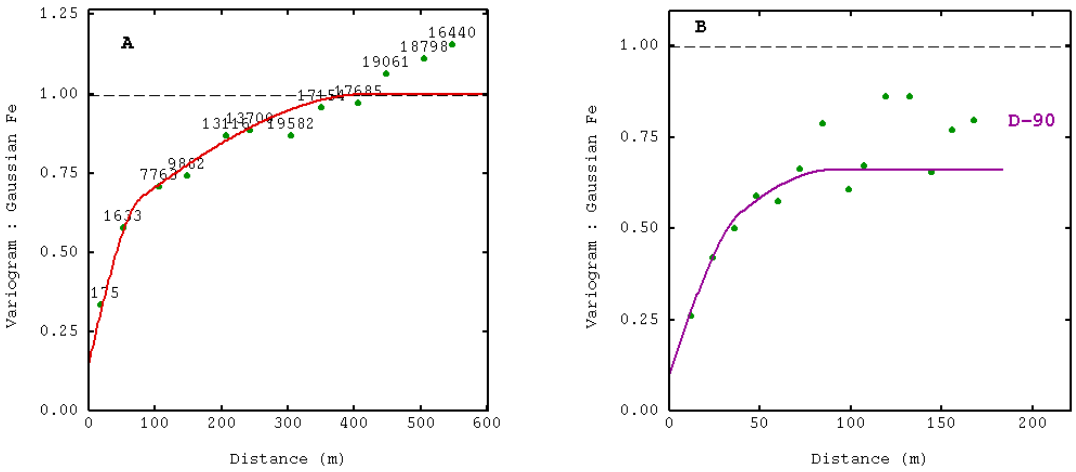


Figure 8.3 Semi-variogram model of Gaussian data of Fe, modelled with two spherical models with nugget effect in horizontal direction (A), and vertical direction (B).

## 8.3 Turning band method

Stationary random fields (also called stationary stochastic process) occur naturally in several areas of science, and the study of stationary processes has been an active field of research for several years. In the fields of geology, mining, environment, engineering sciences and others, several simulation methods exist for simulating such stationary processes. One method for simulating stationary processes is called the turning bands method (Wright, 1987). The geostatistical turning bands method (TBM) of simulation, proposed by Matheron (1973) and Journel (1974), generates Gaussian random fields in three-dimensional space (Gneiting, 1999).

The turning bands method, an approach of a stochastic simulation based on the theory of random fields, constitutes a model of reality which satisfies a number of requirements and preserves certain structural characteristics of the true pattern, and the simulated data has the same mean, variogram, and histogram as the original data and the accuracy of the simulation is improved by adding the condition that the simulated surface honors the data points (Christakos, 1987). The details of the turning band method are explained in detail by Journel and Huijbregts (1978). Details on the implementation of TBM for simulations are given by various researchers (Journel and Huijbregts, 1981; Mantoglou and Wilson, 1982; Brooker, 1985; Dietrich, 1995; Gneiting, 1998).

The turning band method simulates multidimensional (usually three dimensions) random field by summing contributions from a one-dimenisonal (1D) simulation process with a particular covariance structure. The appropriate one-dimensional covariance model is deduced from the covariance model of the three-dimensional process (Jackson et al., 2003). In one-dimensional simulations, a moving average technique is used (Wright, 1987). In this method, a series of independent one-dimensional realizations are first simulated with an intermediate covariance on set of N lines and the final simulated field is generated by combining the contributions of the simulations along the N lines. These N lines radiate from a central point and are equally distributed in space (Figure 8.4A). The simulated value at a given grid point is obtained by summing values taken at the closest point on each of the lines, by dropping a perpendicular from the grid point to the line (Figure 8.4B). The sum of these values gives the required value at the point in three dimensions (Brooker, 1985).

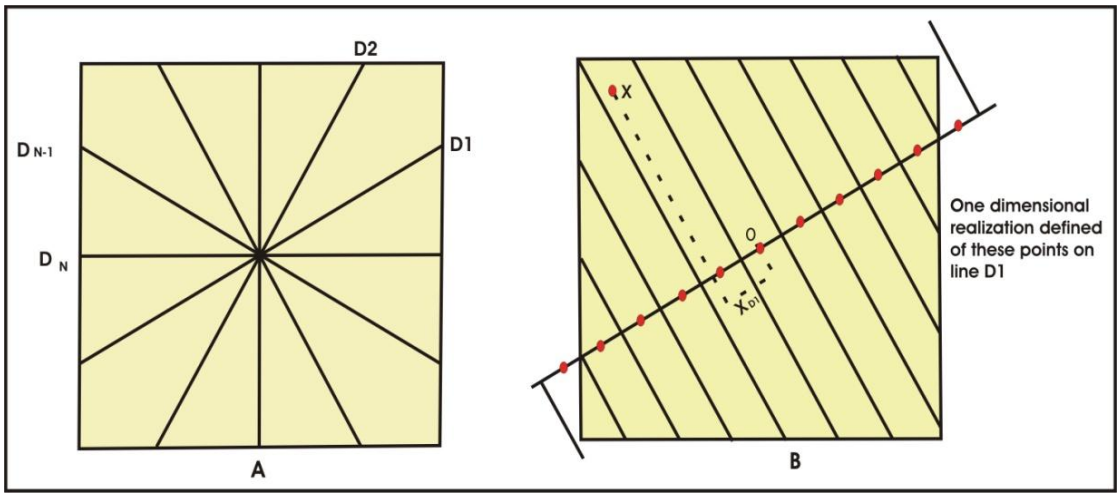


Figure 8.4 (A) Turning bands associated with line D1. Grid points in two dimensions are projected onto this line and take the value from the one-dimensional simulation appropriate to the band within which they fall. (B) Area to be simulated and a uniformly distributed set of N lines $D_1$, $D_2$,…, $D_N$ on which one-dimensional realizations are the first simulated (Brooker, 1985).

The theory requires a dense uniform distribution of N lines on which the intermediate one-dimensional realizations are generated. These N lines are distributed regularly (Lantuejoul, 2002) or independently and uniformly (Journel, 1974) or according to sequences with weak discrepancy on the unit sphere (Bouleau, 1986). Journel (1974) suggests that the 15 axes of the regular icosahedrons – the maximum number of uniformly distributed lines in three dimensions –

gives an adequate approximation to the theoretical infinite sum. However, earlier studies have employed only 15 lines (Brooker, 1985). The method produces realizations $Z_i(x)$ on N (say 15) lines distributed in 3D. The realizations $Z_i(x)$ are averaged to produce a realization $Z_s$ in 3D (Journel and Huijbregts, 1978; Ellefmo and Eidsvik, 2009) as

$$Z_s = \frac{1}{\sqrt{N}} \sum_{i=1}^{N} Z_i(x) \tag{8.1}$$

***Conditioning the data***

The method for conditioning the simulation i.e., obtaining a conditional simulation from a non-conditional simulation to take the same values at sampled locations, is described in Journel and Huijbregts (1981, p.494). The conditioning is performed through a separate kriging step (Chiles and Delfiner, 1999) in which a correlated error obtained from the simulation to a grid kriged from the data is added. As the grid kriged from the data will be smoother than reality, to produce a grid which reproduces the spatial variability of the underlying random function, a new kriged grid is produced by using simulation values at data locations as values used in kriging. This new kriged grid is subtracted from the non-conditional grid to give a grid of correlated errors. This grid of errors is added to the original kriged grid to produce a conditioned simulation (Davis, 1987).

$$\text{So, } Z_{cs} = Z_k + (Z_{ncs} - Z_{kncs}) \tag{8.2}$$

where $Z_{cs}$ is the conditional simulation, $Z_k$ is the grid kriged from real data, $Z_{ncs}$, is the non-conditional) simulation, $Z_{kncs}$, is the grid kriged from non-conditional simulation data. This can be rewritten as

$$Z_{cs} = Z_{ncs} + (Z_k - Z_{kncs}) \tag{8.3}$$

Because data locations are the same, $(Z_k - Z_{kncs})$ can be obtained by kriging differences between data values (Z) and simulated values ($Z_{ncs}$) at data locations (Catherine Bleines et al., 2011).

$$Z_{cs} = Z_{ncs} + (Z - Z_{ncs})_k \tag{8.4}$$

The explicit representation of a kriged grid for the case of simple kriging with a zero mean gives the estimate for a single point as

$$Z^* = A^{-1}B\ Z \tag{8.5}$$

where A is the matrix of covariances between the data points, Z is the vector of data values, and B is the vector of covariances between the target block and the data (Davis and Culhane, 1984, p. 602). For a grid of m points this can be rewritten as

$$Z^* = A^{-1}C\ Z \tag{8.6}$$

where $Z^*$ is a vector of estimated grid values and C is an $m \times n$ matrix containing vectors k for each individual value estimated.

The two significant input parameters that TB method depends on are 'number of turning bands' and 'seed number'. The number of turning bands is the critical parameter involved as the quality of the simulation relies on this single parameter; this number should be large enough to ensure the quality of the resulting simulations. This number must be greater than the number of grid nodes along X, Y directions and less than the total number of grid nodes (Catherine Bleines et al., 2011b). Artifacts are reported when the number of lines is small (Deutsch and Journel, 1992; David Grimes and Pardo_Iguzquiza, 2010). Thus, several attempts are made in this study taking different number of turning bands (300, 500, 1000, 1500, and 2000) and finally a total number of 2000 turning bands are used as there is no significant change in the simulation results beyond this number.

The other input parameter defined in turning band simulation is a 'seed number' for generating random numbers. According to Catherine Bleines et al. (2011b), there is no genuine rule for setting a seed; nevertheless a common practice is to define the seed as a large prime number, avoiding 1 or 2 digit numbers. In several statistical applications, there is a need to generate random values and thus manufacturers always provide a built in function in the software to generate random values based on variable events such as process id, the time of the day and CPU time elapsed. This option has not been used in *Isatis* software as it cannot replicate a whole series of random numbers if we wish to produce twice the same simulation. For this reason, Isatis defined a machine and time independent system for generating series of random numbers. For a 32 bits version of Isatis, random numbers are generated based on the parameters- Modulo 20,000,159 and multiplier 105 resulting the seed value to be 423141 (Geovariances, 2013b).

In this study, conditional simulation employing TB method is carried out for Fe variable using Gaussian data, Gaussian semi-variogram, 2000 turning bands and 100 realizations with seed value 423141. A block of dimensions 25 x 25 x 12 mts is considered for simulation and a total number of 17057 blocks within the ore boundaries of 32 benches of the deposit are simulated. The simulated Gaussian data is back transformed using Gaussian anamorphosis function. Subsequently, the simulated results of TB for 7 typical different realizations which include (i) basic statistics (Table 8.1), (ii) histograms (Figure 8.6) and (iii) semi-variograms (Figure 8.8A) are presented in section 8.6.

## 8.4 Sequential Gaussian simulation method

Another method for simulating stationary random fields is sequential Gaussian simulation, which differs from the turning bands method. Sequential Gaussian Simulation (SGS) is efficient and also widely used in the mining industry for prediction of uncertainty of estimates (Wang et al., 2002; Baskan et al., 2010). Like turning bands method, SGS requires normalized data and a variogram model for the normalized data to proceed with algorithm. A grid consisting of blocks of dimensions 25 x 25 x 12 mts is defined and initially estimated using simple kriging. Kriging is done at each node of the grid following a random path generated from equation 8.7.

$$\begin{aligned} \mathrm{R}_i &= \mathrm{mod}(5R_{i-1} + 1.2^m) \\ &= (5R_{i-1}) + 1 - \mathrm{int}\left\{\frac{(5R_{i-1}+1)}{2^m}\right\}.2^m \end{aligned} \tag{8.7}$$

Where, Ri is a random indicator for node i, m is a great number which makes (2m) greater than number of network's nodes (Asghari et al., 2009).

Based on kriging mean and variance, a Gaussian probability distribution has been determined in each node. A random value which is drawn from Gaussian probability distribution is known as a simulated value in each node (Ersoy and Yunsel, 2009). All grid nodes (points) in the path generated by equation 8.7 are progressively simulated. Each new simulated value is then added to the conditioning data and the next point in the path is simulated (and so on) (Jackson et al., 2003). Once all the nodes in the block model are visited, one realization is generated. A new realization is generated simply rerunning the process with a new random seed (Hansen and

Mosegaard, 2008). The resulting simulated values are transformed into another set of variables to reproduce the input global histogram using 'Simulation Post-processing' (Journel and Xu, 1994; Caers, 2000a; Oz et al., 2003).

The following steps have been adapted in generating equally probable models by using SGS algorithm as suggested by various researchers (Deustch, C. V., Journel, 1992; Goovaerts 1997; Costa et al., 2000; Asghari et al., 2009; Ersoy and Yunsel, 2009) and are shown in Figure 8.5.

- Histogram of regularized raw data is calculated.
- Regularized raw data is transformed into Gaussian distribution.
- Semi-variogram model of Gaussian data is calculated.
- A grid consisting of 3D blocks is defined
- A random path is defined.
- Each node in the grid is kriged from all other values (known and simulated) and Gaussian is defined.
- A random value from Gaussian distribution is drawn which is known as simulated value.
- Other nodes are simulated sequentially
- Simulated value is back transformed (in this step a realization is generated) and
- Step 1 to 9 are repeated to generate another realization.

Several authors have employed sequential Gaussian simulation (SGS) in Earth science related fields. For ex., SGS was applied for grade estimation of a copper deposit (Xavier Emery, 2007), iron ore deposit (Asghari et al., 2009), coal deposit (Costa et al., 2000), lignite deposit (Ersoy and Yunsel, 2009), uranium deposit (Dimitrakopoulos, 1998), gold deposit (Godoy et al., 2001; Jackson et al., 2003; Leuangthong et al., 2004), in optimization of sampling design (Englund and Heravi, 1992), linear inversion in geophysics (Hansen et al., 2006), and soil erosion (Baskan et al., 2010).

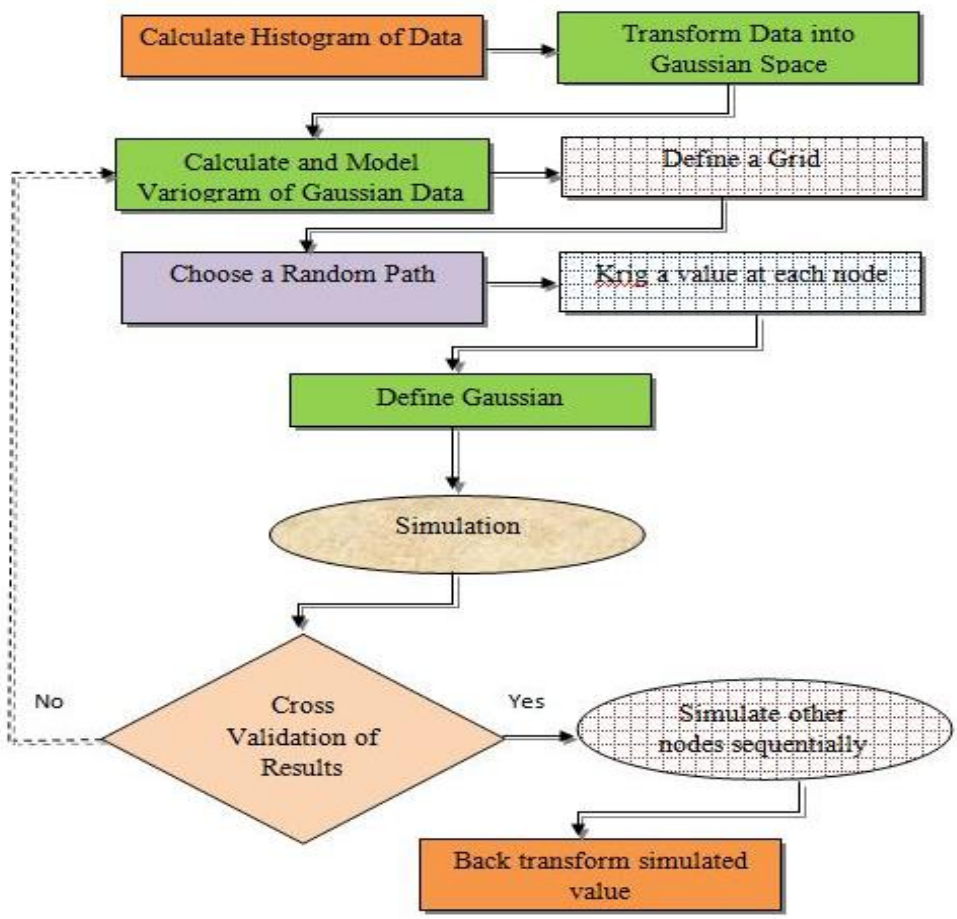


Figure 8.5 Flow chart showing the basic steps in SGS algorithm (Asghari et al., 2009).

In this study, conditional simulation employing SGS method is carried out for Fe variable using Gaussian data, Gaussian semi-variogram model and 100 realizations with seed value 423141. A grid of block dimensions 25 x 25 x 12 mts is considered for simulation and a total number of 17107 blocks are simulated. The simulated Gaussian data is back transformed using Gaussian anamorphosis function. The simulated results of SGS for 7 typical different realizations which include (i) basic statistics (Table 8.2), (ii) histograms (Figure 8.7), semi-variograms (Figure 8.8B) are presented in section 8.6.

## 8.5 Simulation post-processing

At an early stage of a project, where mining is yet to be commenced, like the Bailadila Iron Ore Deposit under study, the risk associated in resource estimation needs to be quantified. As the mining operations progress an additional drilling and geological information are acquired,

the degrees of uncertainty on both grade and geological interpretation will reduce substantially. However, geological risk at early stages could easily have a dramatic impact on financial outcomes. Therefore, in practice, conditional simulation studies are often performed for early stage risk analysis (Jackson et al., 2003). The iron ore will be supplied mostly as run-of-mine material directly to steel plants, respecting the quality technical specifications for Fe. Variations in the grades at the mine site must be predicted in order to forecast possible loss that might arise due to exceeding maximum contractual limits. For this purpose, the results of simulations are useful to produce the maps which identify the Fe grade that can be mined under quality limitations on the mine site (Erosy and Yunsel, 2009). Multiple realizations of the deposit allow for the assessment of uncertainty (Leuangthong et al., 2004).

In Bailadila Iron ore deposits, the technical specifications of the Fe grade suggest that run-of-mine should have Fe content not less than 45 % for considering as 'ore'. This value is chosen as critical cut-off value in the uncertainty assessment of the quality variables after the simulation process. The conditional probability of exceeding this critical value is computed for Fe variable. In NMDC mines, Fe grade between 45 % and 55 % is considered as 'sub-grade' category and it is mined separately. This sub-grade ore is used for blending with high grade ore to meet the customer requirement of 62 % Fe. For this reason, the conditional probability of exceeding this value is computed. Based on the customer requirement, in general, a cut-off of 62 % Fe is included. Other cut-offs 65 %, 67 %, 68 % and 69 % are considered to find out the tonnage that can be extracted with these cut-offs which can be used for blending with low grade. Thus, a total of 8 cut-offs are considered for simulation post-processing to generate (i) grade-tonnage curves and (ii) probability maps. These are generated from mean of the 100 realizations of the simulation computed for each grid node.

***Grade tonnage curves***

Grade-tonnage curves are useful tools which guide mine managers in scheduling of mining production and in risk assessment (Dimitrakopoulos, and Fonseca, 2003). According to these curves, average grade and total recoverable tonnage for different cut off grades are estimated. Using these curves, the best and the worst alternatives are produced, so the risk of operation is predictable (Vann et al., 2002). The curve provides the uncertainty of potential Fe when analyzing cash flows and other financial aspects in evaluation of project (Asghari et al.,

2009). A comparison of total tonnage recovered and mean grade of Fe for different cut-offs in both TB and SGS methods is given in Table 8.3 and the grade-tonnage curves of the deposit for different cut-offs in both TB and SGS methods as compared to original data is given in Figure 8.9.

***Probability maps***

A simulation method produces a macro variable consisting of range of values at each grid cell. Therefore, a specific simulation post-processing is required to transform such a macro variable into a probability map. A cumulative distribution function is related to each grid node in the macro variable and using this information, the probabilities that a specified threshold value is exceeded are analyzed in each location. Such analysis was based on the threshold of inverse cumulative distribution functions. After assigning a specified probability to each grid node then the probability maps are produced (Hlasny, 2009). In this study, 25 x 25 x 12 m grid is used to produce the probability maps for different cut-offs using mean of 100 realization values at each grid node. The probability maps for different cut-offs in a typical 1068 Mean Sea Level, showing the areas with probability of exceeding the cut-off value using SGS data is represented in Figure 8.10.

Geostatistical simulation is much more computationally demanding than geostatistical estimation. However, the exponential increase in computer processing speed, memory and data storage capacity have brought these tools into wide operational use in the mining industry over the past decade and as a result one can generate several simulated images (Jackson et al., 2003).

## 8.6 Results and Discussion

Kriging provides the most accurate linear estimation. However, the spatial structure of the estimated values differs from that of the actual ones. Therefore, the kriged values cannot be used as a suitable numerical model when the variability has to be taken into account (Fouquet 1994), but can be used as good interpolation results (Wang and Zhang, 1999). For the purpose of obtaining minimum variance of the prediction error, smoothening the variability of observed values by kriging (Eggleston et al., 1996; Lin et al., 2000) increases with a nugget effect

(Goovaerts, 1997). Conditional simulations can overcome the above short coming (Jang and Liu, 2004).

Jackson et al., (2003) employing both TB and SGS methods quantified grade risk in an underground gold deposit. Their study demonstrates that the geostatistical simulation method used is a robust and useful tool to quantify grade risk. Prior to their study, three branches geologists (exploration geologist, resource geologist and mine geologist) did a three-dimensional interpretation of the orebody using identical information of this deposit and generated three different models with a tonnage variation of ± 25 %. Authors concluded that with some exceptions in global mean, judged in terms of adequacy of replication of input histogram and variogram, compared to SGS method, turning bands method performed well on the gold deposit, although the differences were not highly significant. Therefore, turning bands simulations were used for their study.

Asghari et al. (2009) compared conditional simulation employing sequential Gaussian simulation (SGS) and geostatistical estimation through ordinary kriging (OK) for a magnetitic iron ore deposit. Authors have shown that there is a close match between histograms, statistical parameters and variograms of the raw data and 4 realizations of SGS. They have found that both SGS and OK provided similar results in terms of grade and tonnage. A difference of only 4 million tons was observed in OK (112 MT) as compared to SGS (108 MT) and the average grade changed from only 55.4 % Fe to 56 % Fe.

### 8.6.1 Validation and Reproduction of Results

Before proceeding with the use of simulated models into resource modelling and further in mining planning, validation of simulated models has been carried out. Reproduction of the original data, histogram and variogram by the simulated models are checked as suggested by Costa et al., (2000). Although, simulations are carried out for several realizations, the check is performed only for few realizations, and any departures from the original data are typically attributed to ergodic fluctuations (Srivastava, 1996). Hence it is restricted to seven realizations for validation purpose. Slight deviations may be the result of numerical precision of the back transformation of simulated values to the original values (Leuangthong et al., 2004). Some realizations generated may have probability distributions and semi-variograms that are

substantially different from the input distributions and semi-variograms. This may be due to the fact that original statistics are inferred from sparse samples and cannot be deemed exactly representative of the population statistics (Deutsch and Journel, 1992). It is necessary to look for realizations that would reproduce accurately the input statistics in each realization (Deutsch and Journel, 1992; Pachepsky and Timlin, 1998). Thus, a typical 7 realizations are considered for validation purpose and the validation tests such as summary statistics, histograms and variograms are carried out in this study. Further, mean of 100 realizations at each grid node are considered for post processing the simulations results which include global mean, grade tonnage curves and probability maps.

***(i) Summary statistics Results***

For each realization, minimum, maximum, global mean and a global variance in both TB and SGS simulated data sets are presented. Summary statistics of the simulated data generated in both these methods for 7 realizations are presented in Table 8.1 and 8.2. It can be observed from 7 realizations in TB method (Table 8.1) that, the mean varies from 64.40 to 64.71 with a variance of 42.04 - 47.81; whereas from 7 realizations in in SGS method (Table 8.2), the mean varies from 64.70 to 65.28 with a variance of 36.79 - 41.20. It can be further observed that all the seven realizations honor the original data individually in both TB and SGS methods. In both the cases, the mean of the 100 realizations also honour the original data (mean 64.84 and variance 43.03). Thus the means of the original data and of the simulated block grades are in excellent agreement. The variances of the simulated quality variable Fe are close to those of the original Fe. It is also observed that the minimum and maximum values of simulated Fe % are in line with the input data. In total, the statistical values of the simulated data are similar to the statistics of the original data.

***(ii) Histogram Reproduction***

The histograms of the simulated models of TB and SGS methods are examined to verify global reproduction of the histogram of the original data. Figures 8.6 and 8.7 show the histograms of seven realizations generated from TB and SGS simulated data respectively, in comparison with the histogram of the original sampling. It can be observed from these two

figures that the suite of distributions honors the input histogram with some statistical fluctuations which are within the acceptable limits.

Table 8.1 Basic Statistics of Simulated data in different realizations (n = 17057 blocks) using TB method.

| Realization | Min | Max | Mean | Std.Dev | Variance |
|---|---|---|---|---|---|
| 8 | 11.21 | 69.99 | 64.40 | 6.49 | 42.11 |
| 17 | 11.13 | 69.99 | 64.71 | 6.48 | 42.04 |
| 47 | 11.04 | 70.00 | 64.61 | 6.59 | 43.43 |
| 54 | 11.19 | 69.98 | 64.41 | 6.80 | 46.26 |
| 72 | 11.04 | 69.99 | 64.44 | 6.91 | 47.81 |
| 82 | 11.04 | 70.00 | 64.38 | 6.52 | 42.58 |
| 92 | 12.94 | 70.00 | 64.40 | 6.34 | 40.22 |

Table 8.2 Basic Statistics of Simulated data in different realizations (n= 17107 blocks) using SGS method.

| Realization | Min | Max | Mean | Std.Dev | Variance |
|---|---|---|---|---|---|
| 4 | 11.04 | 70.00 | 64.98 | 6.06 | 36.79 |
| 11 | 11.16 | 70.00 | 65.05 | 6.19 | 38.31 |
| 22 | 11.04 | 70.00 | 64.94 | 6.30 | 39.67 |
| 44 | 11.04 | 70.00 | 64.86 | 6.23 | 38.85 |
| 52 | 11.04 | 70.00 | 65.28 | 6.17 | 38.04 |
| 72 | 11.04 | 70.00 | 64.70 | 6.42 | 41.20 |
| 85 | 11.04 | 70.00 | 64.90 | 6.32 | 40.00 |

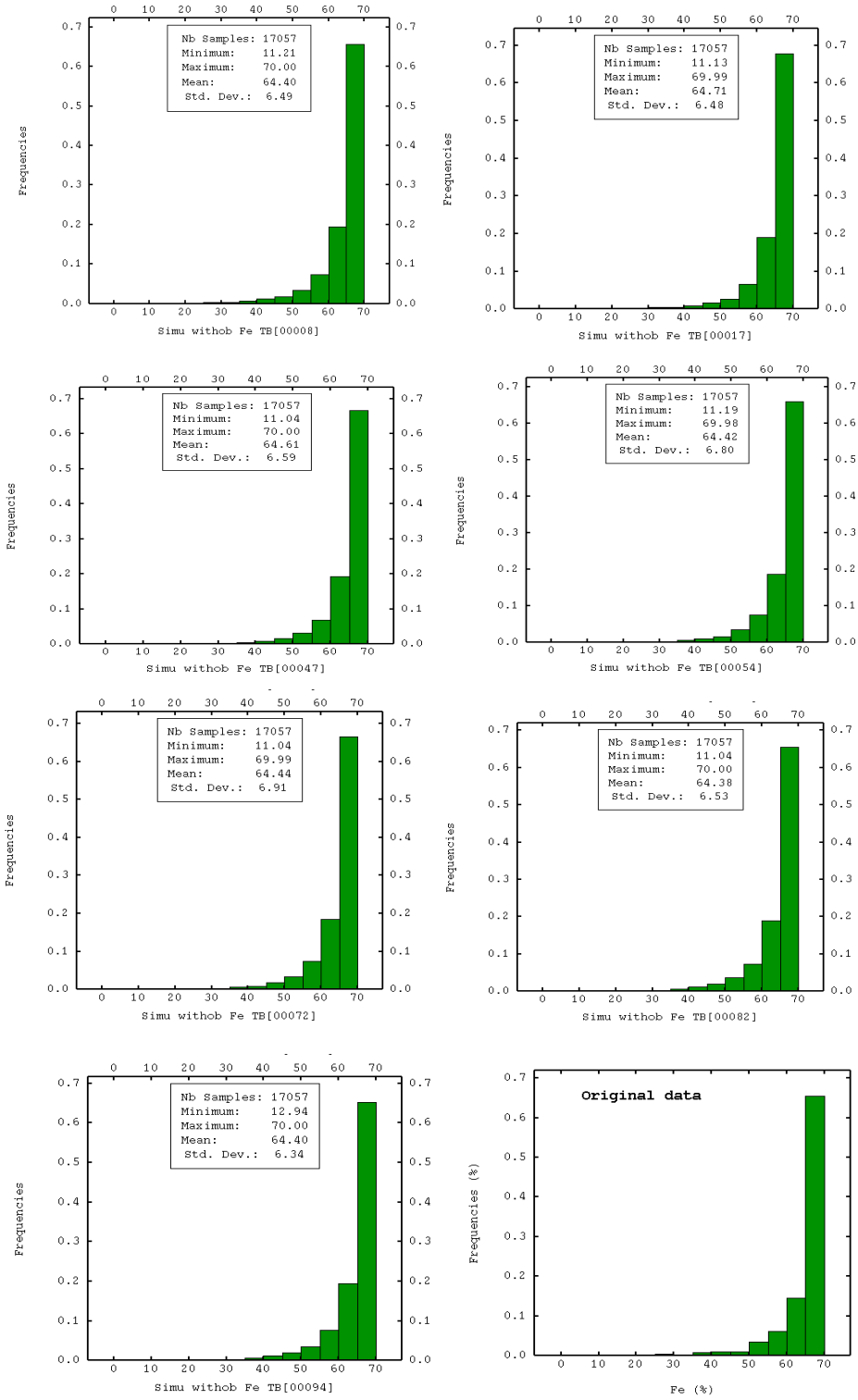


Figure 8.6. Histograms for seven different realizations 8, 17, 47, 54, 72, 82 and 94 of conditionally simulated data using turning bands method and of original data. Each one representing equally probable representation of Fe.

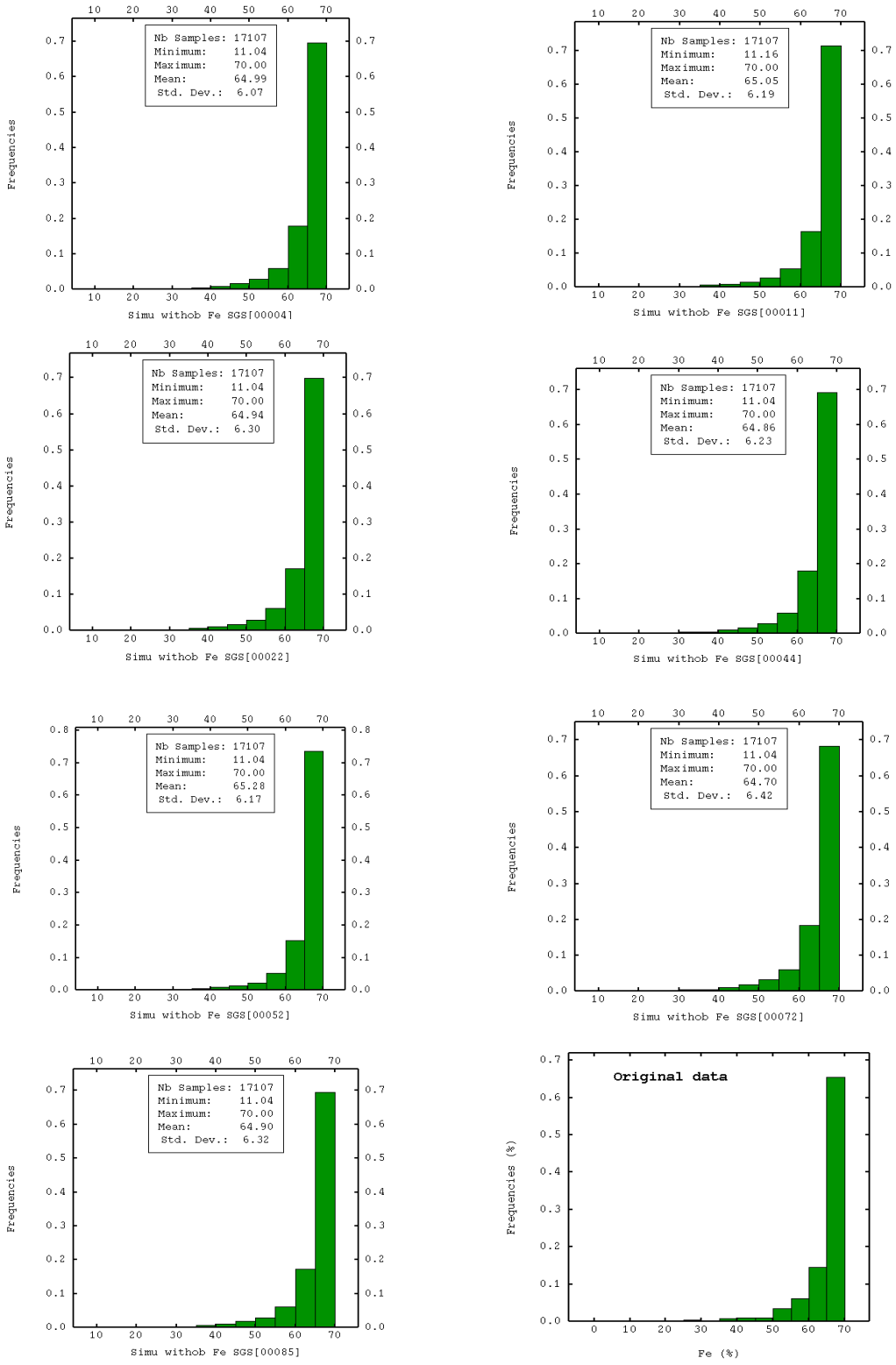


Figure 8.7. Histograms for seven different realizations 4, 11, 22, 44, 52, 72 and 85 of conditionally simulated data using sequential Gaussian method and of original data. Each one representing equally probable representation of Fe.

***(iii) Semi-variogram reproduction***

After the data and the histograms are checked for reproduction of the original data, the second order statistics i.e. the semi-variogram is checked for reproduction. According to Leuangthong et al., (2004), this check must be performed in normal or transformed space (prior to back transformation), since only the normal scores semi-variogram is imposed directly. In both TB and SGS methods, the semi-variograms calculated for the 7 realizations and compared with the input semi-variogram model are illustrated in Figure 8.8. The variogram model is satisfactorily reproduced in both TB and SGS methods. It is observed from the Figure 8.8A, that the semi-variograms of simulated realizations are almost same and slightly deviated from the semi-variogram model of the original data. However, it can be observed from Figure 8.8B, that the semi-variograms of the simulated realizations are very similar to the model fitted to the semi-variogram parameters of the original data in SGS method and the reproduction is almost excellent for all the realizations. In total, the semi-variogram model is satisfactorily reproduced in both TB and SGS methods.

Based on summary statistics, histogram statistics and semi-variogram reproduction, it is observed that simulations carried out using TB and SGS are found to be valid and the simulation reproduction applied to the original data have not altered the intrinsic spatial characteristics of the data. Hence, these two simulated data are used further for simulation post-processing to obtain global statistics of 100 realizations, grade-tonnage curves and probability maps.

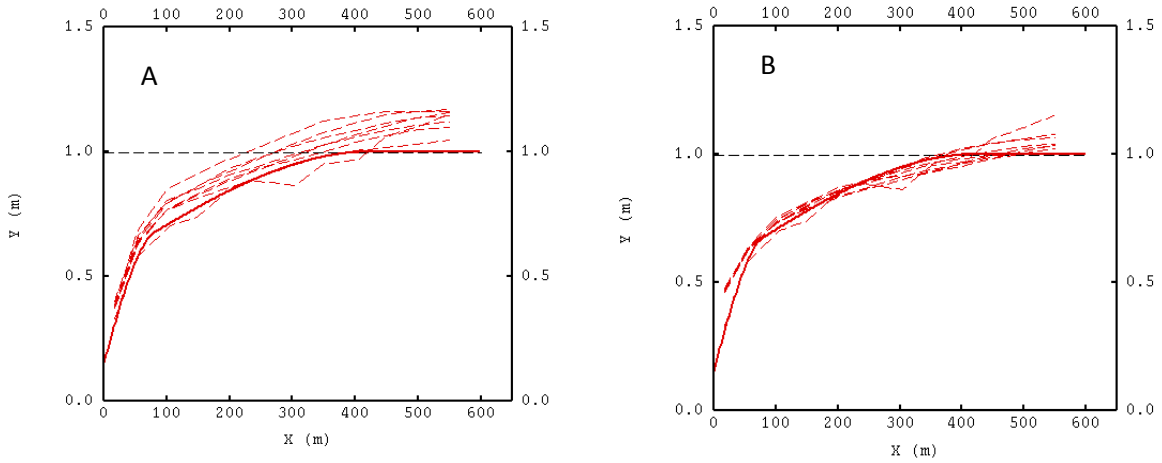


Figure 8.8 Experimental semi-variograms calculated for different realizations (dashed lines) and the input spherical model for Gaussian data used for these simulations (Continuous thick line) using TB method (A) and SGS method (B).

### 8.6.2 Simulation post-processing results

After validation and reproduction results for 7 realizations, simulation post-processing results for different cut-off grades, generated from mean of 100 realizations are represented in the form of (i) Grade Tonnage curves, and (ii) Probability maps.

***(i) Grade tonnage curves***

In general, grade-tonnage curves depict that by increasing cut off grades, the tonnage decreases and whereas average grade increases. These results can also be used in optimization of excavation scheduling (Vann, et al., 2002). It can be observed from Table 8.3 and Figure 8.9A that total recoverable tonnage is identical in both TB and SGS methods and are matching with original data. It is further observed from Table 8.3 & Figure 8.9B that the mean grade of both the methods slightly differs from the mean grade of the original data upto a cut-off of 45 % Fe which is insignificant in this deposit. As the cutoff for considering the material as 'ore' is 45 % Fe, area of interest in the results is above 45 % Fe. It can be further observed from Figure 8.9B that SGS data is matching with original data for the different cut-offs above 45 % Fe, as compared to TB method. In this study, TB method shows underestimated mean grade values, which is evident from the Figure 8.9B.

Though the simulated statistics and histograms reproduced original data in both TB and SGS methods, based on reproduction of semi-variogram and grade-tonnage curves, it is observed that SGS method outperformed TB method slightly in this deposit. Thus further analysis is carried out using SGS data and probability maps are generated.

***(ii) Probability Maps***

It can be observed from the Figure 8.10 that the lower the cut-off of Fe, the greater part of the region is indicated being above the threshold. The figures also suggest that the probability of exceeding 45 % Fe is considerably high and probabilities of exceeding 55 %, 60 % and 62 % Fe are moderately high and probabilities are gradually low further. These maps allow the identification and selection of sub-areas of the deposit based on the required grade and consequently, these maps can be incorporated directly into mine planning. The relevant information obtained from these maps provides a reduction in the installation/operating costs for

the project, because sufficient information is available with a high level of confidence that will be in accordance with agreed quality limits.

Table 8.3 Comparison of total tonnage and mean grade of Fe for different cut-offs using TB and SGS methods.

| Cutoff Grade % | Turning Band Simulation | | Sequential Gaussian Simulation | |
|---|---|---|---|---|
| | Tonnage | Mean Grade | Tonange | Mean Grade |
| 0 | 1.00 | 64.38 | 1.00 | 65.24 |
| 45 | 0.97 | 64.97 | 0.98 | 65.70 |
| 55 | 0.92 | 65.69 | 0.94 | 66.29 |
| 60 | 0.84 | 66.34 | 0.88 | 66.81 |
| 62 | 0.79 | 66.71 | 0.84 | 67.10 |
| 65 | 0.64 | 67.45 | 0.71 | 67.71 |
| 67 | 0.46 | 68.17 | 0.52 | 68.32 |
| 68 | 0.30 | 68.66 | 0.35 | 68.77 |
| 69 | 0.11 | 69.28 | 0.15 | 69.28 |

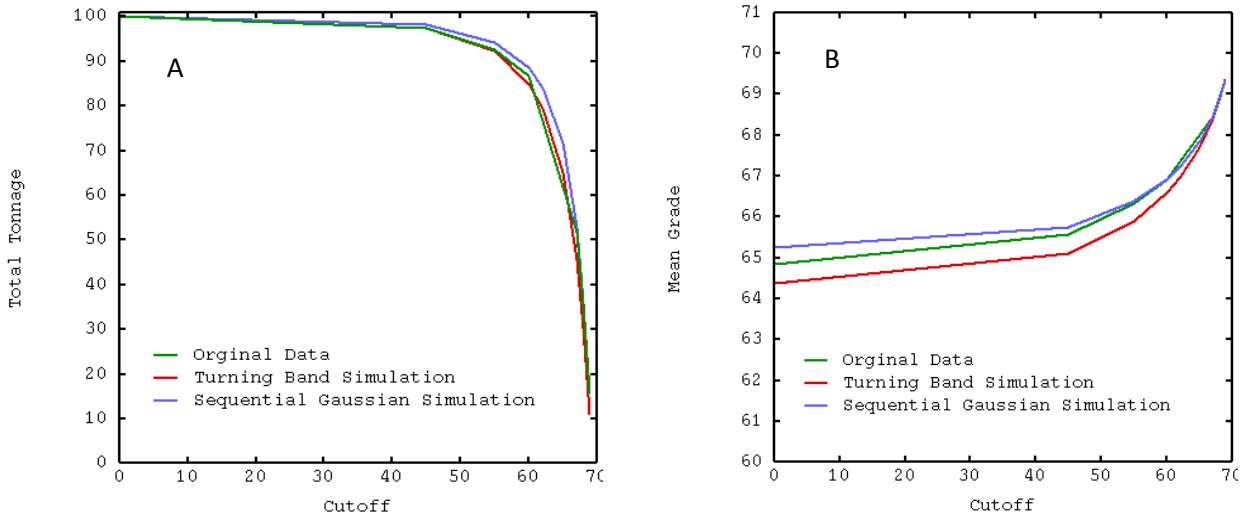


Figure 8.9 Comparison of grade-tonnage curves using TB and SGS methods with original data (A) Cut-off grade Vs Total tonnage; (B) Cut-off grade Vs Mean grade.

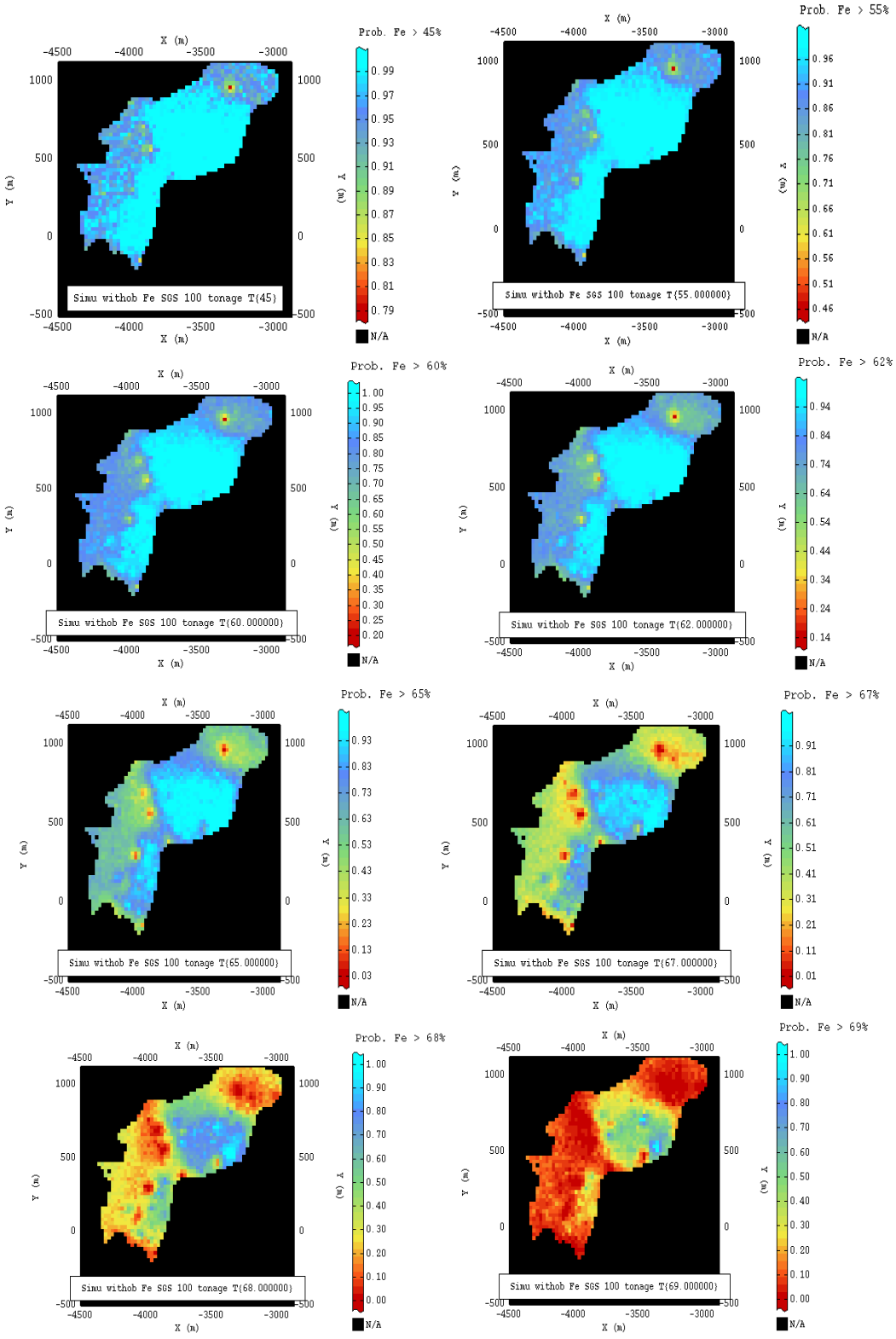


Figure 8.10 Probability maps for different cut-offs in 1068 MRL showing the probability of exceeding the cut-off value using SGS.

## 8.7 Summary

A study that demonstrates the performance of the turning band method in comparison with sequential Gaussian simulation methods is presented. The variable Fe is simulated on a three dimensional grid of dimensions 25 x 25 x 12 mts. Prior to conditional simulation, composited Fe data is transformed to Gaussian data using Gaussian anamorphosis modelling and semi-variograms are modelled in both horizontal and vertical directions. Further conditional simulation is carried out using Gaussian data and Gaussian semi-variograms employing TB and SGS methods. In order to evaluate the simulation results, the summary statistics, histograms and semi-variograms of the original and the simulated Fe values were compared. It is observed that the mean, minimum, maximum, standard deviations of the original and the simulated values were almost similar and both these methods performed quite well in that they reproduced input statistics adequately (Tables 8.1 and 8.2; Figure 8.4A). The mean of 100 realizations is well within the range of values, as is the variance. In both the methods, histograms of different realizations (Figures 8.6 and 8.7) also replicated the input raw data histogram. Likewise, experimental variograms generated from a sample of the realizations show the spatial variability was being replicated well as compared to original data in SGS (Figure 8.8B) and reasonably good in TB (Figure 8.8A).

A comparison is made between the results of total recoverable tonnage and mean grade obtained from TB and SGS methods for different cut-offs. It is observed that total recoverable tonnage is identical in both TB and SGS methods and are matching with original data (Table 8.3 and Figure 8.9A). However, the mean grades of both the methods slightly differs from the mean grade of the original data upto a cut-off of 45 % Fe (Table 8.3 & Figure 8.9B). It is further observed from Figure 8.9B that SGS data is matching with original data for the different cut-offs above 45 % Fe, as compared to TB method which underestimated the mean grade slightly. Though the simulated statistics and histograms reproduced original data in both TB and SGS methods, based on reproduction of semi-variogram and grade-tonnage curves, it is observed that SGS method outperformed TB method slightly in this deposit. This indicates that SGS method is comparatively better and accurate than TB method for estimation of recoverable resources in this deposit.

The resulting blocks provide a basis for early stage of mining studies. The results showed that the summary statistics, histogram, and semivariogram of the simulation results were close to the observed values. Therefore, simulation application should be preferred to kriging, where the knowledge of variability is more important than local estimates (Ersoy and Yunsel, 2009). The simulated models can be incorporated into mine planning and scheduling (Yunsel and Ersoy, 2011).

# CHAPTER 9

# SUMMARY AND CONCLUSIONS

# CHAPTER 9

# Summary and Conclusions

Ore reserve estimates are assessments of the quantity and grade of a mineral that may be profitably extracted from a mineral deposit. A resource estimate is based on prediction of the physical characteristics of a mineral deposit through collection and analysis of sample data, and modelling the size, shape, and grade of the deposit. Important physical characteristics of the ore body that must be predicted include (i) the size, shape, and continuity of ore zones, (ii) the frequency distribution of mineral grade, and (iii) the spatial variability of mineral grade.

There are several interpolation methods for ore reserve estimation, which are broadly categorized in to two main categories: 'deterministic' (nearest neighborhood, triangulation, inverse distance weighting, polygonal functions (splines), linear regression and artificial neural network) and 'probabilistic' (ordinary kriging, simple kriging, universal kriging, residual kriging, indicator kriging, probability kriging and disjunctive kriging). The deterministic methods create a continuous surface by only using the geometric characteristics of point observations and whereas probabilistic methods are based on probabilistic theory and use the concept of randomness, the realized interpolated field is one out of many realizations. Probabilistic methods allow to include the variance in the interpolation process and to compute the statistical significance of the predicted values.

The main focus of this study is a comprehensive geostatistical modelling of an iron ore deposit employing linear, non-linear and simulation methods. The objectives of this study include: (i) to assess grade domains of the deposit in a rapid way in 2D prior to 3D modelling of the deposit, (ii) to investigate the feasibility of a novel approach for delineating various litho types in the iron ore deposit employing a non-linear method and to correlate and validate the grade estimation results of two different approaches, (iii) to compare and validate the recoverable resource estimation results of different types of non-linear geostatistical estimation methods and evaluate the suitable methods for different purpose, and (iv) to assess the uncertainty in the

resource estimates and risk involved in the deposit by employing two conditional simulation methods and compare them to find the suitable model for the deposit.

The deposit under study is a green field unmined deposit on the western ridge of Bailadila range in Dantewada District, Chhattisgarh. It is observed from the outcrops and the lithounits that the enriched ore within the Banded Iron Formations (BIF) is concentrated in the swelled portions of the synclinal depressions.

A total number of 93 exploratory vertical boreholes drilled and 4537 samples recovered by NMDC and GSI are used in this study. Chemical analyses of Fe, $SiO_2$, $Al_2O_3$ and LOI of 4482 samples (out of 4537), along with information on the lithology are considered for geostatistical modelling of the deposit. The iron ore is associated with eight different litho units such as steel grey hematite (SGH), blue grey hematite (BGH), laminated hematite (LH), lateritic/limonitic ore (LO), blue dust (BD), banded hematite quartzite (BHQ), shale (Sh) and transition zone (TZ). The data are divided into two domains as ore and waste; based on geology and chemistry of the deposit. The domain 'ore' consists of 4058 samples pertaining to litho units - SGH, BGH, LH, LO, BD and TZ; whereas the domain 'waste' contains 424 samples pertaining to litho units - BHQ and Sh.

The geostatistical methods such as linear estimator (ordinary kriging) to assess grade domains of the deposit in 2D and to estimate grade estimation in 3D blocks; non-linear estimators (indicator kriging and disjunctive kriging) to determine the recoverable resources for different cut-off grades; and conditional simulation methods ('turning band and sequential Gaussian simulation methods) for assessment of uncertainty and risk that are associated with estimates are employed.

Descriptive statistics, histograms and correlation diagrams are computed to understand the nature of data sets. The basic statistics of exploratory data reveal that the overall Fe content is very high in the iron ore deposit with an average grade of 64.62 % , and majority (91 %) of the data representing the domain 'ore' with an average Fe 66.55 %, and only 9 % of the data represents the domain 'waste' with an average Fe 46.12 %. Scatter diagrams between Fe vs $SiO_2$, Fe vs $Al_2O_3$ and $SiO_2$ vs $Al_2O_3$ show that Fe has significant negative correlation with both the

variables $SiO_2$ (-0.85) and $Al_2O_3$ (-0.77), whereas no significant correlation (0.3) between $SiO_2$ and $Al_2O_3$.

Ore deposit evaluation is carried out in 2D, for rapid assessment of grade domains and grade variation of the deposit. The comparison of kriged results of Fe in 2D with borehole data indicate that minimum and maximum values are almost same whereas the mean value changed from 63.71 % to 59.7 % and CV has come down from 9.2 to 6.97 indicating lesser variation of kriged estimates of Fe than that of raw data. Domain maps show that the deposit broadly can be distributed in to three zones (60-70 % Fe, 50-60% Fe and 40-50% Fe) depending on the estimated Fe grade. It is also observed that the central part of the ore body has very high grade (60-70%) of Fe with a very less variation (0 – 20%). The medium grade (50-60 %) Fe is scattered in pockets, whereas low grade (40-50%) Fe occurs only at two locations. The scatter plot between kriged estimates of Fe and CV shows very strong negative correlation (-0.93) between these two estimates.

As the samples extracted from boreholes are not of uniform length, regularization is done using '*compositing by domain'* and '*compositing by bench*' methods. 'Compositing by domain' was done for each domain i.e., 'ore' and 'waste' separately for estimation of Fe, $SiO_2$, and $Al_2O_3$ grades by linear geostatistical method and 'compositing by bench' was done for estimation of grade by non-linear geostatistical methods and conditional simulations. After compositing by domain, it is observed that there is no significant change in mean Fe % in domain 'ore', whereas in domain 'waste' mean Fe % is decreased by < 2 %. After regularizing the total data using 'compositing by bench', it is observed that the average Fe grade is 64.84 % which is in line with original raw data (64.62 %). In both the methods, the compositing data are inline with the original data.

Semi-variograms, in both the domains 'ore' and 'waste', are calculated separately in the XY plane (horizontal direction) with anisotropy modelled in the Z direction (vertical direction). In domain 'ore', semi-variogram models of Fe, $SiO_2$ and $Al_2O_3$ in both the horizontal and vertical directions show a very good spatial structure with a small nugget effect. For all the three variables, anisotropy is recorded in horizontal and vertical directions. Semi-variogram models indicate Fe ranges 400 m and 90 m in horizontal and vertical directions respectively. Cross-

validation of semi-variogram models of Fe, $SiO_2$ and $Al_2O_3$ indicate that the models are satisfactory and can be further used in estimation.

Initially the geological cross-sectional method was applied for delineating litho types and preparation of geological model of the deposit. A 3D block model is then created using *Surpac software* taking into account the extent of samples in the drill holes, topography and geological model of the deposit prior to grade estimation and resources of the deposit. Block model reveals the total resources of the domain '*ore*' at ~ 362 Million Tonnes (MT) (without any cut-off) and of the domain '*waste*' at ~ 46 MT.

A novel method - non-linear geostatistical indicator kriging method is also applied for categorizing the litho units in the block model using *Isatis software* and subsequently lithological maps are generated. It is observed from the lithological maps of 32 benches that the low grade Fe content bearing litho units - BHQ and shale - occur mostly in the peripheral blocks, whereas high grade Fe bearing litho units - SGH, BGH, LH, LO, and BD occur in the middle portion of the deposit.

Grade estimation of Fe, $SiO_2$ and $Al_2O_3$ employing ordinary kriging in both the block models - geological cross sectional approach and indicator kriging approach - indicate that, kriged grades of the litho units SGH, BGH, LH and BD in domain 'ore' are almost similar and exhibit Fe grade > 65 %, whereas in litho unit LO, kriged grades are differing where Fe grade is 65.10 % in geological cross section method, and 60.52 % in indicator kriging method. It is observed from the comparative results of Fe content by geological cross sectional model and indicator kriging model that the estimated mean grades of litho units SGH, BGH, LH and BD are almost the same, whereas estimated mean grade of litho unit LO is slightly higher (4.6 %) in geological model. It is further observed that the results obtained from IK model are in line with the original drilling data and composited data when compared to the results of geological model. Indicator kriging approach is more suitable for delineating litho units and can be a suitable replacement of traditional geological cross sectional approach.

Grade maps, generated using kriged estimates, show that the Fe grade is distributed mostly between 65 -70 % and partly between 60-65 % in the entire deposit. The medium grade (50-60 %) Fe is scattered in pockets and low grade (40-50%) Fe occurs only in peripheral areas of

the deposit. On the other hand, error maps generated using kriged standard deviations indicate that the central part of the ore body has a very low kriged standard deviation as compared to peripheral areas. This may be due to fluctuations observed in the estimated values in the peripheral areas. The scatter plot between kriged grades and kriged standard deviation of Fe depicts very strong negative correlation (-0.83), suggesting that most of the estimated grades of Fe exhibit less error of estimate. It is inferred from the grade maps and error maps that the deposit has mostly high grade areas with less error of estimate which indicates that the deposit is enriched with high Fe content.

Mineral resource classification carried out using kriging standard deviation of Fe show that most parts (92.16 %) of the estimated block model is classified as 'Measured' category with 0-20 % error. Very few blocks (5.41 %) are classified as 'Indicated' category with 30-40 % error, and remaining (2.39 %) blocks are classified as 'Inferred' category with 40-50% error. On the other hand, mineral resource classification carried out using kriging efficiency of Fe show that 87.8 % of the estimated block model is classified as 'Measured', 3.11 % blocks are classified as 'Indicated' category and remaining 9.08 % blocks are classified as 'Inferred' category.

Indicator semi-variograms modelled in both horizontal and vertical directions for the indicator transformed data of 67 % Fe cut-off, (median value of Fe composited data) show a good structure with a small nugget effect. Anisotropy is observed in horizontal and vertical directions with ranges 320 and 60 respectively. It is observed from indicator kriged estimates that the total recovered tonnage is 95 % i.e., ~ 340 MT (out of total 362 MT) with a cut-off of 45 % Fe. It is also observed that 41 % of the total estimated blocks have greater than 67 % Fe and 10 % of total estimated blocks have greater than 69 % Fe. The basic statistics of indicator kriged results for mean grade indicate that majority of the blocks have Fe grade > 45 %, with a mean of 63.70 %. As per prevailing market requirement, the mean grade is 62 % Fe and supply of iron ore with + 62 % Fe will fetch add on value from the customer for every 1 % increase of Fe.

Semi-variograms modelled in both horizontal and vertical directions for the raw Fe data, required for support correction and for Gaussian variogram, show a very good structure with a small nugget effect. The 'support correction' calculated for a block support of 5 x 5 x 12 m resulted in a factor of 0.91. Semi-variogram for gaussian block variable also shows a very good

structure with a small nugget effect. It is observed that the ranges of semi-variogram models in horizontal and vertical directions are same for punctual Fe data and block Gaussian Fe data. This indicates that gaussian block anamorphosis modelling and semi-variogram modelling are accurate.

The results through the disjunctive kriging method indicate that the total recovered tonnage is 97 % at a cut-off grade of 45 % Fe, 41 % of the blocks exhibit > 67 % Fe, while 9 % of blocks exhibit > 69 % Fe. It is further observed that disjunctive kriged estimates resulted in a mean of 64.02 % at a cutoff grade of 45 % Fe. It is also observed that there is no significant difference in the average grade from a cut-off of zero (i.e., no cut-off) to a cut-off of 45 % Fe. This may be due to very less number of samples in the original data with Fe grade < 45 % and without much variance.

A comparison of estimated results obtained from different kriging methods (viz., indicator kriging, disjunctive kriging and ordinary kriging methods), using grade-tonnage curves, suggests that the total tonnage estimated by DK and OK are in line for the cut-offs 45, 55 and 60 % Fe, whereas IK method underestimates the total tonnage as compared to DK and OK methods. For the cut-offs 67 and 68 % Fe, the estimated tonnage by DK and IK methods show similar values, whereas the values are underestimated in OK method. For the cut-off 69 % Fe, OK estimates are underestimated as compared to DK and OK methods.

From these grade-tonnage curves, it is observed that the mean grade estimated by DK method is slightly higher than IK and OK methods for the cut-offs 45 and 55 % Fe. For the cut-off 60 % Fe, DK and IK estimates are almost same and OK estimates are slightly less. For the cut-offs 67, 68 and 69 % Fe, the mean grade estimated by OK, IK and DK methods are almost same. In totality, it can be observed that IK estimated mean is less than that of OK method up to a cutoff of 35 % Fe, IK estimates are more than OK estimates above 35.5 % Fe cut-off, whereas DK estimates are globally consistent.

Conditional simulation, carried out using Gaussian data and Gaussian semi-variograms employing turning band (TB) and sequential Gaussian simulation (SGS) methods, shows that the mean, minimum, maximum, standard deviations of the simulated values and the original values are almost similar. Both these methods performed quite well in that they reproduced input

statistics adequately. The mean and variance of 100 realizations are also well within the range of values. In both the methods, histograms of different realizations also replicated the input raw data histogram quite well. Likewise, experimental variograms generated from a sample of the realizations show the spatial variability was being replicated well as compared to original data in SGS and reasonably good in TB.

A comparison between the results of total recoverable tonnage (T) and mean grade (M) obtained from turning band simulation and sequential Gaussian simulation methods shows that the total recoverable tonnage is identical in both the methods and is matching with original Fe data for different cut-offs. However, the mean grades of both the methods slightly differ from the mean grade of the original data up to a cut-off of 45 % Fe. It is further observed that SGS data is matching with original data for the different cut-offs above 45 % Fe, as compared to TB method which underestimated the mean grade slightly. It is observed that SGS method outperformed TB method in this deposit. This indicates that SGS method is comparatively better and accurate than TB method for estimation of recoverable resources in this deposit.

This study confirms the general theory that no single spatial geostatistical method can be consistently best or worst for all purposes and it is essential to use appropriate method for different purposes. The practicality of the proposed non-linear 'indicator kriging' approach to delineate litho units in the block model consists of the probabilistic assessment of the Fe grade parameters, which explicitly incorporates spatial variability of Fe grade and uncertainty in iron ore deposit characterization. Therefore, it is suggested that this novel method has superiority in terms of accuracy to the traditional geological cross sectional model approach.

The linear estimator 'ordinary kriging' provides not only the best estimates but also error of estimates. The non-linear methods 'median indicator kriging' and 'disjunctive kriging' provide recoverable resources for different cut-offs. It is suggested that conditional simulation using SGS method is appropriate to generate equally probable maps for risk analysis in mine planning. The combination of multiple simulated models provides the necessary tool to assess uncertainty associated with predictions of the attribute under study. Our study suggests that simulation approach has an edge/superiority over kriging method in assessment of uncertainty of estimates.

The conditional variances generated by simulation models provide a more realistic assessment of the uncertainty and risk than the error variances obtained with kriging estimations. The resulting simulated blocks provide a basis for early stage of mining studies. Therefore, simulation application should be preferred to kriging, where the knowledge of variability is more important than local estimates. The simulated models can be incorporated into mine planning and scheduling.

The results presented in this study are potentially useful for a wide range of practitioners, geologists, mining engineers, and decision-makers for steel plants generating steel from good quality iron ore. However, the suitability of a particular estimation method - linear, non-linear and conditional simulations - can be ascertained only after comparing these estimated results with the real production data. As this deposit is yet to be mined, it is suggested that these results are to be validated with the production data i.e., the blast hole data of the mining benches in order to establish the most accurate method.

# *REFERENCES*

# References


Abdullah., 1990. Effects of search parameters on kriged reserve estimation. International Journal of Mining and Geological Engineering 8, 319-331.

Akinrinsola, E.O., Adekeye, J.I.D., 1993. A geostatistical ore reserve estimation of the Itakpe iron ore deposit okene, Kogi state. Journal of Mining and Geology 29 (1), 19-25.

Annels, A.E., 1996. Mineral deposit evaluation: A practical approach. Chapman and Hall London, 436 pp.

Armstrong, M., 1981. A geostatistical approach to predicting the washability characteristics of coal in-situ. Mathematical Geology 3 (4), 321-329.

Armstrong, M., 1984. Common problems seen in variograms. Mathematical Geology 16 (3), 305-313.

Armstrong, M., 1998. Basic linear geostatistics. Springer-Verlag (Berlin), 256 pp.

Armstrong, M., Jabin, R., 1981. Variogram models must be positive-definite. Mathematical Geology 13(5), 455-459.

Armstrong, M., Matheron, G., 1986a. Disjunctive kriging revisited, Part 1. Mathematical Geology 18 (8), 711-728.

Armstrong, M., Matheron, G., 1986b. Disjunctive kriging revisited, Part 2. Mathematical Geology, 18 (8), 729-742.

Armstrong, M., Champigny, N., 1989. Study on kriging small blocks. CIM Bulletin V82, N923, International Journal of Rock Mechanics and Mining Sciences & Geomechanics 26, 128-133.

Armstrong, M., Dowd, P.A. 1994. Geostatistical simulations. Kluwer Academic Publishers, Dordtrecht, 255 pp.

Arvidson, H., 1998. KCGM – Fimiston ore resource estimation practice, In: proceedings of gold and nickel ore reserve estimation practice seminar (held 31 October 1997), (The Australasian Institute of Mining and Metallurgy, Kalgoorlie Branch: Kalgoorlie), 59-69.

Asghari, O., Soltni, F., Hassan B. A., 2009. The comparison between sequential Gaussian simulation (SGS) of Choghart ore deposit and geostatistical estimation through ordinary kriging. Australian Journal of Basic and Applied Science, ISSN 1991-8178 3 (1), 330-341.

AusIMM (Australasian Institute of Mining and Metallurgy). 1996. Australasian code for reporting of identified mineral resources and ore reserves: AusIMM Bull. 4, 2-19.

Bachmaier, M., Backes, M., 2011. Variogram or semivariogram? Variance or semivariance? Allan variance or introducing a new term?, Math Geosci 43, 475-740.

Badel, M., Angorani, S., Panahi, M. S., 2011. The application of median indicator kriging and neural network in modeling mixed population in an iron ore deposit. Computers & Geosciences 37, 530-540.

Bandyopadhyay, D., Hishikar, A.K., 1977. Stratigraphic in southern part of Bailadila Range, Bastar District, M.P. Journal Geological Society of India, 18, 240-245.

Baskan, O., Cebel, H., Akgul, S., Erpul, G., 2010. Conditional simulation of USLE/RUSLE soil erodibility factor by geostatistics in a Mediterranean catchment, Turkey. Environmental Earth Sciences 60, 1179–1187.

Bertoli1, O., Job, M., Vann, J., Dunham, S., 2003. Two-Dimensional geostatistical methods — Theory, practice and a case study from the 1A shoot nickel deposit, Leinster, Western Australia, 5th International Mining Geology Conference, Bendigo, Vic., 1-8.

Berterretche, M., Hudak, A.T., Cohen, W.B., Maiersperger, T.K., Gower, S.T., Dungan, J., 2005. Comparison of regression and geostatistical methods for mapping Leaf Area Index (LAI) with Landsat ETM+ data over a boreal forest. Remote Sensing of Environment. Published by Elsevier Inc., 96, 49-61.

Betzhold, J., Roth, C., 2000. Characterizing the lithological variability of a Chilean copper deposit using plurigaussian simulations. Journal of the South African Institute of Mining and Metallurgy 100(2), 111-120.

Bouleau, N., 1986. Probabilities de l'Ingeniur. Variables Aleatoires et Simulation. Herman, Paris.

Bristol, R., 2009. Geostatistics in *surpac 6.1*, Gemcom software International Inc. 225 pp.

Brooker, P.I., 1979. "Kriging", Engineering And Mining Journal, 148-153.

Brooker, P.I., 1985. Two - Dimensional simulation by turning bands. Mathematical Geology 17(1), 81-90.

Caers, J., 2000. Adding local accuracy to direct sequential simulation. Mathematical Geology 32 (7), 815–850.

Carr, J.R., Deng, E.D., Glass, C.E., 1986. An application of disjunctive kriging for earthquake ground motion estimation. Mathematical Geology 18(2), 197-213.

Catherine, B., Matthieu, B., Deraisme, J., Francois, G., Nicolas, J., Ophelie, L., Sebastien, P., Jerome, P., Rambert, F., Didier, R., Touffait, Y., Laurent, W., 2011a. Mining case studies. *ISATIS*, Geovariances, Avon, France, 232 pp.

Catherine, B., Matthieu, B., Deraisme, J., Francois, G., Nicolas, J., Ophelie, L., Sebastien, P., Jerome, P., Rambert, F., Didier, R., Touffait, Y., Laurent, W., 2011b. Technical References. *ISATIS*, Geovariances, Avon, France, 220 pp.

Champigny, N., Armstrong, M., 1993. Geostatistics for the estimation of gold deposits. Mineralium Deposita, International Journal for Geology, Mineralogy and Geochemistry of Mineral Deposits 28, 279-282.

Chatterjee, A., 1970. Structure, tectonics and metamorphism in part of southern Bastar, M.P. Journal of Mining, Geological, Metallurgical Society of India 42, 75-95.

Chatterjee A. K., Murthy, P.S.N., 1994. Ore reserve estimation with special reference to open cast mines – An overview in the text book entitiled "Computers in Industry", Oxford & IBH publishing Co. Pvt. Ltd., 151-161.

Chatterjee, S., Bhattacherjee, A., Samanta, B., Pal, S.K., 2006. Ore grade estimation of a limestone deposit in India using an artificial neural network. Applied GIS DOI: 10.2014/ag060003 2(1), 2.1-2.2.

Chica-Olmo, M., Luque-Espinar, J.A., 2002. Applications of the local estimation of the probability distribution function in environmental sciences by kriging methods. Inverse Problems 18 (1), 25–36.

Chiles, J.P., Delfiner, P., 1999. Geostatistics: Modeling spatial uncertainty. Wiley, Inter-Science, New York, 695 pp.

Chilès, J.P., Delfiner, P., 2009. Geostatistics: Modeling Spatial Uncertainty. John Wiley & Sons, 720 pp.

Christakos, G., 1987. Stochastic simulation of spatially correlated geo-processes. Mathematical Geology 19(8), 807-831.

Clark, I., 1976a. Regularization of a semi-variogram. Computers & Geosciences 3, 341-346.

Clark, I., 1976b. Some practical computational aspects of mine planning. In: Guarascio, M., et al (Eds.), Proceedings of the Advanced geostatistics in the mining industry. D. Reidel publishing company, Dordrech-Holland , 391-399.

Clark, I., 1977. Practical kriging in three dimensions. Computers & Geosciences 3, 173-180.

Clark, I., 1979a. The Semi-Variogram-Part 1. Engineering And Mining Journal 180, 90-94.

Clark, I., 1979b. Does Geostatistics Work ?. In: O'Neil, T.J. (Ed), Proceedings of the 16th International APCOM Symposium, McGraw-Hill, New York, 213-225.

Clark, I., 1979c. Practical Geostatistics. Applied Science Publishers Ltd., London, 129 pp.

Clark, I., 1983a. Regression revisited. Mathematical Geology 15(4), 517-536.

Clark, I., 1983b. Block by block reserve estimation – A case study. In: Proceedings of the Second international surface mining and quarrying symposium organized by the Institute of Mining and Metallurgy in association with the Institute of Quarrying and held in Bristol, England, from 4 to 6 October, 1983, "Reserve estimation—a geostatistical case study on the comparability of drilling methods" in Surface Mining and Quarrying, Inst. Min. Metall., London, 135 – 144.

Clark, I., 1986. The art of cross validation in geostatistical applications. In: Ramani, R.V. (Ed.), Proceedings of the 19th Application of computers and operations research in the mineral industry, April 14 – 16, 1986, Published by Society of mining engineers, Inc., Littleton, Colorado.

Clark, I., 1993. Practical reserve estimation in a shear-hosted gold deposit, Zimbabwe. In: Proceedings of the International mining geology Conference, Kalgoorlie WA, 157-160.

Clark, I., 1998. Predicting variability in coal quality parameters. Coal Indaba, Johannesburg, 1-5.

Clark, I., 1999. Geostatistical modelling for realistic mine planning. Mining Pribram Symposium in Science and Technology, Prague, Czechoslovakia, 1-7.

Cochrane, L. B., Thompson, B. D., McDowell, G. D., 1998. The application of geophysical methods to improve the quality of resource and reserve estimates. Exploration and Mining Geology Journal 7, 63–75.

Collings, P. S., Khosrowshahi, S., Ness, P. K., 1997. Geological modelling and geostatistical resource estimation of the Hope North Deposit. In: Misra, V.N., Dunloop, J.S. (Eds.), Proceedings of the national Conference on Iron Making Resources and Reserves Estimation (The Australasian Institute of Mining and Metallurgy: Melbourne) 105-116.

Coombes, J., 1997. Handy hints for variography. In: Misra, V.N., Dunloop, J.S. (Eds.), Proceedings of the national Conference on Iron Making Resources and Reserves Estimation (The Australasian Institute of Mining and Metallurgy: Melbourne) 127-130.

Coombes, J., 2008. The Art and Science of Resource Estimation. Publisher: Coombes Capability, Subiaco, W.A., 245 pp.

Costa, J.F., Zingano, A.C., Koppe, J.C., 2000. Simulation - An approach to risk analysis in coal mining. Exploration and Mining Geology Journal 9 (1), 43-49.

Cressie, N., Hawkins, D.M., 1980. Robust estimation of the variogram. Mathematical Geology 12(2), 115-125.

Cressie, N., 1990. The origins of kriging. Mathematical Geology 22 (3), 239–252.

Cressie, N., 1991. Statistics for spatial data. John Wiley and Sons, New York, 920 pp.

Cressie, N. A. C., 1993. Statistics for spatial data, revised edition. John Wiley & Sons, New York, 461 pp.

Crookshank, H., 1938a. The western margin of the eastern ghats in southern Jeypore. Geological survey of India 73(3), 398-434.

Crookshank, H., 1938b. Iron ores of the Bailadila Range. Journal of Mining Geological & Metallurgical Institute of India (MGMI) 34(3) 254-281.

Crookshank, H., 1963. Geology of southern Bastar and Jeypore from Bailadila range to Eastern ghats., Geological Survey of India, Memoir 87, 150pp.

Dagbert, M., David, M., 1977. Geostatistical mineral resources appraisal. Mathematical Geology 9 (3), 313-317.

Da Rocha, M.M., Yamamoto, J.K., 2000. Comparison between kriging variance and interpolation variance as uncertainty measurements in the Capanema iron mine, State of Minas Gerais, Brazil. Natural resources research, International Association for Mathematical Geology 9(3), 223-235.

David, M., 1977. Geostatistical ore reserve estimation. Developments in Geomathematics 2, Elsevier, Amsterdam, 364pp.

David, M., 1988. Handbook of applied advanced geostatistical ore reserve estimation. Developments in Geomathematics 6, Elsevier Amsterdam, 216 pp.

David, M., Dowd, P.A., Korobov, S., 1974. Forecasting departure from planning in open pit design and grade control. In: Proceedings of the 12th Symposium on the Application of Computers and Operations Research in the Mineral Industries (APCOM), Colorado School of Mines, 2, 131 - 142.

Davis, J. C., 1973. Statistics and data analysis in geology, John Wiley and Sons, New York, 550 pp.

Davis, J. C., 1986. Statistics and data analysis in geology, second edition, John Wiley and Sons, New York, 646 pp.

Davis, J. C., 2002. Statistics and data analysis in geology, third edition, John Wiley and Sons, New York, 638 pp.

Davis, M. W., 1987. Production of conditional simulations via the LU triangular decomposition of the covariance matrix. Mathematical Geology 19 (2), 91-98.

Davis, M. W., Culhane, P. G., 1984. Contouring very large datasets using kriging, In: Verly, G., David, M., Journel, A. G., and Marechal, A. (Eds.), Geostatistics for Natural Resource Characterization, Part 2: Reidel, Dordrecht, Netherlands.

Daya, A. A., Hossein, H., 2010. Geostatistical grade modeling of Choghart north anomaly iron ore deposit through disjunctive kriging. Journal of the Earth Sciences Application and Research Centre of Hacettepe University, Yerbilimleri 31 (1), 45-52.

Daya, A. A., 2014. Application of disjunctive kriging for estimating economic grade distribution in an iron ore deposit: A case study of the Choghart north anomaly, Iran. Journal Geological Society of India 83, 567-576.

Delfiner, P., 1979. Basic introduction to geostatistics. Centre de Geostatistique (Fontainebleau) Research report CGMM - C78.

Delfiner, P., Delhomme, P., 1973. Optimum interpolation by kriging. Display and analysis of spatial data, NATO Advanced study institute, Wiley, London, 96-114.

Delfiner, P., Chiles, J. P., 1977. Conditional simulation - A new Monte-Carlo approach to probabilistic evaluation of hydrocarbons in place. Internal Report N-526, Centre de Geostatistique, Fontainebleau, 30 pp.

Delfiner, P., Delhomme, J.P., 1975. Optimum interpolation by Kriging. In: Davis, E.C., McCullagh, M.J. (Eds.), Proceedings of the NATO ASI for Display and analysis of spatial data. Wiley, 96-114.

Deraisme, J. 1977. Utilisation de simulations de gisements pour la planification de l'exploitation. In : Proceedings of the Symposium on Science and Technique "Mathematical Methods in Geology", Pribram, Tcheckoslovakia, 203-216.

Deraisme, J., 1996. The geostatistical approach for reserves. Article published in The Mining Magazine. C. De Fouquet (ENSMP) 2-5.

Deraisme, J., Farrow, D., 2005. Geostatistical simulation techniques applied to Kimberlite orebodies and risk assessment of sampling Strategies. In: Leauangthong, O., Deutsch, C.V., (Eds.), Proceedings of the Geostatistics Banff. Springer, 429-438.

De Souza, L.E., Costa, J.F.C.L., Koppe, J.C., 2004. Uncertainty estimate in resources assessment: A geostatistical contribution. Natural Resources Research 13(1), 1-15.

Deutsch, C.V., 2002. Geostatistical reservoir modelling, Oxford University Press 376 pp.

Deustch, C.V., Journel, A. G., 1992. GSLIB, Geostastical software library and user's guide. Oxford University Press, New York, 340 pp.

Deutsch, C. V., Journel, A. G., 1998. GSLIB: Geostatistical software library and user's guide. 2nd edition. Oxford University Press, New York, pp. 369.

De-vitry, C., 2003. Resource classification – A case study from the Joffre-hosted iron ore of BHP Billition's mount whaleback operations. J. Mining Tech., Trans. Inst. Min. Metall.Asso., 112, 185-196.

De-vitry, C., Vann, J., Arvidson, H., 2007. A Guide to selecting the optimal method of resource estimation for multivariate iron ore deposits. In: Proceedings of the Iron ore Conference, Perth, WA, 1-12.

Didier, R., 2010. Non-linear Geostatistics. http://www.geosciences.minesparistech.fr/enseignements-formations/formations-postgrade/cfsg.

Diehl, P., David, M., 1982. Classification of ore reserves/resources based on geostatistical methods. CIM Bull., 75 (838), 127-136.

Dietrich, C.R. 1995. A simple and efficient space domain implementation of the turning bands method. Water Resources Research 31 (1), 147–156.

Dimitrakopoulos, R., 1988. Stochastic modelling of reservoir-rock properties: Petroleum society of CIM, Paper No. 88-39-113.

Dimitrakopoulos, R., 1990. Conditional simulation of intrinsic random functions of order k. Mathematical Geology 22 (3), 361-380.

Dimitrakopoulos, R., 1994. Geostatistics for the next century. Kluwer Academic Publishers, Dordrecht, 499 pp.

Dimitrakopoulos, R., 1997. Indicator kriging course notes. W H Bryan Centre, University of Queensland.

Dimitrakopoulos, R., 1998. Conditional simulation algorithms for modelling orebody uncertainty in open pit optimization. International Journal of Surface Mining, Reclamation and Environment 12, 173-179.

Dimitrakopoulos, R., Fonseca, M.B., 2003. Assessing risk in grade - tonnage curves in a complex copper deposit, northern Brazil, based on an efficient joint simulation of multiple correlated variables, APCOM, 373-382.

Dowd, P.A., 1982. Lognormal kriging – the general case. Mathematical Geology 14 (5), 475-489.

Dowd, P.A., 1992. A review of recent developments in geostatistics. Computers & Geosciences 17 (10), 1481-1500.

Dowd, P.A., 1994a. Risk assessment in reserve estimation and open-pit planning. Transactions of the Institution of Mining and Metallurgy, AusIMM (Section A: Mining Industry) 103, A148-A154.

Dowd, P.A., 1994b. The use of conditional simulation in grade control. In: Proceedings of the conference on mining geostatistics, South Africa, 19-24 September, Geostatistical Association of South Africa, 11-25.

Dowd, P.A., 1996. Structural controls in the geostatistical simulation of mineral deposits. In: Baafi, E.Y., Schofield, N.A., (Eds.), Proceedings of the Geostatistics Wollongong '96. Netherlands, 647-657.

Dowd, P.A., 1997. Risk in minerals projects: Analysis, perception and management. Transactions of the Institution of Mining and Metallurgy AusIMM (Section A: Mining Industry) 106, A9-A18.

Dowd, P.A., David, M., 1976. Planning from estimates: Sensitivity of mine production schedules to estimation methods. In: Guarascio, M., David, M., Huijbregts, C. (Eds.), Proceedings of the Advanced geostatistics in the mining industry, NATO ASI Series C: Mathematical and physical sciences, Dordrecht: Reidel 24, 163- 183.

Dowd, P.A., Pardo-IguÂ zquiza., 2002. The incorporation of model uncertainty in geostatistical simulation. Geographical & Environmental Modelling 6 (2), 147-169.

Duval, R., Levy, R., Matheron, G., 1955. Travaux de D. G. Krige sur l'´evaluation des gisements dans les mines d'or Sud-Africaines. Annales des Mines 12, 3-49.

Eggleston, J.R, Rojstaczer, S.A and Peirce, J.J., 1996. Identification of hydraulic conductivity structure in sand and gravel aquifers: Cape Cod dataset. Water Resources Research 32, 1209–1222.

Ellefmo, S.L., Eidsvik, J., 2009. Local and spatial joint frequency uncertainty and its application to rock mass characterisation. Rock Mechanics and Rock Engineering 42, DOI 10.1007/s00603-008-0009-x, 667-688.

Elliott, S.M., Snowden, D.V., Bywater, A., Standing, C.A., Ryba, A., 1997. Reconciliation of the McKinnons gold deposit, Cobar, New South Wales. In: Proceedings of the Third international mining geology conference, (The Australasian Institute of Mining and Metallurgy: Melbourne) 113-122.

Emery, X., 2005a. Simple and ordinary multigaussian kriging for estimating recoverable reserves. Mathematical Geology 37 (3), 295–319.

Emery, X., 2005b. Geostatistical simulation of random fields with bivariate isofactorial distributions by adding mosaic models. Stochastic Environmental Research Risk Assessment Journal 19, DOI 10.1007/s00477-005-0240-x, 348–360.

Emery, X., 2006a. Ordinary multigaussian kriging for mapping conditional probabilities of soil properties. Geoderma 132, 75–88.

Emery, X., 2006b. A disjunctive kriging program for assessing point-support conditional distributions. Computer & Geosciences 32, 965–983.

Emery, X., 2007. Conditional simulations of Gaussian random fields by ordinary kriging. Mathematical Geology 39, DOI 10.1007/s11004-007-9112-x, 607-623.

Emery, X., 2012. Co-simulating total and soluble copper grades in an oxide ore deposit. Mathematical Geosciences 44, DOI 10.1007/s11004-011-9366-1, 27–46.

Emery, X., Ortiz, J.M., 2005. Estimation and mineral resources using grade domains: critical analysis and a suggested methodology. The Journal of the South African Institute of Mining and Metallurgy 105, 247-255.

Emery, X., Gonzalez, K.E., 2007. Probabilistic modelling of lithological domains and its application to resource evaluation. The Journal of the South African Institute of Mining and Metallurgy 107, 803-809.

Emery, X., Ortiz J.M., Cáceres. A. M., 2008. Geostatistical modelling of rock type domains with spatially varying proportions: Application to a porphyry copper deposit, The Journal of the Southern African Institute of Mining and Metallurgy 108, 285-292.

Emery, X., Silva, D.A., 2009. Conditional co-simulation of continuous and categorical variables for geostatistical applications. Computers & Geosciences 35, 1234–1246.

Englund, E.J., Heravi, N., 1992. Conditional simulation: Practical application for sampling design optimization. In: Soares, A. (Ed.), Proceedings of the Geostatistics Troia '92, Kluwer Academic Publishers , Dordreeht, 613-624.

Ersoy, A., Yunsel, T.Y., 2009. Assessment of lignite quality variables: A practical approach with sequential Gaussian simulation. Energy sources, Part A, 31, Taylor & Francis Group, LLC ISSN: 1556-7036. 175–190.

Fabbri, P., Trevisani, S., 2005. A Geostatistical simulation approach to a pollution case in Northeastern Italy. Mathematical Geology 37 (6), 569-586.

FitzGerald, D., Chiles, J.P., Guillen, A., 2009. Delineate 3D iron ore geology and resource models using the potential field method. In: Proceedings of the 11th SAGA Biennial Technical Meeting and Exhibition, Swaziland, 227-235.

Fouquet, C., 1994. In: Reminders on the conditional Kriging. In: Armstrong, M., and Dowd, P. A. (Eds.), Proceedings of the Geostatistical simulations, Kluwer Academic, Netherlands, 131–145.

Froidevaux, R., 1982. Geostatistics and ore reserve classification: CIM Bulletin, 75(843), 77-83.

Gandin, L. S., 1963. Objective analysis of meteorological fields. Translated from Russian in 1965 by Israel program for scientific translations, Jerusalem, Gidrometeorologicheskoe Izdatel'stvo (GIMIZ), Leningrad.

Geovariances 2013a. *Isatis* Mining case study, Géovariances, Fontainebleau.

Geovariances 2013b. *Isatis* Technical references, Géovariances, Fontainebleau.

Gholamnejad, J., Ansari, A.H., Bafghi, Y., Taqizadeh, M., 2010. Determination of ore/waste boundary using indicator kriging, Case study: Choghart iron mine of Iran. IJE Transactions B: Applications 23 (3 & 4), 269-276.

Glacken, I. M., 1996. Change of support and use of economic parameters in block selection. In: Baafi, E.Y., Schofield, N.A. (Eds.), Proceedings of the Geostatistics Wollongong '96 , Kluwer, Netherlands, 811-821.

Glacken, I.M., Blackney, P.A., 1998. A practitioners implementation of indicator kriging. In: Proceedings of a one day symposium: Beyond ordinary kriging. Perth, Western Australia. Geostatistical Association of Australasia, 26-39.

Glaken, I.M., Snowden, D.V., 2001. Mineral resource estimation. In: Edwards, A.C. (Ed.), Proceedings of the Mineral Resource and ore Reserve Estimation. The AusIMM guide to good practice (The Australasian Institute of Mining and Metallurgy, Melbourne) 189-198.

Glacken, I. M, Sommerville, B. L., Arnold, C.G., 1998. Reserve estimation at Kambalda nickel operations – from 1970 to 2000. In: Proceedings Gold and Nickel ore reserve Estimation Practice seminar, The Australasian Institute of Mining and Metallurgy, Kalgoorlie, 35-38.

Gneiting, T., 1998. Closed form solutions of the two-dimensional turning bands equation. Mathematical Geology 30 (4), 379–390.

Gneiting, T., 1999. The correlation bias for two-dimensional simulations by turning bands. Mathematical Geology 30 (4), 195–211.

Gneiting, T., Sasvari, Z., Schlather, M., 2001. Analogies and correspondences between variograms and covariance functions. Advances in Applied Probability Journal 33(3), 617-630.

Godoy, M.C., Dimitrakopoulos, R., and Costa, J.F., 2001. Economic functions and geostatistical simulation applied to grade control. In: Edwards, A.C. (Ed.), Proceedings of the Mineral Resource and the Reserve Estimation – The AusIMM guide to good practice, 591-600.

Goovaerts, P., 1997. Geostatistics for natural resources evaluation. Oxford University Press, New York, 483 pp.

Goovaerts, P., 1999. Impact of simulation algorithm, magnitude of ergodic fluctuations and number of realizations on the spaces of uncertainty of flow properties. Stochastic Environmental Research and Risk Assessment 13, 161-182.

Goovaerts, P., 2000. Estimation or simulation of soil properties ? An optimization problem with conflicting criteria. Geoderma 97, 165–186.

Goria, S., Armstrong, M., Galli, A., 2001. Quantifying the impact of additional drilling, on an open pit gold project. In: Proceedings of the International Association of Mathematical Geology Conference, Cancun, Mexico, 1-15 pp.

Gossage, B., 1998. The application of indicator kriging in the modelling of geological data. In: Proceedings of a one day symposium: Beyond ordinary kriging. Perth, Western Australia. Geostatistical Association of Australasia.

Gouda, M.A., Moharam, M.R., Ashworth, E., 1995. Geostatistical modelling of El-Gidida iron ore deposit. In: Mitr, H. (Ed.), Proceedings of the CAMT95, 3rd Canadian conference Application in the mineral industry, Montreal, Quebec, Canada, 103-112.

Gouda, M.A., Moharam, M.R., 2001. Effect of indicator kriging on recoverable ore reserves of El-Gidida iron deposit. In: proceedings of the 17th International mining congress and exhibition of Turkey- IMCET2001, ISBN 975-395-417-4, 595-601.

Grace, K.A. 1986. The critical role of geology in reserve determination. In: Ranta, D.E. (ed.), Applied mining geology: Ore reserve estimation, SME, Littleton, Colorado 1-7.

Grimes, D. I. F., Pardo-Iguzquiza, E., 2010. Geostatistics analysis of rainfall. Geographical analysis 42, ISSN 0016-7363 136-160.

GSI (Geological Survey of India) 2006. Detailed Information Dossier on Iron Ores in India. 194 pp.

Guibal, D.,1987. Recoverable reserves estimation of an Australian gold project. In: Matheron, G., Armstrong, M., (Eds.), Geostatistical case studies. Reidel (Dordrecht) publishing Company 149-168.

Guibal, D., Ramacre, A., 1984. Local estimation of the recoverable reserves: Comparing various methods with the reality of a porphyry copper deposit: in Geostatistics for Natural Resource Characterization, Part I, Edited by G. Verly et al.: NATO ASI SERIES C: Mathematical and physical Sciences, Vol. D. Reidel Publishing Company, Holland 435-448.

Guibal, D, Humphreys, M, Sanguinetti, H and Shrivastava, P,, 1997. Geostatistical conditional simulation of a large iron orebody of the Pilbara Region in Western Australia. In: Baafi, E.Y., Schofield, N.A.(Eds.), Proceedings Fifth International Geostatistical Congress, Geostatistics Wollongong '96, Kluwer Academic Publishers, Dordrecht, 695-706.

Haldar, S.K., 2004. Grade and tonnage relationships in sediment-hosted lead-zinc suphide deposits of Rajasthan, India. In: Deb, M., Goodfellow, W. D., (Eds.), Proceedings of the Sediment hosted lead-zinc sulfide deposits: Attributes and models of some major deposits in India, Australia and Canada: Narosa Publishing House, New Delhi 264–272.

Haldar. S.K. 2010. Geostatistical applications in base metal deposits - A case study. In: Sarkar, .C. (Ed.), Proceedings of the Science and economics of rocks - A primer on mineral geostatistics. 95-109.

Haldar, S.K. 2013. Mineral Exploration - Principles and Applications, Elsevier Publication, 374 pp.

Haldar, S.K., 1990. Bhatnagar, S.N., Paliwal, H.V., Application of geostatistics to exploration data for sample optimisation, mine sub-block estimation and grade forecast system at Rampura-Agucha lead-zinc mine, India. In: Proceedings of the XXII APCOM-90, Berlin, 1-11 pp.

Hammah, R.E., Curran, J.H., 2006. Geostatistics in geotechnical engineering: Fad or Empowering ? In: Don, J.D., Jason, T., Dejons, D.F., Laurie G.B. (Eds.), Proceedings Geocongress 2006: Geotechnical engineering in the information technology age Publisher: American Society of Civil Engineers, 1-5.

Hansen, T.M., Mosegaard, K., 2008. VISIM: Sequential simulation for linear inverse problems. Computers & Geosciences 34, 53-76.

Hansen, T.M., Journel, A.G., Tarantoia, A., Mosegaard, K., 2006. Linear inverse Gaussian theory and geostatistics. Geophysics 71(6), R101–R111.

Hardy, R.L., Rashad, M.Z., Sirayanone, S., 1986. Geostatistical prediction of grade fluctuations of Bahariya iron ore components after blasting a certain volume. In: Proceedings of Large open pit mining Conference, Alaska, 169-175.

Hassani, Pak, A.A., 1998. Geostatistics. Tehran University Press, 314 pp.

Hassani, Pak, A.A., 2005. Exploration Data Analysis. Tehran University Press, 642-646.

Hengl T, Toomanian, N., 2006. Maps are not what they seem: representing uncertainty in soil-property maps. In: Caetano M, Painho M, (eds) Proceedings of the 7th international symposium on spatial accuracy assessment in natural resources and environmental sciences (Accuracy 2006), Lisbon, Portugal, 805–813.

Hengl, T., Minasny, B., Gould, M., 2009. A geostatistical analysis of geostatistics. Jointly published by Akadémiai Kiadó, Budapest Scientometrics, and Springer, Dordrecht , DOI: 10.1007/s11192-008-2088-6, 80 (2), 493–516.

Henstridge, J., 1998. Non-linear modelling of geological continuity. In: Proceedings of a one day symposium: Beyond ordinary kriging. Perth, Western Australia. Geostatistical Association of Australasia, 41-49.

Hill, D.,Mueller, U., Bloom, L., 1998. Comparison of median and full indicator kriging in the analysis of a gold mineralization. In: Proceedings of a one day symposium, Beyond ordinary kriging. Perth, Western Australia. Geostatistical Association of Australasia, 50-62.

Hlasny, T., Vizi, L., Turcani, M., Korean, M., Kulla, L., Sitkova, Z., 2009. Geostatistical simulation of bark beetle infestation for forest protection purposes. Journal of Forest Science 55 (11), 518-525.

Huijbregts, C.J., 1975. Regionalized variables and quantitative analysis of spatial data. Proc. NATO ASI for display and analysis of spatial data; Ed. J.C. Davis and M.J. McCullagh, Wiley, 38-53.

Humphreys, M., 1998. Local recoverable estimation: A case study in uniform conditioning on the Wandoo Project for Boddington Gold Mine. In: Proceedings of a one day symposium: Beyond ordinary kriging, Perth Western Australia. Geostatistical Association of Australasia, 63-75.

Humphreys, M., Shrivastava, P., 1997. Choosing an exploration drillhole spacing: A case-study in an iron mine. In: Baafi, E.Y., Schofield, N.A. (Eds.), Proceedings of the fifth international geostatistical congress, Geostatistics Wollongong ’96. Kluwer Academic Publishers, Dordrecht, 780-791.

Indian Bureau of Mines (IBM), 2014. Indian Minerals Year Book 2012, Part III, Minerals Review, 51st Edition, Ministry of Mines, Govt. of India, February, 2014, Iron ore 28:1 - 28:35.

Ingalls, R.G., 2001. Introduction to simulation. In: Peters, B.A., Smith, J.S., Medeiros, D.J., Rohrer, M.W. (Eds.), Proceedings of the 2001 winter simulation conference, Stillwater, Oklahoma, U.S.A. 7-16.

Isaaks, E.H., 1990. The application of Monte carlo methods to the analysis of spatially correlated data. Ph.D. thesis, Stanford University, Stanford, 213 pp.

Isaaks, E.H., Srivastava, R.M., 1989, Applied geostatistics. Oxford University Press, New York, 561.

Jackson, M., Marechal, A., 1979. Recoverable reserves estimated by disjunctive kriging: A case studv. In: Proceedings of the 16th APCOM Symposium, Tucson, Arizona, AIME, New York, 240-249.

Jackson, S., Fredericksen, D., Stewart, M., Vann, J., Burke, A., Dugdale, J., Bertoli, O., 2004. Geological and grade risk at the Golden Gift and Magdala gold deposits Stawell, Victoria, Australia. In: Proceedings of the 5th International Mining Geology Conference, Bendigo, 1-8.

Jang, C.S., Liu, C.W., 2004. Geostatistical analysis and conditional simulation for estimating the spatial variability of hydraulic conductivity in the Choushui river alluvial fan, Taiwan. Hydrological processes 18, 1333–1350.

Jones, I., 1998. A case study using indicator kriging – the Mount Morgan gold-copper deposit, Queensland. In: Proceedings of a one day symposium: Beyond ordinary kriging, Perth, Western Australia. Geostatistical Association of Australasia, 76-87.

Journel, A. G., 1974. Geostatistics for conditional simulation of ore bodies. Economic Geology 69, 673-687.

Journel, A.G., 1980. The lognormal approach to predicting local distributions of selective mining unit grades. Journal of the International Association for Mathematical Geology 12, 285-304.

Journel, A.G., 1982. The indicator approach to estimation of spatial data. In: Proceedings of the 17th APCOM, Port City Press, New York, 793-806.

Journel, A.G., 1983a. Geostatistics, simple tools applied to difficult problems. In: Proceedings of the 50th Iowa Statistical Lab. Anniversary, 237-255.

Journel, A.G., 1983b. Non-parametric estimation of spatial distributions. Mathematical Geology 15 (3), 445-468.

Journel, A.G., 1985. Recoverable reserves – the geostatistical approach. Mining Engineering, 563-568.

Journel, A. G., 1986. Mining geostatistics. Mathematical Geology 18, 119–140.

Journel, A.G., 1989. Fundamentals of geostatistics in five lessons. Short Course in Geology: Volume 8. American Geophysical Union ,Washington. In: Proceedings of 28th International Geological Congress, Washington, 57 pp.

Journel, A.G., 1994. Modeling uncertainty: Some conceptual thoughts. In: Dimitrakopoulos, R. (Ed.), Proceedings of the Geostatistics for the Next Century. Kluwer Academic Publishers, Dordrecht 30–43.

Journel, A.G., Huijbregts, Ch.J., 1978. Mining geostatistics. Academic Press, London 600 pp.

Journel, A.G., Huijbregts, Ch.J., 1981. Mining geostatistics. Academic Press, London 600 pp.

Journel, A.G., Isaaks, E.H., 1984. Conditional indicator simulation: Application to a Saskatchewan uranium deposit. Mathematical Geology 16 (7), 685- 718.

Journel, A.G., Alabert, F., 1989. Non-gaussian data expansion in the earth sciences. Terra Nova, 1, 123- 134.

Journel,A.G., Xu, W., 1994. Posterior identification of histograms conditional to local data. Mathematical Geology 26 (6), 323–359.

Juang, K.W., Lee, D.Y., 1998. Simple indicator kriging for estimating the probability of incorrectly delineating hazardous areas in a contaminated site. Environmental Science & Technology 32, 2487–2493.

Juang, K.W., Lee, D.Y., 2000. Application of disjunctive kriging on delineation of heavy-metal contaminated soils. Journal of the Chinese Institute of Environmental Engineering 10 (4), 291-299.

Kamel, H.F.E, Slimani, M., Cudennec, C., 2010. A comparison of three geostatistical procedures for rainfall network optimization. International Renewable Energy Congress 260-267.

Kameshwara Rao, V., Rao, C.R., Narayana, A.C., 2014. Assessing grade domain of iron ore deposit using geostatistical modelling: A Case study. Journal Geological Society of India 83, 549-554.

Kar, P., Chakravarthy, D.C., 1970. Final report on the north block of the deposit no.13, Bailadila iron ore range, Bastar Dist., M.P, GSI, Central Region, 111 pp.

Keogh, A., Moulton, C., 1998. Median indicator kriging - A case study in iron ore. In: Proceedings of a one day symposium: Beyond ordinary kriging. Perth, Western Australia. Geostatistical Association of Australasia, 106-120.

Khosrowshahi, S., Shaw, W. J., 1997. Conditional simulation for resource estimation and grade control – principles and practice. In: Proceedings of the World Gold 97 Conference, Singapore, Australasian Institute of Mining and Metallurgy, 275-282.

Khosrowshahi, S., Gaze, R., and Shaw, B., 1998. A proposed approach to change of support correction for multiple indicator kriging, based on p-field simulation. In: Proceedings of a one day symposium: Beyond ordinary kriging, Perth Western Australia. Geostatistical Association of Australasia, 121-131.

King H.F., McMahon, D.W., Bujtor, G.J., 1982. A guide to the understanding of ore reserve estimation. The Australasian Institute of Mining and Metallurgy, Melbourne, Supplement to Proceedings No. 281, 21 pp.

King H.F., McMahon, D.W. Bujtor, G.J., Scott, A.K., 1986. Geology in the understanding of ore reserve estimation: An Australian viewpoint. In: Ranta, D.E. (Ed.), Proceedings of the Applied mining geology: Ore reserve estimation, SME, Littleton, Colorado 53-68.

Kitandis, P.K., 1997. Introduction to geostatistics: Applications to hydrogeology, Cambridge University Press 249 pp.

Knudsen, H. P., KimY.C., 1978. A short course on Geostatistical ore reserve estimation, Department of mining and geological engineering, college of mines, The University of Arizona, Tuscon, Arizona, 224 pp.

Koike, K., Matsuda, S., 2003. Characterizing content distributions of impurities in a limestone mine using a feed forward neural network. Natural resources research 12 (3), 209–222.

Kok, M.V., Ulker, B., 2008. Reserve estimation using geostatistics, Energy sources, Part A, Taylor & Francis Group, LLC, ISSN:1556-7036 DOI: 10.1080/15567030601100597 30, 93–100.

Krige, D.G., 1951. A statistical approach to some basic mine valuation problems on the Witwatersrand. Journal of the Chemical, Metallurgical and Mining Society of South Africa 52 (6), 119–139.

Krige, D. G., 1962. Effective pay limits for selective mining. Journal of the South African Institute of Mining and Metallurgy, 345-363.

Krige, D.G., 1994a. A basic perspective on the roles of classical statistics, data search routines, conditional biases, and information and smoothing effects in ore block valuations. In: Bafi, E.Y., Schofield, N.A. (Eds.), Proceedings of the Conference on Mining Geostatistics, Geostatistical Association of Southern Africa, Cape Town, 1-10.

Krige, D.G., 1994b. An analysis of some essential basic tenets of geostatistics not always practiced in ore valuations Regional APCOM: Slovenia.

Krige, D.G., 1996. A practical analysis of the effects of spatial structure and data available and accessed, on conditional biases in ordinary kriging. In: Bafi, E.Y., Schofield, N.A. (Eds.), Proceedings of the Fifth International Geostatistics Congress, Geostatistics Wollongong' 96 799-810.

Khan, M.W.Y., Bhattacharyya, T.K., 1993. A reappraisal of the stratigraphy of Bailadila group, Bacheli, Bastar District, Madhya Pradesh. Journal Geological Society of India 42, 549-562.

Khan, M.W.Y., Bhattacharyya, T.K., 1994. Geochemistry and Tectonic Significancc of Late Archean-Early proterozoic Metabasalts from Bacheli, Bastar District, Madhya Pradesh. Journal Geological Society of India 43, 361-369.

Lantuejoul, C., 1994. Non-conditional simulation of stationary isotropic multigaussian random functions. In: Armstrong, M., Dowd, P.A. (Eds), Proceedings of the Geostatistical simulations. Kluwer Academic, Dordrecht, 147–177.

Lantuejoul, C., 2002. Geostatistical simulation Models and algorithms. Springer, Heidelberg 256 pp.

Lemmer, I.C., 1984a. Estimating local recoverable reserves via indicator kriging, in, Verly, *et. al.*, eds., Geostatistics for Natural Resource Characterization, D. Reidel, Dordrect, Netherlands 349-364.

Lemmer, I.C., 1984b. The Mononodal cutoff – Application to robust variography and spatial distribution estimation. Ph.D. Dissertation, Stanford University, Stanford, California, 396 pp.

Leuangthong, O., McLennan, J. A., Deutsch, C. V., 2004. Minimum acceptance criteria for geostatistical realizations. Natural Resources Research 13, (3), 131-141.

Lin, Y.P., Lee, C.C., Tan, Y.C., 2000. Geostatistical approach for identification of transmissivity structure at Dulliu area in Taiwan. Environmental Geology 40, 111–120.

Lipton, I., Gaze, R., Horton, J., Khosrowshahi, S., 1998. Practical application of multiple indicator kriging and conditional simulation to recoverable resource estimation for the Halley's lateritic

nickel deposit. In: Proceedings of a one day symposium: Beyond ordinary kriging. Perth Western Australia. Geostatistical Association of Australasia, 88-105.

Lloyd, C.D., Atkinson, P.M., 2004. Archaeology and geostatistics, Journal of Archaeological Science 31, 151–165.

Longley-Sinitsyna, D., Snowden, V., 1997. Using geostatistics as a tool in fine tuning of iron ore resource modelling. In: Misra, V.N., Dunlop, D,S. (Eds.), Proceedings of the conference Iron making Resources and Reserves Estimation, Perth, 95-97.

Luster, G.R., 1985. Raw materials for Portland cement - Applications of conditional simulation of co-regionalization: Ph.D. thesis, Stanford University, Stanford, California 531pp.

Lutherborrow, C., 1999. Evolution of resource and reserve estimation methods at Pasminco Broken Hill Mine southern underground operations. In: Stegman, C.L. (Ed.) Proceedings of the Resource/Reserve Estimation Practice in the central west New South Wales mining industry. The Australasian Institute of Mining and Metallurgy, Melbourne, 3-10.

Mantoglou, A., 1987. Digital simulation of multivariate two-and three-dimensional stochastic processes with a spectral turning bands method. Mathematical Geology 19, 129-149.

Mantoglou, A., Wilson, J. L., 1982. The turning bands method for simulation of random fields using line generation by a spectral method, Water Resources Research 18 (5), 1379–1394.

Marechal, A., 1976a. Selecting mineable blocks: Experimental results observed on a simulated orebody. In: Guarascio, M|. (Ed.), Advanced geostatistics in the mining industry, D. Reidel, Dordrecht, Netherlands, 137-l6l.

Marechal, A., 1976b. The practice of transfer functions: Numerical methods and their applications. In: Guarascio, M., David, M., Huijbregts, Ch. (Eds.), Proceedings of the Advanced geostatistics in the mining industry Reidel, Dordrecht, Holland 253-276.

Marechal, A., 1981. Local estimation of co-products by disjunctive kriging: CGMM Internal Report N-728, Fontainebleau (Presented at the 17th APCOM symposium, Golden, Colorado), 19-23.

Marechal, A., 1984. Recovery estimation: A review of models and methods. In: Verly, G. (Ed.), Proceedings of the Geostatistics for Natural resources characterization, NATO A.S.I.: Reidel Publishing Co, Dordrecht, 385-420.

Marechal, A., Shrivastava P., 1977. Geostatistical study of a lower protozoic iron orebody in the Pilbara region of Western Australia. In: Proceedings of the 15th APCOM Symposium, Brisbane Australia, 221-230.

Marechal, A., Touffait, Y., 1980. Recovery estimation of a non-stationary ore body using disjunctive kriging. In: Proceedings of the 17th symposium on the Application of computers in the mining industry, Moscow, 1-8.

Marinoni, O., 2003. Improving geological models using a combined ordinary – indicator kriging approach. Engineering Geology 69, 37-45.

Marzeihe, S.K., Hassan, M., Hossein, H., Parvizz, M., 2013. Determining the best search neighborhood in reserve estimation, using geostatistical method: A case study anomaly No. 12A iron deposit in central Iran. Journal Geological Society of India 81, 581-585.

Mata Lima, H., 2005. Geostatistic in reservoir characterization: From Estimation to Simulation methods. Estudios Geologicos 61, 135-145.

Matheron, G., 1955a. Applications des methodes statistiques a l'evaluation des gisements, in Annales des Mines 12, Paris, 50-75.

Matheron, G., 1955b. Etude geostatistique du gisement de plomb de Bou-Kiama, Technical report, Ecole des mines de Paris, Centre de Geostatistique, Fontainebleau.

Matheron, G., 1962. Traite de geostatistique appliquee. Memoires du bureau de recherches geologiques et minieres. Tome I, no 14, Editions Technip, Paris, Tome II: le krigeage, no 24, Editions BRGM, Paris.

Matheron, G., 1963. Principles of Geostatistics. Economic Geology 58, 1246-1266.

Matheron, G., 1965. Les variables régionalisées et leur estimation: Une application de la théorie des fonctions aléatoires aux sciences de la nature. Paris, Masson, 306 pp.

Matheron, G., 1971. The theory of regionalized variables and its applications; Les cahiers du Centre de morphologie mathematique, Ecole des mines de Paris Fontainebleau, No. 5, 211 pp.

Matheron, G., 1973. The intrinsic random functions and their applications: Advances in applied probabability 5, 439–468.

Matheron, G., 1974. Les fonctions de transfert des petits panneaux, note geostatistique No. 127, Fontainebleau Series No. N-395.

Matheron, G., 1975a. A simple substitute for conditional expectations: the disjunctive kriging. In: Guarascio, M. (Ed.), Proceedings of the Advanced Geostatistics in the Mining Industry D. Reidel, Hingman, Massachusetts, 221-236.

Matheron, G., 1975b. The transfer functions and their estimation. In: Proceedings of the Nato A.S.I., Geostats75, D. Reidel Publ.Co., Netherlands.

Matheron, G., 1976a. A simple substitute for conditional expectation: The disjunctive kriging. In Guarascio, M., et. al. (Eds.), Advanced geostatistics in the mining industry. Proceedings of NATO A.S.I.. Reidel (Dordrecht) 221-236.

Matheron, G., 1976b. Forecasting block grade distributions: The transfer functions. In: Guarascio, M. (Ed.), Proceedings of the Advanced Geostatistics in the Mining Industry. D. Reidel, Dordrecht (Netherlands) 237-251.

Matheron, G., 1978. Le krigeage disjonctif et le parametrage local des reserves. Internal report, Centre de Geostatistique, Fontainebleau, C-76.

Mathews, S., Van Luyt, P., Smart, G., 1999. Grade domains versus geological domains at the Browns Creek gold mine, NSW. In: Stegman, C. L (Ed.), Proceedings of the Resource/reserve estimation

practice in the central West New South Wales mining industry. The Australasian Institute of Mining and Metallurgy, Melbourne, 89-94.

Mendes, R.M., Lorandi, R., 2006. Indicator kriging geostatistical methodology applied to geotechnics project planning, The Geological Society of London, IAEG paper No. 527, 1-12.

Miller, J. W., 1991. Optimization of grid drilling using computer simulation. Mathematical Geology 23(2), 201-218.

Mishra, V.P., Singh, P., Dutta, N.K., 1988. Stratigraphy, structure and metamorphic history of Bastar Craton. Geological Survey of India Record, 117, 1-26.

Mol, O., Gillies, A.D.S., 1984. Use of a reorientation-strategy for geostatistical ore reserve estimation of a complex dipping tabular orebody as an aid to open pit mine planning. In: Proceedings of the Australian Institute of Mining and Mettalurgy 289, 265-270.

Monestiez, P., Dubroca, L., Bonnin, E., Durbec, J.P., Guinet, C., 2006. Geostatistical modelling of spatial distribution of Balaenoptera physalus in the Northwestern mediterranean sea from sparse count data and heterogeneous observation efforts. Ecological modelling 193, 615–628.

Moorhead, C.F, Dunham, P.B, Eastwood, G.J., Leckie, J.F., 1999. Cadia Hill – From discovery to a mine – A case history. In: Stegman, C. L. (Ed.), Proceedings of the Resource/reserve estimation practice in the central west New South Wales mining industry, The Australasian Institute of Mining and Metallurgy, Melbourne, 67-78.

Mukherjee, A., Mondal, R.P., Rajeev Wadhwa, Prabhakhar, G., 2010. Disposition of banded iron formation of Bailadila range, south Bastar Dantewada Dist., Chhattisgarh: Its implications on exploration. Journal of Applied Geochemistry 12 (3), 469-477.

Mukhopadhyay, J., Gosh, G., Nandy, A., Choudhri, A.K., 2006. Depositional setting of the Kolhan group. Its implications for the development of a meso to neoproterozoic deep water basin on the South Indian craton. South African Journal of Geology 109, 183-192.

Mukhopadhyay, J., Beukes, N.J., Bhattacharyya, H.N., 2008. Geology and genesis of major banded iron formation - Hosted high grade iron deposits of India. Economic Geology 15, 291-316.

Murphy, R., Landmark, J., Warner, J., Riddington, D., Ekers, B., 1998. Towards a better resource estimate – The GCML experience. In: Proceedings of the Gold and nickel ore reserve estimation Practice Seminar, The Australasian Institute of Mining and Metallurgy, Kalgoorlie, 101-120.

Murthy, P.S.N., 1989a. Some aspects of the selection of block size and neighborhood in kriging – A case study, IM & EJ, September, 3-14.

Murthy, P.S.N., 1989b. Comparison of ordinary and disjunctive kriging in an Indian iron ore deposit. Mathematical Geology 21 (4), 443-461.

Murthy, P.S.N., 1996. Selective studies on multivariables under constraint in an Indian iron ore deposit. In: Baafi, E.Y., Schofield, N.A. (Eds.), Proceeding of the Geostatistics Wollongong 2, 851-863.

Murthy, P.S.N., 2007. Corrections needed for conceptual errors in some ore reserve estimation methods. Journal Geological Society of India 70, 1077-1085.

Murthy, P.S.N., Chatterjee, A.K. 2007. Some aspects of fixation of exploratory parameters including optimum drilling grid in the context of multivariables of secondary enriched iron ore deposits. Journal Geological Society of India 70, 846-860.

Mwasinga, P., 2001. Approaching resource classification: general practices and the integration of geostatistics. In: Xie, Wang, Jiang (Eds.), Proceedings of the 29th International Symposium on Computer Applications in the Mineral Industries (APCOM02001), Beijing, China, 97–104.

Noble, A.C., 1993. Ore reserve/resource estimation. Mining engineering hand book, In: Peter, D. (Ed.), Published by Society for Mining, Metallurgy and Exploration Inc., Chapter 5.6, 344-359.

Nowak, M.S., Srivastava, R.M., Sinclair, A.J., 1993. Conditional simulation: A mine planning tool for a small gold deposit. In: Soares, A. (Ed.), Proceedings of the Fourth International Geostatistics Congress, Geostat Troia, Portugal, Vol. 2, 977-987.

Olea, R.A., 1999. Geostatistics for engineers and earth scientists. Kulwer Academic publishers 303 pp.

Oliver, M.A., Webster, R., McGrath, S.P., 1996. Disjunctive kriging for environmental management. Environmetrics 7 (3), 333–357.

Omre, H. 1994. Introduction to geostatistical theory and examples of practical applications, Norwegian Computing Center, Oslo, Norway, 1-20.

Osterholt, V., Herod, O., Arvidson, H., 2009. Regional three dimensional modelling of iron ore exploration targets. In: Proceedings of the Orebody Modelling and Strategic Mine Planning. Perth, 35-41.

Oz, B., Deutsch, C.V., Thomas.Tran, T., Xie, Y., 2003. A Fortran 90 program for direct sequential simulation with histogram reproduction. Computers & Geosciences 29, 39–51.

Pachepsky, Y., Timlin, D., 1998. Generating spatially correlated fields with a genetic algorithm. Computers & Geosciences 24 (8), 765-769.

Pandey, S., Sarkar, B.C., 2006. Geostatistical modelling of a bauxite deposit. In: Proceedings of the National Conference on frontier areas in geological and technological aspects of fossil fuel and mineral resources, Allied Publishers, New Delhi, 151-163.

Parker, H.M., 1975, The geostatistical evaluation of ore reserves using conditional probabilitv distributions - A case study for the areas prospect, Warren Maine, Ph.D. dissertation, Stanford University, Stanford, Ca.

Parker, H.M., Switzer, P., 1976, Use of conditional probability distributions in ore reserve estimation: A case study. In: Proceedings of the l3th APCOM Symposium, Clausthal , West Germany Verlag Gluckauf, GMBH, Essen, MII-1 – MII-16.

Parker, H.M., Journel, A.G., Dixon., 1979. Conditional lognormal probability distributions for the estimation of open-pit ore reserves in Stratabound Uranium Deposits: A Case study. In: Proceedings of the 16th APCOM Symposium, Tucson, Arizona, AIME, New York 33-148.

Pasti, H.A. Costa, J.F.C.L., Boucher, A., 2012. Multiple–point geostatistics for modelling lithological domains at a Brazilian iron ore deposit using the single normal equations simulation algorithm. Quantitative Geology and Geostatistics 17, 397-407.

Pebesma, E.J, Karssenberg, D, de Jong, K., 2000. The stochastic dimension in a dynamic GIS. In: Bethlehem, J.G., van der Heijden, P.G.M. (Eds.), Proceedings of the Compstat 2000, computational statistics. Physica, Heidelberg, 379–384.

Perez, V.S., 1988. Indicator kriging based on principal component analysts MSc thesis, Department of Applied Earth Sciences, Stanford University, 336 pp.

Petitgas, P., 1993. Use of disjunctive kriging to model areas of high pelagic fish density in acoustic fisheries surveys, Aquatic Living Resources, 6, 201-209.

Pettijohn, F.J., 1975. Sedimentary rocks, 3rd edition, Harper and Row publishers, New York, 628 pp.

Pocock, J., 1999. Why feasibility resource estimates under-valued the peak orebody. In: Stegman, C.L. (Ed.), Proceedings of the Resource/reserve Estimation practice in the central west New South Wales mining industry, The Australasian Institute of Mining and Metallurgy, Melbourne, 13-28.

Radhakrishna, B.P., 1989. Suspect tectonostratigraphic terrane element in the Indian subcontinent. Journal Geological Society of India 34, 1-24.

Ramachandra, H.M., Roy, A., Mishra, V.P., Dutta, N.K., 2001. A critical review of the tectonothermal evolution of the Bastar craton. Geological Survey of India Special Publication 55, 161-180.

Ramacre, A., 1987. Conditioning by the panel grade for recovery estimation of non-homogenous ore bodies. In: Matheron, G., Armstrong, M. (Eds.), Proceedings of the Geostatistical case studies. D. Reidel Publishing Company, Holland 135-148.

Ramakrishnan, M., 1990. Crustal development in Southern Bastar Central Indian Craton. In: Datta, K.K., Choudhury, S.V., Rajurkar, S.T.and Desmukh, S.S., (Eds.) Precambrian of central India. Geological Survey of India Special Publication 28, 44-66.

Ramakrishnan, M., Vaidyanathan, R., 2010. Geology of India. Geological Society of India 2, 428 pp.

Rambert, F., 2014. Introduction to mining geostatistics. www.geovariances.com. 1-4.

Reeve, J.S., Glacken, I.M., 1998. The evolution of resource and reserve practices within WMC – past, present, and future. In: Proceedings of the Gold and nickel Ore Reserve Estimation Practice seminar. The Australasian Institute of Mining and Metallurgy, Kalgoorlie 19-34.

Renard, P., Straubhaar, J., Caers, J., Mariethoz, G., 2011. Conditioning facies simulations with connectivity data. DOI 10.1007/s11004-011-9363-4 International Association for Mathematical Geosciences 43, 879–903.

Rendu, J.M., 1979. Normal and lognormal estimation. Journal of the International Association of Mathematical Geology 11 (4), 87-102.

Rendu, J.M., 1980a. An Introduction to geostatistical methods of mineral evaluation, The Journal of the South African Institute of Mining and Metallurgy, Johannesburg, 84 pp.

Rendu, J.M., 1980b. Disjunctive kriging: Comparison of theory with actual results. Mathematical Geology 12 (4), 305-320.

Rivoirard, J., 1987. Two key parameters when choosing the kriging neighborhood. Mathematical Geology 19 (8), 851-856.

Rivoirard, J., 1989. Models with orthogonal indicator residuals. In: Armstrong, M., (Ed), Proceedings of the 3rd International Geostatistical Congress, Avignon, France. 91-107.

Rivioriard, J., 1994. Introduction to disjunctive kriging and non-linear geostatistics, Clarendon Press, Oxford, 180 pp.

Rivoirard, J., 2005. Concepts and methods of geostatistics. In: Bilodeau et al. (Eds.) Proceedings of Space, structure and randomness, Springer, 17-37.

Rossi, M.E., Alvarado, S.B., 1998. Conditional simulations applied to recoverable reserves. In: Proceedings of APCOM '98, 27th International Symposium on Computer Applications in the Minerals Industries, The Institution of Mining and Metallurgy, London, 187-199.

Rossi, M.E., Deutsch, C.V., 2014. Mineral resource estimation, Springer Dordrecht Heidelberg, New York 332 pp.

Rostad, O.H., 1986. Geologic and Allied consideration in ore reserve estimation for vein-type deposits. In: Ranta, D.E. (Ed.), Proceedings of the Applied mining geology: Ore reserve estimation, SME, Littleton, Colorado 19.

Roy, A., Ramchandra, H.M., Bandopadhyay, B.K., 2001. Supracrustal belts and their significance in the crustal evolution of central India. Geoligical Survey of India Special Publication 55, 361-380.

Roy, I., Sarkar, B.C., Chattopadhyay, A., 2001. MINFO – a prototype mineral information database for iron ore resources of India, Computers & Geostatistics 27, 357-361.

Royle, A.G., 1977. Why Geostatistics? Engineering And Mining Journal, 92-101.

Sabourin, R., 1983. Geostatistics as a tool to define various categories of resources. Mathematical Geology 15 (1), 131-143.

Sahin, A., Fuseni, A., 1998. Conditional simulation of grain-size distributions in a beach sand deposit. Proceedings of the APCOM, London, UK, Transactions of Institution of Mining and Metallurgy and published In: Sarah Goria, Margaret Armstrong, and Alain Galli, (Eds.), Proceedings of the Quantifying the Impact of Additional Drilling on an Open pit Gold Project, IAMG conference, Cancun, Mexico, 215-224.

Samanta, B., Ganguli, R., Bandopadhyay, S., 2005. Comparing the predictive performance of neural network technique with ordinary kriging technique in a bauxite deposit. Transactions of the Institute of Mining and Metallurgy 114(3), 129-139.

Samui, P., Sitharam, T.G., 2007. Spatial variability of SPT data using ordinary and disjunctive Kriging. In: Proceedings of the First international symposium on geotechnical safety & risk, ISGSR2007, Shanghai, Tongji University, China. 253-264.

Sanguinetti, H., Shrivastava, P., Deraisme, J., Guibal, D., Humphreys, M., 1994. Control of product variability in a large open pit iron mine. In: Proceedings of the Fourth large open pit mining conference. Perth, Australia. The Australasian Institute of Mining and Metallurgy, Melbourne, 133-138.

Saikia, K., Sarkar, B.C., 2006. Exploration drilling optimization using Geostatistics – A case in Jharia coalfield, India. Applied Earth Science 115 (1), London, 13-22.

Saikia, K., Sarkar, B.C., 2013. Coal exploration modelling using geostatistics in Jharia coalfield, India. International Journal of Coal Geology 112, 36-52.

Sarkar, B.C., 2005a. Geostatistics in mineral deposit modelling and evaluation – State of Art. Journal of Economic Geology and Georesource Management, 2 (1-2), 9-22.

Sarkar, B.C., 2005b. Developments in geomathematical modelling and computer applications in mineral resources assessment. Journal Geological Society of India 66 (6), 713-724.

Sarkar, B.C., 2014, Geostatistics: Concepts and applications in mineral deposit modelling for exploration and mining. IGC's sixth Prof. P.B. Verma memorial lecture, Society of Geosciences and Allied Technologies (SGAT), Bhubaneshwar, 1-35.

Sarkar, B.C., Roy, I., 2005. A geostatistical approach to resource evaluation of Kala iron ore deposit, Sundergarh Dist., Orissa, Journal Geological Society of India 65 (5) 553-561.

Sarkar, B.C., Saikia, K., and Paul, P.R., 2006. Geostatistical modelling of coal seams in Jharia coalfield using kriging and simulated annealing simulation. In: Proceedings of the 1st Asian Mining Congress, MGMI, Kolkata, 561-568.

Sarkar, G., Corfu, F., Paul, D.K., MeNaughton, N.J., Gupta, S.N., Bishui, P.K., 1993. Early archen crust in Bastar craton, central India_ageochemical and isotopic study: Precambrian Research 62, 127-137.

Sarma, D.D., 2002. Geostatistics with Applications in Earth Sciences, Capital Publishing Company. 170 pp.

Sarma D.D., 2009. Geostatistics with Applications in Earth Sciences, 2nd Ed., Springer, ISBN 978-1-4020-9 379-1, 205 pp.

Schofield, N.A., 1989a. Ore reserve estimation at the enterprise gold mine, Pine Creek, northern territory, Australia. Part 1: Structural and variogram analysis. C.I.M. Bulletin, 81 (909), 56-61.

Schofield, N.A., 1989b. Ore reserve estimation at the enterprise gold mine, Pine Creek, northern territory, Australia. Part 2: the Multigaussian kriging model. C.I.M. Bulletin, 81 (909), 62-66.

Shahbeik, S., Afzal, P., Moarefvand, P., and Qumarsy, M., 2013. Comparison between ordinary kriging (OK) and inverse distance weighted (IDW) based on estimation error. Case study: Dardevey iron ore deposit, NE Iran. Arab Journal of Geosciences, DOI 10.1007/s12517-013-0978-2, 1-12.

Shannon, R.E., 1975. Systems Simulation: the art and science, Prentice-Hall, 387 pp.

Singh, T.R.P., 1982. Statistical properties of accumulated values and their applications in mining estimations. Mathematical geology 14(2), 107-123.

Skvortsova, T., Armstrong, M., Beucher, H., Forkes, J., Thwaites, A., Turner, R., 2001. Applying plurigaussian simulations to a granite-hosted orebody. In: Kleingeld, W.J., and Krige, D.G. (Eds.), Proceedings of the international conference Geostats 2000, Cape Town, Johannesburg. Geostatistical Association of Southern Africa, 904–911.

Skvortsova, T., Beucher, H., Armstrong, M., Forkes, J., Thwaites, A., Turner, R., 2000. Simulating the geometry of a granite-hosted uranium orebody. In: Armstrong, M., Bettini, C., Champigny, N., Galli, A., and Remacre, A. (Eds.), Proceedings of the conference Geostatistics Rio. Kluwer Academic, Dordrecht, 85–99.

Sluiter, R., 2009. Interpolation methods for climate data, KNMI intern rapport; IR 2009-04, R&D Information and Observation Technology, De Bilt, Netherlands, 28 pp.

Snowden, V., 2001. Practical interpretation of mineral resource and ore reserve classification guidelines. The AusIMM Guide to Good Practice (Monograph 23) 1-21.

Soares, A., 1992. Geostatistical estimation of multi-phase structures. Mathematical geology 24(2), 149-160.

Srivastava, R.M., 1996, Matheronian geostatistics: where is it going? In: Baafi, E.Y., Schofield, N.A., (Eds.), Proceedings of the International Conference Geostatistics Wollongong ’96, vol.1, Kluwer Academic Publishers, Dordrecht, Holland, 53–66.

Srivastava, R.K., Singh R.K., Verma, S.P., 2004. Neoarchaean mafia volcanic rocks from the southern Bastar greenstone belt. Central India: Petrological and tectonic significance: Precambrian research, 131, 305-322.

Stegman, C., 1999. How domain envelopes impact on the resource estimate – Case studies from the Cobar Gold Field, NSW, Australia. In: Edwards, A.C. (Ed.), Proceedings of the Mineral resource and ore reserve estimation – The AusIMM guide to good practice. The Australasian Institute of Mining and Metallurgy, Melbourne, 221-236.

Stein, M. L., 1999. Interpolation of spatial data: Some theory for kriging. Springer, New York, 257 pp.

Stephenson, P. R., 1990. Mineral resource/ore reserve estimation – A common sense approach. In: Proceedings of ore reserves symposium, March 1990, (The Australasian Institute of Mining and Metallurgy, Melbourne).

Sullivan, J., 1984. Conditional recovery estimation through probability kriging – theory and practice. In: Geostatistics for Natural Resources Characterisation, Part 1. Verly, G. et al. (Eds.), Reidel (Dordrecht), 365-384.

Switzer, P., 1977. Estimation of distribution functions from correlated data. Bulletin of the International Statistical Institute, 47 (2), 123-137.

Taboada, J., Vaamonde, A., Saavedra, A., Ordóñez, C., 2002. Geostatistical study of the feldspar content and quality of a granite deposit, Engineering Geology 65, 285-292.

Tahmasebi, P. Hezarkhani, A., 2010. Application of adaptive neuro-fuzzy inference system for grade estimation; Case study, Sarcheshmeh porphyry copper deposit, Kerman, Iran. Australian Journal of Basic and Applied Sciences 4, ISSN 1991–8178, 408-420.

Tavares, M.T., Sousa, A.J., Abreu, M.M., 2008. Ordinary kriging and indicator kriging in the cartography of trace elements contamination in Sao Domingos mining site, Portugal. Journal of Geochemical exploration 98, 43-56.

Thwaites, Deraisme, J., 1998. On the use of non-linear geostatistical techniques for recoverable reserves estimation: A practical case study. Article presented at the APCOM'98, 1-11.

Torcal, F., Posadas, A.M., Chica, M., Serrano, I., 1999. Application of conditional geostatistical simulation to calculate the probability of occurrence of earthquakes belonging to a seismic series, Geophysics Journal International 139, 703-725.

Vallee, M., Cote, D., 1992. The guide to the evaluation of gold deposits: Integrating deposit evaluation and reserve inventory practices: CIM (Canadian Institute of Mining) Bulletin 85 (957), 50-61.

Vann, J., Sans, 1995. Global resource estimation and change of support at the enterprise gold mine, Pine Creek, Northern Territory - Application of the geostatistical discrete Gaussian model. In: Proceedings of APCOM XXV, AusIMM. Parkville, 171-179.

Vann, J., Guibal, D., 1998. An overview of non-linear estimation. In: Proceedings of a one day symposium: Beyond ordinary kriging. Perth, Western Australia. Geostatistical Association of Australasia, 6-25.

Vann, J., Bertoli, O., Jackson, S., 2002. Geostatistical simulation for quantifying risk. In: Proceedings of the Geostatistical Association of Australian symposium, 1-12.

Vann, J., Guibal, D., Harley, M., 2000. Multiple indicator kriging - is it suited to my deposit? In: Proceedings of the 4th International mining geology conference. The Australasian Institute of Mining and Metallurgy, Melbourne, 187-194.

Vann, J., Jackson, S., Bertoli, O., 2003. Quantitative kriging neighborhood analysis for the mining geologist – A description of the method with worked case examples. In: Proceedings of the 5th International Mining Geology Conference, Bendigo, Vic., 1-10.

Verly, G., 1983. The multigaussian approach and its applications to the estimation of local reserves. Journal of the International Association for Mathematical Geology 15 (2), 259–286.

Verly, G., 1984. Estimation of spatial point and block distributions: The Multigaussian model. Ph.D. Dissertation, Stanford Universitv, Stanford, Ca.

Verly, G., Sullivan, J., 1984. Multigaussian and probability kriging – Application to the Jerritt Canyon deposit, presented at the SME-AIME Annual meeting, Los Angeles, California, February, 1984 84-52.

Verly, G., Sullivan, J., 1985. Multigaussian and probability krigings – An application to the Jerritt Canyon deposit. Mining Engineering, 568-574.

Virdee, T.S., Kottegoda, N.T., 1984. A brief review of kriging and its application to optimal interpolation and observation well selection, Hydrological Sciences – Journal – des Sciences Hydrologiques 29 (4), 367-387.

Wackernagel, H., 1995. Multivariate geostatistics. Springer-Verlag (Berlin), 256 pp.

Wackernagel, H., 1998. Principal component analysis for autocorrelated data: A geostatistical perspective: Technical Report N-22/98/G. Centre de Géostatistique, Fontainebleau, France.

Wang, X.J., Zhang, Z.P., 1999. A Comparison of conditional simulation, kriging and trend surface analysis for soil heavy metal pollution pattern analysis. Journal of Environment Science and Health 34(1), 73-89.

Wellmer, F.W., 1983. Classification of ore reserves by geostatistical methods: ERZMETALL 36 (7/8), 315-321.

Worboys, M.F., 1995. GIS – a computing perspective. Taylor and Francis, London, 376 pp.

Wright, A.L., 1987. Some methods for simulating random fields. In: Thesen, A., Grant, H., Kelton, W.D. (Eds.), Proceedings of the winter simulation conference, 295-299.

Wang, G., Gertner, G., Singh, V., Shinkareva, S., Parysow, P., Anderson, A.B., 2002. Spatial and temporal prediction and uncertainty of soil loss using the revised universal soil loss equation: A case study of the rainfall–runoff erosivity R factor. Ecological Modelling 153, 143-155.

Webster, R., Oliver, M.A., 1989. Optimal interpolation and isarithmic mapping of soil properties: Disjunctive kriging and mapping the conditional probability. Journal of Soil Science 40, 497-512.

Webster, R., Oliver, M.A., 2001. Geostatistics for environmental scientists. Wiley, Chichester, 271 pp.

Webster, R., Oliver, M.A., 2007. Geostatistics for environmental scientists. Statistics in Practice, 2nd Ed., John Wiley & Sons Inc., ISBN-13: 978-0-470-02858-2, Chichester, England, 315 pp.

Williamson, D.R., Mueller, E., 1976. Ore estimation at Cyprus Pima mine. In: Proceedings of AIME annual meeting, Las vegas. Nevada.

Wober, H. H., Morgan, P. J., 1993. Classification of ore reserves based on geostatistical and economic parameters. CIM Bull., 86 (966), 73-76.

Wood, G., Oliver, M.A., Webster, R., 1990. Estimating soil salinity by disjunctive kriging. Soil use and management 6 (3), 97-104.

Yamamoto, J. K., 1999. Quantification of uncertainty in ore-reserve estimation: Applications to Chapada copper deposit, State of Goias, Brazil, Natural Resources Research 89(2), 153-163.

Yang, J., Huang, Z.-C., Chen, T.-B., Lei, M., Zheng, Y.-M., Zheng, G-D., Song, B., Liu, Y-Q., Zhang, C., 2008, Predicting the probability distribution of Pb-increased lands in sewage-irrigated region: A case study in Beijing, China. Geoderma 147, 192-196.

Yang, F., Cao, S., Liu, X., Yang, K., 2008. Design of ground water level monitoring network with ordinary kriging. Journal of Hydrodynamics 20 (3), 339-346.

Yates, S.W., Arricka, A.W., Myers, D.E., 1986a. Disjunctive kriging: I. Overview of estimation and conditional probability. Water Resources Research 22, 615-621.

Yates, S.W., Arricka, A.W., Myers, D.E., 1986b. Disjunctive kriging: II. Examples. Water Resources Research 22, 623-630.

Yates, S.R., Yates, M.V., 1988. Disjunctive kriging as an approach to management decision making. Soil Science Society of America Journal 52 (6), 1554–1558.

Youden, W. J., 1951. Statistical methods for Chemists. John Wiley & Sons, New York, 126 pp.

Young, D., 1982. Development and application of the disjunctive kriging model: Discrete Gaussian model. In: Proceedings of the 17th APCOM Symposium, Golden, Colorado, AIME, New York 544-561.

Yunsel, T.Y., Ersoy, A., 2011. Geological modelling of gold deposit based on grade domaining using plurigaussian simulation technique. Natural Resources Research 20(4), 231-249.

Yu, Chen., Yu, Xianchuan., Hou, Jingru., 2004. The theory of disjunctive kriging and its application in grade estimate. 0-7803-8742-2/04/$20.00 (c) 2004 IEEE, 4176-4179.

Zimmerman, D., Pavlik, C., Rugglesv, A., Armstrong. M.P, 1999. An experimental comparison of ordinary and universal kriging and inverse distance weighting, Mathematical Geology 31 (4), 375-390.

Zirschky, J., 1985. Geostatistics for environmental monitoring and survey design. Environmental International 11, 512-524.

## List of Publications

1. Assessing Grade Domain of Iron Ore Deposit using Geostatistical Modelling: A Case Study, *Journal Geological Society of India*, Vol.83, pp.549-554, 2014.
2. Application of non-linear geostatistical indicator kriging in lithological categorization of an Iron ore deposit. *Current Science* (in press).

## Papers Presented in Seminars

1. Some Aspects of the Selection in Domaining and Regularization for Structural Analysis of an Iron ore Deposit – A Case Study, presented in "*National Symposium on Challenges of Mineral Development for Sustainable Growth of India's Mineral-based Industries with emphasis on Iron & Steel Sector*", Organized by South Asian Association of Economic Geologists (SAAEG) at Andhra University, Visakhapatnam, 8 - 10 March, 2013.
3. Geostatistical Modeling and Resource Estimation of Bailadila Iron Ore Deposit through Ordinary Kriging Method, India, presented in the International conference on *"Geostatistical and Geospatial Approaches for the Characterization of Natural Resources in the Environment: Challenges, Processes and Strategies"* organized by International Association for Mathematical Geosciences, 17-20 October, 2014 at JNU, New Delhi.

## Synopsis / Summary of thesis

Geostatistics is a relatively new interdisciplinary field that encompasses geology, mathematics, statistics and mining. The most common goal of geostatistical modelling is to model the spatial data to interpolate the data at unsampled locations and provide resource estimates. Geostatistics not only estimates the ore reserve and grade in mineral deposits but also gives error of estimates.

The main focus of the thesis is a comprehensive geostatistical modelling of an iron ore deposit of Bailadila area, Chhattisgarh, India employing linear, non-linear and simulation methods. The objectives of this study include: to assess grade domains of the deposit in a rapid way in 2D prior to 3D modelling of the deposit, to investigate the feasibility of a novel approach for delineating various litho types in the iron ore deposit employing a non-linear method and to correlate and validate the grade estimation results of two different approaches, to compare and validate the recoverable resource estimation results of different types of non-linear geostatistical estimation methods and evaluate the suitable methods for different purpose, and to assess the uncertainty in the resource estimates and risk involved in the deposit by employing two conditional simulation methods and compare them to find the suitable model for the deposit.

Various geostatistical methods are used for different purposes, viz., - linear estimator such as ‘ordinary kriging’ is used to assess grade domains of the deposit in 2D and to estimate grade estimation in 3D blocks. Non-linear estimators such as ‘indicator kriging’ and ‘disjunctive kriging’ are used to determine conditional probability that the estimated grade in a block is greater than a specified cut-off grade. Conditional simulation methods such as ‘turning band and sequential Gaussian simulation methods are used for assessment of uncertainty and risk that are associated with an estimate.

It is observed from the lithological maps obtained from novel approach indicator kriging method, that the low grade Fe content bearing litho units - BHQ and shale - occur mostly in the peripheral blocks, whereas high grade Fe bearing litho units - SGH, BGH, LH, LO, and BD occur in the middle portion of the deposit.

Block model generated from geological cross section evaluates the total resources of the domain ‘ore’ at ~ 362 Million Tonnes (MT) and of the domain ‘waste’ at ~ 46 MT. The ratio of ore to waste is 1:0.13.

It is observed from the comparative results of Fe content by geological cross sectional model and indicator kriging model that the estimated mean grades of litho units SGH, BGH, LH and BD are almost same, whereas estimated mean grade of litho unit LO is slightly higher (4.6 %) in case of geological model. It is further observed that the results obtained from IK model are in line with the original drilling data and composited data when compared to the results of geological model. It is inferred that the indicator kriging approach provided satisfactory results and it is suggested that this novel approach is more suitable for delineating litho units and can be a suitable replacement of traditional geological cross sectional approach which is time consuming.

It is inferred from the grade maps and error maps that the deposit has mostly high grade areas with less error of estimate which indicates that the deposit is enriched with high Fe content. As the low grade Fe occurs in peripherals, it is a good indication for extracting ore economically. As the quantity of waste is only 46 MT as compared to ore (362 MT), it is inferred that the mining is profitable in this deposit and techno-economically feasible.

It is observed from indicator kriged estimates that the total recovered tonnage is 95 % i.e., ~ 340 MT (out of total 362 MT) with a cut-off of 45 % Fe. The basic statistics of indicator kriged results for mean grade indicate that majority of the blocks have Fe grade > 45 %, with a mean of 63.70 %. Indicator kriged estimates show that about 50 % of the total resources i.e., 180 MT have Fe grade > 67 %, which can fetch bonus or can be used for blending with low grade.

The results through the disjunctive kriging method indicate that the total recovered tonnage is 97 % at a cut-off grade of 45 % Fe. It is further observed that disjunctive kriged estimates resulted in a mean of 64.02 % at a cutoff of grade 45 % Fe.

As this deposit is yet to be mined and production data is not available, based on the relative comparison of OK, IK and DK, in totality, it is concluded that DK estimates are globally consistent.

A comparison is made between the results of total recoverable tonnage (T) and mean grade (M) obtained from turning band simulation and sequential Gaussian simulation methods for different cut-offs. It is observed that the total recoverable tonnage is identical in both the methods and is matching with original Fe data for different cut-offs. However, the mean grades of both the methods slightly differ from the mean grade of the original data upto a cut-off of 45 % Fe. It is further observed that SGS data is matching with original data for the different cut-offs above 45 % Fe, as compared to TB method which underestimated the mean grade slightly. This indicates that

SGS method is comparatively better and accurate than TB method for estimation of recoverable resources in this deposit.

The results presented in this study are potentially useful for different purposes. However, the suitability of a particular estimation method in linear, non-linear and conditional simulations can be ascertained only after comparing these estimated results with the real production data. As this deposit is yet to be mined, it is suggested that these results are to be validated initially with the production data i.e., the blast hole data of the mining benches and the most accurate methods are to be identified.

The thesis is organized in nine chapters. The first chapter of the thesis introduces the thesis and gives introduction to geostatistics with an overview about iron ore. In addition, various resource estimation methods and the objectives of the thesis are given. Chapter 2 contains geology of the study area.

Chapter 3 presents the data available for modelling and describes the concepts of domaining and regularization followed by classical statistical analysis of these data sets. The theoretical study of geostatistics begins in Chapter 4. In this chapter, the probabilistic model of geostatistics in introduced, together with the important concepts of semi-variogram analysis, cross-validation and neighborhood selection. This chapter also reviews categorization of litho units in the block model using *geological cross section* method and proposes a new approach using non-linear *indicator kriging* approach.

In Chapter 5, the concept of *ordinary kriging* is discussed and results obtained using *ordinary kriging* are presented. Chapter 6 presents non-linear geostatistical methods and discusses *indicator kriging* for recoverable resource estimation followed by presentation of results. Chapter 7 focuses on the recoverable resource estimation using *disjunctive kriging*. A comparison of estimated recoverable resources in different methods such as ordinary kriging, indicator kriging and disjunctive kriging is provided in this chapter.

Chapter 8 deals with conditional simulation. Recoverable resource estimation by using *turning band simulation* and *sequential Gaussian simulation* approaches are presented in this chapter. In Chapter 9 summary & conclusion are presented.